TRANSITION METAL VINYLIDENE AND ACETYLIDE COMPLEXES FOR NONLINEAR OPTICS

Stephanie K. Hurst

B. App. Sci. (Hons) (U.W.S.)

A thesis submitted for the degree of Doctor Of Philosophy of The Australian National University

October 2001

Contents

Statement

I certify that the content of this Thesis has never been submitted for any degree and is not currently being submitted for any other degree or qualification, that all the work and results described are original unless due reference is made, and that any help received has been acknowledged.

Stephanie K. Hurst

Summary

The aims of this Thesis were to synthesize a series of linear and octopolar transition metal complexes and to examine their second- and third-order nonlinear optical (NLO) properties.

Chapter 1 briefly discusses the theoretical background of NLO effects and experimental techniques used to measure these effects. A literature review examining the measured NLO responses of organometallic complexes from the previous five years is discussed and related to previous major reviews.

Chapter 2 is concerned with the synthesis of a series of ruthenium vinylidene and acetylide complexes and the measurement of their quadratic (β) and cubic (γ) hyperpolarizabilities. Chain extension leads to increased NLO response, while the vinylidene complexes are shown to possess significant values for β and γ, comparable in strength to the analogous acetylide complexes.

Chapter 3 covers the synthesis and characterization of ruthenium complexes derived from protected and free formylphenylacetylenes. Measurement of the NLO properties of these donor-acceptor complexes showed moderate responses for β and γ resulting from the weak electron-withdrawing capability of the formyl acceptor group.

Chapter 4 is concerned with bimetallic complexes of ruthenium and gold with systematically-varied bridging units. Increasing the π-conjugation through the ligated ruthenium centre had a positive effect on the NLO response. The ferrocenyl-linked complexes gave strong $|\gamma|$ responses.

Chapter 5 contains the synthesis of dendritic organometallic complexes and their linear analogues, with comparison between gold complexes and ruthenium vinylidene and acetylide metal complexes. An improved synthetic methodology was developed to allow the rapid construction of multi-generational dendrimer complexes. The octopolar complexes have favourable optical transparency / NLO efficiency as well as significant γ values. Replacement of yne-linkages with (*E*)-ene-linkages leads to an increase in the measured γ responses.

Acknowledgements

I sincerely thank my supervisor, Dr Mark Humphrey, for his continual support and encouragement, and for a generous allocation of his time.

Dr Stephan Houbrechts, Ms Inge Asselberghs, and Prof. André Persoons are thanked for hyper-Rayleigh scattering measurements and Dr Marek Samoc is thanked for assistance with Z-scan measurements.

Drs Ian Whittall, David Hockless, Tony Willis and Nigel Lucas are thanked for the crystal structure determinations. Drs Marie Cifuentes and Graham Heath are thanked for assistance with electrochemical measurements.

I wish to thank my parents and all my friends for their enduring support over the course of these studies described herein this Thesis.

Abbreviations

a.c.	alternating current
Bu^n	normal butyl
Bu^t	tertiary butyl
CA	*p*-chloroanil
c.c.	complex conjugate
CT	charge-transfer
d.c.	direct current
DDQ	2,3-dichloro-5,6-dicyano-1,4-benzoquinone
DFWM	degenerate four-wave mixing
dppe	bis(diphenylphosphino)ethane
dppm	bis(diphenylphosphino)methane
EFISH	electric field-induced second harmonic generation
EI	electron impact
Et	ethyl
Fc	ferrocenyl
HRS	hyper-Rayleigh scattering
LMCT	ligand to metal charge transfer
Me	methyl
MLCT	metal to ligand charge transfer
NLO	nonlinear optical
OPL	optical power limiting
Ph	phenyl
RSA	reverse saturable absorption
SHG	second harmonic generation
SI	secondary ion
TCNE	tetracyanoethylene
TCNQ	7,7′,8,8′-tetracyanoquinodimethane

thf	tetrahydrofuran
THG	third harmonic generation
Tp^{An}	hydrotris(3-*p*-methoxyphenylpyrazol-1-yl)borate
TPA	two-photon absorption
TPAF	two-photon absorption fluorescence

Published Results

1. A. M. McDonagh, G. J. Deeble, S. K. Hurst, M. P. Cifuentes and M. G. Humphrey.
   J. Chem. Educ., **2001**, *78*, 232.
   "Ruthenium vinylidene and acetylide complexes - An advanced undergraduate multi-technique inorganic/organometallic chemistry experiment".

2. S. K. Hurst, M. P. Cifuentes, J. P. L. Morrall, N. T. Lucas, I. R. Whittall, M. G. Humphrey, I. Asselberghs, A. Persoons, M. Samoc and B. Luther-Davies.
   Organometallics, **2001**, *20(22)*, 4664.
   "Organometallics for Nonlinear Optics. 22. Quadratic and cubic hyperpolarizabilities of *trans*-bis(bidentate phosphine)ruthenium σ-aryl-vinylidene and -alkynyl complexes".

3. S. K. Hurst, N. T. Lucas, M. P. Cifuentes, M. G. Humphrey, M. Samoc, B. Luther-Davies, I. Asselberghs and A. Persoons.
   J. Organomet. Chem., **2001**, *633(1-2)*, 114.
   "Organometallics for Nonlinear Optics. 23. Quadratic and cubic hyperpolarizabilities of acetylide and vinylidene complexes derived from protected and free formylphenylacetylenes".

4. S. K. Hurst, M. P. Cifuentes, M. G. Humphrey, M. Samoc, B. Luther-Davies and A. C. Willis.
   J. Organomet. Chem., **2001**, in press.01/431/Hurst
   "Organometallics for Nonlinear Optics. 25. Quadratic and cubic hyperpolarizabilities of some dipolar and quadrupolar gold and ruthenium complexes".

5. M. H. Garcia, M. P. Robalo, A. R. Dias, M. T. Duarte, W. Wenseleers, G. Aerts, E. Goovaerts, M. P. Cifuentes, S. K. Hurst, M. G. Humphrey, M. Samoc and B. Luther-Davies
   Organometallics, **2001**, Manuscript submitted.
   "Synthesis and Nonlinear Optical Properties of Monocyclopentadienyliron(II) Acetylide Derivatives".

6. S. K. Hurst, N. T. Lucas, M. G. Humphrey, I. Asselberghs and A. Persoons and A. C. Willis.
   Aust. J. Chem., **2001**, in press.
   "Organometallics for Nonlinear Optics. 26. Quadratic hyperpolarizabilities of some 4-methoxytetrafluorophenylalkynyl gold and ruthenium complexes".

7. S. K. Hurst, M. G. Humphrey, M. Samoc, B. Luther-Davies, G. A. Heath and A. C. Willis.

Organometallics, **2001**, Manuscript in preparation.

"Organometallics for Nonlinear Optics. 28. Cubic hyperpolarizabilities of some ferrocenyl-linked gold and ruthenium complexes".

8. S. K. Hurst, M. P. Cifuentes and M. G. Humphrey.

J. Am. Chem. Soc., **2001**, Manuscript submitted.

"A rapid convergent approach to organometallic dendrimers: Sterically-controlled dendron synthesis".

9. S. K. Hurst, N. T. Lucas, M. G. Humphrey, M. Samoc and B. Luther-Davies.

Macromolecules, **2001**, Manuscript in preparation.

"Organometallics for Nonlinear Optics. 29. Cubic hyperpolarizabilities of some octopolar ruthenium and gold complexes".

Chapter 1

Organo-transition metal complexes for nonlinear optics

Contents

Chapter 1

Organo-transition metal complexes for nonlinear optics

1.1. Introduction

Nonlinear optics (NLO) deals with the interactions of electromagnetic fields (light) with matter. The incident light may be altered in phase, frequency or other physical properties, by exploiting processes such as harmonic generation, frequency mixing and Raman shifting. Materials capable of large nonlinear optical effects may be of technological importance for optical data storage, optical communication, dynamic image processing and, ultimately, optical computing.

Materials currently utilized for their NLO properties are mostly inorganic solids such as $LiNbO_3$ and KH_2PO_4. These and similar inorganic salts have found application in frequency mixing and electrooptic modulation. In these complexes, the purely electronic NLO-based effects are accompanied by crystal lattice distortions where small, loosely bound positive ions within the crystals produce an asymmetric field which gives rise to NLO effects on the nanosecond time scale. This relatively slow response is suitable for some applications, e.g. the electrooptic effect, but is not ideal for frequency conversions which require a purely electronic NLO response. Inorganic salts have desirable properties

for materials applications including a large transparency range, high optical damage threshold and the ability to be grown as large crystals. Second-harmonic generation with efficiencies up to 10 % have been observed in $LiNbO_3$, $LiTaO_3$ and $KTiOPO_4$ (KTP) crystals. Inorganic salts possess disadvantages, though, including restricted structural diversity and difficulty in fabrication.

Semiconductors such as gallium arsenide and cadmium sulfide, particularly those with reduced dimensions (quantum wires, quantum dots and quantum wells), possess NLO effects which arise from saturable absorption, with third-order responses that are amongst the highest known. However, the NLO response of these systems may be relatively slow on account of the NLO process being due to resonant interactions, i.e. one and two-photon absorption. Although some semiconductors such as $Al_xGa_{1-x}As$ have reasonably high nonresonant nonlinearities, many organics [for example π-conjugated polymers such as polyacetylenes and poly(*p*-phenylenevinylenes)] offer similar or higher nonlinearities along with inherently greater architectural flexibility.

Many organic molecules (in solution or as crystals, or in guest-host systems) have been probed for their NLO responses.[1-3] In these complexes, the main source of the NLO response is usually the electronic nonlinearities. Organic systems possess certain advantages over inorganic systems, such as fast nonlinear responses, they are generally cheaper and easier to fabricate than inorganic materials, and they have a greater degree of structural diversity. This architectural flexibility allows for precise molecular design and the determination of structure-property relationships. Low lying electronic transitions in the UV-visible region improve the NLO efficiencies of organic systems, but lead to a disadvantage due to a trade-off between nonlinear efficiency and optical transparency.

Other disadvantages of organics include lower thermal stability and facile relaxation of the chromophore in poled guest-host systems to random orientations.

Experimentation with organic materials for nonlinear optics has afforded various structure-property relationships. Additionally, the rapid development of theoretical/computational techniques has provided a basis to appraise optical chromophores and structural approaches. Historically, chromophores possessing the largest second-order nonlinearities have been composed of donor and acceptor substituents linked through a π-conjugated backbone. Experimentation has demonstrated that second-order nonlinearities can be enhanced by using strongly electron polarized substituents (to increase electron asymmetry) or by lengthening the π-conjugated backbone (to improve electron delocalization). High polarizability of any order is associated with the existence of low energy molecular excited states which, because they are close in energy to the ground state, mix easily when the molecule is perturbed. Donor-acceptor systems possessing large nonlinearities include substituted stilbenes, azo dyes and oligothiophenes.

Similar properties are important for third-order materials. Lengthening the π-conjugated chain increases the excited-state dipole, allowing for long-distance intramolecular charge transfer. In addition, varying the donor and acceptor end groups increases the charge asymmetry, leading to concomitant enhancement of cubic hyperpolarizability. Shifting from one-dimensional donor-acceptor systems to two-dimensional (phthalocyanines or tetraethynylethenes) or three-dimensional systems (fullerene derivatives), the use of heterocycles (rather than phenyl moieties) and modification of bond-length alternation (the difference in length between C—C single and double bonds in a π-conjugated system) all impact favorably on third-order nonlinearities.

Octopolar compounds have also been investigated for their NLO potential. The higher symmetry of octopolar compounds allows for a better NLO efficiency/transparency trade-off. Additionally, octopolar complexes may possess highly polarized substituents, but the absence of a molecular dipole moment should reduce the possibility of centrosymmetric packing of the material in the bulk phase.

Like organic molecules, organometallic complexes possess large NLO responses, fast response times, ease of fabrication and integration into composites, as well as having greater design flexibility. Organometallics can be formed using a wide range of metals with different oxidation states, ligands and geometry which permit fine tuning the molecule in ways not possible with purely organic molecules. The metal may act variously as a donor or acceptor group, and mixed-metal systems are also easily accessible. Because of the enormous diversity of possible organometallic complexes, structure-property relationships may be determined for systematically varied systems. Organic fragments which would otherwise be too unstable to examine may be stabilized by complexation to a metal (e.g. carbenes). Organometallics may also be incorporated into polymers either directly into the polymer backbone or as part of the side chains.

The NLO properties of organometallic compounds have been recently reviewed along with some related coordination complexes.[4-6] The present work reviews the organo-transition metal-containing component of the field through mid-2001.

1.2. Background

1.2.1. Theory of nonlinear optics

Optical nonlinearities can be explained by considering the interaction of strong electric fields with matter. If the fields have optical frequencies, the phenomena resulting from the nonlinear interactions are called nonlinear optical (NLO) phenomena. Most texts on nonlinear optics (e.g. references 7-10) begin the discussion of this area from considerations of macroscopic relations between the vector quantities **P** (the polarization vector), **D** (the displacement vector) and **E** (the electric field vector). Chemists, however, consider the molecular origin of physical phenomena, so the description of NLO phenomena which follows starts from consideration of the behaviour of a single molecule in a strong electric field.

An electric field $\mathbf{E}_{loc}$ acting on a molecule is termed a *local* field since it may differ substantially from the macroscopic field outside the medium (because of the influence of neighbouring molecules). The field will, in general, distort the electron density distribution $\rho(\mathbf{r})$ in a molecule. Such a distortion may be described in terms of changes in the electron distribution moments. The first moment of the electron distribution, the dipole moment μ, is the most important quantity from the aspect of optical properties (hence, one often talks about a so-called dipolar approximation). The changes in the dipole moment induced by a relatively weak field can be expected to be linear with the magnitude of the field. However, this will not be the case for the field $\mathbf{E}_{loc}$ comparable in strength to the internal electric fields within the molecule. In these circumstances, the distortion and the induced dipole moment have to be treated as nonlinear functions of the field strength, usually being presented in terms of a power series:

$$\mu = \mu_0 + \alpha \mathbf{E}_{loc} + \beta \mathbf{E}_{loc}\mathbf{E}_{loc} + \gamma \mathbf{E}_{loc}\mathbf{E}_{loc}\mathbf{E}_{loc} + \ \ldots \qquad (1.1)$$

In many texts (e.g. some of those relating to quantum chemical calculations), equation (1.1) is treated as a Taylor series and therefore has 1/n! multipliers in front of the consecutive $(\mathbf{E}_{loc})^n$ terms.

The tensorial α, β and γ quantities defined by the above equation are called the linear polarizability, the second-order or quadratic hyperpolarizability (or, sometimes, the first hyperpolarizability) and the third-order or cubic hyperpolarizability (the second hyperpolarizability), respectively. As both μ and $\mathbf{E}_{loc}$ are vectors, the relation between the three Cartesian components of μ and the three Cartesian components of $\mathbf{E}_{loc}$ needs nine proportionality factors, and so α is a second-rank tensor (or a 3 x 3 matrix). A full description of the second-order and third-order interactions involves assessing the effect on the dipole moment of *combinations* of Cartesian components of the field, so β is a third-rank tensor (or a 3 x 3 x 3 matrix) and γ is a fourth-rank tensor (or a 3 x 3 x 3 x 3 matrix). Fortunately, many of the tensor components of α, β, and γ are equivalent by various symmetry rules or equal to zero. The most straightforward simplification comes from permutation symmetry (the products of the Cartesian components of the field can be freely permuted), which results in some indices in the tensor elements of the polarizabilities being permuted, too.[9] Additional simplification comes from polarizabilities being invariant with respect to all point group symmetry operations. The latter rule is especially important when considering the second-order hyperpolarizability β: in the same way that a vectorial property must be absent in an object which has a centre of symmetry (the only vector which stays invariant after inverting it through a centre of symmetry is a vector of zero length), all the components of β (and any third-rank tensor) must vanish in centrosymmetric point groups.

The electric field of a light wave can be expressed as:

$$\mathbf{E}(t) = \mathbf{E}_0 \cos(\omega t) = \frac{\mathbf{E}_0}{2}[\exp(i\omega t) + \exp(-i\omega t)]$$

Therefore, for an arbitrary point in space, Equation 1.1. can be written as:

$$\begin{aligned}\mu(t) &= \mu_0 + \alpha\mathbf{E}_0\cos(\omega t) + \beta\mathbf{E}_0^2\cos^2(\omega t) + \gamma\mathbf{E}_0^3\cos^3(\omega t) + \ \ldots \\ &= \mu_0 + \tfrac{1}{2}\alpha\mathbf{E}_0\exp(i\omega t) + \tfrac{1}{2}\beta\mathbf{E}_0^2 \\ &\quad + \tfrac{1}{4}\beta\mathbf{E}_0^2\exp(2i\omega t) + \tfrac{3}{8}\gamma\mathbf{E}_0^3\exp(i\omega t) + \tfrac{1}{8}\gamma\mathbf{E}_0^3\exp(3i\omega t) + \text{c.c.} + \ \ldots\end{aligned} \qquad (1.2)$$

where c.c. stands for complex conjugate terms. It is easily seen from the above expansions in terms of exponential factors or, equivalently, trigonometric relations such as $\cos^2(\omega t) = 1/2 + 1/2\cos(2\omega t)$ that the effect of the nonlinear terms in the dipole moment expansion has been to introduce contributions at different frequencies: the second-order (β) term has introduced a time-independent (d.c.) contribution (optical rectification) as well as a term oscillating at the frequency of 2ω (the second-harmonic generation component). It can readily be verified that the quadratic term also provides a frequency mixing phenomenon if the input field is a sum of two components with different frequencies, and that a constant (dc) field may influence an oscillating field if the two are combined in a medium containing second-order nonlinear molecules [the linear electrooptic (Pockels) effect]. In a similar way, the cubic term in Equation (1.1) leads to various nonlinear optical effects, one being oscillation of the induced dipoles at 3ω (third-harmonic generation).

Equation (1.1) is, strictly speaking, not suitable for optical fields, which are rapidly varying in time. Even for linear polarization, the oscillation of the induced dipole moment may be damped (by material resonances) and thereby phase shifted with respect to the oscillation of the external electric field. The usual way of expressing this phase shift is by considering the relationship between the Fourier components of the induced effect (oscillation of the

induced dipole) and the stimulus (the electric field), with the damping and phase shift conveniently expressed by treating the terms involved as complex. Thus, the linear polarizability can be written as:

$$\Delta\mu^{(1)}(\omega) = \alpha(\omega)E(\omega)$$

where $\alpha(\omega)$ is complex, $E(\omega)$ is the Fourier amplitude of the field at frequency ω and $\Delta\mu^{(1)}(\omega)$ is the linear component of the oscillation of the dipole at the same frequency. Dispersion of α (the frequency dependence of the linear polarizability) will show characteristic rapid changes of the real part of α and enhanced values of the imaginary part of α near to the resonance frequencies of the molecule.

In the same way, frequency-dependent hyperpolarizabilities can be defined as complex quantities by considering the relations between the nonlinear (quadratic and cubic) components of the induced dipole moment oscillations at particular frequencies. A complication is that, in general, more than a single field frequency is involved. The usual notation is:

$$\Delta\mu^{(2)}(\omega_3) = \beta(-\omega_3;\omega_1,\omega_2)E(\omega_1)E(\omega_2)$$

and:

$$\Delta\mu^{(3)}(\omega_4) = \gamma(-\omega_4;\omega_1,\omega_2,\omega_3)E(\omega_1)E(\omega_2)E(\omega_3)$$

for the quadratic and cubic NLO effects, respectively. The first frequency in the brackets describing the frequency dependence of the hyperpolarizability refers to the output frequency and the remaining frequencies are those of the input fields. Positive and negative signs of the frequencies can occur, depending on the type of interaction; for example, the β responsible for second-harmonic generation is represented as $\beta(-2\omega;\omega,\omega)$ whereas β for

optical rectification is written as $\beta(0;-\omega,\omega)$. Dispersion of β and γ is therefore quite complicated, the dispersion of β being a function in two-variable space (the frequency ω_3 is always $\omega_3 = \omega_1 + \omega_2$) and the dispersion of γ needing three-variable space for a full description. It should be noted that resonant behaviour of the hyperpolarizabilities (a rapidly changing real part and enhanced imaginary part) is expected not only when any of the frequencies in $\beta(-\omega_3;\omega_1,\omega_2)$ or $\gamma(-\omega_4;\omega_1,\omega_2,\omega_3)$ approaches a resonance but also for some combination of the input frequencies being close to a resonance. One of the best known examples of such behaviour is that the so-called degenerate third-order hyperpolarizability $\gamma(-\omega;\omega,-\omega,\omega)$ can be expected to exhibit resonant behaviour when 2ω approaches resonance.

1.2.2. Nonlinear optical processes

Second-order nonlinearities are mostly used for various frequency mixing schemes. Among the possible processes, there are several which have specific technological applications and are therefore of significant interest: (i) second-harmonic generation, i.e. the $\omega + \omega \rightarrow 2\omega$ mixing process which doubles the energy of photons (e.g. to convert infrared into visible), (ii) the linear electrooptic (Pockels) effect, i.e. the $\omega + 0 \rightarrow \omega$ process which is often used to modulate the phase or amplitude of a light wave (to make it carry information), and (iii) parametric generation, i.e. the $\omega \rightarrow \omega_1 + \omega_2$ process which involves splitting an energetic photon into a sum of two less energetic ones (a popular way of generating laser beams at tunable wavelengths).

There are many possible third-order nonlinear processes, some of which are important as valuable tools for nonlinear spectroscopy, while others have technological significance. The presence of $\chi^{(3)}$ in any substance (even air) means that all materials exhibit third-harmonic generation of laser frequencies. The direct process of third-harmonic generation

is, however, not usually exploited for generation of short wavelength laser beams, a cascade of two second-order mixing processes ($\omega + \omega \rightarrow 2\omega$ and $2\omega + \omega \rightarrow 3\omega$) being preferred for generation of 3ω from ω (one reason for this is that phase matching is virtually impossible to obtain for third-harmonic generation). From the technological point of view, the most interesting applications of $\chi^{(3)}$ are those which correspond to all-optical interactions of light beams. For interacting fields of the same frequency (the degenerate case), the frequency mixing scheme is $\omega - \omega + \omega \rightarrow \omega$, which means that the interaction of three fields of the same frequency generates a fourth field of the same frequency.

Optical power limiting (OPL) has attracted considerable interest with applications such as the protection of sensors from damage resulting from exposure to high energy laser pulses. In principle, the direct two-photon absorption process is suitable for optical limiting, but practical estimates show that power limiting properties of existing materials (even those with the largest two-photon absorption coefficients) are insufficient for the most important applications, namely, the protection of sensors from laser pulses of duration of the order of nanoseconds. Another important process which affords optical limiting behaviour is reverse saturable absorption (RSA). If a substantial proportion of the population of molecules is excited from the ground state to the excited state, then the absorption of the material is no longer the same as that of the population of ground state molecules. A common phenomenon is saturable absorption (absorption bleaching), i.e. increase of sample transmission as the ground state molecules are depleted. In order for reverse saturable absorption to take place, it is necessary that the excited state molecules exhibit a higher absorptivity at a given wavelength than the ground state molecules. The RSA phenomenon is thus a "photodarkening" effect. The difference between the RSA process and two-photon absorption is that the two-photon absorption is virtually instantaneous whereas processes involving intermediate absorbing states exhibit certain kinetic behaviour, which is

dependent upon the lifetimes of the states which are involved. As with refractive third-order nonlinearity, time-resolved investigations of the changes of absorptive properties are necessary to evaluate the mechanism of power limiting in a given system.

1.2.3. Systems of units

The two common unit systems employed for the description of nonlinear optical properties are the SI (or MKS) and Gaussian (or cgs) systems (Boyd[9] mentions an alternative system of SI units which will not be discussed further, as it has not been used with organometallic complexes). In the Gaussian system, properties are described in units of esu. The main source of confusion arises from the fact that not only do the units vary between each system, but the dimensions of the properties also vary: for example, the polarizability α has dimensions of length^3 in the Gaussian system (units: cm^3) but dimensions of charge length^2 potential^{-1} (units: C m^2 V^{-1}) in the SI system. Furthermore, vacuum permittivity ε_0 exists in the SI system (having units of F m^{-1}) but has no equivalent in the Gaussian system (i.e. ε_0 = 1). It is important to be able to convert between the two systems, but care must be taken to ensure that not only are the units converted correctly, but that the quantities of interest are treated according to their different definitions in different systems.

The dimensions of the first-, second- and third-order susceptibilities in both systems are simply derived from the polarizability power series equation.[9] In the Gaussian system, polarization **P** and electric field strength **E** have equivalent dimensions (units: statV cm^{-1} = statC cm^{-2} = (erg cm^{-3})$^{1/2}$), and are related by:

$$\mathbf{P} = \chi^{(1)}\mathbf{E} + \chi^{(2)}\mathbf{E}^2 + \chi^{(3)}\mathbf{E}^3 + \ldots$$

so that the electrostatic units of the susceptibilities are as follows:

$\chi^{(1)}$ dimensionless

units of $\chi^{(2)}$ = units of $1/E$ = cm statV^{-1} = (erg cm^{-3})$^{-1/2}$

units of $\chi^{(3)}$ = units of $1/E^2$ = cm^2 statV^{-2} = (erg cm^{-3})$^{-1}$

The above units are traditionally written as esu for any of the above quantities.

In the SI system, **P** and **E** have different dimensions (units of **P**: C m^{-2}, and units of **E**: V m^{-1}), and **P** is related to **E** by:

$$\mathbf{P} = \varepsilon_0 [\chi^{(1)}\mathbf{E} + \chi^{(2)}\mathbf{E}^2 + \chi^{(3)}\mathbf{E}^3 + ...]$$

where $\varepsilon_0 = 8.85 \times 10^{-12}$ F m^{-1}. The units of the susceptibilities in the SI system are:

$\chi^{(1)}$ dimensionless

units of $\chi^{(2)}$ = units of $1/E$ = m V^{-1}

units of $\chi^{(3)}$ = units of $1/E^2$ = m^2 V^{-2}

Similarly, the units for α, β and γ in both SI and Gaussian systems can be derived from the equation describing polarization on the molecular scale (noting units μ_{SI}: C m, and units μ_{cgs}: statV cm^2) and are given in Table 1.1.

To convert $\chi^{(1)}$, $\chi^{(2)}$ and $\chi^{(3)}$ between the systems of units, it is also necessary to include a factor of 4π as the displacement vector **D** is defined differently for the two systems. In the Gaussian system:

$$\mathbf{D}_{cgs} = \mathbf{E}_{cgs} + 4\pi\mathbf{P}_{cgs} = \mathbf{E}_{cgs}(1 + 4\pi\chi^{(1)}{}_{cgs})$$

and in the SI system:

$$\mathbf{D}_{SI} = \varepsilon_0 \mathbf{E}_{SI} + \mathbf{P}_{SI} = \varepsilon_0 \mathbf{E}_{SI}(1 + \chi^{(1)}_{SI})$$

so that:

$$4\pi\chi^{(1)}_{cgs} = \chi^{(1)}_{SI}$$

To convert α, β and γ between the systems of units, we utilize the fact that μ in SI (units: C m) and μ in cgs (units: StatC cm) are defined the same way and, since 1 C = 3 x 10^9 StatC, the conversion factor is μ_{SI} = 1/3 x 10^{-11} μ_{cgs}. The unit system conversions for the polarizability and hyperpolarizabilities can be deduced by analogy to the derivation of the susceptibilities (i.e. rearranging the equations and equating $\alpha_{SI}E_{SI}/\mu_{0SI} = \alpha_{cgs}E_{cgs}/\mu_{0cgs}$, etc). A summary of units and conversion factors for important properties is shown in Table 1.1. Butcher *et al.*[10] provides a discussion of the pitfalls which arise when applying conversion procedures between nonlinear properties defined in different ways.

Table 1.1. Units and conversion factors for important properties.

Property		System of units: SI	System of units: cgs	Conversion factor
Dipole moment	μ	C m	statC cm = statV cm^2	$\mu_{SI} = 1/3 \times 10^{-11}\ \mu_{cgs}$
Electric field	E	V m^{-1}	statV cm^{-1} = (erg cm^{-2})$^{1/2}$	$E_{SI} = 3 \times 10^4\ E_{cgs}$
Linear polarizability	α	C m^2 V^{-1}	cm^3	$\alpha_{SI} = (1/3)^2 \times 10^{-15}\ \alpha_{cgs}$
Hyperpolarizability	β	C m^3 V^{-2}	cm^2 $statV^{-1}$ = esu	$\beta_{SI} = (1/3)^3 \times 10^{-19}\ \beta_{cgs}$
Second hyperpolarizability	γ	C m^4 V^{-3}	cm^5 $statV^{-2}$ = esu	$\gamma_{SI} = (1/3)^4 \times 10^{-23}\ \gamma_{cgs}$

1.3. Experimental Techniques

A variety of experimental techniques have been used to obtain both qualitative and quantitative information about the optical nonlinearities of materials. This section includes descriptions of those techniques which have been used, or have potential use, for the measurements of NLO properties of organometallics. Reference 8 is an excellent source of information about other techniques.

1.3.1. Solvatochromism[11,12]

Solvatochromism is the shift of the absorption spectrum of a molecule with varying solvent. The use of this phenomenon for the determination of β is based on the two-level microscopic model of the first hyperpolarizability, in which the infinite sum-over-states quantum perturbation expression for β is reduced to two states, the ground and excited states. This model allows β_{CT} (β in the direction of the charge-transfer axis) to be determined in terms of other measurable microscopic quantities, namely the ground to excited state transition energy ω_{eg} (from λ_{max} in the electronic absorption spectrum), the transition dipole moment μ_{eg} (from integration of the absorption band in the UV-vis spectrum), the ground state dipole moment μ_g (measured separately) and the excited state dipole moment μ_e. The last quantity is found by measuring the solvatochromic shift of λ_{max} of the solute, in solvents of varying polarity for which the dielectric constant and refractive index are known (or can be measured). The value for β_{CT} is then obtained from:

$$\beta_{CT} = \frac{3}{2}\hbar^2 \left[\frac{\mu_{eg}^2 (\mu_e - \mu_g)}{(\omega_{eg}^2 - \omega^2)(\omega_{eg}^2 - 4\omega^2)} \right]$$

This technique has been applied to organic compounds where charge-transfer is dominated by one transition; this is not often the case for organometallics. The applicability of this

technique to organometallics thus far has not been tested; there are no reports where solvatochromism has been used to examine the second-order nonlinearities of transition metal organometallics, and only one report of its application to two organoboron compounds.[13]

1.3.2. Electric-field induced second-harmonic generation (EFISH)

In the EFISH technique, a liquid or solution sample is subjected to a high voltage d.c. pulse to align molecules, the pulse being synchronized with the laser beam pulse. $\chi^{(2)}$ can then be observed in what was previously an isotropic medium. All materials will produce an EFISH signal as it is formally a third-order nonlinear process described by the susceptibility $\chi^{(3)}$ $(-2\omega;\omega,\omega,0)$. There are two contributions to this susceptibility, one of them arising from the sum of the orientationally-averaged third-order hyperpolarizabilities $\gamma(-2\omega;\omega,\omega,0)$ of the medium, and another due to the vectorial sum of the components of the second-order hyperpolarizabilities. Molecules that possess a permanent dipole μ partially align with the d.c. field, the degree of the alignment usually described in terms of the Langevin function. The nett second-order effect can be shown to depend on the $\mu\cdot\beta_{vec}$ product where μ is the dipole moment of the molecule and β_{vec} is the vectorial component of the second-order hyperpolarizability (the hyperpolarizability β is a symmetric third-rank tensor which can be treated as being composed of a vector part and a septor part).[14] In general, the directions of β_{vec} and of μ do not coincide. The effective hyperpolarizability measured by the EFISH technique can be defined as β_{EFISH}, and is given by $\mu\cdot\beta_{vec} = \mu\beta_{EFISH}$. For molecules with strong electron donor and acceptor groups (at opposing ends of the molecule), β_{CT} (the hyperpolarizability along the charge-transfer axis) usually accounts for most of β_{EFISH}.

A wedge shaped cell is used to hold a solution of the sample. This is translated in a direction perpendicular to the incident laser beam, creating Maker fringes whose

periodicity is related to the wedge design and to the coherence length, which can therefore be determined. An analogous measurement can also be made on a reference wedge such as quartz, but most often a measurement on a pure solvent of well-known properties, e.g. chloroform, is used to calibrate the system.

The EFISH third-order macroscopic susceptibility defined as $\Gamma = 3\chi^{(3)}(-2\omega;\omega,\omega,0)$ is related to the microscopic second hyperpolarizability γ' by local field factors and the molecule number density. In turn, β can be obtained from $\gamma' = \gamma + \mu\beta_{EFISH}/(5k_bT)$, where γ' is the effective second hyperpolarizability (third-order hyperpolarizability), γ is the intrinsic second hyperpolarizability consisting of electronic and vibrational parts, k_b is Boltzmann's constant and T is the temperature in K. In the experiment, comparison against a reference enables Γ values to be determined. In order to determine the $\mu\beta_{EFISH}$ product of an unknown substance, one usually performs EFISH measurements as a function of concentration in a well-characterized solvent; this concentration dependence study is necessary in order to resolve ambiguities occurring because the $\mu\beta_{EFISH}$ products for the solvent and the solute may be of the same or of opposite signs, and the SHG signal is proportional to the square of the EFISH susceptibility. Other quantities that may be required for the interpretation of the results are the dielectric constant, the permanent dipole moment, and the intrinsic second hyperpolarizability of the solute (found from a separate experiment or ignored).

The application of EFISH to organometallics is limited to neutral complexes. The presence of ionic species makes it impossible to apply high electric fields to a solution. It is also not possible to utilize EFISH when the complex has no nett dipole moment.

1.3.3. Hyper-Rayleigh scattering (HRS)[15,16]

The HRS technique involves detecting the incoherently-scattered second-harmonic light generated from an isotropic solution in order to determine the first hyperpolarizability. HRS is due to orientational fluctuations of asymmetric molecules in solution which give rise to local asymmetry, on a microscopic scale, in an isotropic liquid.[16] The light scattered from such a system can have a component at the second-harmonic that depends only on the first hyperpolarizability of the solute molecules, and varies quadratically with the incident intensity; an example of the data obtained from an HRS experiment is displayed in Figure 1.1.

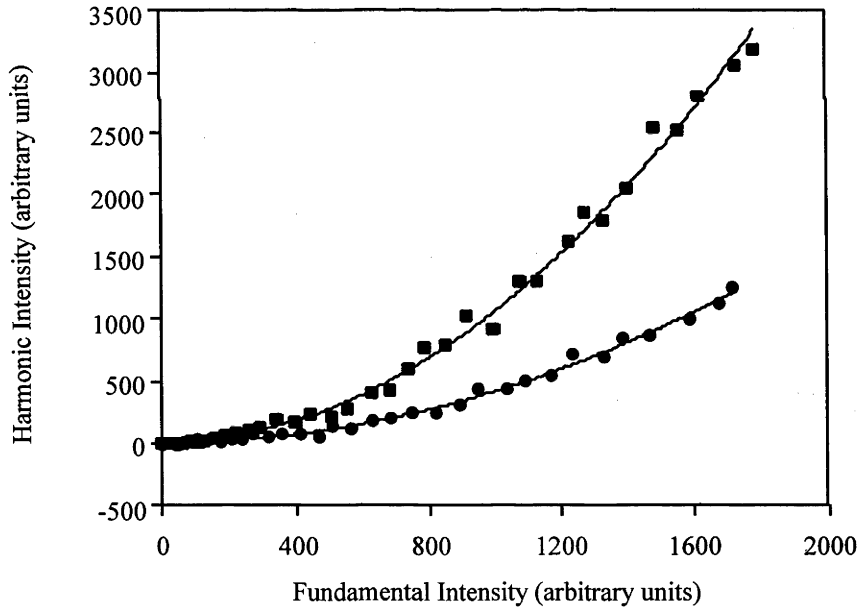

Figure 1.1. Quadratic dependence of $I_{2\omega}$ vs I_{ω} for $[Ru(4,4'\text{-}C{\equiv}CC_6H_4C{\equiv}CC_6H_4NO_2)(PPh_3)_2(\eta\text{-}C_5H_5)]$.[4]

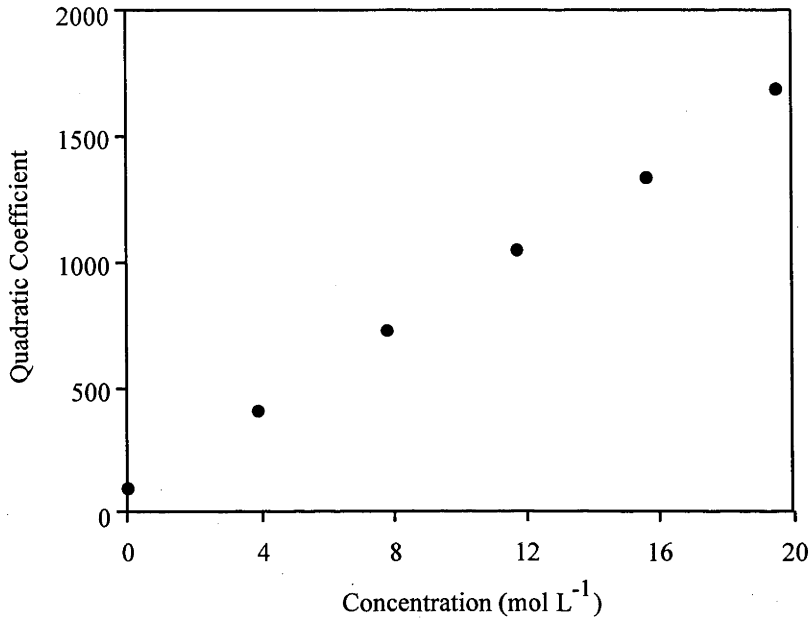

Figure 1.2. Quadratic coefficient $GB^2 = G[N_{solvent}\beta^2_{solvent} + N_{solute}\beta^2_{solute}]$, obtained from the curves in Fig. 1.1., vs N_{solute} for the complex $[Ru(4,4'\text{-}C{\equiv}CC_6H_4C{\equiv}CC_6H_4NO_2)(PPh_3)_2(\eta\text{-}C_5H_5)]$.[4]

The solute concentration has a linear relationship with the square of the nonlinearity of all of the molecules in the system (Figure 1.2.), so measurements of different concentrations of solute allow β^2 to be extracted.

The experimental setup for HRS is shown in Figure 1.3. A seed injected, Q-switched laser is used to pump the HRS cell. The incident intensity and polarization are controlled by a half-wave plate polarizer combination and monitored by a photodiode or energy meter. The incident beam is focussed into the sample solution. A concave mirror, with its focus at the interaction focal volume, and a lens are used to collect the scattered light which is filtered

to isolate the second-harmonic light, detected by a photomultiplier tube and averaged by a gated integrator.

Advantages of HRS are: (i) its simplicity when compared to EFISH (there is no need for a d.c. field to be applied, and it does not need complementary measurements of μ or γ), (ii) its sensitivity to non-vector components of the β tensor and (iii) unlike EFISH, it can be used to measure octopolar molecules and ionic molecules, the latter having important implications for organometallics where a particular system may have a range of accessible oxidation states. Disadvantages of HRS include: (i) the need for sensitive detection and high intensity of the fundamental, due to the low intensity of the second-harmonic light (high intensity of the fundamental may be detrimental to the experiment due to stimulated Raman or Brillouin scattering, self-focussing, or dielectric breakdown),[8] (ii) it is only possible to find the magnitude of β, due to the quadratic dependence on the HRS signal, and (iii) HRS can give unreliable results when the complex fluoresces at the frequency-doubled wavelength.[17]

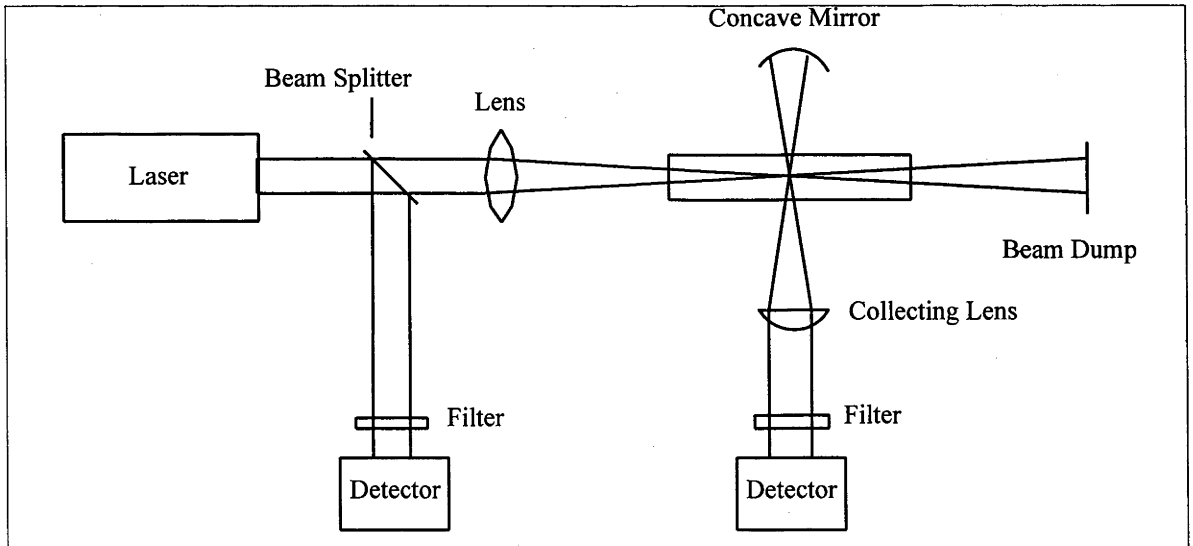

Figure 1.3. Schematic diagram of the HRS experiment.

1.3.4. Third-harmonic generation (THG)

Third-harmonic generation is used to study the purely electronic molecular second hyperpolarizability of centrosymmetric materials; no other mechanism but the nonresonant electron cloud distortion can respond rapidly enough to produce a nonlinear polarization oscillating at the third-harmonic.[8] It is technically difficult because all materials exhibit THG, including any glass used for a sample cell and even air. One technique that avoids some of these problems involves placing the sample in a vacuum sealed cell inside a vacuum chamber. A simpler method involves using thick glass windows which allow the contribution from air to be ignored; the third-order susceptibility of the glass and solvent must be known. THG has been used to study $\chi^{(3)}$ in many organic and organometallic molecules, particularly those measured by EFISH for which an estimation of γ is required to extract an accurate value of β.

1.3.5. Z-scan[18]

Z-scan is a technique used to derive the nonlinear refractive index intensity coefficient n_2 (from which $\chi^{(3)}$ and γ can be determined) by examining self-focussing or self-defocussing phenomena in a nonlinear material. Using a single Gaussian laser beam in a tight focus geometry (Figure 1.4.), the transmittance of a nonlinear medium through a fixed aperture in the far field is measured as the position of the material is varied through the z direction. An example of a Z-scan trace is shown in Figure 1.5. for a nonlinear material with a positive nonlinear refractive index. At the start (A) (and end (E)) of the scan the sample is far from the focal plane, the intensity of the beam is low and so lensing is not observed. As the material approaches the focal-plane (B), lensing causes the beam to focus earlier and hence reduces the measured transmittance. At the focal plane, z = 0 (C), there will be no change in transmittance as a thin lens at the focus will cause no change in the far-field. After the

focal plane (D), slight focussing of the beam by the lensing of the material causes an increase in the measured transmittance. The measured, normalized energy transmittance from a Z-scan experiment is numerically fitted to equations derived from theory and allows the determination of n_2, $\chi^{(3)}$ and γ.

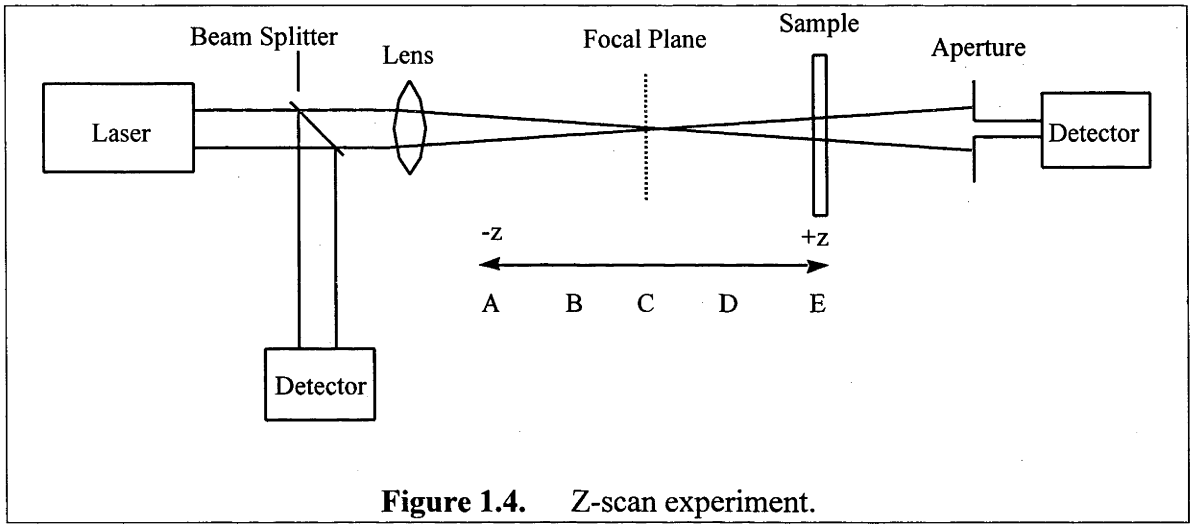

Figure 1.4. Z-scan experiment.

The shape of the Z-scan curve can be modified if a nonlinear absorption or nonlinear transmission (absorption bleaching) takes place in the sample, e.g. due to the presence of an imaginary part of $\chi^{(3)}$ of the material. The curves then become asymmetrical due to increased absorption or transmission when the sample is close to the focal plane. By analyzing the shape of such a modified Z-scan curve one can determine the nonlinear absorption coefficient β_2 or the related imaginary part of $\chi^{(3)}$. Alternatively, to determine the nonlinear absorption properties of a sample, the total transmission through the sample can be monitored, i.e. the total intensity of the transmitted beam can be measured without an aperture, as a function of the sample position with respect to the focal plane. Such an experiment is usually referred to as an "open aperture Z-scan". It is often used for the investigations of materials with potential optical limiting properties. For solutions, the

changes of the nonlinearity with concentration of the solution can be determined and measurements performed in an absolute manner, or results can be referenced to a known standard (e.g. the nonlinear refractive index of silica equal to $n_2 = 3 \times 10^{-16}$ cm^2 W^{-1} can be used).

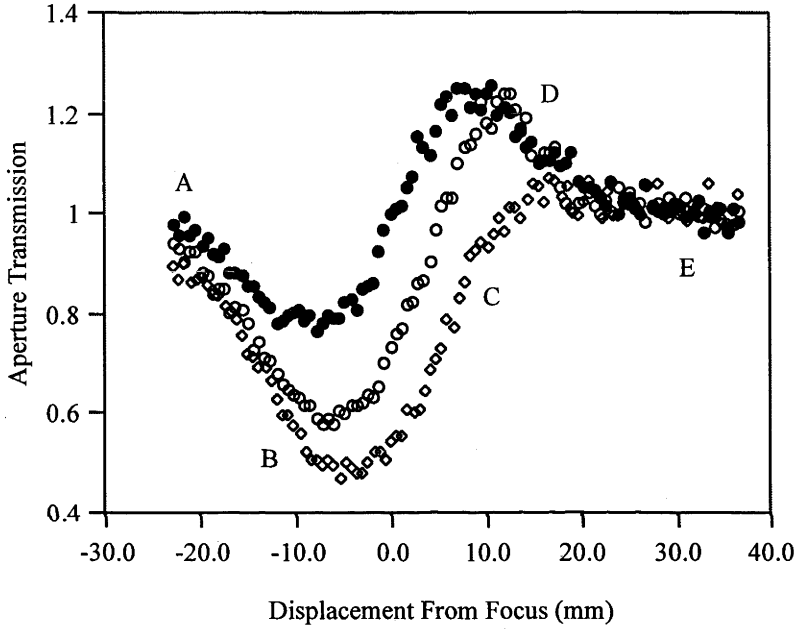

Figure 1.5. Comparison of closed aperture Z-scans for pure thf and solutions of [Au(4,4'-C≡CC$_6$H$_4$C≡CC$_6$H$_4$NO$_2$)(PPh$_3$)]; • thf, o 1.56 weight %, ◊ 3.08 weight %.[5]

Advantages of the Z-scan technique include: (i) the ability to determine the sign and magnitude of the nonlinear refractive index, (ii) the ability to determine both the real and imaginary parts of $\chi^{(3)}$, and (iii) simplicity (compared to DFWM) due to the single beam configuration. Disadvantages of Z-scan include: (i) the necessity for a high quality Gaussian beam and good optical quality of samples, and (ii) the absence of information on the temporal behaviour of the nonlinear response. The Z-scan technique has been used to

determine the third-order nonlinear optical properties of organometallics as solutions and as thin films.

1.3.6. Power dependent transmission

Information about nonlinear absorptive properties of a sample can be derived simply by measuring the sample transmission as a function of the incident light intensity. A linear dependence of the inverse transmission on the incident intensity can be used to determine the value of the nonlinear absorption coefficient (β_2). Because of the ease of determining the value of β_2 with open-aperture Z-scan, Z-scan is often the preferred method for quickly determining the nonlinear absorption coefficient.

1.3.7. Comparisons between experimental results

There are several problems in comparing results obtained by different groups using the many experimental techniques which are available to investigate the NLO properties of molecules; the most important of these include dispersion effects, the measurement of different tensorial components, different physical processes contributing to nonlinearity, and solubility problems.

The dispersion of NLO properties is a major source of problems. Measurements are frequently available at one wavelength only and the degree to which the results are influenced by material resonances close to the measurement wavelength is often difficult to quantify. It is possible to compensate for some of the dispersion effects in certain cases. For example, off-resonant dispersion of the second-order hyperpolarizability for linear intramolecular charge-transfer type molecules is reasonably well described by a two-state model in which parameters of the dominant excited state are assumed. A two-state model is probably not sufficient for more complicated second-order molecules, e.g. those with

significant contribution to the nonlinearity from octopolar origins. Also, the simple two-state model is generally considered insufficient for describing the dispersion of the third-order nonlinearity; at least two excited states have to be considered.

The tensorial character of the nonlinear polarizabilities is another experimental complication. Experimental techniques only provide access to specific tensorial components or combinations thereof, e.g. the vector part of β or orientationally averaged γ. An especially challenging issue is the correct measurement and interpretation of the third-order nonlinear effects when the degenerate susceptibility $\chi^{(3)}(-\omega;\omega,-\omega,\omega)$ or the nonlinear refractive index n_2 is being investigated. Variations of the refractive index may be due to a plethora of physical processes, not just changes in the charge density distributions in molecules; the measured NLO response may therefore contain many contributions which need to be identified and properly separated. The use of very short laser pulses (usually in the sub-picosecond range) and time-resolved techniques is helpful in resolving unclear cases.

An issue with NLO measurements on many organometallics is that the most convenient technique for investigating the nonlinearity (as solutions in common solvents) is of little value if the solubility of the compounds is not sufficiently high. For example, if the nonlinearity of a solution can be measured with a 10% accuracy and the compound being investigated can only be dissolved at 1% concentration, the practical limit of detection is that the nonlinearity of the organometallic has to be at least 10 times higher than that of the solvent.

Finally, a source of major frustration for anybody trying to compare NLO results obtained by different techniques and from different research groups is the use of varying definitions of the measured quantities and of varying measurement standards. This problem has been

discussed in several monographs.[8-10] Several different definitions of $\chi^{(3)}$ are possible depending, for example, on the use or absence of the factor of 1/2 before the Fourier components of the a.c. electric field, and on the inclusion or exclusion in $\chi^{(3)}$ of so-called degeneracy factors which are dependent on the type of nonlinear process considered [as seen, for example, in Equation (1.2), different multipliers are present in front of the nonlinear terms responsible for different processes]. Thus, it is very helpful if the optical nonlinearities of well-known standards used or determined in a given series of experiments are provided by the authors of original papers in which data on new compounds are published. In many cases, because of the factors mentioned above, direct comparison of numbers quoted in different papers is unfortunately not possible: trends observed for a series of compounds in a single set of experimental results are relatively reliable, though.

1.4. Organo-transition metal complexes for second-order nonlinear optics

Determination of second-order molecular hyperpolarizabilities (β) for organometallics have generally been carried out using either the EFISH or HRS techniques. This area has attracted substantial interest since the first report of NLO properties for a ferrocenyl derivative in 1987.[19] Whittall *et al.*[4] noted the preponderance of ferrocenyl- and ruthenocenyl-based complexes for which β had been measured. This can be attributed to several factors including large observed nonlinearities, well known synthetic methodologies and high thermal and oxidative stabilities. Some metallocene complexes and their measured β values illustrated in Figure 1.6.

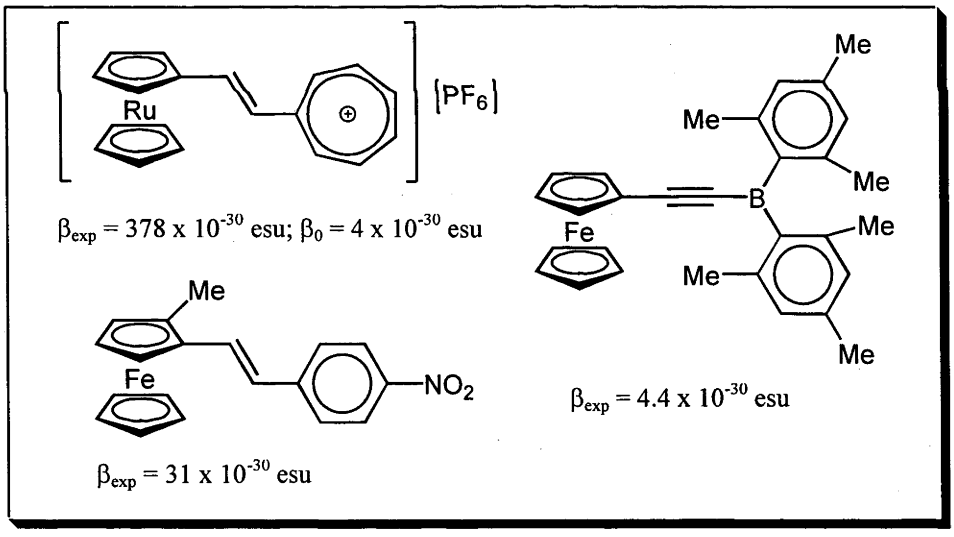

Figure 1.6. Metallocene complexes and their measured β values.

Table 1.2. contains second-order molecular NLO data for ferrocenyl and ruthenocenyl complexes reported since the last major review.[4] Some of these complexes have quite large

Table 1.2. Molecular second-order NLO results for ferrocenyl and ruthenocenyl complexes

Complex	Solvent	λ_{max} (nm)	β_{exp} (10^{-30} esu)	β_0 (10^{-30} esu)	Technique	Fund. (μm)	Ref.
$[Ru(\eta\text{-}C_5H_5)(\eta\text{-}C_5H_4\text{-}C_7H_6)][PF_6]$	$MeNO_2$	536	378	4	HRS	1.06	20
$[Ru(\eta\text{-}C_5H_5)(\eta\text{-}C_5H_4\text{-}(E)\text{-}CH{=}CH\text{-}C_7H_6)][PF_6]$	$MeNO_2$	600	649	120	HRS	1.06	20
$[FcC(=CH_2)Si(OCH_2CH_2)_3N]$	CH_2Cl_2	446	13	--	HRS	1.3	21
$[FcCH{=}CHSi(OCH_2CH_2)_3N]$	CH_2Cl_2	446	23	--	HRS	1.3	21
$[Fe(\eta\text{-}C_5H_5)(\eta\text{-}C_5H_3\text{-}1\text{-}CH_2NMe_2\text{-}2\text{-}Si(OCH_2CH_2)_3N]$	$CHCl_3$	400	23	--	HRS	1.3	21
$[FcCH{=}CHCO_2Me]$	MeCN	295	35	--	HRS	--	22
$[Fc(CH{=}CH)_2CO_2Me]$	MeCN	320	39	--	HRS	--	22
$[Fc(CH{=}CH)_3CO_2Me]$	MeCN	346	42	--	HRS	--	22
$[FcCH{=}NC_6H_4\text{-}4\text{-}OCH_3]$	MeCN	457	11.9	2.5	HRS	1.06	23
[FcCH=NPh]	MeCN	448	13.8	3.3	HRS	1.06	23
$[FcCH{=}NC_6H_4\text{-}4\text{-}Cl]$	MeCN	463	20.9	4.1	HRS	1.06	23
$[FcCH{=}NC_6H_4\text{-}4\text{-}NO_2]$	MeCN	490	51.2	6.1	HRS	1.06	23

Table 1.2. Molecular second-order NLO results for ferrocenyl and ruthenocenyl complexes (continued)

Complex	Solvent	λ_{max} (nm)	β_{exp} (10^{-30} esu)	β_0 (10^{-30} esu)	Technique	Fund. (μm)	Ref.
[$FcSiMe_2Ph$]	Acetone	456	--	0.5	EFISH	--	24
[$FcSiMe_2SiMe_2Ph$]	Acetone	455	--	-0.6	EFISH	--	24
[$FcSiMe_2SiMe_2SiMe_2Ph$]	Acetone	457	--	0.4	EFISH	--	24
[$Fc(SiMe_2)_3SiMe_2Ph$]	Acetone	456	--	6.4	EFISH	--	24
[$Fc(SiMe_2)_4SiMe_2Ph$]	Acetone	456	--	1.8	EFISH	--	24
[$Fc(SiMe_2)_5SiMe_2Ph$]	Acetone	456	--	1.0	EFISH	--	24
[$FcSiMe_2SiMe_2C_6H_4$-4-Cl]	Acetone	456	--	1.6	EFISH	--	24
[$FcSiMe_2SiMe_2C_6H_4$-4-OMe]	Acetone	456	--	-0.26	EFISH	--	24
[$FcSiMe_2SiMe_2C_6H_4$-4-NMe_2]	Acetone	455	--	3.5	EFISH	--	24
[$FcSiMe_2SiMe_2C_6H_4$-3-CF_3]	Acetone	457	--	2.2	EFISH	--	24
[$FcSiMe_2SiMe_2C_6H_4$-4-CH=$C(CN)_2$]	Acetone	342	--	7	EFISH	--	24
[Fc(*E*)-CH=CHC_6H_4-4-NO_2]	Dioxane	356	31	--	EFISH	1.9	25
[Fe(η-C_5H_5)(η-C_5H_3-1-Me-2-{(*E*)-CH=CHC_6H_4-4-NO_2}]	Dioxane	359	24	--	EFISH	1.9	25
[Fe(η-C_5H_5)(η-C_5H_3-1-CH_2OH-2-{(*E*)-CH=CHC_6H_4-4-NO_2}]	Dioxane	362	43	--	EFISH	1.9	25
[Fe(η-C_5H_5)(η-C_5H_3-1-$SiMe_3$-2-{(*E*)-CH=CHC_6H_4-4-NO_2}]	Dioxane	357	36	--	EFISH	1.9	25

Table 1.2. Molecular second-order NLO results for ferrocenyl and ruthenocenyl complexes (continued)

Complex	Solvent	λ_{max} (nm)	β_{exp} (10^{-30} esu)	β_0 (10^{-30} esu)	Technique	Fund. (μm)	Ref.
[Fc-(*E*)-CH=CH-2-C_4H_2S-5-NO_2]	CH_2Cl_2	644	316	95	HRS	1.06	26
[Fc-(*E*)-CH=CH-2-C_4H_2S-5-NO_2][PF_6]	CH_2Cl_2	851	25	10	HRS	1.06	26
[Fc-(*E*)-CH=CHC_6H_4-4-(*Z*)-CH=CHC_6H_4-4-NO_2]	CH_2Cl_2	315	122	--	HRS	1.06	27
[Fc-(*E,E*)-$(CH=CH)_2C_6H_4$-4-NO_2]	CH_2Cl_2	387	103	--	HRS	1.06	27
[Fc-(*E,E,Z*)-$(CH=CH)_3C_6H_4$-4-NO_2]	CH_2Cl_2	364	209	--	HRS	1.06	27
[Fc-(azulene)][BF_4]	CH_2Cl_2	716	326	145	HRS	1.06	28
[Fc-(*E,E*)-CH=CHCH=CH(azulene)][BF_4]	CH_2Cl_2	866	810	451	HRS	1.06	28
[Fc-(1,4-dimethyl-7-isopropylazulene)][PF_6]	CH_2Cl_2	724	220	101	HRS	1.06	28
[Fc-(*E*)-CH=CH(1,4-dimethyl-7-isopropylazulene)][BF_4]	CH_2Cl_2	782	1539	821	HRS	1.06	28
[Fc-(*E,E*)-CH=CHCH=CH-(1,4-dimethyl-7-isopropylazulene)][BF_4]	CH_2Cl_2	827	1373	770	HRS	1.06	28
[Fc-(*E,E*)-CH=CHCH=CH-(1,4-dimethyl-7-isopropylazulene)][BF_4]	CH_2Cl_2	827	360	132	HRS	1.3	28
[Fc{(*E*)-CH=CH-4-C_5H_4N}]	$CHCl_3$	468	21	--	HRS	1.06	29
[Fc{(*E*)-CH=CH-4-C_6H_4-(*E*)-CH=CH-4-C_5H_4N}]	$CHCl_3$	459	146	--	HRS	1.06	29
[Fc{(*E*)-CH=CH-4-C_5H_4NMe}][PF_6]	Acetone	553	40	--	HRS	1.06	29

Table 1.2. Molecular second-order NLO results for ferrocenyl and ruthenocenyl complexes (continued)

Complex	Solvent	λ_{max} (nm)	β_{exp} (10^{-30} esu)	β_0 (10^{-30} esu)	Technique	Fund. (μm)	Ref.
[Fc{(*E*)-CH=CH-4-C_6H_4-(*E*)-CH=CH-4-C_5H_4NMe}][PF_6]	Acetone	503	197	--	HRS	1.06	29
[Fc{(*E*)-(CH=CH-4-C_6H_4)}$_2$-(*E*)-CH=CH-4-C_5H_4NMe][PF_6]	Acetone	462	458	--	HRS	1.06	29

Table 1.2. Molecular second-order NLO results for ferrocenyl and ruthenocenyl complexes (continued)

Complex	Solvent	λ_{max} (nm)	$\mu\beta_{exp}$ (10^{-48} esu)	$\mu\beta_0$ (10^{-48} esu)	Technique	Fund. (μm)	Ref.
[Fc{(*E*)-CH=CH-4-C_6H_4CH=C$(CN)_2$}]	CH_2Cl_2	543	450 ± 50	200 ± 20	EFISH	1.54	30
[Fc{(*Z*)-CH=CH-4-C_6H_4CH(2,5,7-trinitrofluorene-4-carboxylic acid(triethyleneglycol monomethylether)ester)}]	CH_2Cl_2	570	1300 ± 130	830 ± 80	EFISH	1.54	30
[Fc{(*E,E*)-CH=CH-4-C_6H_4CH=CH-4-C_6H_4CH=C$(CN)_2$}]	CH_2Cl_2	500	570 ± 30	370 ± 20	EFISH	1.54	30
[Fc{(*E,E*)-CH=CH-4-C_6H_4CH=CH-4-C_6H_4CH(2,5,7-trinitrofluorene-4-carboxylic acid(triethyleneglycol monomethylether)ester)}]	CH_2Cl_2	570	410 ± 35	240 ± 20	EFISH	1.54	30
[Fc{(*E,E*)-$(CH=CH)_2$CH(2,5,7-trinitrofluorene-4-carboxylic acid(methylether)ester)}]	CH_2Cl_2	663	5000 ± 1500	900 ± 300	EFISH	1.54	30
[Fc{(*E,E*)-$(CH=CH)_2$CH(2,5,7-trinitrofluorene-4-carboxylic acid(triethyleneglycol monomethylether)ester)}]	CH_2Cl_2	660	2700 ± 200	470 ± 50	EFISH	1.54	30
[Fc{C≡CCH(2,5,7-trinitrofluorene-4-carboxylic acid(triethyleneglycol monomethylether)ester}]	CH_2Cl_2	616	700 ± 100	170 ± 30	EFISH	1.54	30

nonlinearities, which is consistent with the ferrocene acting as an efficient electron donor similar in strength to an anisyl group; metallocene complexes have therefore attracted continued interest.[25,31-33] Complexes with strong acceptor groups are able to make use of this electron reservoir and generally have large nonlinearities. Metallocene complexes such as the sesquifulvalene, azulene and guaiazulene-containing compounds synthesized by Heck and co-workers often possess absorption bands close to the second-harmonic wavelength.[34] Calculation of the frequency-independent hyperpolarizability using the two-level model indicates that these complexes are significantly resonance-enhanced. The applicability of the two-level model to these complexes is questionable because of the presence of contributions to the NLO response from a donor-acceptor charge-transfer band and an intraligand $\pi \rightarrow \pi^*$ transition.[35] Analysis of the fluorescence properties of these complexes indicates that two-photon absorption fluorescence (TPAF) can significantly contribute to an overestimation of β.[36] Several techniques have been applied to avoid or determine the TPAF contribution to the quadratic hyperpolarizability in metallocenes, including measurement at longer wavelengths,[28] high frequency demodulation,[37] time resolved HRS ,[38] and application of a damping parameter after measurement of the TPAF contribution.[39]

Chain lengthening of the π-conjugated backbone to increase the quadratic hyperpolarizability has been investigated for several metallocene systems. Insertion of an (*E*)-ene linkage between the five and seven membered rings of a monometallic sesquifulvalene leads to a dramatic enhancement of both the experimental and frequency-independent second-order results and is in accordance with well-established NLO structure-property trends.[20] The synthesis of a series of ferrocenyl complexes with 1 to 3 (*E*)-ene units in the bridging group resulted in a gradual increase in the second-order molecular

NLO response.[22] Optimization of linker components has been investigated to a lesser extent, replacement of the (*E*)-ene linkage with an imine bond to afford the complex [FcCH=NC$_6$H$_4$-4-NO$_2$] leading to an increase in the experimentally-derived β response. Unfortunately, not only have the two complexes been measured using different techniques (EFISH and HRS) and solvents (dioxane and acetonitrile), but the NLO response of the imine complex is strongly-resonance enhanced, and therefore any proper assessment of variation in the bridging unit in this case is impossible to make. Use of a polysilane chain can give good optical transparency,[24] but previous work[4] has established that these complexes have low nonlinearities even when the chain length is relatively long, due to the non-planar silicon-arene geometry. Attachment of a strong acceptor group such as 4-C$_6$H$_4$-CH=C(CN)$_2$ results in a minor increase in the experimental second-order nonlinearity. Replacement of a π-bridging phenyl ring with a thiophene ring should lead to enhanced β response due to the lower delocalization energy of the thiophene, but no systematic studies utilizing identical measurement conditions have been undertaken to examine the effect of ring substitution upon quadratic nonlinearity. Modification of the cyclopentadienyl ring has also been undertaken with the introduction of a chiral center into a material with known NLO response [Fc-(*E*)-CH=CHC$_6$H$_4$-4-NO$_2$] which crystallizes in the centrosymmetric space group $P2_1/c$.[27] Substitution at the 2 position with Me, SiMe$_3$ and CH$_2$OH lead to only small increases in the molecular second-order response, but the effect of the substituents on the crystal packing lead to large increases in the bulk response through prevention of centrosymmetric crystal packing. Previous work[40] has already determined that increases in the second-order nonlinearities may also be obtained by methylation of the cyclopentadienyl rings. Malaun *et al.*[26] synthesized [Fe(η-C$_5$Me$_5$){η-C$_5$Me$_4$-(*E*)-CH=CH-2,5-C$_4$H$_2$S-NO$_2$}], which was subsequently chemically oxidized with either ferrocenium hexafluorophosphate or (NBu$_4$)Br$_3$. Upon oxidation of the metal centre there was a

significant decrease in both β_{exp} and β_0. In the neutral complex there is a significant absorption band near to the second-harmonic wavelength which disappears upon oxidation; it is therefore possible that the significant change in β may be due to loss of resonance enhancement in proceeding from the neutral to the charged complex. The cationic complex could be reduced to the neutral form through addition of hydrazine.

Although metallocene complexes have been widely investigated for their molecular second-order response, they possess numerous drawbacks including strong resonance enhancement, tendency to pack in centrosymmetric space-groups in the bulk phase and poor optical transparency / NLO trade-off. Consequently, research has branched into other organometallics of potential NLO interest.

Table 1.3. contains data from metal carbonyl complexes, the nonlinear response being presumed to arise from ligands other than the carbonyls. Most of the complexes listed are based upon the dipolar donor-π-conjugated linker-acceptor pattern. Previous work[4] has shown that the effect of metal substitution may vary greatly depending upon the type of ligands present and that suggested design strategies (positioning the metal in the plane of the charge-transfer excitation or lengthening the π-conjugated backbone) are justified. The chromium tricarbonyl fragment in (arene)$Cr(CO)_3$ acts as a ground-state acceptor but an excited state donor.[41] Previous work[42] has shown that the charge-transfer electron density is nearly equally divided between the carbonyl and arene ligands, and, as such, the size of $\Delta\mu$ is modest and limits the magnitude of the second-order nonlinearity. By introducing electron donating ligands around the metal centre, greater asymmetry can be produced and this in turn should lead to a greater value for β. This is supported by experimental results, [43] where substitution of a CO ligand for a PPh_3 unit leads to drastically enhanced quadratic

Table 1.3. Molecular second-order NLO results for metal carbonyl complexes

Complex	Solvent	λ_{max} (nm)	β (10^{-30} esu)	β_o (10^{-30} esu)	Technique	Fund. μm	Ref.
$[Mn(CO)_3(\eta^5\text{-}C_5H_4C_7H_6)][BF_4]$	$MeNO_2$	510	240	15	HRS	1.06	44
$[Mn(CO)_2(PPh_3)(\eta^5\text{-}C_5H_4C{\equiv}CC_7H_6)][BF_4]$	CH_2Cl_2	751	226	113	HRS	1.06	44
$[Mn(CO)_3(\eta^5\text{-}C_4H_3SCH{=}CHC_6H_4\text{-}4\text{-}OMe][BF_4]$	$MeNO_2$	415	42	14	HRS	1.06	45
$[Mn(CO)_3(\eta^5\text{-}C_4H_3SCH{=}CHC_6H_4\text{-}4\text{-}CH_3][BF_4]$	$MeNO_2$	405	59	21	HRS	1.06	45
$[Mn(CO)_3(\eta^5\text{-}C_4H_3SCH{=}CHPh][BF_4]$	$MeNO_2$	390	68	27	HRS	1.06	45
$[Mn(CO)_3(\eta^5\text{-}C_4H_3SCH{=}CHC_6H_4\text{-}4\text{-}Br][BF_4]$	$MeNO_2$	393	88	35	HRS	1.06	45
$[Mn(CO)_3(\eta^5\text{-}C_4H_3SCH{=}CHC_6H_4\text{-}4\text{-}NO_2][BF_4]$	$MeNO_2$	400	101	38	HRS	1.06	45
$[Mn(CO)_2(PPh_3)(\eta^5\text{-}C_4H_3S\text{-}CH{=}CHC_6H_4\text{-}4\text{-}NO_2][BF_4]$	$MeNO_2$	384	115	48	HRS	1.06	45
$[Mn(CO)_3(\eta^6\text{-}C_6H_4\text{-}4\text{-}NMe_2\text{-}1\text{-}CH{=}CH\text{-}2\text{-}C_4H_3S)][BF_4]$	$MeNO_2$	470	62	11	HRS	1.06	45
$[Cr(CO)_3(\eta^6\text{-}C_6H_5\text{-}(E)\text{-}CH{=}CH\text{-}4\text{-}C_6H_4NO_2)]$	$CHCl_3$	455	15	12	HRS	1.5	46
$[Cr(CO)_3(\eta^6\text{-}C_6H_5\text{-}(E,E)\text{-}(CH{=}CH)_2\text{-}4\text{-}C_6H_4NO_2)]$	$CHCl_3$	457	33	25	HRS	1.5	46
$[Cr(CO)_3(\eta^6\text{-}C_6H_5\text{-}(E,E,E)\text{-}(CH{=}CH)_3\text{-}4\text{-}C_6H_4NO_2)]$	$CHCl_3$	453	44	31	HRS	1.5	46
$[Cr(CO)_3(\eta^6\text{-}C_6H_5\text{-}(E)\text{-}CH{=}CH\text{-}4\text{-}C_6H_4NMe_2)]$	$CHCl_3$	418	20	14	HRS	1.5	46
$[Cr(CO)_3(\eta^6\text{-}C_6H_5\text{-}(E,E)\text{-}(CH{=}CH)_2\text{-}4\text{-}C_6H_4NMe_2)]$	$CHCl_3$	438	38	27	HRS	1.5	46
$[Cr(CO)_3(\eta^6\text{-}C_6H_5\text{-}(E)\text{-}CH{=}CH\text{-}2\text{-}C_4H_2S\text{-}5\text{-}NO_2)]$	$CHCl_3$	488	30	22	HRS	1.5	46

Table 1.3. Molecular second-order NLO results for metal carbonyl complexes (continued)

Complex	Solvent	λ_{max} (nm)	β (10^{-30} esu)	β_o (10^{-30} esu)	Technique	Fund. μm	Ref.
$[Cr(CO)_2(PPh_3)(\eta^6\text{-}C_6H_5C{\equiv}C\text{-}4\text{-}C_6H_4NO_2)]$	$CHCl_3$	481	52	41	HRS	1.5	46
$[Cr(CO)_3(\eta^6\text{-}C_6H_4\text{-}2\text{-}CHO\text{-}1\text{-}C{\equiv}CC_6H_4\text{-}4\text{-}NMe_2)]$	$CHCl_3$	378	52	39	HRS	1.5	46
$[Cr(CO)_3(\eta^6\text{-}C_6H_5C{\equiv}CC{\equiv}C\text{-}4\text{-}C_6H_4NO_2)]$	$CHCl_3$	437	18	14	HRS	1.5	46
$[Cr(CO)_3(\eta^6\text{-}C_6H_5C{\equiv}CC{\equiv}C\text{-}4\text{-}C_6H_4NMe_2)]$	$CHCl_3$	414	34	26	HRS	1.5	46
$[Cr(CO)_3(\eta^6\text{-}C_6H_5C{\equiv}C\text{-}4\text{-}C_6H_4NO_2)]$	$CHCl_3$	435	10	8	HRS	1.5	46
$[Cr(CO)_3(\eta^6\text{-}C_6H_5C{\equiv}C\text{-}4\text{-}C_6H_4NMe_2)]$	$CHCl_3$	405	11	9	HRS	1.5	46
$[(CpFeCO)_2(\mu\text{-}CO)(\mu\text{-}CCH{=}CH\text{-}4\text{-}C_6H_4\text{-}(E)\text{-}CH{=}CH\text{-}4\text{-}C_6H_4\text{-}NO_2][BF_4]$	CH_2Cl_2	463	346	68	HRS	1.06	47
$[(CpFeCO)_2(\mu\text{-}CO)(\mu\text{-}CCH{=}CH\text{-}4\text{-}C_6H_4\text{-}(E)\text{-}CH{=}CHPh][BF_4]$	CH_2Cl_2	513	792	43	HRS	1.06	47
$[(CpFeCO)_2(\mu\text{-}CO)(\mu\text{-}CCH{=}CH\text{-}2,5\text{-}C_4H_2S\text{-}(E)\text{-}CH{=}CH\text{-}4\text{-}C_6H_4\text{-}NMe_2][BF_4]$	CH_2Cl_2	765	2443	1260	HRS	1.06	47
	MeCN	696	1623	661	HRS	1.06	
$[(CpFeCO)_2(\mu\text{-}CO)(\mu\text{-}C{=}CHCH{=}CH\text{-}4\text{-}C_6H_4CH{=}C(CN)_2]$	CH_2Cl_2	523	456	--	HRS	1.5	48
$[(CpFeCO)_2(\mu\text{-}CO)(\mu\text{-}C{=}CHCH{=}CH\text{-}2,5\text{-}C_4H_2SCH{=}C(CN)_2]$	CH_2Cl_2	565	227	--	HRS	1.5	48

Table 1.3. Molecular second-order NLO results for metal carbonyl complexes (continued)

Complex	Solvent	λ_{max} (nm)	$\beta_{1.06}$ (10^{-30} esu)	$\beta_{1.34}$ (10^{-30} esu)	$\beta_{1.91}$ (10^{-30} esu)	Technique	Ref.
$[Ir(CO)_2Cl(4\text{-}NMe_2C_5H_4N)]$	$CHCl_3$	291	9	8	6.5	EFISH	49
$[Rh(CO)_2Cl(4\text{-}NMe_2C_5H_4N)]$	$CHCl_3$	289	8.7	12	6.4	EFISH	49
$[Os(CO)_3Cl_2(4\text{-}NMe_2C_5H_4N)]$	$CHCl_3$	290	6	5	4.4	EFISH	49
$[Ir(CO)_2Cl(4\text{-}Bu^tC_5H_4N)]$	$CHCl_3$	--	0.1	--	--	EFISH	49
$[Rh(CO)_2Cl(4\text{-}Bu^tC_5H_4N)]$	$CHCl_3$	--	~0	--	--	EFISH	49
$[W(CO)_5(4\text{-}Bu^nC_5H_4N)]$	Dioxane	--	--	--	-3.4	EFISH	49
$[Rh(CO)_2Cl(C_5H_5N)]$	$CHCl_3$	--	2.6	--	--	EFISH	49
$[Os(CO)_3Cl_2(C_5H_5N)]$	$CHCl_3$	--	~0	--	--	EFISH	49
$[W(CO)_5(C_5H_5N)]$	Toluene	--	--	--	-4.4	EFISH	49
$[Os(CO)_2Cl_2(4\text{-}MeCOC_5H_4N)]$	$CHCl_3$	--	~2	--	--	EFISH	49
$[W(CO)_5(4\text{-}MeCOC_5H_4N)]$	$CHCl_3$	--	--	--	-9.3	EFISH	49
$[Ir(CO)_2Cl(4\text{-}NCC_5H_4N)]$	$CHCl_3$	--	-9	--	--	EFISH	49
$[Rh(CO)_2Cl(4\text{-}NCC_5H_4N)]$	$CHCl_3$	--	-4.3	--	--	EFISH	49
$[Os(CO)_3Cl_2(4\text{-}NCC_5H_4N)]$	$CHCl_3$	--	~2	--	--	EFISH	49
$[Ir(CO)_2Cl(4,4'\text{-}NC_5H_4CH{=}CHC_6H_4NMe_2)]$	$CHCl_3$	431	242	128	--	EFISH	49

Table 1.3. Molecular second-order NLO results for metal carbonyl complexes (continued)

Complex	Solvent	λ_{max} (nm)	$\beta_{1.06}$ (10^{-30} esu)	$\beta_{1.34}$ (10^{-30} esu)	Technique	Ref.
$[Ir(COT)_2Cl(4,4'\text{-}NC_5H_4CH{=}CHC_6H_4NMe_2)]$	$CHCl_3$	413	137	82	EFISH	49
$[Rh(CO)_2Cl(4,4'\text{-}NC_5H_4CH{=}CHC_6H_4NMe_2)]$	$CHCl_3$	421	177	111	EFISH	49
$[Rh(COD)_2Cl(4,4'\text{-}NC_5H_4CH{=}CHC_6H_4NMe_2)]$	$CHCl_3$	397	119	77	EFISH	49
$[Os(CO)_3Cl_2(4,4'\text{-}NC_5H_4CH{=}CHC_6H_4NMe_2)]$	$CHCl_3$	435	160	83	EFISH	49
$[Ir(CO)_2Cl(4,4'\text{-}NC_5H_4(CH{=}CH)_2C_6H_4NMe_2)]$	$CHCl_3$	449	285	135	EFISH	49
$[Ir(COT)_2Cl(4,4'\text{-}NC_5H_4(CH{=}CH)_2C_6H_4NMe_2)]$	$CHCl_3$	430	280	152	EFISH	49
$[Rh(CO)_2Cl(4,4'\text{-}NC_5H_4(CH{=}CH)_2C_6H_4NMe_2)]$	$CHCl_3$	442	262	131	EFISH	49
$[Os(CO)_3Cl_2(4,4'\text{-}NC_5H_4(CH{=}CH)_2C_6H_4NMe_2)]$	$CHCl_3$	456	260	116	EFISH	49

hyperpolarizability. Lengthening the π-conjugated backbone for the same $[Cr(CO)_3(\eta^6\text{-}C_6H_5\text{-}(E)\text{-}(CH{=}CH)_x\text{-}4\text{-}C_6H_4NO_2)]$ system (where x = 1 – 3) leads to only small incremental increases in β, but replacement of the phenyl linker with a thiophene ring leads to an approximate doubling of the NLO response, as expected for an arene ring with a lower resonance stabilization energy. Replacement of an (*E*)-ene linkage with an alkyne bridge leads to a drop in second-order NLO response, in accordance with well known NLO structure-property relationships. Chung and co-workers[50] have prepared a series of systematically-varied $[Mn(CO)_3(\eta\text{-}SC_4H_3X)]$ complexes. Variation of the terminal group (R) in the system $[Mn(CO)_3(\eta\text{-}SC_4H_3CH{=}CHC_6H_4\text{-}4\text{-}R]BF_4$ lead to the NLO response varying as $MeO < CH_3 < H < Br < NO_2$, which follows the electron accepting power of the substituent. Again, replacement of a carbonyl ligand with a PPh_3 group leads to an improvement in the second-order NLO response, presumably due to increased electron donation to the metal centre.

Roberto *et al.*[49] measured the EFISH responses of different metal carbonyl complexes coordinated to a systematically varied set of substituted pyridines. Coordination of substituted pyridines to metal carbonyl moieties produced an enhancement of up to 2 orders of magnitude of the quadratic hyperpolarizability of the free pyridine. In these complexes, the role of the metal centre as either an acceptor or donor is dependent on the nature of the pyridine substituent, with strong electron-withdrawing groups leading to negative values of β_{exp}. The quadratic hyperpolarizability of complexes of more π-delocalized *para*-substituted pyridine ligands was dependent upon the length of the π-delocalized bridge and upon the nature of the metal centre, with the oxidation state and nature of the ligated metal centre playing an important role.

Table 1.4. contains the second-order NLO data for acetylide, vinylidene and nitrile complexes. Theory suggests that metal-carbon multiple bonding should lead to enhanced values for the quadratic hyperpolarizability. Direct comparison between the acetylide [Ru(C≡C-4-$C_6H_4NO_2$)(PPh_3)$_2$(η^5-indenyl)] and its precursor vinylidene reveals that the vinylidene has a poorer second-order response, even after correction for resonance enhancement. This is attributed to the net positive charge on the ruthenium centre causing a decrease in electron donor ability as compared to the metal acetylide. The effect on second-order nonlinearities of systematic structural variation of aryldiazovinylidenes has also been assessed.[51] These results indicate that the size of β is consistent with the relative strength and position of electron-withdrawing substituents. Lengthening the π-conjugated backbone leads to the expected increase in nonlinearities, with insertion of an aryl imine bridge leading to a large measured nonlinearity. However, calculation of the frequency-independent hyperpolarizability using the two-level model suggests that a *para*-substituted arylalkyne is, overall, a more efficient linker group. The tendency for linear π systems to possess larger nonlinearities is apparent, since the complex possessing two *m*-NO_2 groups has a β value considerably lower than the identical ligated metal centre possessing a single *p*-NO_2 functionality. Weyland *et al.*[52] have synthesized a series of mono-, bis- and tris-Fe(dppe)(η-C_5Me_5) acetylide complexes and have measured the β response of these complexes and their chemically oxidized derivatives. In a simple donor-acceptor organometallic where the metal is acting as an electron donor, increasing the charge on the metal centre should lead to a drop in β as it becomes harder to remove electrons from the metal. The results for the Fe(dppe)(η-C_5Me_5) acetylides are not straightforward, with oxidation leading to increases and decreases in β depending upon the total charge of the complex and the substitution pattern. Oxidation of the acetylides leads to the appearance of ligand-metal charge-transfer transitions close to the second-harmonic which

Table 1.4. Molecular second-order NLO results for vinylidene, acetylide and nitrile complexes

Complex	Solvent	λ_{max} (nm)	β (10^{-30} esu)	β_o (10^{-30} esu)	Technique	Fund. μm	Ref.
$[Ru(C{=}CH\text{-}4\text{-}C_6H_4NO_2)(PPh_3)_2(\eta^5\text{-indenyl})][PF_6]$	CH_2Cl_2	379	116	50	HRS	1.06	53
$[Ru(C{\equiv}C\text{-}4\text{-}C_6H_4NO_2)(PPh_3)_2(\eta^5\text{-indenyl})]$	CH_2Cl_2	476	746	119	HRS	1.06	53
$[Ru(C{\equiv}C\text{-}4\text{-}C_6H_4NO_2)(dppe)(\eta^5\text{-indenyl})]$	CH_2Cl_2	459	516	107	HRS	1.06	53
$[Ru(C{\equiv}C\text{-}4\text{-}C_6H_4NO_2)(dppm)(\eta^5\text{-indenyl})]$	CH_2Cl_2	456	540	117	HRS	1.06	53
$[Ru(C{\equiv}C\text{-}4\text{-}C_6H_4C{\equiv}C\text{-}4\text{-}C_6H_4NO_2)(PPh_3)_2(\eta^5\text{-indenyl})]$	CH_2Cl_2	463	1027	202	HRS	1.06	53
$[Ru(C{\equiv}C\text{-}4\text{-}C_6H_4N{=}CH\text{-}4\text{-}C_6H_4NO_2)(PPh_3)_2(\eta^5\text{-indenyl})]$	CH_2Cl_2	509	1295	85	HRS	1.06	53
$[Ru(C{\equiv}CCH{=}CH\text{-}4\text{-}C_6H_4NO_2)(PPh_3)_2(\eta^5\text{-indenyl})]$	CH_2Cl_2	507	1257	89	HRS	1.06	53
$[Ru(C{\equiv}C(CH{=}CH)_2\text{-}4\text{-}C_6H_4NO_2)(PPh_3)_2(\eta^5\text{-indenyl})]$	CH_2Cl_2	523	1320	34	HRS	1.06	53
$[Ru(C{\equiv}CCH{=}CH\text{-}2\text{-}C_4H_2O\text{-}5\text{-}NO_2)(PPh_3)_2(\eta^5\text{-indenyl})]$	CH_2Cl_2	550	908	43	HRS	1.06	53
$[Ru(C{\equiv}C\text{-}(E)\text{-}CH{=}CH\text{-}2\text{-}C_4H_2S\text{-}5\text{-}NO_2)(PPh_3)_2(\eta^5\text{-indenyl})]$	CH_2Cl_2	598	487	88	HRS	1.06	53
$[Ru(C{\equiv}CCH{=}C\{3\text{-}C_6H_4NO_2\}_2)(PPh_3)_2(\eta^5\text{-indenyl})]$	CH_2Cl_2	345	48	25	HRS	1.06	53
$[Ru(C{\equiv}N)(PPh_3)_2(\eta^5\text{-indenyl})]$	CH_2Cl_2	396	13	5	HRS	1.06	53
$[Ru(C{\equiv}CCH{=}CH\text{-}4\text{-}C_6H_4C{\equiv}N)(PPh_3)_2(\eta^5\text{-indenyl})]$	CH_2Cl_2	427	238	71	HRS	1.06	53
$[Ru(C{\equiv}C\text{-}(E)\text{-}CH{=}CH\text{-}4\text{-}C_5H_4N)(PPh_3)_2(\eta^5\text{-indenyl})]$	CH_2Cl_2	399	100	37	HRS	1.06	53

Table 1.4. Molecular second-order NLO results for vinylidene, acetylide and nitrile complexes (continued)

Complex	Solvent	λ_{max} (nm)	β (10^{-30} esu)	β_o (10^{-30} esu)	Technique	Fund. μm	Ref.
[Ru(C=CPhN=NPh)(PPh_3)$_2$(η-C_5H_5)][BF_4]	Acetone	363	14	6.6	HRS	1.06	51
[Ru(C=CPhN=NC_6H_4OMe-2)(PPh_3)$_2$(η-C_5H_5)][Cl]	Acetone	373	22	10	HRS	1.06	51
[Ru(C=CPhN=NC_6H_4OMe-3)(PPh_3)$_2$(η-C_5H_5)][BF_4]	Acetone	382	23	10	HRS	1.06	51
[Ru(C=CPhN=NC_6H_4OMe-4)(PPh_3)$_2$(η-C_5H_5)][BF_4]	Acetone	370	26	12	HRS	1.06	51
[Ru(C=CPhN=$NC_6H_4NO_2$-4)(PPh_3)$_2$(η-C_5H_5)][BF_4]	CH_2Cl_2	413	184	62	HRS	1.06	51
[Ru(C=CPhN=$NC_6H_4NO_2$-4)(PPh_3)$_2$(η-C_5H_5)][Cl]	CH_2Cl_2	413	137	46	HRS	1.06	51
[Ru(C=CPhN=$NC_6H_4NO_2$-4)(PPh_3)$_2$(η-C_5H_5)][Br]	CH_2Cl_2	413	136	45	HRS	1.06	51
[Ru(C=CPhN=$NC_6H_4NO_2$-4)(PPh_3)$_2$(η-C_5H_5)][I]	CH_2Cl_2	413	134	45	HRS	1.06	51
	Acetone	417	150	48	HRS	1.06	51
[Ru(C=CPhN=$NC_6H_4NO_2$-4)(PPh_3)$_2$(η-C_5H_5)][4-$MeC_6H_4SO_3$]	CH_2Cl_2	413	164	55	HRS	1.06	51
[Ru(C=CPhN=$NC_6H_4NO_2$-4)(PPh_3)$_2$(η-C_5H_5)][NO_3]	CH_2Cl_2	413	181	61	HRS	1.06	51
[Ru{C=CPhN=N-3,5-$C_6H_3(NO_2)_2$}(PPh_3)$_2$(η-C_5H_5)][Cl]	Acetone	395	33	13	HRS	1.06	51
[Ru{(*E*)-4,4′-C≡CC_6H_4N=$NC_6H_4NO_2$}(PPh_3)$_2$(η-C_5H_5)]	THF	565	1627	149	HRS	1.06	54
trans-[Ru{(*E*)-4,4′-C≡CC_6H_4N=$NC_6H_4NO_2$}Cl($dppm_2$)$_2$]	THF	583	1649	232	HRS	1.06	54
[Au{(*E*)-4,4′-C≡CC_6H_4N=$NC_6H_4NO_2$}(PPh_3)]	THF	398	180	68	HRS	1.06	54

Table 1.4. Molecular second-order NLO results for vinylidene, acetylide and nitrile complexes (continued)

Complex	Solvent	λ_{max} (nm)	β (10^{-30} esu)	β_o (10^{-30} esu)	Technique	Fund. μm	Ref.
1,3,5-{*trans*-[RuCl(dppe)$_2$(C≡C-4-C$_6$H$_4$C≡C)]}$_3$C$_6$H$_3$	THF	414	94	--	HRS	1.06	55
1,3,5-{*trans*-{Ru(C≡CPh)(dppe)$_2$(C≡C-4-C$_6$H$_4$C≡C)]}$_3$C$_6$H$_3$	THF	411	93	--	HRS	1.06	55
trans-[Ru(C≡CPh)(C≡C-4-C$_6$H$_4$C≡CPh)(dppe)$_2$]	THF	383	34	--	HRS	1.06	55
trans-[Ru(C≡CPh)Cl(dppe)$_2$]	THF	319	6	--	HRS	1.06	55
[Fe(C≡CPh)(dppe)(η-C$_5$Me$_5$)]	CH_2Cl_2	348	52	24	HRS	1.06	52
[Fe(C≡CPh)(dppe)(η-C$_5$Me$_5$)][PF$_6$]	CH_2Cl_2	663	80	--	HRS	1.06	52
1,3-C$_6$H$_4$[(C≡C)Fe(dppe)(η-C$_5$Me$_5$)]$_2$	CH_2Cl_2	349	210	98	HRS	1.06	52
[1,3-C$_6$H$_4${(C≡C)Fe(dppe)(η-C$_5$Me$_5$)}$_2$][PF$_6$]	CH_2Cl_2	650	150	--	HRS	1.06	52
[1,3-C$_6$H$_4${(C≡C)Fe(dppe)(η-C$_5$Me$_5$)}$_2$][PF$_6$]$_2$	CH_2Cl_2	662	200	--	HRS	1.06	52
1,3,5-C$_6$H$_3$[(C≡C)Fe(dppe)(η-C$_5$Me$_5$)]$_3$	CH_2Cl_2	351	175	87	HRS	1.06	52
[1,3,5-C$_6$H$_3${(C≡C)Fe(dppe)(η-C$_5$Me$_5$)}$_3$][PF$_6$]	CH_2Cl_2	710	190	--	HRS	1.06	52
[1,3,5-C$_6$H$_3${(C≡C)Fe(dppe)(η-C$_5$Me$_5$)}$_3$][PF$_6$]$_2$	CH_2Cl_2	688	170	--	HRS	1.06	52
[1,3,5-C$_6$H$_3${(C≡C)Fe(dppe)(η-C$_5$Me$_5$)}$_3$][PF$_6$]$_3$	CH_2Cl_2	662	53	--	HRS	1.06	52
1,4-C$_6$H$_4$[(C≡C)Fe(dppe)(η-C$_5$Me$_5$)]$_2$	CH_2Cl_2	413	180	60	HRS	1.06	52
[1,4-C$_6$H$_4${(C≡C)Fe(dppe)(η-C$_5$Me$_5$)}$_2$][PF$_6$]	CH_2Cl_2	702	400	--	HRS	1.06	52

Table 1.4. Molecular second-order NLO results for vinylidene, acetylide and nitrile complexes (continued)

Complex	Solvent	λ_{max} (nm)	β (10^{-30} esu)	β_o (10^{-30} esu)	Technique	Fund. μm	Ref.
$[1,4\text{-}C_6H_4\{(C{\equiv}C)Fe(dppe)(\eta\text{-}C_5Me_5)\}]_2][PF_6]_2$	CH_2Cl_2	702	200	--	HRS	1.06	52
$[Fe(4\text{-}N{\equiv}CC_6H_4NO_2)\{(+)\text{-diop}\}(\eta\text{-}C_5H_5)][PF_6]$	CH_2Cl_2	454	380	86	HRS	1.06	56
$[Fe(4\text{-}N{\equiv}CC_6H_4NO_2)(dppe)(\eta\text{-}C_5H_5)][PF_6]$	CH_2Cl_2	460	395	115	HRS	1.06	56
$[Fe(4\text{-}N{\equiv}CC_6H_4C_6H_4NO_2)\{(+)\text{-diop}\}(\eta\text{-}C_5H_5)][PF_6]$	CH_2Cl_2	430	190	78	HRS	1.06	56
$[Fe(4\text{-}N{\equiv}CC_6H_4C_6H_4NO_2)(dppe)(\eta\text{-}C_5H_5)][PF_6]$	CH_2Cl_2	372	240	108	HRS	1.06	56
$[Fe\{(E)\text{-}4\text{-}N{\equiv}CCH{=}CHC_6H_4NO_2\}\{(+)\text{-diop}\}(\eta\text{-}C_5H_5)][PF_6]$	CH_2Cl_2	466	520	105	HRS	1.06	56
$[Fe\{(E)\text{-}4\text{-}N{\equiv}CCH{=}CHC_6H_4NO_2\}(dppe)(\eta\text{-}C_5H_5)][PF_6]$	CH_2Cl_2	484	570	112	HRS	1.06	56
$[Ru\{C{\equiv}CC_6H_4N{=}\overline{CCH{=}C^tBuC(O)C^tBu{=}CH}\}Cl(dppm)_2]$	THF	645	417	124	HRS	1.06	57
$[Ru\{C{\equiv}CC_6H_4N{=}\overline{CCH{=}C^tBuC(O)C^tBu{=}CH}\}(PPh_3)_2(\eta\text{-}C_5H_5)]$	THF	622	658	159	HRS	1.06	57

may have as-yet-undetermined effects upon the β response. The possibility of being able to switch between two distinct "on" and "off" responses may be of potential utility for technological applications.

Combinations of organic complexes with monometallic centres has produced a wealth of NLO-active complexes; extension to bimetallic complexes has therefore been a logical progression. Table 1.5. lists some of the bimetallic complexes for which β values have been recently reported. Some metallocene complexes and their measured β values are illustrated in Figure 1.7. Examination of the work of Heck and co-workers[20,28,44,58] permits comparison of several related bimetallic complexes. Use of a ferrocene moiety leads to a higher quadratic NLO response than does use of the cymantrene unit $[Mn(CO)_3(\eta\text{-}C_5H_4R)]$, probably due to the stronger electron-donating capability of the former. In otherwise identical complexes, replacement of a cyclopentadienyl ring with an indenyl ring leads to a modest increase in β_{exp} and β_0, as demonstrated previously,[53] and increasing chain-length

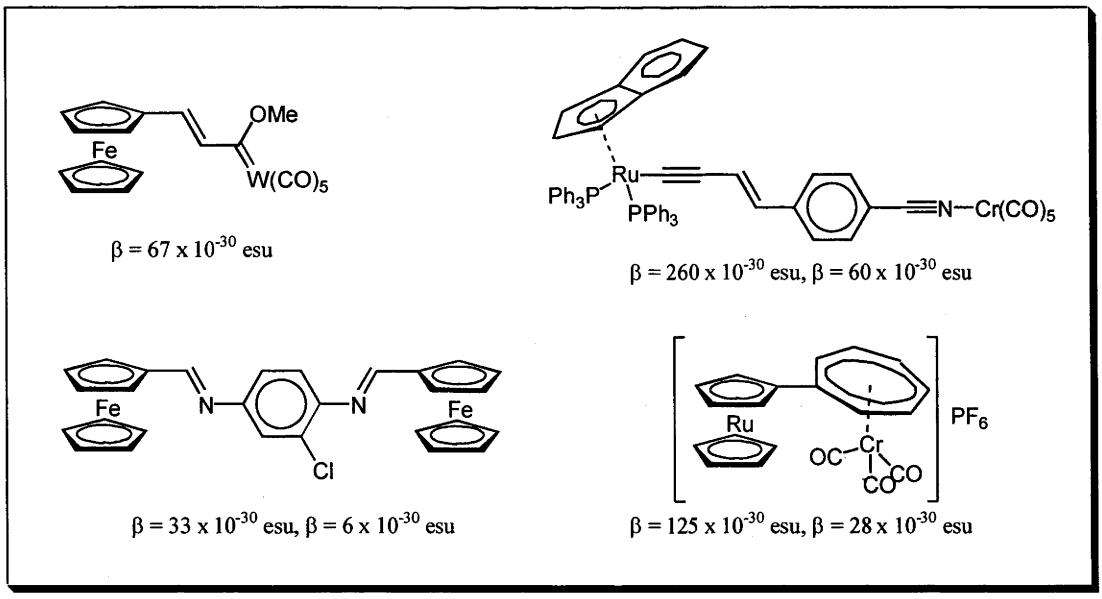

Figure 1.7. Some bimetallic complexes and their measured β values.

Table 1.5. Molecular second-order NLO results of bimetallic complexes

Complex	Solvent	λ_{max} (nm)	β (10^{-30} esu)	β_o (10^{-30} esu)	Technique	Fund. μm	Ref.
$[Fc(\eta^7\text{-}C_7H_6)Ru(\eta\text{-}C_5H_5)][PF_6]_2$	$MeNO_2$	615	125	28	HRS	1.06	20
$[Ru(\eta\text{-}C_5H_5)(\eta\text{-}C_5H_4\text{-}\eta^7\text{-}C_7H_6)Cr(CO)_3][PF_6]$	$MeNO_2$	536	378	4	HRS	1.06	20
$[Ru(\eta\text{-}C_5H_5)(\eta\text{-}C_5H_4\text{-}\eta^7\text{-}C_7H_6)Ru(\eta\text{-}C_5H_5)][PF_6]_2$	$MeNO_2$	462	264	53	HRS	1.06	20
$[Ru(\eta\text{-}C_5H_5)(\eta\text{-}C_5H_4\text{-}(E)\text{-}CH{=}CH\text{-}\eta^7\text{-}C_7H_6)Ru(\eta\text{-}C_5H_5)][PF_6]_2$	$MeNO_2$	549	358	17	HRS	1.06	20
$[Mn(CO)_3(\eta\text{-}C_5H_4\text{-}\eta^7\text{-}C_7H_6)Cr(CO)_3][BF_4]$	$MeNO_2$	445	77	19	HRS	1.06	44
$[Mn(CO)_3(\eta^5\text{-indenyl-}\eta^7\text{-}C_7H_6)Cr(CO)_3][BF_4]$	$MeNO_2$	435	112	31	HRS	1.06	44
$[Mn(CO)_3(\eta\text{-}C_5H_4C{\equiv}C\text{-}\eta^7\text{-}C_7H_6)Cr(CO)_3][BF_4]$	CH_2Cl_2	449	244	58	HRS	1.06	44
$[(Fc\text{-}2\text{-}\eta^5\text{-}SC_4H_3)Mn(CO)_3][BF_4]$	$MeNO_2$	514	43	2	HRS	1.06	45
$[(FcCH{=}CH\text{-}2\text{-}\eta^5\text{-}SC_4H_3)Mn(CO)_3][BF_4]$	$MeNO_2$	536	110	-1	HRS	1.06	45
$[(Fc(CH{=}CH)_2\text{-}2\text{-}\eta^5\text{-}SC_4H_3)Mn(CO)_3][BF_4]$	$MeNO_2$	548	127	-6	HRS	1.06	45
$[(FcCH{=}CH\text{-}3\text{-}\eta^5\text{-}SC_4H_3)Mn(CO)_3][BF_4]$	$MeNO_2$	480	50	7	HRS	1.06	45
$[(FcCH_2\text{-}2\text{-}\eta^5\text{-}SC_4H_3)Mn(CO)_3][BF_4]$	$MeNO_2$	--	36	--	HRS	1.06	45
$[Cr(CO)_3(\eta^6\text{-}C_6H_5C{\equiv}CFc)]$	$CHCl_3$	387	9	7	HRS	1.5	46
$[Cr(CO)_3(\eta^6\text{-}C_6H_5C{\equiv}CC{\equiv}CFc)]$	$CHCl_3$	419	11	9	HRS	1.5	46

Table 1.5. Molecular second-order NLO results of bimetallic complexes (continued)

Complex	Solvent	λ_{max} (nm)	β (10^{-30} esu)	β_o (10^{-30} esu)	Technique	Fund. μm	Ref.
[Ru(C≡NCr(CO)$_5$)(PPh$_3$)$_2$(η^5-indenyl)]	CH_2Cl_2	392	25	10	HRS	1.06	53
[Ru(C≡NW(CO)$_5$)(PPh$_3$)$_2$(η^5-indenyl)]	CH_2Cl_2	392	40	15	HRS	1.06	53
[Ru(C≡NRu(NH$_3$)$_5$)(PPh$_3$)$_2$(η^5-indenyl)][CF_3SO_3]$_3$	Acetone	621	108	26	HRS	1.06	53
[Ru(C≡CCH=CH-4-C_6H_4C≡NCr(CO)$_5$)(PPh$_3$)$_2$(η^5-indenyl)]	CH_2Cl_2	442	465	119	HRS	1.06	53
[Ru(C≡CCH=CH-4-C_6H_4C≡NW(CO)$_5$)(PPh$_3$)$_2$(η^5-indenyl)]	CH_2Cl_2	456	700	150	HRS	1.06	53
[Ru(C≡CCH=CH-4-C_6H_4C≡NRu(NH$_3$)$_5$)(PPh$_3$)$_2$(η^5-indenyl)][CF_3SO_3]$_3$	Acetone	442	315	80	HRS	1.06	53
[Ru(C≡C-(*E*)-CH=CH-4-C_5H_4NCr(CO)$_5$)(PPh$_3$)$_2$(η^5-indenyl)]	CH_2Cl_2	451	260	60	HRS	1.06	53
[Ru(C≡C-(*E*)-CH=CH-4-C_5H_4NW(CO)$_5$)(PPh$_3$)$_2$(η^5-indenyl)]	CH_2Cl_2	462	535	71	HRS	1.06	53
[Ru(C≡C-(*E*)-CH=CHFc)(PPh$_3$)$_2$(η^5-indenyl)]	CH_2Cl_2	345	273	141	HRS	1.06	53
[Ru(C=CH-(*E*)-CH=CHFc)(PPh$_3$)$_2$(η^5-indenyl)][BF_4]	CH_2Cl_2	301	117	73	HRS	1.06	53
[Fc-(1,4-dimethyl-7-isopropylazulene)Ru(η-C_5H_5)][PF_6]	CH_2Cl_2	698	326	134	HRS	1.06	28
[Fc-(*E*)-CH=CH-4-C_6H_4C≡NRu(PPh$_3$)$_2$(η-C_5H_5)][PF_6]	$CHCl_3$	485	186	25	HRS	1.06	59
[Fc-(*E*)-CH=CH-4-C_6H_4C≡NRu(PPh$_3$)$_2$(η-C_5H_5)][BF_4]	$CHCl_3$	484	325	44	HRS	1.06	59
[Fc-(*E*)-CH=CH-4-C_6H_4C≡NFe(CO)$_2$(η-C_5H_5)][PF_6]	$CHCl_3$	474	171	28	HRS	1.06	59

Table 1.5. Molecular second-order NLO results of bimetallic complexes (continued)

Complex	Solvent	λ_{max} (nm)	β (10^{-30} esu)	β_o (10^{-30} esu)	Technique	Fund. μm	Ref.
[Fc{(*E*)-CH=CH-4-C_6H_4-(*E*)-CH=CH-4-C_5H_4NCr$(CO)_5$}]	CH_2Cl_2	477	63	--	HRS	1.06	29
[Fc{(*E*)-CH=CH-4-C_6H_4-(*E*)-CH=CH-4-C_5H_4NMo$(CO)_5$}]	CH_2Cl_2	487	95	--	HRS	1.06	29
[Fc{(*E*)-CH=CH-4-C_6H_4-(*E*)-CH=CH-4-C_5H_4N}W$(CO)_5$]	CH_2Cl_2	491	101	--	HRS	1.06	29
[Fc{(*E,E*)-(CH=CH-4-C_6H_4)$_2$-(*E*)-CH=CH-4-C_5H_4NCr$(CO)_5$}]	CH_2Cl_2	462	369	--	HRS	1.06	29
[Fc{(*E,E*)-(CH=CH-4-C_6H_4)$_2$-(*E*)-CH=CH-4-C_5H_4NMo$(CO)_5$}]	CH_2Cl_2	476	448	--	HRS	1.06	29
[Fc{(*E,E*)-(CH=CH-4-C_6H_4)$_2$-(*E*)-CH=CH-4-C_5H_4NW$(CO)_5$}]	CH_2Cl_2	487	535	--	HRS	1.06	29

leads to increased β. However, the sesquifulvalene complexes exhibit significant two-photon fluorescence which hinders accurate determination of β_{1064}. High frequency demodulation HRS at 1300 nm has been used to attempt to circumvent this problem.[28] Significant work on bimetallic ruthenium acetylides has been undertaken by Gimeno and co-workers.[53] The presence of the ruthenium centre in the plane of the charge-transition, and the domination of the charge-transfer state by a single transition has been suggested as a reason for the effectiveness of the [$Ru(PPh_3)_2(\eta^5$-indenyl)] ligated metal centre for NLO effects.

Samuelson and co-workers[23,39] synthesized a series of bisferrocenyl complexes where two ferrocene moieties were linked through an aromatic Schiff base spacer (Table 1.6.). Despite the apparent centrosymmetric nature of these complexes, the β_{exp} values of the bisferrocenyl complexes are much higher than the corresponding monoferrocenyl complexes, but in all of the former there is a strong resonant contribution to β due to the MLCT transition around 532 nm. The authors also synthesized a series of charge-transfer complexes of the bisferrocenyl compounds with acceptors such as iodine, *p*-chloroanil (CA), 2,3-dichloro-5,6-dicyano-1,4-benzoquinone (DDQ), tetracyanoethylene (TCNE) and 7,7,8,8-tetracyanoquinodimethane (TCNQ). Although the authors corrected for two-photon fluorescence, the β values were strongly resonance enhanced, and hence the β_0 values (which were calculated using the two-level model) should be viewed with caution. In a later paper, Samuelson and co-workers[39] calculated the two-photon absorption to be up to 25% in certain bisferrocenyl complexes with Schiff base linkers, and by fitting a Gaussian curve to the absorption band obtained the frequency-independent hyperpolarizability β_0, confirming the very strong resonance enhancement present in these ferrocene complexes.

Table 1.7. shows series of bimetallic complexes prepared by Jayaprakash et al.[31] Lengthening of the π-conjugated backbone led to a predictable increase in β_{exp}.

Replacement of chromium by tungsten also led to greater quadratic nonlinearities, which is be expected on the basis of the tungsten complexes having more efficient back-donation to the CO ligand from the metal, a result supported by previous studies.[60,61] The quadratic hyperpolarizabilities of this series of complexes were measured in four different solvents and were shown to be highly dependent upon the solvent polarity. $[Fc(CH=CH)_4C(OMe)=W(CO)_5]$ exhibited a three-fold increase in β upon progressing from hexane as solvent to acetonitrile.

Given the wealth of possible combinations of metal centres, ligands and oxidation states, bi- and multi-metallic systems are potentially a rich source of materials for molecular second-order NLO. The results of the studies summarized above are sufficiently promising as to suggest that this will continue to be a focus of organometallic-NLO studies.

Table 1.6. Molecular second-order NLO results of bisferrocenyl complexes

Complex	Solvent	λ_{max} (nm)	β (10^{-30} esu)	β_o (10^{-30} esu)	Technique	Fund. μm	Ref.
[FcCH=NC_6H_3-2-(OMe)-4-N=CHFc]	MeCN	453	18	4	HRS	1.06	23
[FcCH=NC_6H_3-2-(OMe)-4-N=CHFc]·I_5	MeCN	514	126	6	HRS	1.06	23
[FcCH=NC_6H_3-2-(OMe)-4-N=CHFc]·$(DDQ)_2$	MeCN	546	174	7	HRS	1.06	23
[FcCH=NC_6H_3-2-(OMe)-4-N=CHFc]·$(TCNE)_2$	MeCN	498	259	25	HRS	1.06	23
[FcCH=NC_6H_3-2-(OMe)-4-N=CHFc]·$(TCNQ)_2$	MeCN	482	166	24	HRS	1.06	23
[FcCH=NC_6H_3-2-(OMe)-4-N=CHFc]·$(CA)_2$	MeCN	634	135	37	HRS	1.06	23
[FcCH=NC_6H_4-4-N=CHFc]	MeCN	460	23	5	HRS	1.06	23
[FcCH=NC_6H_4-4-N=CHFc]·$I_{4.5}$	MeCN	510	137	8	HRS	1.06	23
[FcCH=NC_6H_4-4-N=CHFc]·$(DDQ)_2$	MeCN	582	150	21	HRS	1.06	23
[FcCH=NC_6H_4-4-N=CHFc]·$(TCNE)_2$	MeCN	479	181	27	HRS	1.06	23
[FcCH=NC_6H_4-4-N=CHFc]·$(TCNQ)_2$	MeCN	476	144	23	HRS	1.06	23
[FcCH=NC_6H_4-4-N=CHFc]·$(CA)_2$	MeCN	570	263	28	HRS	1.06	23
[FcCH=NC_6H_3-2-Cl-4-N=CHFc]	MeCN	474	33	5	HRS	1.06	23
[FcCH=NC_6H_3-2-Cl-4-N=CHFc]·$I_{4.5}$	MeCN	521	160	5	HRS	1.06	23

Table 1.6. Molecular second-order NLO results of bisferrocenyl complexes (continued)

Complex	Solvent	λ_{max} (nm)	β (10^{-30} esu)	β_o (10^{-30} esu)	Technique	Fund. μm	Ref.
[FcCH=NC_6H_3-2-Cl-4-N=CHFc]·$(DDQ)_2$	MeCN	588	175	27	HRS	1.06	23
[FcCH=NC_6H_3-2-Cl-4-N=CHFc]·$(TCNE)_2$	MeCN	490	125	34	HRS	1.06	23
[FcCH=NC_6H_3-2-Cl-4-N=CHFc]·$(TCNQ)_2$	MeCN	476	204	32	HRS	1.06	23
[FcCH=NC_6H_3-2-Cl-4-N=CHFc]·$(CA)_2$	MeCN	601	279	52	HRS	1.06	23
[FcCH=$NC_6(Me)_4$-4-N=CHFc]	MeCN	455	23	5	HRS	1.06	23
[FcCH=$NC_6(Me)_4$-4-N=CHFc]·I_3	MeCN	502	13	10	HRS	1.06	23
[FcCH=$NC_6(Me)_4$-4-N=CHFc]·$(DDQ)_2$	MeCN	494	153	17	HRS	1.06	23
[FcCH=$NC_6(Me)_4$-4-N=CHFc]·$(TCNE)_2$	MeCN	478	161	25	HRS	1.06	23
[FcCH=$NC_6(Me)_4$-4-N=CHFc]·$(TCNQ)_2$	MeCN	475	171	28	HRS	1.06	23
[FcCH=$NC_6(Me)_4$-4-N=CHFc]·$(CA)_3$	MeCN	438	170	45	HRS	1.06	23
[FcCH=NC_6H_4-4-C_6H_4-N=CHFc]	MeCN	465	36	7	HRS	1.06	23
[FcCH=NC_6H_4-4-C_6H_4-N=CHFc]·I_3	MeCN	524	149	3	HRS	1.06	23
[FcCH=NC_6H_4-4-C_6H_4-N=CHFc]·$(DDQ)_2$	MeCN	590	132	21	HRS	1.06	23
[FcCH=NC_6H_4-4-C_6H_4-N=CHFc]·$(TCNE)_2$	MeCN	505	288	22	HRS	1.06	23

Table 1.6. Molecular second-order NLO results of bisferrocenyl complexes (continued)

Complex	Solvent	λ_{max} (nm)	β (10^{-30} esu)	β_o (10^{-30} esu)	Technique	Fund. μm	Ref.
$[FcCH{=}NC_6H_4\text{-}4\text{-}C_6H_4N{=}CHFc]\cdot(TCNQ)_2$	MeCN	478	173	26	HRS	1.06	23
$[FcCH{=}NC_6H_4\text{-}4\text{-}C_6H_4N{=}CHFc]\cdot(CA)_3$	MeCN	448	197	47	HRS	1.06	23

Table 1.7. Molecular second-order NLO results for bimetallic complexes in different solvents

Complex	Solvent	λ_{max} (nm)	β_{exp} (10^{-30} esu)	Technique	Fund. (μm)	Ref.
$[FcCH=CHC(OMe)=W(CO)_5]$	Hexane	559	67	HRS	1.06	31
	CH_2Cl_2	--	82	HRS	1.06	31
	Acetone	--	102	HRS	1.06	31
	MeCN	--	160	HRS	1.06	31
$[Fc(CH=CH)_2C(OMe)=W(CO)_5]$	Hexane	558	220	HRS	1.06	31
	CH_2Cl_2	--	402	HRS	1.06	31
	Acetone	--	520	HRS	1.06	31
	MeCN	--	600	HRS	1.06	31
$[Fc(CH=CH)_3C(OMe)=W(CO)_5]$	Hexane	551	408	HRS	1.06	31
	CH_2Cl_2	--	580	HRS	1.06	31
	Acetone	--	840	HRS	1.06	31
	MeCN	--	1140	HRS	1.06	31

Table 1.7. Molecular second-order NLO results for bimetallic complexes in different solvents (continued)

Complex	Solvent	λ_{max} (nm)	β_{exp} (10^{-30} esu)	Technique	Fund. (μm)	Ref.
$[Fc(CH=CH)_4C(OMe)=W(CO)_5]$	Hexane	541	780	HRS	1.06	31
	CH_2Cl_2	--	960	HRS	1.06	31
	Acetone	--	1720	HRS	1.06	31
	MeCN	--	2420	HRS	1.06	31
$[FcCH=CHC(OMe)=Cr(CO)_5]$	Hexane	543	47	HRS	1.06	31
	CH_2Cl_2	--	69	HRS	1.06	31
	Acetone	--	89	HRS	1.06	31
	MeCN	--	110	HRS	1.06	31
$[Fc(CH=CH)_2C(OMe)=Cr(CO)_5]$	Hexane	546	161	HRS	1.06	31
	CH_2Cl_2	--	240	HRS	1.06	31
	MeCN	--	410	HRS	1.06	31
	Acetone	--	306	HRS	1.06	31

Table 1.7. Molecular second-order NLO results for bimetallic complexes in different solvents (continued)

Complex	Solvent	λ_{max} (nm)	β_{exp} (10^{-30} esu)	Technique	Fund. (μm)	Ref.
$[Fc(CH=CH)_3C(OMe)=Cr(CO)_5]$	Hexane	550	343	HRS	1.06	31
	CH_2Cl_2	--	440	HRS	1.06	31
	Acetone	--	760	HRS	1.06	31
	MeCN	--	1030	HRS	1.06	31

1.5. Organo-transition metal complexes for third-order nonlinear optics

Significantly less work has been undertaken to study the third-order NLO properties of organometallic complexes in comparison with the abundance of work on quadratic hyperpolarizabilities. Since the last major review[5] there have been fewer papers in this area than for second-order nonlinear optics, due to the lack of immediate technological applications for third-order effects and, additionally, because all materials exhibit third-order NLO effects, including glass used for a sample cell and even air, so that obtaining a signal free from additional contributions can be experimentally challenging.

Humphrey and co-workers have examined a range of ruthenium and gold acetylide complexes using the Z-scan technique. Table 1.8. lists the cubic nonlinearities measured for gold complexes. Electron polarization can be induced in the complexes by the presence of a strong electron-withdrawing group such as NO_2 which leads to an increase in γ_{real}. Lengthening the π-conjugated backbone leads to a systematic increase in the cubic nonlinearity, a structure-NLO property relationship well established for organic systems. The composition of the π-conjugated backbone has a significant effect upon the cubic nonlinearity, with (*E*)-CH=CH > C≡C > (*Z*)-CH=CH > (*E*)-N=CH.

The ruthenium acetylide complexes listed in Table 1.9. have increasingly large $|\gamma|$ values upon increasing the π-conjugation through the metal centre. Formation of the dendritic complex [1,3,5-C_6H_3(4-C≡CC_6H_4C≡C-*trans*-[Ru(dppe)$_2$]C≡C-3,5-C_6H_3-{4-C≡CC_6H_4C≡C-*trans*-[Ru(C≡CPh)(dppe)$_2$]}$_2$)$_3$] leads to a very large $|\gamma|$ value without a subsequent increase in λ_{max}, thereby avoiding the NLO efficiency / transparency trade-off which occurs in many materials. The significant γ_{imag} values for these complexes are indicative of two-photon absorption.

Table 1.8. Molecular third-order NLO data for gold acetylide complexes.

	λ_{max} (nm) [ε (10^4 M^{-1} cm^{-1})]	Technique	Solvent	Fund. (μm)	γ_{real}	γ_{imag}	Ref.
PPN[Au(C≡C-4-$C_6H_4NO_2$)$_2$]	376 [5.4]	Z-scan	CH_2Cl_2	0.8	-800 ± 400	115 ± 50	62
NPr_4[Au(C≡C-4-$C_6H_4NO_2$)$_2$]	374 [3.1]	Z-scan	CH_2Cl_2	0.8	90 ± 150	190 ± 50	62
[Au(C≡C-4-$C_6H_4NO_2$)(CNBu^t)]	332 [2.6]	Z-scan	CH_2Cl_2	0.8	≤ 130	≤ 50	62
[Au(C≡C-4-C_6H_4-4-$C_6H_4NO_2$)(CNBu^t)]	343 [3.1]	Z-scan	CH_2Cl_2	0.8	20 ± 100	70 ± 50	62
[Au(C≡C-4-C_6H_4-(*E*)-CH=CH-4-$C_6H_4NO_2$)(CNBu^t)]	381 [4.1]	Z-scan	CH_2Cl_2	0.8	390 ± 200	1050 ± 300	62
[Au(C≡C-4-C_6H_4-4-$C_6H_4NO_2$){C(NHBu^t)(NEt$_2$)}]	354 [0.4]	Z-scan	CH_2Cl_2	0.8	10 ± 100	160 ± 40	62
[Au(C≡C-4-C_6H_4-(*E*)-CH=CH-4-$C_6H_4NO_2$){C(NHBu^t)(NEt$_2$)}]	389 [0.6]	Z-scan	CH_2Cl_2	0.8	-200 ± 360	610 ± 200	62
[Au(C≡CPh)(PPh_3)]	296 [1.3]	Z-scan	THF	0.8	39 ± 20	--	63
[Au(C≡C-4-$C_6H_4NO_2$)(PPh_3)]	338 [2.5]	Z-scan	THF	0.8	120 ± 40	20 ± 50	63
[Au(C≡C-4-C_6H_4-4-$C_6H_4NO_2$)(PPh_3)]	350 [2.9]	Z-scan	THF	0.8	540 ± 150	120 ± 50	63
[Au(C≡C-4-C_6H_4C≡C-4-$C_6H_4NO_2$)(PPh_3)]	362 [3.6]	Z-scan	THF	0.8	1300 ± 400	560 ± 150	63
[Au(C≡C-4-C_6H_4-(*E*)-CH=CH-4-$C_6H_4NO_2$)(PPh_3)]	386 [3.8]	Z-scan	THF	0.8	1200 ± 200	470 ± 150	63
[Au(C≡C-4-C_6H_4-(*Z*)-CH=CH-4-$C_6H_4NO_2$)(PPh_3)]	362 [2.0]	Z-scan	THF	0.8	420 ± 150	92 ± 30	63
[Au(C≡C-4-C_6H_4-(*E*)-N=CH-4-$C_6H_4NO_2$)(PPh_3)]	392 [2.1]	Z-scan	THF	0.8	130 ± 30	330 ± 60	63

Table 1.9. Molecular third-order NLO data for organometallic complexes at 800 nm.

	λ_{max} (nm) [ε (10^4 M^{-1} cm^{-1})]	Technique	Solvent	γ_{real} (10^{-36} esu)	γ_{imag} (10^{-36} esu)	$\lvert\gamma\rvert$ (10^{-36} esu)	σ_2	Ref.
1,3,5-[*trans*-RuCl(dppe)$_2$(C≡C-4-C$_6$H$_4$C≡C)]$_3$C$_6$H$_3$	414 [10.4]	Z-scan	THF	-330 ± 100	2200 ± 500	2200 ± 600	530 ± 120	55
1,3,5-{*trans*-[Ru(C≡CPh)(C≡C-4-C$_6$H$_4$C≡C)(dppe)$_2$]}$_3$C$_6$H$_3$	411 [11.6]	Z-scan	THF	-600 ± 200	2900 ± 500	3000 ± 600	700 ± 120	55
trans-[Ru(C≡CPh)(C≡C-4-C$_6$H$_4$C≡CPh)(dppe)$_2$]	383 [3.8]	Z-scan	CH_2Cl_2	-670 ± 300	1300 ± 300	1500 ± 500	--	55
trans-[Ru(C≡CPh)Cl(dppe)$_2$]	319 [1.8]	Z-scan	CH_2Cl_2	-170 ± 40	71 ± 20	200 ± 50	--	55
1-(Me$_3$SiC≡C)-C$_6$H$_3$-3,5-{4-C≡CC$_6$H$_4$C≡C-*trans*-[RuCl(dppe)$_2$]}$_2$	411 [6.8]	Z-scan	THF	-510 ± 500	4700 ± 1500	4700 ± 2000	1100 ± 360	64
1-(Me$_3$SiC≡C)-C$_6$H$_3$-3,5-{4-C≡CC$_6$H$_4$C≡C-*trans*-[Ru(C≡CPh)(dppe)$_2$]}$_2$	407 [6.4]	Z-scan	THF	-700 ± 100	2270 ± 300	2400 ± 300	550 ± 70	64
1-(HC≡C)-C$_6$H$_3$-3,5-{4-C≡CC$_6$H$_4$C≡C-*trans*-[Ru(C≡CPh)(dppe)$_2$]}$_2$	408 [7.3]	Z-scan	THF	-830 ± 100	2200 ± 300	2400 ± 300	530 ± 70	64
1,3,5-C$_6$H$_3$(4-C≡CC$_6$H$_4$C≡C-*trans*-[Ru(dppe)$_2$]C≡C-3,5-C$_6$H$_3$-{4-C≡CC$_6$H$_4$C≡C-*trans*-[Ru(C≡CPh)(dppe)$_2$]}$_2$)$_3$	402 [42]	Z-scan	THF	-5050 ± 500	20100 ± 2000	20700 ± 2000	4800 ± 500	64

Table 1.10. Molecular third-order NLO data for ferrocenyl complexes.

	λ_{max} (nm)	Technique	Solvent	Fund. (μm)	γ_{real} (10^{-36} esu)	γ_{imag} (10^{-36} esu)	$\lvert\gamma\rvert$ (10^{-36} esu)	Ref.
[MoCl(HNC$_6$H$_4$-4-Fc)(NO)(Tp^{An})]	598	THG	$CHCl_3$	1.91	-450	460	640	65
[MoCl(HNC$_6$H$_4$-4-N=N-4-C$_6$H$_4$Fc)(NO)(Tp^{An})]	537	THG	$CHCl_3$	1.91	-3450	3210	4710	65
[MoCl(HNC$_6$H$_3$-3-Me-4-N=NC$_6$H$_4$-4-Fc)(NO)(Tp^{An})]	540	THG	$CHCl_3$	1.91	-467	1320	1400	65
[MoCl(HNC$_6$H$_3$-3-Me-4-N=NC$_6$H$_3$-3-Me-4-Fc)(NO)(Tp^{An})]	530	THG	$CHCl_3$	1.91	-428	5770	5790	65
[MoCl(HNC$_6$H$_3$-3-Me-4-N=NC$_6$H$_3$-5-Me-2-Fc)(NO)(Tp^{An})]	571	THG	$CHCl_3$	1.91	-180	410	448	65
[Fc-4-C$_6$H$_4$CH=CH-4-C$_6$H$_4$NO$_2$]	469	THG	$CHCl_3$	1.91	605	860	1050	65
[Fe{η-C$_5$H$_4$-(*E*)-CH=CHC$_6$H$_4$-4-NO$_2$}{η-C$_5$H$_4$-(*Z*)-CH=CHC$_6$H$_4$-4-NO$_2$}]	488	Z-scan	THF	0.8	840 ± 400	770 ± 200	1140 ± 430	66
[Fe{η-C$_5$H$_4$-(*Z*)-CH=CHC$_6$H$_4$-4-NO$_2$}$_2$]	481	Z-scan	THF	0.8	600 ± 300	0 ± 50	600 ± 300	66
[Fe{η-C$_5$H$_4$-(*Z*)-CH=CHC$_6$H$_4$-4-CN}$_2$]	492	Z-scan	THF	0.8	280 ± 150	30 ± 20	280 ± 150	66
[Fe{η-C$_5$H$_4$-(*E*)-CH=CHC$_6$H$_4$-4-CN}{η-C$_5$H$_4$-(*Z*)-CH=CHC$_6$H$_4$-4-CN}]	469	Z-scan	THF	0.8	310 ± 200	50 ± 30	310 ± 200	66
[Fe(η-C$_5$H$_5$){η-C$_5$H$_4$-(*E*)-CH=CH-4-C$_6$H$_4$-(*E*)-CH=CH-η-C$_5$H$_4$}Fe(η-C$_5$H$_5$)]	457	Z-scan	THF	0.8	640 ± 300	30 ± 20	640 ± 300	66
[Fe(η-C$_5$H$_5$)(η-C$_5$H$_4$-(*E*)-CH=CH-4-{η^6-C$_6$H$_4$)-Cr(CO)$_3$}-(*E*)-CH=CH-η-C$_5$H$_4$)Fe(η-C$_5$H$_5$)]	455	Z-scan	THF	0.8	850 ± 300	95 ± 30	860 ± 300	66

Rojo *et al.*[65] have synthesized a series of push-pull organobimetallic Mo/Fe compounds and measured the cubic hyperpolarizability (Table 1.10.). Although the authors did not report errors for their experimental values, similar trends to previous reports were observed, including an increase in γ which correlated with an increase in length of the π-conjugated linkers, non-linear complexes having lower responses, and a decrease in γ when substituents are attached to the bridge. Mata *et al.*[66] have synthesized a series of mono-, bi- and tri-metallic ferrocenyl complexes, where γ was observed to increase upon increasing electron-donor strength and increasing the number of metal centres. Large γ values are generally reported for π-delocalized systems containing more than one metal center, although Tykwinski and co-workers[67] have previously shown that ferrocenyl centres are relatively inefficient π-electron donors. Therefore, future materials with potentially high third-order NLO responses may be expected to contain multiple in-plane metal centres connected by an extended π-delocalized framework.

1.6. Conclusions

The studies summarized above have reinforced the previously established structure/NLO property relationships for organometallic systems, but a great deal of work investigating variation in metal, charge-transfer ligands, oxidation state, co-ligands, and geometry remains to be done. The molecular nonlinearities obtained for some of the complexes are extremely large, suggesting significant potential for application of organometallics.

In the current work, the results of studies addressing some of the points mentioned above are presented, namely the effect of chain-lengthening the π-delocalized bridge (Chapter 2), acceptor group strength (Chapter 3), presence of multiple metal centers (Chapter 4) and variation in molecular geometry (Chapter 5) upon the optical nonlinearities.

1.7. References

[1] Eaton, D.F., Nonlinear Optical-Materials - the Great and Near Great, ACS Symposium Series, **1991**, *455*, 128.

[2] Kaino, T., Tomaru, S., *Adv. Mater.*, **1993**, *5*, 172.

[3] Bredas, J.L., Adant, C., Beljonne, D., Meyers, F., Shuai, Z., *Synth. Met.*, **1993**, *57*, 3933.

[4] Whittall, I.R., McDonagh, A.M., Humphrey, M.G., Samoc, M., *Adv. Organomet. Chem.*, **1998**, *42*, 291.

[5] Whittall, I.R., McDonagh, A.M., Humphrey, M.G., Samoc, M., *Adv. Organomet. Chem.*, **1999**, *43*, 349.

[6] Roundhill, D.M., Fackler, J.P.: Optoelectronic Properties of Inorganic Compounds, Plenum Publishing Corporation, New York, 1999.

[7] Shen, Y.R.: The Principles of Nonlinear Optics, Wiley, New York, 1984.

[8] Sutherland, R.L.: Handbook of Nonlinear Optics, Marcel Dekker, New York, 1996.

[9] Boyd, R.W.: Nonlinear Optics, Academic Press, New York, 1992.

[10] Butcher, P.N., Cotter, D.: The Elements of Nonlinear Optics, Cambridge University Press, New York, 1990.

[11] Bosshard, C., Knöpfle, G., Prêtre, P., Günter, P., *J. Appl. Phys.*, **1992**, *71*, 1594.

[12] Paley, M.S., Harris, J.M., Looser, H., Baumert, J.C., Bjorklund, G.C., Jundt, D., Twieg, R.J., *J. Org. Chem.,* **1989**, *54*, 3774.

[13] Lequan, M., Lequan, R.M., Ching, K.C., *J. Mater. Chem.,* **1991**, *1*, 997.

[14] Chemla, D.S., Oudar, J.L., Jerphagnon, J., *Phys. Rev. B,* **1975**, *12*, 4534.

[15] Clays, K., Persoons, A., *Phys. Rev. Lett.,* **1991**, *66*, 2980.

[16] Clays, K., Persoons, A., *Rev. Sci. Instrum.,* **1992**, *63*, 3285.

[17] Hendrickx, E., Dehu, C., Clays, K., Brédas, J.L., Persoons, A., in G.A. Lindsay, K.D. Singer (Eds.), Polymers for Second-Order Nonlinear Optics, ACS, Washington, DC, 1995, p. 82.

[18] Sheik-bahae, M., Said, A.A., Wei, T., Hagan, D.J., van-Stryland, E.W., *IEEE J. Quantum Electron.,* **1990**, *26*, 760.

[19] Green, M.L.H., Marder, S.R., Thompson, M.E., Bandy, A.J., Bloor, D., Kolinsky, P.V., Jones, R.J., *Nature,* **1987**, *330*, 360.

[20] Heck, J., Dabek, S., Meyer-Friedrichsen, T., Wong, H., *Coord. Chem. Rev.,* **1999**, *192*, 1217.

[21] Pedersen, B., Wagner, G., Herrmann, R., Scherer, W., Meerholz, K., Schmalzlin, E., Brauchle, C., *J. Organomet. Chem.,* **1999**, *590*, 129.

[22] Naskar, D., Das, S.K., Giribabu, L., Maiya, B.G., Roy, S., *Organometallics,* **2000**, *19*, 1464.

[23] Pal, S.K., Krishnan, A., Das, P.K., Samuelson, A.G., *J. Organomet. Chem.,* **2000**, *604*, 248.

[24] Sharma, H.K., Pannell, K.H., Ledoux, I., Zyss, J., Ceccanti, A., Zanello, P., *Organometallics,* **2000**, *19*, 770.

[25] Balavoine, G.G.A., Daran, J.C., Iftime, G., Lacroix, P.G., Manoury, E., Delaire, J.A., Maltey-Fanton, I., Nakatani, K., Di Bella, S., *Organometallics,* **1999**, *18*, 21.

[26] Malaun, M., Reeves, Z.R., Paul, R.L., Jeffery, J.C., McCleverty, J.A., Ward, M.D., Asselberghs, I., Clays, K., Persoons, A., *Chem. Commun.,* **2001**, 49.

[27] Mata, J.A., Peris, E., Asselberghs, I., Van Boxel, R., Persoons, A., *New J. Chem.,* **2001**, *25*, 299.

[28] Farrell, T., Meyer-Friedrichsen, T., Malessa, M., Haase, D., Saak, W., Asselberghs, I., Wostyn, K., Clays, K., Persoons, A., Heck, J., Manning, A.R., *J. Chem. Soc., Dalton Trans.,* **2001**, 29.

[29] Mata, J.A., Peris, E., Asselberghs, I., Van Boxel, R., Persoons, A., *New J. Chem.,* **2001**, *25*, 1043.

[30] Moore, A.J., Chesney, A., Bryce, M.R., Batsanov, A.S., Kelly, J.F., Howard, J.A.K., Perepichka, I.F., Perepichka, D.F., Meshulam, G., Berkovic, G., Kotler, Z., Mazor, R., Khodorkovsky, V., *Eur. J. Org. Chem.,* **2001**, 2671.

[31] Jayaprakash, K.N., Ray, P.C., Matsuoka, I., Bhadbhade, M.M., Puranik, V.G., Das, P.K., Nishihara, H., Sarkar, A., *Organometallics,* **1999**, *18*, 3851.

[32] Calabrese, J.C., Cheng, L.T., Green, J.C., Marder, S.R., Tam, W., *J. Am. Chem. Soc.,* **1991**, *113*, 7227.

[33] Polin, J., Buchmeiser, M., Nock, H., Schottenberger, H., *Mol. Cryst. Liq. Cryst.,* **1997**, *293*, 287.

[34] Tamm, M., Bannenberg, T., Baum, K., Frohlich, R., Steiner, T., Meyer-Friedrichsen, T., Heck, J., *Eur. J. Inorg. Chem.,* **2000**, 1161.

[35] Barlow, S., Bunting, H.E., Ringham, C., Green, J.C., Bublitz, G.U., Boxer, S.G., Perry, J.W., Marder, S.R., *J. Am. Chem. Soc.,* **1999**, *121*, 3715.

[36] Olbrechts, G., Wostyn, K., Clays, K., Persoons, A., Kang, S.H., Kim, K., *Chem. Phys. Lett.,* **1999**, *308*, 173.

[37] Olbrechts, G., Strobbe, R., Clays, K., Persoons, A., *Rev. Sci. Instrum.,* **1998**, *69*, 2233.

[38] Noordman, O.F.J., van Hulst, N.F., *Chem. Phys. Lett.,* **1996**, *253*, 145.

[39] Krishnan, A., Pal, S.K., Nandakumar, P., Samuelson, A.G., Das, P.K., *Chem. Phys.,* **2001**, *265*, 313.

[40] Marder, S.R., Sohn, J.E., Stucky, G.D.: Materials for Nonlinear Optics, Washington DC, 1991.

[41] Cheng, L.T., Tam, W., Meredith, G.R., Marder, S.R., *Mol. Cryst. Liq. Cryst.,* **1990**, *189*, 137.

[42] Kanis, D.R., Ratner, M.A., Marks, T.J., *Chem. Rev.,* **1994**, *94*, 195.

[43] Muller, T.J.J., Netz, A., Ansorge, M., Schmalzlin, E., Brauchle, C., Meerholz, K., *Organometallics,* **1999**, *18*, 5066.

[44] Tamm, M., Bannenberg, T., Baum, K., Frohlich, R., Steiner, T., Meyer-Friedrichsen, T., Heck, J., *Eur. J. Inorg. Chem.,* **2000**, 1161.

[45] Lee, I.S., Seo, H.M., Chung, Y.K., *Organometallics,* **1999**, *18*, 5194.

[46] Muller, T.J.J., Netz, A., Ansorge, M., Schmalzlin, E., Brauchle, C., Meerholz, K., *Organometallics,* **1999**, *18*, 5066.

[47] Farrell, T., Meyer-Friedrichsen, T., Heck, J., Manning, A.R., *Organometallics,* **2000**, *19*, 3410.

[48] Farrell, T., Meyer-Friedrichsen, T., Malessa, M., Wittenburg, C., Heck, J., Manning, A.R., *J. Organomet. Chem.,* **2001**, *625*, 32.

[49] Roberto, D., Ugo, R., Bruni, S., Cariati, E., Cariati, F., Fantucci, P., Invernizzi, I., Quici, S., Ledoux, I., Zyss, J., *Organometallics,* **2000**, *19*, 1775.

[50] Lee, I.S., Seo, H., Chung, Y.K., *Organometallics,* **1999**, *18*, 1091.

[51] Cifuentes, M.P., Driver, J., Humphrey, M.G., Asselberghs, I., Persoons, A., Samoc, M., Luther-Davies, B., *J. Organomet. Chem.,* **2000**, *607*, 72.

[52] Weyland, T., Ledoux, I., Brasselet, S., Zyss, J., Lapinte, C., *Organometallics,* **2000**, *19*, 5235.

[53] Cadierno, V., Conejero, S., Gamasa, M.P., Gimeno, J., Asselberghs, I., Houbrechts, S., Clays, K., Persoons, A., Borge, J., Garcia-Granda, S., *Organometallics,* **1999**, *18*, 582.

[54] McDonagh, A.M., Lucas, N.T., Cifuentes, M.P., Humphrey, M.G., Houbrechts, S., Persoons, A., *J. Organomet. Chem.,* **2000**, *605*, 193.

[55] McDonagh, A.M., Humphrey, M.G., Samoc, M., Luther-Davies, B., Houbrechts, S., Wada, T., Sasabe, H., Persoons, A., *J. Am. Chem. Soc.,* **1999**, *121*, 1405.

[56] Garcia, M.H., Robalo, M.P., Dias, A.R., Piedade, M.F.M., Galvao, A., Wenseleers, W., Goovaerts, E., *J. Organomet. Chem.,* **2001**, *619*, 252.

[57] McDonagh, A.M., Cifuentes, M.P., Lucas, N.T., Humphrey, M.G., Houbrechts, S., Persoons, A., *J. Organomet. Chem.,* **2000**, *605*, 184.

[58] Wong, H., Meyer-Friedrichsen, T., Farrell, T., Mecker, C., Heck, J., *Eur. J. Inorg. Chem.,* **2000**, 631.

[59] Mata, J.A., Peris, E., Uriel, S., Llusar, R., Asselberghs, I., Persoons, A., *Polyhedron,* **2001**, *20*, 2083.

[60] Houbrechts, S., Clays, K., Persoons, A., Cadierno, V., Gamasa, M.P., Gimeno, J., *Organometallics,* **1996**, *15*, 5266.

[61] Houbrechts, S., Clays, K., Persoons, A., Cadierno, V., Gamasa, M.P., Gimeno, J., Whittall, I.R., Humphrey, M.G., *Proc. SPIE-Int. Soc. Opt. Eng.,* **1996**, *2852*, 98.

[62] Vicente, J., Chicote, M.T., Abrisqueta, M.D., de Arellano, M.C.R., Jones, P.G., Humphrey, M.G., Cifuentes, M.P., Samoc, M., Luther-Davies, B., *Organometallics,* **2000**, *19*, 2968.

[63] Whittall, I.R., Humphrey, M.G., Samoc, M., Luther-Davies., B., *Angew. Chem., Int. Ed. Engl.,* **1997**, *36*, 370.

[64] McDonagh, A.M., Humphrey, M.G., Samoc, M., Luther-Davies, B., *Organometallics,* **1999**, *18*, 5195.

[65] Rojo, G., Agullo-Lopez, F., Campo, J.A., Heras, J.V., Cano, M., *J. Phys. Chem. B,* **1999**, *103*, 11016.

[66] Mata, J.A., Peris, E., Llusar, R., Uriel, S., Cifuentes, M.P., Humphrey, M.G., Samoc, M., Luther-Davies, B., *Eur. J. Inorg. Chem.,* **2001**, 2113.

[67] Tykwinski, R.R., Gubler, U., Martin, R.E., Diederich, F., Bosshard, C., Gunter, P., *J. Phys. Chem. B,* **1998**, *102*, 4451.

Chapter 2

Ruthenium complexes incorporating extended arylalkynyl ligands and their nonlinear optical properties

---

Contents

Chapter 2

Ruthenium complexes incorporating extended arylalkynyl ligands and their nonlinear optical properties

---

2.1. Introduction

It has been shown that an important factor in the magnitude of β is the length (L) of the conjugated chain linking the donor group and acceptor group of a molecule.[1] This relationship can be expressed as:

$$\beta = \kappa L^{\eta} \qquad 2.1.$$

(where κ is a constant). As the length of the conjugated backbone increases, β increases. Provision of an extended π-conjugated backbone between strong donor and acceptor groups facilitates electron polarization, with a corresponding increase in β. Lengthening of the π-conjugated backbone and the consequent increase in β is strongly dependent upon the nature of the π-linker group. Recent research has examined a diverse range of compounds and linker groups including polyacetylenes,[2] tetraethynylethenes,[3] thiophene oligomers[4] and metallocene derivatives.[5] Regardless of the linker group utilized, a point is reached where β does not increase despite further π-system lengthening, this point being referred to as saturation. Calculations on polyphenylenic compounds[6] indicate that saturation of the β response for these systems will occur at very short conjugation lengths. ZINDO/SOS calculations suggest that polyyne-linked systems should saturate when the number of linkages (n) > 2 or 3. In related polyene compounds, saturation is not expected until n ≥ 20 (Figure 2.1.).[1] Several explanations

have been put forward to explain these differences, specifically, additional π electron contributions opposing (in sign) the usual charge-transfer contribution in the polyyne chain,[7] configuration mixing of π → π* transitions,[8] breakdown in the two-level approximation as conjugation length increases,[9] or partial breaking of the charge-transfer plane being more likely in the polyyne.[10] Cheng *et al.*[11] reported a comprehensive study of the conjugation length dependencies of the second- and third-order NLO properties and suggested that the significant differences between yne- and ene-linked architectures are due mainly to differences in orbital hybridization, leading to less effective π delocalization in the yne-linked compounds. Increasing the π-conjugation length is a common method to increase β in organic systems, and has also been applied to organometallics. For example, Whittall *et al.*[12] synthesized a systematically varied series of gold acetylide complexes which demonstrated significant enhancement of the quadratic hyperpolarizability upon extension of the π-conjugated backbone.

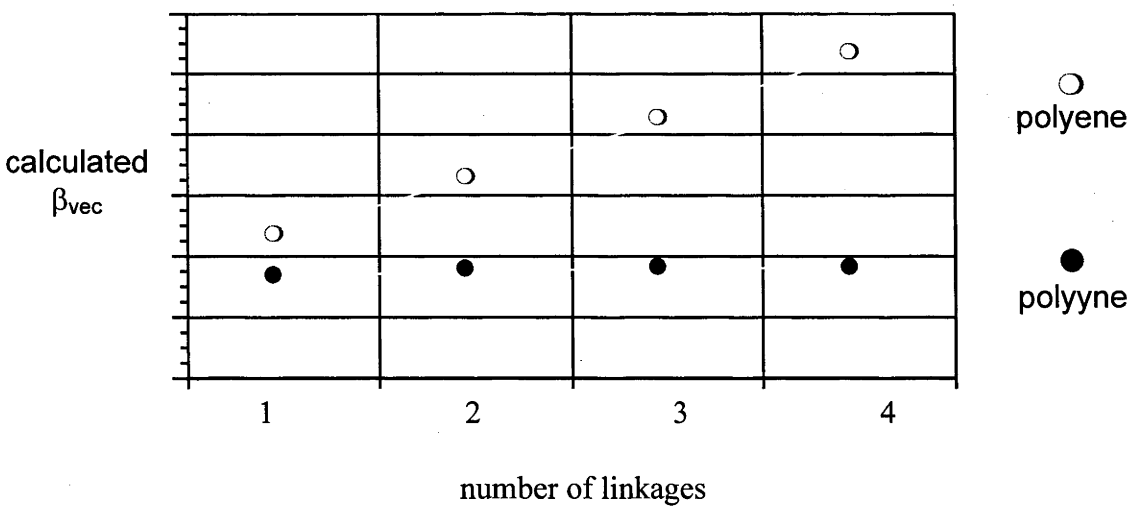

Figure 2.1. Computed β_{vec} values for π-system chain-lengthening in analogous oligo-ene and oligo-yne systems.[1]

The length and composition of π-conjugated chains is also expected to have an effect on the third-order NLO properties of donor- and acceptor-substituted molecules, and there has been significant research undertaken on conjugated, semiconducting, organic polymers.[13-15] The presence of low-energy optical absorptions and poor thermal and environmental stability has meant that initially promising materials such as polyacetylene have given way to oligomers with tunable characteristics. For third-order measurements of materials at π-system conjugation lengths shorter than those corresponding to saturation, a simple power law can be used to describe the cubic NLO response (Equation 2.2.):

$$\gamma \alpha L^{\eta} \qquad 2.2.$$

where L is the number of repeat units and η is an exponent dependent upon the nature of the repeating unit. Polyacetylene has an experimentally determined value of $\eta \approx 2.5$ with saturation at L = 120 double bonds,[16] while poly(thienylenevinylene) has $\eta = 3.82$ with the onset of saturation at L = 7-8.[17] Organometallic complexes also give enhanced γ response upon extension of the π-conjugated system.[5,18,19] Extension of the π-conjugated arylyne bridge in *trans*-bis{bis(diphenylphosphino)methane}-chlororuthenium acetylide and vinylidene complexes should therefore be a convenient method to enhance second- and third-order NLO response. Examination of this possibility is one focus of this Chapter.

The NLO merit of *trans*-bis{bis(diphenylphosphino)methane}chlororuthenium acetylide complexes has attracted significant attention recently.[20-25] Ruthenium complexes of this type have the advantage that the intermediate vinylidene complex can be isolated (Touchard *et al.*[26]) and their NLO properties examined. However, the NLO responses of organometallic vinylidene complexes have received little attention in the literature.[27-29] Cadierno *et al.*[30] compared two acetylide / vinylidene pairs coordinated to a [$Ru(PPh_3)_2$(η-indenyl)] unit and attributed the lower β and β_0 response of the

vinylidene complexes to the net positive charge on the ruthenium centre. In contrast to this result, Marder has suggested that introduction of some metal to carbon multiple-bond character should result in increased second-order hyperpolarizabilities.[31]

The first aim of the studies described in this Chapter is the synthesis of a series of organometallic complexes with extended arylyne ligands, to assess the enhancement of the quadratic and cubic nonlinearities upon π-lengthening, and examine evidence for saturation of the NLO response.

The second aim is the synthesis of a series of acetylide / vinylidene complex pairs and to contrast their second- and third-order NLO responses.

2.2. *Synthesis of terminal alkynes*

Examination of the effect of π-conjugated bridge lengthening on NLO response necessitated the preparation of extended arylalkynes. The preparation of the new organic alkynes proceeded by extending the general method of Lavastre *et al.*[32] for the preparation of substituted phenylacetylenes (Scheme 2.1.). 4,4'-$HC{\equiv}CC_6H_4C{\equiv}CC_6H_4NO_2$ was coupled with 4-$IC_6H_4C{\equiv}CSiMe_3$ under standard Sonogashira conditions[33] using $[PdCl_2(PPh_3)_2]$ and CuI as catalysts, to give the new acetylene, 4,4',4''-$Me_3SiC{\equiv}CC_6H_4C{\equiv}CC_6H_4C{\equiv}CC_6H_4NO_2$ (**3**). This method led to the synthesis of small amounts of an unidentified, intensely coloured material which was believed to be the homo-coupled product 4,4',4'',4'''-$O_2NC_6H_4C{\equiv}CC_6H_4C{\equiv}CC{\equiv}CC_6H_4C{\equiv}CC_6H_4NO_2$. This by-product could either be removed by use of column chromatography, or the side-reaction itself could be eliminated by utilizing $[Pd(PPh_3)_4]$, eliminating the CuI, and by rigorous deoxygenation of the solvent. Deprotection of **3** to the terminal alkyne **4** could be accomplished by stirring the material with tetra-*n*-butylammonium fluoride (TBAF) in dichloromethane. The new acetylenes were characterized by EI mass spectrometry, satisfactory microanalyses, UV-vis and IR spectroscopy, ^1H and ^{13}C NMR spectroscopy.

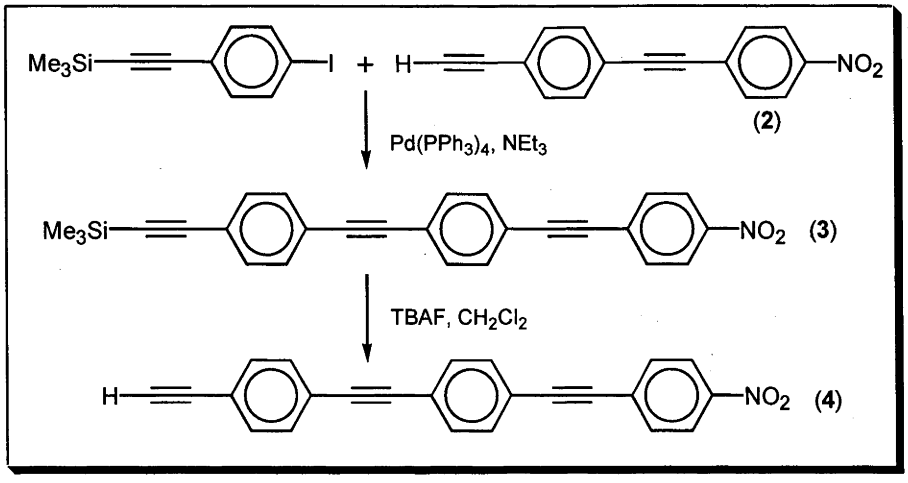

Scheme 2.1. Syntheses of extended arylalkynes.

2.3. Synthesis and characterization of ruthenium complexes

2.3.1. Synthesis of ruthenium complexes

The synthetic methodology employed for the preparation of the new complexes has been utilized previously for the preparation of the corresponding phenylacetylides. Thus, the new bis{bis(diphenylphosphino)methane}ruthenium complexes were prepared by extending the method of Touchard *et al.*,[34] a procedure which also permits isolation of the stable vinylidene intermediates. Reaction of *cis*-$[RuCl_2(dppm)_2]$, ammonium hexafluorophosphate and an excess of the terminal alkyne afforded the air-stable vinylidene complexes in good yield (Scheme 2.2.). Ammonium hexafluorophosphate was found to be superior to the literature salt sodium hexafluorophosphate in the vinylidene complex preparation due to its lower cost, and the deliquescent nature of sodium hexafluorophosphate. Deprotonation of the vinylidene complexes then resulted in the formation of the corresponding acetylide complexes (Scheme 2.2.). The new vinylidene and acetylide complexes were characterized by SI mass spectrometry, satisfactory microanalyses, UV-vis and IR spectroscopy, ^1H, ^{31}P and ^{13}C NMR spectroscopy and, in the case of **8**, by a single-crystal X-ray diffraction study.

2.3.2. Characterization of ruthenium complexes

Selected ^1H NMR data for compounds **1** - **14** are listed in Table 2.1. and the numbering scheme is displayed in Figure 2.2. The terminal acetylenes **1**, **2** and **4** all have resonances corresponding to ≡C*H* in the range 3.17 to 3.34 ppm. Hydrogen atoms on non-nitro substituted phenylene groups are in very similar environments, as indicated by a singlet for H_4 and H_5 in the ^1H NMR spectrum of **2**, and two singlets in the spectra of both **3** and **4** corresponding to the H_4/H_5 and H_{10}/H_{11} protons. The H_4 protons in the

vinylidene complexes are shifted upfield by 0.4 - 0.5 ppm compared with the analogous acetylides, probably because of the greater positive charge on the nearby ruthenium centre. Attaching acetylenes **2** or **4** to a ruthenium centre leads to differing chemical shifts for protons on the phenyl ring immediately adjacent to the ruthenium. All vinylidene and alkynyl complexes incorporating a nitro substituent possess ^{1}H NMR spectra in which protons of the adjacent phenylene group are shifted downfield due to the strong deshielding effect of the electronegative substituent. The dppm methylene groups give rise to one resonance in the ^{1}H NMR spectra of acetylide complexes but two resonances in the spectra of the corresponding vinylidene complexes; this is presumably due to the restricted rotation around the ruthenium-carbon axis in the vinylidene complex leading to a loss of a plane of symmetry present in the acetylide complex.

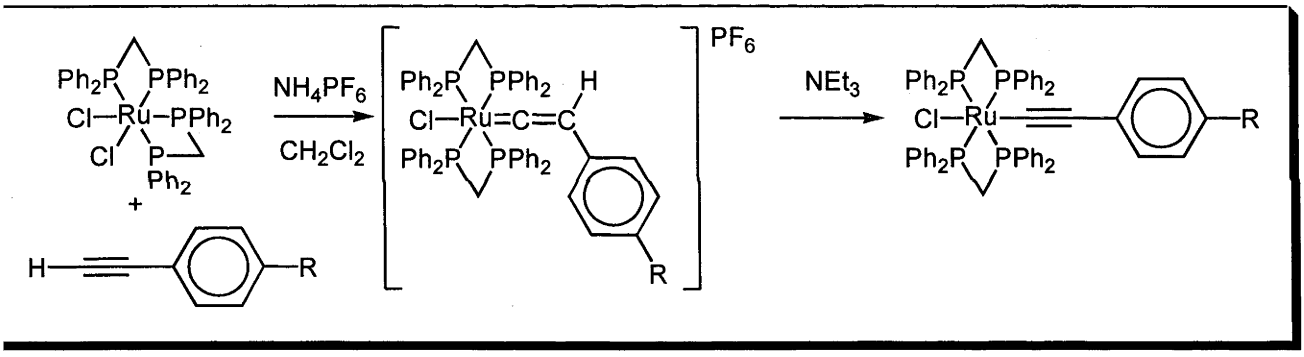

R	Vinylidene Complex	Alkynyl Complex
H	**5**	**6**
C≡CPh	**7**	**8**
NO_2	**9**	**10**
4-C≡C$C_6H_4NO_2$	**11**	**12**
4,4′-C≡CC_6H_4C≡C$C_6H_4NO_2$	**13**	**14**

Scheme 2.2. Syntheses of *trans*-bis{bis(diphenylphosphino)methane}chlororuthenium acetylide and vinylidene complexes

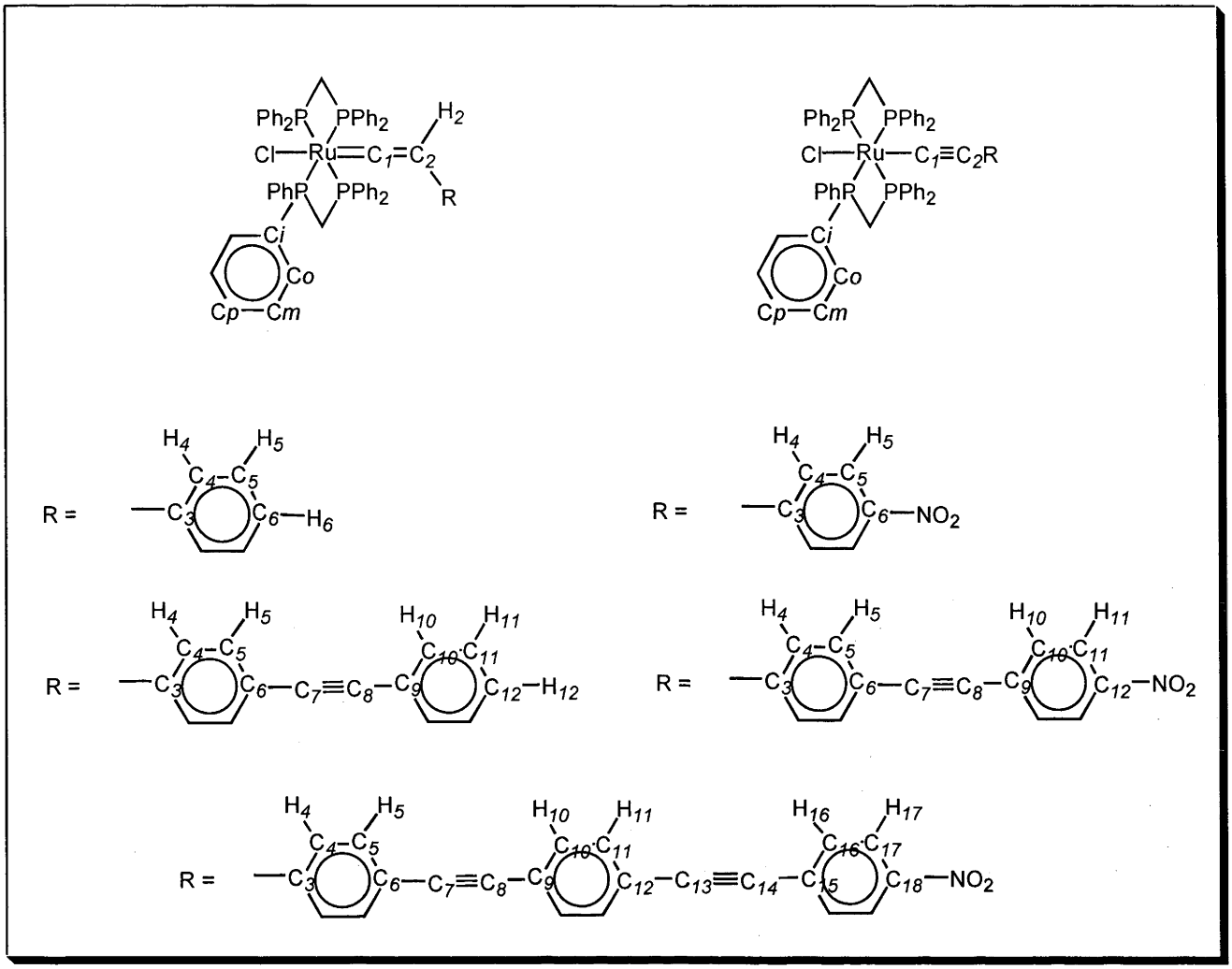

Figure 2.2. NMR numbering scheme

Table 2.2. contains IR and UV-vis data for compounds **1** - **14**. The IR spectra of the terminal alkynes possess a band corresponding to ν(C≡CH) at 2116 – 2107 cm^{-1}. The corresponding band for the trimethylsilyl-protected alkyne group in **3** occurs at 2157 cm^{-1}. The internal alkyne groups give ν(C≡C) bands at approximately 2218 cm^{-1}. Coupling **1**, **2** or **4** to a ruthenium centre shifts the ν(C≡C) band to lower frequency. Comparison of the UV-vis spectra of complexes **5** - **14** show that there is generally only a small difference in λ_{max} between the vinylidenes and their corresponding acetylide complexes, the acetylides tending to have slightly greater ε. Although replacement of the unsubstituted phenyl ring in **6** with a nitrophenyl group to afford **10** results in a

Table 2.1. Selected ^{1}H NMR data (ppm) (J_{HH}, Hz)

Compound	H_4	H_5	H_{10}	H_{11}	H_{16}	H_{17}	Ph	$P(CH_2)P$
4-HC≡$CC_6H_4NO_2$ (**1**)	7.62 (9)	8.18 (9)	--	--	--	--	--	--
4,4′-HC≡CC_6H_4C≡$CC_6H_4NO_2$ (**2**)	7.49		7.65 (9)	8.21 (9)	--	--	--	--
4,4′,4″-Me_3SiC≡CC_6H_4C≡CC_6H_4C≡$CC_6H_4NO_2$ (**3**)	7.44		7.52		7.65 (9)	8.21 (9)	--	--
4,4′,4″-HC≡CC_6H_4C≡CC_6H_4C≡$CC_6H_4NO_2$ (**4**)	7.44		7.52		7.65 (9)	8.22 (9)	--	--
trans-[Ru(C=CHPh)Cl(dppm)$_2$]PF_6 (**5**)	5.52	[a]	--	--	--	--	6.70 - 7.45	5.10, 5.33
trans-[Ru(C≡CPh)Cl(dppm)$_2$] (**6**)	[a]	[a]	--	--	--	--	6.70 - 7.55	4.89
trans-[Ru(4-C=CHC_6H_4C≡CPh)Cl(dppm)$_2$]PF_6 (**7**)	5.45 (8)	6.02 (8)	6.77 (8)	[a]	--	--	7.10 - 7.60	5.12, 5.32
trans-[Ru(4-C≡CC_6H_4C≡CPh)Cl(dppm)$_2$] (**8**)	5.97 (8)	[a]	[a]	[a]	--	--	7.00 - 7.60	4.89
trans-[Ru(4-C=$CHC_6H_4NO_2$)Cl(dppm)$_2$]PF_6 (**9**)	5.58 (9)	[a]	--	--	--	--	7.10 - 7.60	5.18, 5.30
trans-[Ru(4-C≡$CC_6H_4NO_2$)Cl(dppm)$_2$] (**10**)	5.89 (9)	7.72 (9)	--	--	--	--	7.00 - 7.70	4.91
trans-[Ru(4,4′-C=CHC_6H_4C≡$CC_6H_4NO_2$)Cl(dppm)$_2$]PF_6 (**11**)	5.50 (8)	6.89 (8)	7.64 (9)	8.20 (9)	--	--	7.10 - 7.50	5.15, 5.34
trans-[Ru(4,4′-C≡CC_6H_4C≡$CC_6H_4NO_2$)Cl(dppm)$_2$] (**12**)	5.97 (8)	[a]	7.57 (9)	8.18 (9)	--	--	7.00 - 7.50	4.90
trans-[Ru(4,4′,4″-C=CHC_6H_4C≡CC_6H_4C≡$CC_6H_4NO_2$)Cl(dppm)$_2$]PF_6 (**13**)	5.48 (8)	[a]	[a]	[a]	7.65 (8)	8.21 (9)	6.90 - 7.55	5.34, 5.13
trans-[Ru(4,4′,4″-C≡CC_6H_4C≡CC_6H_4C≡$CC_6H_4NO_2$)Cl(dppm)$_2$] (**14**)	5.97 (8)	[a]	[a]	[a]	7.65 (8)	8.22 (9)	7.00 - 7.50	4.90

[a] Obscured by other resonances.

Table 2.2. Selected IR[a] and UV-vis[b] data for compounds **1-14**.

Compound	ν(C≡C) (cm^{-1})	λ_{max} (nm) [ε (10^4 M^{-1} cm^{-1})]
4-HC≡$CC_6H_4NO_2$ (**1**)	2116	288 [1.5]
4,4′-HC≡CC_6H_4C≡$CC_6H_4NO_2$ (**2**)	2107, 2218	331 [2.8]
4,4′,4″-Me_3SiC≡CC_6H_4C≡CC_6H_4C≡$CC_6H_4NO_2$ (**3**)	2157, 2217	346 [2.5]
4,4′,4″-HC≡CC_6H_4C≡CC_6H_4C≡$CC_6H_4NO_2$ (**4**)	2109, 2218	351 [1.7]
trans-[Ru(C=CHPh)Cl(dppm)$_2$]PF_6 (**5**)	--	320 [2.1]
trans-[Ru(C≡CPh)Cl(dppm)$_2$] (**6**)	2080	313 [1.3]
trans-[Ru(4-C=CHC_6H_4C≡CPh)Cl(dppm)$_2$]PF_6 (**7**)	2064	381 [2.1]
trans-[Ru(4-C≡CC_6H_4C≡CPh)Cl(dppm)$_2$] (**8**)	2066	380 [2.9]
trans-[Ru(4-C=$CHC_6H_4NO_2$)Cl(dppm)$_2$]PF_6 (**9**)	--	471 [1.1]
trans-[Ru(4-C≡$CC_6H_4NO_2$)Cl(dppm)$_2$] (**10**)	2046	473 [1.7]
trans-[Ru(4,4′-C=CHC_6H_4C≡$CC_6H_4NO_2$)Cl(dppm)$_2$]PF_6 (**11**)	2069	461 [1.2]
trans-[Ru(4,4′-C≡CC_6H_4C≡$CC_6H_4NO_2$)Cl(dppm)$_2$] (**12**)	2064, 2059	468 [2.3]
trans-[Ru(4,4′,4″-C=CHC_6H_4C≡CC_6H_4C≡$CC_6H_4NO_2$)Cl(dppm)$_2$]PF_6 (**13**)	2211, 2065	427 [1.4]
trans-[Ru(4,4′,4″-C≡CC_6H_4C≡CC_6H_4C≡$CC_6H_4NO_2$)Cl(dppm)$_2$] (**14**)	2205, 2070	439 [2.0], 359 [3.6]

[a] In dichloromethane. [b] In thf.

red-shift in λ_{max}, insertion of an additional arylyne spacer does not automatically increase λ_{max}. For the nitro-substituted complexes, increasing the number of arylalkyne spacers from 1 to 2 (in proceeding from **8** to **12**) results in a decrease in λ_{max} for the vinylidene and acetylide complexes. Further lengthening of the arylalkyne chain (in proceeding from **12** to **14**) leads to an additional decrease in λ_{max}. Replacing the alkene bridging unit in the previously-synthesized complex *trans*-[Ru(4,4′-(*E*)-C≡CC_6H_4CH=$CHC_6H_4NO_2$)Cl(dppm)$_2$] (λ_{max} 490 nm) with an alkyne bridging unit in **8** (473 nm) results in a small blue-shift in λ_{max}. Cheng *et al.*[11] found no clear red-shifting of λ_{max} with lengthening of an acetylenic bridge and that this bridge system is poorly

delocalized, with the extent of the charge-transfer relatively independent of the length of the bridge. Previous work on ruthenium acetylides[35] has also demonstrated that extended acetylide ligands have equal or smaller values of λ_{max} than their one-ring analogues. A simple correlation between increasing chain-length and red-shifting of λ_{max} for this series of complexes cannot be assumed.

Selected ^{13}C NMR data are presented in Table 2.3. C_1 carbon atoms in the terminal acetylenes possess a chemical shift around ~79 ppm. Assigning individual resonances is difficult due to the large number of closely-spaced resonances arising from the phenyl rings of the dppm ligands. In the ^{13}C NMR spectra of the vinylidene complexes the C_1 signal is a multiplet in the region of 350 - 360 ppm. In the acetylide complexes it could not be definitively assigned. The C_2 signal generally remains invariant between corresponding vinylidene and acetylide complexes and between varying terminal groups. In the vinylidene complexes, the resonance corresponding to the bridging PCH_2P carbon is shifted upfield by 4 - 5 ppm as compared with that of the neutral acetylide complex.

Table 2.3. Selected ^{13}C NMR data (ppm)

Compound	C_1	C_2	Ph	$P(CH_2)P$
4-$HC{\equiv}CC_6H_4NO_2$ (**1**)	82.3	81.5	123.0 - 147.5	--
4,4′-$HC{\equiv}CC_6H_4C{\equiv}CC_6H_4NO_2$ (**2**)	79.6	83.0	122.0 - 147.0	--
4,4′,4″-$Me_3SiC{\equiv}CC_6H_4C{\equiv}CC_6H_4C{\equiv}CC_6H_4NO_2$ (**3**)	104.4	96.5	121.8 - 147.0	--
4,4′,4″-$HC{\equiv}CC_6H_4C{\equiv}CC_6H_4C{\equiv}CC_6H_4NO_2$ (**4**)	79.1	83.1	121.5 - 147.0	--
trans-$[Ru(C{=}CHPh)Cl(dppm)_2]PF_6$ (**5**)	356.4	109.7	125.6 - 133.0	45.7
trans-$[Ru(C{\equiv}CPh)Cl(dppm)_2]$ (**6**)	[a]	112.3	126.7 - 135.0	50.2
trans-$[Ru(4\text{-}C{=}CHC_6H_4C{\equiv}CPh)Cl(dppm)_2]PF_6$ (**7**)	360.2	110.2	126.5 - 134.0	45.8
trans-$[Ru(4\text{-}C{\equiv}CC_6H_4C{\equiv}CPh)Cl(dppm)_2]$ (**8**)	[a]	[a]	127.0 - 135.5	50.2
trans-$[Ru(4\text{-}C{=}CHC_6H_4NO_2)Cl(dppm)_2]PF_6$ (**9**)	351.4	109.4	123.0 - 144.7	45.3
trans-$[Ru(4\text{-}C{\equiv}CC_6H_4NO_2)Cl(dppm)_2]$ (**10**)	[a]	115.7	122.5 - 141.7	50.3
trans-$[Ru(4,4'\text{-}C{=}CHC_6H_4C{\equiv}CC_6H_4NO_2)Cl(dppm)_2]PF_6$ (**11**)	[a]	109.8	119.9 – 147.0	45.5
trans-$[Ru(4,4'\text{-}C{\equiv}CC_6H_4C{\equiv}CC_6H_4NO_2)Cl(dppm)_2]$ (**12**)	[a]	109.8	119.0 - 146.2	50.0
trans-$[Ru(4,4',4''\text{-}C{\equiv}CC_6H_4C{\equiv}CC_6H_4C{\equiv}CC_6H_4NO_2)Cl(dppm)_2]$ (**14**)	[a]	113.3	120.8 – 147.0	50.2

[a] Not observed.

2.4. *Electrochemistry of ruthenium complexes*

The results of cyclic voltammetric investigations of complexes **5 - 14** are summarized in Table 2.4. Alkynyl complexes are potentially useful as electronic or optoelectronic materials, and their electrochemical properties are an important indicator in this regard; the electrochemistry of alkynylmetal complexes is therefore a subject of significant current interest. Of specific relevance to the present studies, a number of reports have considered the electrochemical properties of *trans*-bis(bidentate phosphine)ruthenium alkynyl complexes,[24,36-40] but, with the exception of a brief earlier report by Naulty *et al.*,[24] the focus of these studies has been on bis(alkynyl) complexes.

Table 2.4. Cyclic voltammetry data for complexes **5 – 14** [a]

Complex	E^0_{ox} (V) [i_{pc}/i_{pa}] $Ru^{II/III}$	E^0_{red} (V) [i_{pc}/i_{pa}] $A^{0/-1}$
trans-[$RuCl_2(dppm)_2$] [b]	0.62 [1]	--
trans-[$Ru(C{=}CHPh)Cl(dppm)_2$]PF_6 (**5**)	1.38 [c]	-1.15 [d]
trans-[$Ru(C{\equiv}CPh)Cl(dppm)_2$] (**6**)	0.55 [1]	--
trans-[$Ru(4\text{-}C{=}CHC_6H_4C{\equiv}CPh)Cl(dppm)_2$]$PF_6$ (**7**)	1.34 [c]	-1.11 [d]
trans-[$Ru(4\text{-}C{\equiv}CC_6H_4C{\equiv}CPh)Cl(dppm)_2$] (**8**)	0.55 [0.9]	--
trans-[$Ru(4\text{-}C{=}CHC_6H_4NO_2)Cl(dppm)_2$]$PF_6$ (**9**)	1.56 [c]	-0.82 [0.9], -1.12 [d]
trans-[$Ru(4\text{-}C{\equiv}CC_6H_4NO_2)Cl(dppm)_2$] (**10**)	0.72 [1]	-0.81 [0.7], -1.08 [d]
trans-[$Ru(4,4'\text{-}C{=}CHC_6H_4C{\equiv}CC_6H_4NO_2)Cl(dppm)_2$]$PF_6$ (**11**)	1.42 [c]	-0.83 [0.9]
trans-[$Ru(4,4'\text{-}C{\equiv}CC_6H_4C{\equiv}CC_6H_4NO_2)Cl(dppm)_2$] (**12**)	0.57 [0.9]	-0.90 [0.7]
trans-[$Ru(4,4',4''\text{-}C{\equiv}CC_6H_4C{\equiv}CC_6H_4C{\equiv}CC_6H_4NO_2)Cl(dppm)_2$] (**14**)	0.54 [1]	-0.86 [0.9]

[a] CH_2Cl_2; Pt wire auxiliary, Pt working and Ag/AgCl reference electrodes; ferrocene/ferrocenium couple located at 0.56 V. [b] Ref.[24]. [c] Epa $Ru^{II/III}$(V) for nonreversible process. [d] Epc $A^{0/-1}$ (V) for nonreversible process.

All of the complexes studied here display an anodic wave assigned to the $Ru^{II/III}$ oxidation process. The first oxidation process in the alkynyl complexes occurs with potentials ranging from 0.54 to 0.72 V, the higher potentials being characteristic of complexes with a single-phenyl-ring arylalkynyl ligand containing the electron-withdrawing substituent NO_2. In each case this process is either reversible or quasi-reversible (ΔE 0.06 - 0.08 V, $i_{pc}/i_{pa} \sim 1$, employing standard conditions of 100 mV s^{-1} scan rate at room temperature). As expected, a sizeable shift towards more positive potentials is observed for the oxidation process in the positively charged vinylidene complexes, with the $Ru^{II/III}$ oxidation found at potentials in the range of 1.34 to 1.56 V; again, the higher potentials are observed for complexes containing electron-withdrawing aryl substituents. In contrast to the alkynyl complexes, the $Ru^{II/III}$ couple in the vinylidene complexes is irreversible under our standard conditions, approaching quasi-reversible behaviour on increasing the scan rate. For example, Figure 2.3. shows the oxidative cyclic voltammetric behaviour for the vinylidene complex $[Ru(C{=}CHPh)Cl(dppm)_2]PF_6$ (**5**) using scan rates ranging from 100 to 1200 mV s^{-1}. The $Ru^{II/III}$ oxidation has been labelled A (ΔE = 0.19 V). The signal labelled B is associated with the main $Ru^{II/III}$ oxidation process and displays a signal current independent of the scan rate; it is attributed to a redox process involving the $[Ru(C{=}CHPh)Cl(dppm)_2]^{2+}$ daughter product of the $Ru^{II/III}$ oxidation process. Higher scan rates reveal a cathodic peak (labelled C) at a potential similar to that observed for the corresponding alkynyl complex, suggesting conversion of the $[Ru(C{=}CHPh)Cl(dppm)_2]^{2+}$ product to the corresponding alkynyl cation by loss of a proton, and subsequent reduction to the neutral alkynyl complex (Scheme 2.3.). A similar deprotonation of an oxidized vinylidene complex to afford an alkynyl complex has been noted previously.[41] In some cases a second, less reversible, anodic process is observed at higher potentials, ranging from 1.42 - 1.56 V, attributed to the $Ru^{III/IV}$ oxidation process. The highest potential recorded for this second oxidation is, not

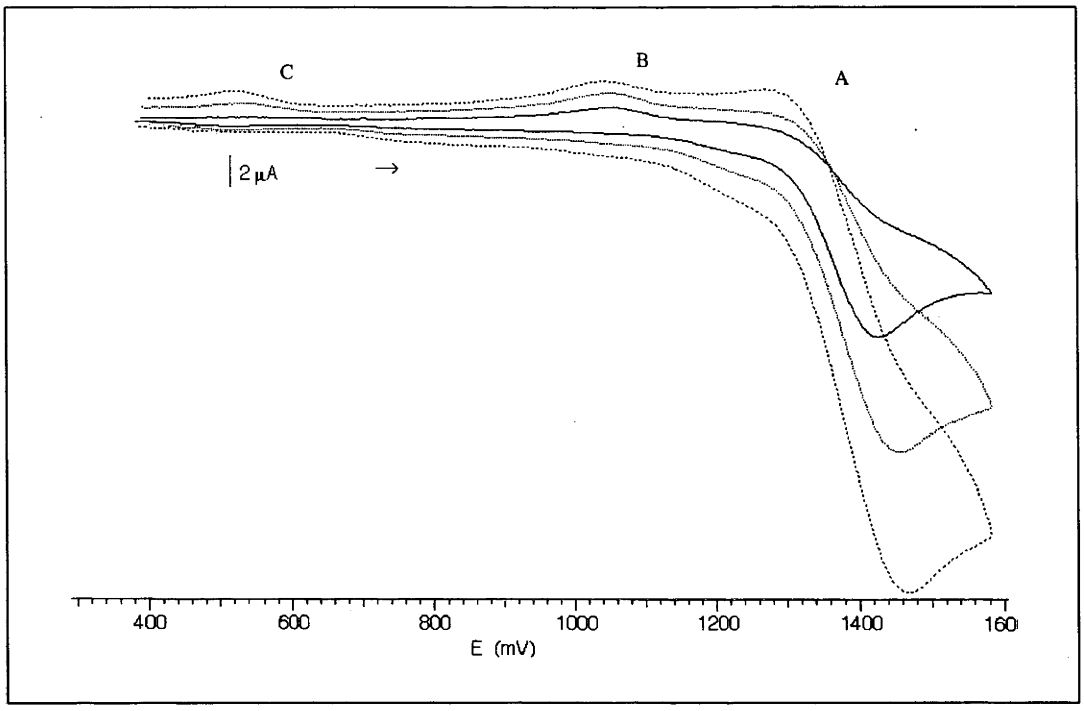

Figure 2.3. Effect of varying the scan rate from 100 (dashed line) through 400 to 1200 (solid line) mV s^{-1} on the oxidation behaviour of $[Ru(C{=}CHPh)Cl(dppm)_2]PF_6$ (**5**)

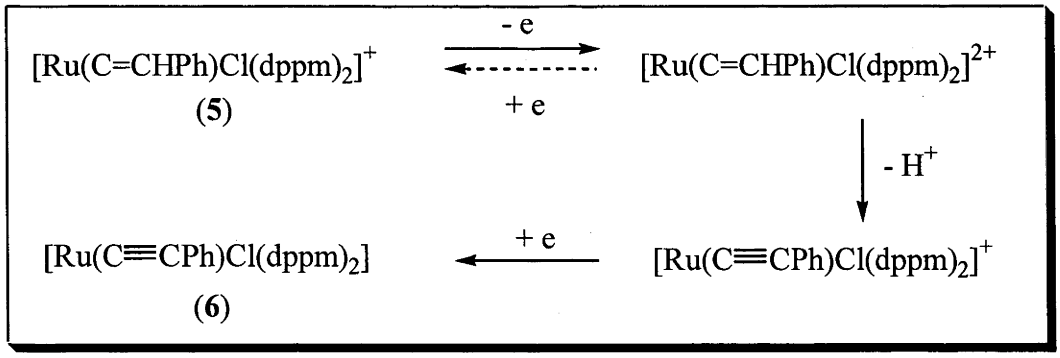

Scheme 2.3. : Proposed anodic behaviour for the vinylidene complex *trans*-$[Ru(C{=}CHPh)Cl(dppm)_2]PF_6$ (**5**)

surprisingly, that of the 4-nitrophenylvinylidene complex *trans*-[Ru(4-C=CHC$_6$H$_4$NO$_2$)Cl(dppm)$_2$]PF$_6$ (**9**).

Examination of the cyclic voltammetric data for these alkynyl and vinylidene complexes affords a series of trends. The familiar increase in the $Ru^{II/III}$ oxidation potential on addition of the electron withdrawing nitro group to the arylalkynyl ligand [35] was observed for all of the relevant complexes in this study, with similar increases found for both the alkynyl and vinylidene groups, e.g. increases of 0.17 and 0.18 V were found on proceeding from *trans*-[Ru(C≡CPh)Cl(dppm)$_2$] (**6**, 0.55 V) to *trans*-[Ru(4-C≡CC$_6$H$_4$NO$_2$)Cl(dppm)$_2$] (**10**, 0.72 V) and from *trans*-[Ru(C=CHPh)Cl(dppm)$_2$]PF$_6$ (**5**, 1.38 V) to *trans*-[Ru(4-C=CHC$_6$H$_4$NO$_2$)Cl(dppm)$_2$]PF$_6$ (**9**, 1.56 V), respectively. Chain-lengthening of the nitro-containing vinylidene ligand was found to produce a decrease in the $Ru^{II/III}$ oxidation potential, e.g. from 1.56 V for *trans*-[Ru(4-C=CHC$_6$H$_4$NO$_2$)Cl(dppm)$_2$]PF$_6$ (**9**) to 1.42 V for *trans*-[Ru(4,4'-C=CHC$_6$H$_4$C≡CC$_6$H$_4$NO$_2$)Cl(dppm)$_2$]PF$_6$ (**11**). Whittall *et al.* have previously noted a similar decrease in the oxidation potential required for the $Ru^{II/III}$ process on chain-lengthening of alkynyl complexes.[35] This effect is attenuated on further chain-lengthening, e.g. in proceeding from *trans*-[Ru(4-C≡CC$_6$H$_4$NO$_2$)Cl(dppm)$_2$] (**10**, 0.72 V) to *trans*-[Ru(4,4'-C≡CC$_6$H$_4$C≡CC$_6$H$_4$NO$_2$)Cl(dppm)$_2$] (**12**, 0.57 V), and then to *trans*-[Ru(4,4',4''-C≡CC$_6$H$_4$C≡CC$_6$H$_4$C≡CC$_6$H$_4$NO$_2$)Cl(dppm)$_2$] (**14**, 0.54 V), with the last-mentioned possessing an E^0_{ox} similar to that of *trans*-[Ru(C≡CPh)Cl(dppm)$_2$] (**6**, 0.55 V) which lacks an acceptor group. In the present study, the absence of an acceptor group influencing the oxidation potential results in chain lengthening from the phenylalkynyl complex **6** to *trans*-[Ru(4-C≡CC$_6$H$_4$C≡CPh)Cl(dppm)$_2$] (**8**) having no effect on the oxidation potentials (both 0.55 V); the corresponding vinylidene complexes were also found to have similar oxidation potentials (1.38 V **5**, and 1.34 V **7**).

Cyclic voltammetric scans to -1.4 V were carried out for each complex; results are summarized in Table 2.4. and were found to be dependent on the length and substituents of the alkynyl ligand, as well as on the charge of the complex. The following trends were noted. Alkynyl complexes **6** and **8** (which lack a formal acceptor substituent) displayed no reduction peaks in the region sampled; however, vinylidene complexes **5** and **7** (lacking formal acceptor groups) showed a single, non-reversible reduction process occurring with potentials in the range -1.11 to -1.15 V. Varying the scan rate from 100 mV s^{-1} to 1000 mV s^{-1} was found to have little effect on the reversibility of this redox process. The 4-nitrophenylalkynyl complex **10** and corresponding vinylidene complex **9** displayed two reduction processes, centred at potentials of -0.8 and -1.1 V, presumably due to the $Ru^{I/II}$ and NO_2 reduction processes. In contrast, complexes **11** and **12** showed only a single reduction process at around –0.85 V. Figure 2.4. shows the cathodic behaviour for *trans*-[Ru(4-C=CHC_6H_4C≡CPh)Cl(dppm)$_2$]PF_6 (**7**), using a starting potential of 0.8 V and a switching potential just beyond that required for the first vinylidene reduction process, in this case -1.4 V. Initial scans and scans using a switching potential of 0 V (dotted lines) show no oxidation peaks around 0.5 V. When the scan is extended past the vinylidene complex reduction process, however, a reversible oxidation process is apparent at 0.5 V, suggesting conversion of the reduced vinylidene complex to the corresponding alkynyl complex via hydrogen loss (Scheme 2.4.). Similar reduction of vinylidene complex to alkynyl complex with loss of hydrogen has been noted previously. [41]

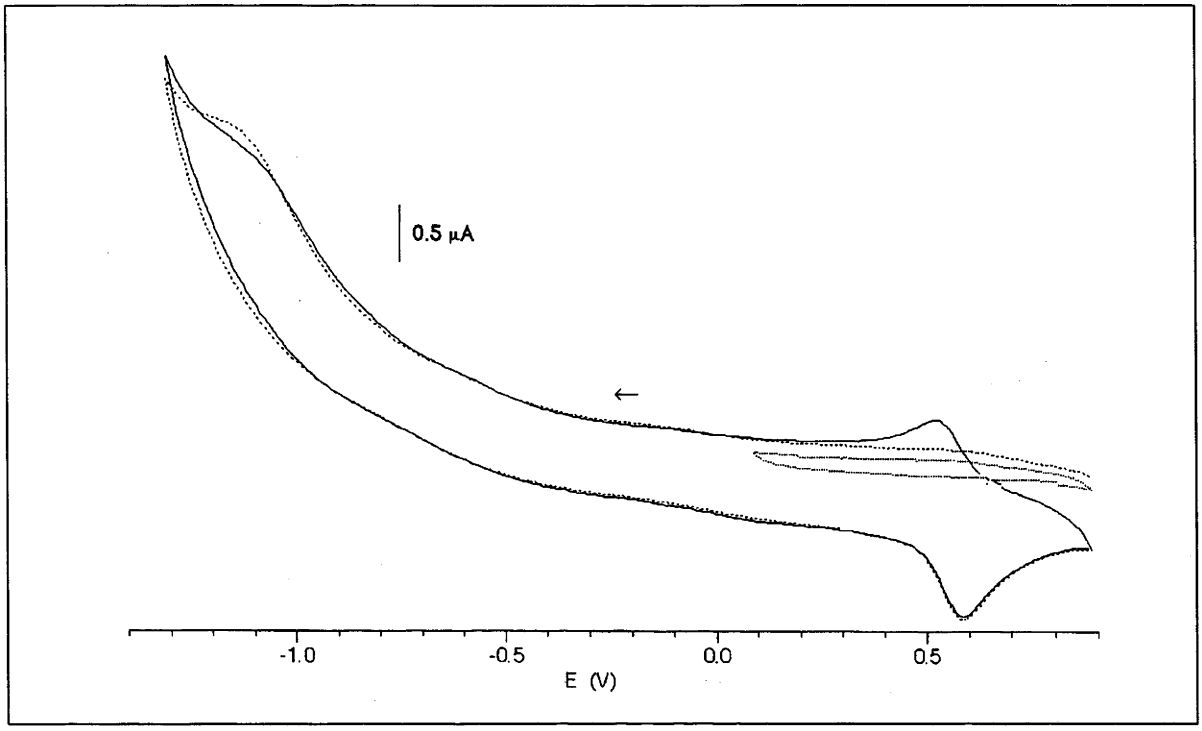

Figure 2.4. Comparison of results from cathodic cyclic voltammetry scans for *trans*-[Ru(4-C=CHC$_6$H$_4$C≡CPh)Cl(dppm$_2$)]PF$_6$ (**7**) using switching potentials of –1.4 (two successive scans) and 0 V

$$2[Ru(4\text{-}C{=}CHC_6H_4C{\equiv}CPh)Cl(dppm)_2]^+ \xrightarrow{+\,e} 2[Ru(4\text{-}C{=}CHC_6H_4C{\equiv}CPh)Cl(dppm)_2]$$

(**7**)

$$2[Ru(4\text{-}C{=}CHC_6H_4C{\equiv}CPh)Cl(dppm)_2] \xrightarrow{-\,H_2} 2[Ru(4\text{-}C{\equiv}CC_6H_4C{\equiv}CPh)Cl(dppm)_2]$$

(**8**)

Scheme 2.4. : Proposed cathodic behaviour for the vinylidene complex *trans*-[Ru(4-C=CHC$_6$H$_4$C≡CPh)Cl(dppm)$_2$]PF$_6$ (**7**)

2.5. X-ray structural study of trans-[Ru(4-C≡CC$_6$H$_4$C≡CPh)Cl(dppm)$_2$] (8)

A single-crystal X-ray diffraction study of *trans*-[Ru(4-C≡CC$_6$H$_4$C≡CPh)Cl(dppm)$_2$] (**8**) has been performed. An ORTEP plot of the complex is displayed in Figure 2.5. and selected bond lengths and angles are gathered in Table 2.5. A comparison of selected bond lengths and angles with those of related complexes appears in Table 2.6.

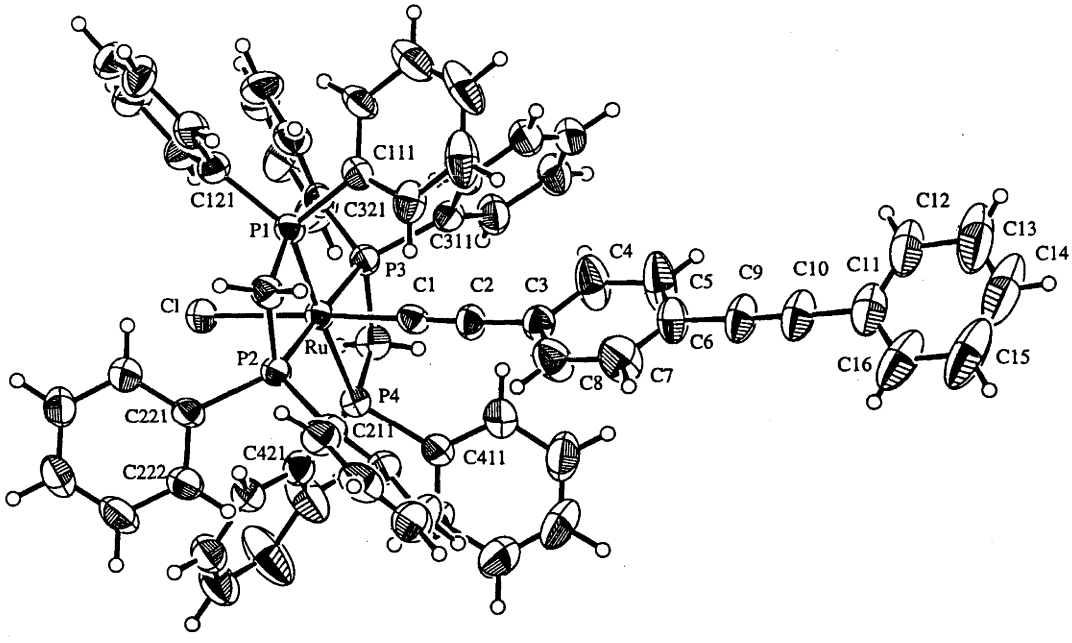

Figure 2.5. Molecular geometry and atomic labeling scheme for *trans*-[Ru(4-C≡CC$_6$H$_4$C≡CPh)Cl(dppm)$_2$] (**8**). 30% thermal ellipsoids are shown for the non-hydrogen atoms. Hydrogen atoms drawn as circles. (Crystal structure provided by A.C. Willis and N.T. Lucas).

No structural studies of complexes with the alkynyl ligand from **8** have been reported previously. The bond lengths and angles about the Cl-Ru-C(1)-C(2)-C(3) unit are not unusual, the Cl-Ru, Ru–C(1) and C(2)-C(3) data falling within the range of those previously reported for related octahedral *trans*-bis(bidentate phosphine)ruthenium alkynyl complexes (Table 2.6.).[22,24,42] Of particular interest for NLO merit is the co-planarity of phenyl rings in the alkynyl ligand; previously, semi-empirical ZINDO has been used to examine the effect upon quadratic optical nonlinearity of phenyl-phenyl rotation in *trans*-[Ru(4,4′-C≡C$C_6H_4C_6H_4NO_2$)Cl(dppm)$_2$], for which a variation of 50 % was found between maximum (co-planarity) and minimum (orthogonality) responses.[42] Co-planarity, and efficient delocalization, is therefore important for maximizing NLO response in the present complexes. The phenyl-phenyl dihedral angle for the 4-(phenylethynyl)phenylethynyl ligand in **8** (26.75 °) is significantly distorted from the idealized coplanarity (0 °).

Table 2.5. Selected bond distances (Å) and angles (deg) for *trans*-[Ru(4-C≡CC$_6$H$_4$C≡CPh)Cl(dppm)$_2$] (**8**)

Ru - Cl	2.482(2)	Ru - P(1)	2.356(2)
Ru - P(2)	2.336(2)	Ru - P(3)	2.356(2)
Ru - P(4)	2.343(2)	Ru - C(1)	1.984(8)
P(1) - C(120)	1.830(9)	P(2) - C(120)	1.822(9)
P(3) - C(340)	1.846(9)	P(4) - C(340)	1.814(9)
C(1) - C(2)	1.20(1)	C(2) - C(3)	1.43(1)
C(3) - C(4)	1.35(1)	C(3) - C(8)	1.36(1)
C(4) - C(5)	1.39(1)	C(7) - C(8)	1.40(1)
C(5) - C(6)	1.33(1)	C(6) - C(7)	1.33(1)
C(6) - C(9)	1.43(1)	C(9) - C(10)	1.18(1)
C(10) - C(11)	1.45(1)	C(11) - C(12)	1.38(2)
C(12) - C(13)	1.43(2)	C(13) - C(14)	1.32(4)
C(14) - C(15)	1.41(4)	C(15) - C(16)	1.40(2)
C(11) - C(16)	1.35(2)		
Cl(1) - Ru - P(1)	96.93(7)	Cl(1) - Ru - P(2)	94.49(8)
Cl(1) - Ru - P(3)	86.64(8)	Cl(1) - Ru - P(4)	86.94(8)
Cl(1) - Ru - C(1)	175.9(2)	P(1) - Ru - P(2)	72.10(8)
P(1) - Ru - P(3)	108.68(8)	P(1) - Ru - P(4)	176.11(8)
P(2) - Ru - P(3)	178.56(8)	P(2) - Ru - P(4)	107.26(8)
P(3) - Ru - P(4)	71.89(8)	Ru - P(1) - C(120)	94.2(3)
Ru - P(2) - C(120)	95.1(3)	Ru - P(3) - C(340)	93.8(3)
Ru - P(4) - C(340)	95.1(3)	Ru - C(1) - C(2)	178.7(8)
C(1) - C(2) - C(3)	178(1)	C(2) - C(3) - C(4)	123.4(9)
C(2) - C(3) - C(8)	122(1)	C(3) - C(4) - C(5)	123(1)
C(3) - C(8) - C(7)	122(1)	C(4) - C(5) - C(6)	121(1)
C(6) - C(7) - C(8)	121(1)	C(5) - C(6) - C(7)	118(1)
C(5) - C(6) - C(9)	120(1)	C(7) - C(6) - C(9)	122(1)
C(6) - C(9) - C(10)	179(1)	C(9) - C(10) - C(11)	178(2)
C(10) - C(11) - C(12)	117(2)	C(11) - C(12) - C(13)	121(2)
C(12) - C(13) - C(14)	118(3)	C(13) - C(14) - C(15)	124(3)
C(14) - C(15) - C(16)	116(2)	C(11) - C(16) - C(15)	123(2)

Table 2.6. Comparison of selected bond lengths in **8** with those of analogous complexes

Compound	Ru-C(1)	C(1)-C(2)	C(2)-C(3)	Cl-Ru-C(1)	Ru-C(1)-C(2)	C(1)-C(2)-C(3)	Reference
trans-[Ru(4-C≡CC_6H_4C≡CPh)Cl(dppm)$_2$] (**8**)	1.984(8)	1.20(1)	1.43(1)	175.9(2)	178.7(8)	178(1)	This work
trans-[Ru(4,4′-C≡C$C_6H_4C_6H_4NO_2$)Cl(dppm)$_2$]	1.994(4)	1.198(6)	1.439(7)	175.2(1)	177.9(4)	179.1(5)	42
trans-[Ru{(*E*)-4,4′-C≡CC_6H_4N=N$C_6H_4NO_2$}Cl(dppm)$_2$]	1.974(7)	1.224(9)	1.406(9)	173.1(2)	175.2(6)	179.8(9)	23
trans-[Ru{(*E*)-4,4′-C≡CC_6H_4CH=CH$C_6H_4NO_2$}Cl(dppe)$_2$]	1.996(4)	1.205(7)	1.434(7)	171.8(1)	177.4(4)	174.4(5)	43

2.6. *Nonlinear optical investigations*

2.6.1. Second-order NLO studies

Measurements of the second-order nonlinearities of the new metal complexes and some of their organic precursors were performed at 1064 nm using the hyper-Rayleigh scattering technique by collaborators at the University of Leuven, Belgium. The results are presented in Table 2.7.

As discussed in Chapter 1, NLO responses are frequency-dependent. To permit estimation of frequency-independent nonlinearities, the two-level model has been developed, which affords two-level corrected nonlinearities β_0. However, the two-state model may not be adequate for the donor-acceptor organometallic complexes in this study. It has been suggested that the two-state model is appropriate in the limited cases where structural change is restricted to the molecular component responsible for the charge-transfer band contributing to the hyperpolarizability.[44] The low-energy band for the present series of complexes is the MLCT band; as the higher-energy bands for chlorobis(bidentate phosphine)ruthenium alkynyl complexes are associated with transitions involving other ligands,[24] with little change in dipole moment between ground and excited states (and hence only a small contribution to the optical nonlinearity), it is possible that the two-level corrected values may have some significance as an indicator of frequency-independent nonlinearity.

Inspection of the data for the precursor acetylenes reveals that β and β_0 increase upon chain-lengthening (proceeding from **1** to **2**) a well-established structure-NLO activity trend for organic donor-bridge-acceptor molecules.

Table 2.7. Second-order NLO results measured by HRS at 1064 nm.

Compound	λ_{max} (nm), [ε (10^4 M^{-1} cm^{-1})]	β_{HRS} [a] (10^{-30} esu)	β_0 [a,b] (10^{-30} esu)
4-HC≡$CC_6H_4NO_2$ (**1**)	288 [1.5]	14	9
4,4′-HC≡CC_6H_4C≡$CC_6H_4NO_2$ (**2**)	331 [2.8]	31	17
trans-[Ru(C=CHPh)Cl(dppm)$_2$]PF_6 (**5**)	320 (sh) [0.6]	24	16
trans-[Ru(C≡CPh)Cl(dppm)$_2$] (**6**)	313 [1.3]	20	12
trans-[Ru(4-C=CHC_6H_4C≡CPh)Cl(dppm)$_2$]PF_6 (**7**)	381 [2.1]	64	31
trans-[Ru(4-C≡CC_6H_4C≡CPh)Cl(dppm)$_2$] (**8**)	380 [2.9]	101	43
trans-[Ru(4-C=$CHC_6H_4NO_2$)Cl(dppm)$_2$]PF_6 (**9**)	471 [3.5]	721	127
trans-[Ru(4-C≡$CC_6H_4NO_2$)Cl(dppm)$_2$] (**10**)	473 [1.7]	767	129
trans-[Ru(4,4′-C=CHC_6H_4C≡$CC_6H_4NO_2$)Cl(dppm)$_2$]PF_6 (**11**)	461 [1.2]	424	122
trans-[Ru(4,4′-C≡CC_6H_4C≡$CC_6H_4NO_2$)Cl(dppm)$_2$] (**12**)	468 [1.4]	833	161
trans-[Ru(4,4′,4″-C≡CC_6H_4C≡CC_6H_4C≡$CC_6H_4NO_2$)Cl(dppm)$_2$] (**14**)	439 [2.0]	1379	365
trans-[Ru{(*E*)-4,4′-C≡CC_6H_4CH=$CHC_6H_4NO_2$}Cl(dppm)$_2$][24]	490 [2.6]	1964	235

[a] All measurements in thf solvent. All complexes are optically transparent at 1064 nm; values ±10 %. [b] HRS at 1064 nm corrected for resonance enhancement at 532 nm using the two-level model with $\beta_0 = \beta[1-(2\lambda_{max}/1064)^2][1-(\lambda_{max}/1064)^2]$; damping factors not included.

Examination of the data reveals that proceeding from organic acetylene to organometallic vinylidene or alkynyl complex by incorporation of the electron-rich ligated metal (functioning as a strong donor group) results in a significant increase in β and β_0. Additionally, introduction of an acceptor group (proceeding from 4-H to 4-NO_2) results in increasing β and β_0. Chain-lengthening in proceeding from **10** and **12** to **14** results in increased β and β_0. Surprisingly, proceeding from **10** to **12** does not result in a significant increase in β or β_0. It has been shown with organic compounds that "chain-lengthening" arylalkynes leads to a saturation of the β response for two repeat units, whereas the β response for oligo-phenylenevinylene compounds does not saturate until the complex contains approximately twenty repeat units.[1] The present compounds afford an unusual series for which minimal increase in β or β_0 (within the error margin of ±10%) is seen on progressing from n = 0 to 1 for *trans*-[Ru{4-C≡C(C_6H_4-4-C≡C)$_n$$C_6H_4NO_2$}Cl(dppm)$_2$] but a significant increase is seen on progressing to n = 2. For this series of complexes, increasing β is not correlated with a red-shift in λ_{max}; chain-lengthening is accompanied by a blue-shift in optical absorption maxima. Replacing an yne-linkage by an ene-linkage results in increased β and β_0 as demonstrated in proceeding from **12** to *trans*-[Ru(4,4′-C≡CC_6H_4CH=CH$C_6H_4NO_2$)Cl(dppm)$_2$], in agreement with previously obtained results.[12,18]

The present series of data also provide the opportunity to assess the effect of deprotonation, in proceeding from vinylidene complex to alkynyl derivative. One would perhaps expect that replacing the electron-rich ruthenium donor in the alkynyl complexes with a cationic ruthenium in the vinylidene complexes would result in a significant decrease in nonlinearity. In this study, some vinylidene / alkynyl complex pairs have similar nonlinearities (e.g. **5**, **6**; **9**, **10**), and in some instances β(vinylidene) < β(alkynyl complex) (e.g. **7**, **8**; **11**, **12**). If β_{exp} and β_0 values for vinylidene / alkynyl

complex pairs differ sufficiently to readily distinguish β signals into bi-stable "off" and "on" states, the alkynyl complexes can be reprotonated to afford the precursor vinylidene complex, and this sequence can be repeated. These complex pairs can provide a protically-switchable NLO-active system where the "on" signal is the alkynyl complex (see Figure 2.6.).

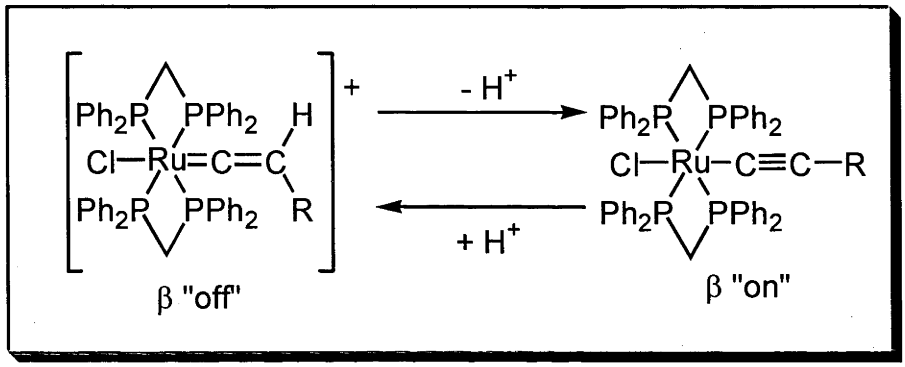

Figure 2.6. Interconversion between a protiovinylidene complex and the related acetylide complex.

2.6.2. Third-order NLO studies

Measurements of third-order optical nonlinearities were carried out by the author with assistance from Dr M. Samoc using the Z-scan technique (see Section 1.3.5.) at 800 nm. The results are presented in Table 2.8. Results for the precursor acetylenes are consistent with their having modest $|\gamma|$ values consisting of a positive real component (γ_{real}) and a small (in some cases, not detectable) imaginary component (γ_{imag}), and with an increase in cubic nonlinearity on chain-lengthening. Nonlinearities of the vinylidene and alkynyl complexes are characterized by large error margins in many instances, rendering extraction of structure-property relationships difficult, and negative real components and significant imaginary components for many complexes, indicative of two-photon resonance effects. Nevertheless, as observed with β_{exp} and β_0 trends, the effect of chain lengthening on $|\gamma|$ is insignificant within error margins on proceeding

Table 2.8. Third-order NLO results measured by Z-scan at 800 nm .[a]

Compound	γ_{real} (10^{-36} esu)	γ_{imag} (10^{-36} esu)	$\lvert\gamma\rvert$ (10^{-36} esu)
4-HC≡CC$_6$H$_4$C≡CPh	25 ± 10	<6	25 ± 10
4,4′-HC≡CC$_6$H$_4$C$_6$H$_4$NO$_2$	20 ± 10	15 ± 7	25 ± 10
4-HC≡CC$_6$H$_4$NO$_2$ (**1**)	< 80	10 ± 5	10 ± 5
4,4′-HC≡CC$_6$H$_4$C≡CC$_6$H$_4$NO$_2$ (**2**)	120 ± 20	0	120 ± 20
trans-[Ru(C=CHPh)Cl(dppm)$_2$]PF$_6$ (**5**)	< 440	0	< 440
trans-[Ru(C≡CPh)Cl(dppm)$_2$] (**6**)	< 120	0	< 120
trans-[Ru(4-C=CHC$_6$H$_4$C≡CPh)Cl(dppm)$_2$]PF$_6$ (**7**)	< 500	0	< 500
trans-[Ru(4-C≡CC$_6$H$_4$C≡CPh)Cl(dppm)$_2$] (**8**)	65 ± 40	520 ± 100	520 ± 200
trans-[Ru(4-C=CHC$_6$H$_4$NO$_2$)Cl(dppm)$_2$]PF$_6$ (**9**)	< 50	3 ± 3	< 50
trans-[Ru(4-C≡CC$_6$H$_4$NO$_2$)Cl(dppm)$_2$] (**10**)[42]	170 ± 34	230 ± 46	290 ± 60
trans-[Ru(4,4′-C=CHC$_6$H$_4$C≡CC$_6$H$_4$NO$_2$)Cl(dppm)$_2$]PF$_6$ (**11**)	< 500	420 ± 60	420 ± 60
trans-[Ru(4,4′-C≡CC$_6$H$_4$C≡CC$_6$H$_4$NO$_2$)Cl(dppm)$_2$] (**12**)	-160 ± 80	160 ± 60	230 ± 100
trans-[Ru(4,4′,4″-C≡CC$_6$H$_4$C≡CC$_6$H$_4$C≡CC$_6$H$_4$NO$_2$)Cl(dppm)$_2$] (**14**)	-920 ± 200	970 ± 200	1300 ± 300

[a] All measurements as thf solutions (all complexes are optically transparent at 800 nm). All results are referenced to silica, nonlinear refractive index $n_2 = 3 \times 10^{-16}$ cm^2 W^{-1}.

from **10** to **12**, but there is a dramatic increase in $|\gamma|$ in proceeding to **14**. The vinylidene / alkynyl pair **9** and **10** have significantly different γ_{imag} values. Since γ_{imag} is related to the two-photon absorption (TPA) cross-section σ_2, the significant variation in γ_{imag} values for this pair provides protically-switchable materials in which the TPA response can be alternatively switched "on" (**10**) and "off" (**9**).

2.7. Conclusions

The complexes *trans*-[Ru(C=CHR)Cl(dppm)$_2$]PF$_6$ (R = 4-C$_6$H$_4$C≡CPh, 4,4′-C$_6$H$_4$C≡CC$_6$H$_4$NO$_2$, 4,4′,4″-C$_6$H$_4$C≡CC$_6$H$_4$C≡CC$_6$H$_4$NO$_2$) and *trans*-[Ru(C≡CR)Cl(dppm)$_2$] (R = 4-C$_6$H$_4$C≡CPh, 4,4′-C$_6$H$_4$C≡CC$_6$H$_4$NO$_2$, 4,4′,4″-C$_6$H$_4$C≡CC$_6$H$_4$C≡CC$_6$H$_4$NO$_2$) have been synthesized and an X-ray structural study of *trans*-[Ru(4-C≡CC$_6$H$_4$C≡CPh)Cl(dppm)$_2$] completed. Cyclic voltammetric, linear optical, and quadratic and cubic nonlinear optical response data for these new complexes have been collected. Oxidation potentials for the $Ru^{II/III}$ couple increase on proceeding from neutral alkynyl complex to analogous cationic vinylidene complex and on introduction of a NO_2 acceptor group; the complexes with 4-C≡CC$_6$H$_4$NO$_2$ ligands are the most difficult to oxidize. In some instances, the $Ru^{I/II}$ processes have been identified together with, where relevant, nitro-centred reduction processes. The vinylidene complexes are capable of being electrochemically converted into the corresponding alkynyl complexes upon oxidation or reduction. Optical absorption maxima undergo a red-shift upon increase of acceptor strength. Proceeding from vinylidene complex to analogous alkynyl complex results in a small red-shift in absorption maxima and a significant increase in extinction coefficient. Quadratic molecular nonlinearities by hyper-Rayleigh scattering measurements at 1064 nm increase upon introduction of ligated metal (proceeding from precursor alkyne to alkynyl or vinylidene complex), increasing acceptor strength and alkynyl chain-lengthening (in the series [4-C≡CC$_6$H$_4$]$_n$-4-NO$_2$, proceeding from n = 1 and 2 to 3). Significant differences in β value for a vinylidene/alkynyl complex pair suggest that they could function as precursors to protically-switchable quadratic NLO materials at 1064 nm. Cubic molecular nonlinearities by Z-scan measurements at 800 nm are in many cases characterized by negative real and significant imaginary components, indicative of two-photon effects; nevertheless, a substantial increase in $|\gamma|$ on

proceeding to the largest molecule, *trans*-[Ru(4,4′,4″-$C{\equiv}CC_6H_4C{\equiv}CC_6H_4C{\equiv}CC_6H_4NO_2$)Cl(dppm)$_2$], is observed. The significant differences in γ_{imag} values (and therefore two-photon absorption (TPA) cross-sections σ_2) for some of the vinylidene / alkynyl complex pairs (i.e. **9** and **10**) suggest that they may have potential as protically-switchable TPA materials at 800 nm.

2.8. Experimental

2.8.1 General Conditions, Reagents and Instruments

General Conditions

All reactions were performed under a nitrogen atmosphere with the use of standard Schlenk techniques unless otherwise stated. Dichloromethane and triethylamine were dried by distilling over calcium hydride, and diethyl ether and tetrahydrofuran were dried by distilling over sodium / benzophenone; other solvents were used as received. "Petroleum spirit" refers to a fraction of petroleum ether of boiling range 60-80 °C. Chromatography was on silica gel (230-400 mesh ASTM) or basic ungraded alumina.

Reagents

The following reagents were prepared by the literature procedures: *cis*-$[RuCl_2(dppm)_2]$,[45] 4-$IC_6H_4C{\equiv}CSiMe_3$,[46] 4-$HC{\equiv}CC_6H_4NO_2$ (**1**),[33] 4-$HC{\equiv}CC_6H_4C{\equiv}CPh$ and 4,4'-$HC{\equiv}CC_6H_4C{\equiv}CC_6H_4NO_2$ (**2**),[32] *trans*-$[Ru(C{=}CHPh)Cl(dppm)_2]PF_6$ (**5**) and *trans*-$[Ru(C{\equiv}CPh)Cl(dppm)_2]$ (**6**),[34] *trans*-$[Ru(4\text{-}C{=}CHC_6H_4NO_2)Cl(dppm)_2]PF_6$ (**9**) and *trans*-$[Ru(4\text{-}C{\equiv}CC_6H_4NO_2)Cl(dppm)_2]$ (**10**).[47] Ammonium hexafluorophosphate (Aldrich), $[PdCl_2(PPh_3)_2]$ (PMO), $NBu^n{}_4F$ (Aldrich) and CuI (Fluka) were used as received. $[Pd(PPh_3)_4]$ was a gift from Dr B.L. Flynn.

Instruments

EI (electron impact) mass spectra (both unit resolution and high resolution (HRS)) were recorded using a VG Autospec instrument (70 eV electron energy, 8 kV accelerating potential) and secondary ion (SI) mass spectra were recorded using a VG ZAB 2SEQ instrument (30 kV Cs^+ ions, current 1 mA, accelerating potential 8 kV, 3-nitrobenzyl alcohol matrix) at the Research School of Chemistry, Australian National University;

peaks are reported as *m/z* (assignment, relative intensity). Microanalyses were carried out at the Research School of Chemistry, Australian National University. Infrared spectra were recorded either as 1% KBr discs or dichloromethane solutions using a Perkin-Elmer System 2000 FT-IR. ^{1}H, ^{31}P, and ^{13}C NMR spectra were recorded using a Varian Gemini-300 FT NMR spectrometer and are referenced to residual chloroform (7.24 ppm), *d*-chloroform (77.0 ppm) or external 85% H_3PO_4 (0.0 ppm), respectively. The assignments follow the numbering scheme shown in Figure 2.2. UV-vis spectra are as solutions in tetrahydrofuran in 1 cm quartz cells using a Cary 5 spectrophotometer. Electrochemical measurements were recorded using a MacLab 400 interface and MacLab potentiostat from ADinstruments. The supporting electrolyte was 0.1 M $[NBu^{n}_4][PF_6]$ in distilled, deoxygenated CH_2Cl_2. Solutions containing *ca.* 1 x 10^{-3} M complex were maintained under nitrogen. Measurements were carried out at room temperature using platinum disc working-, Pt wire auxiliary- and Ag/AgCl reference-electrodes, such that the ferrocene/ferrocenium redox couple was located at 0.56 V with a peak separation of around 0.09 V. Scan rates were typically 100 mVs^{-1}.

2.8.2. Syntheses of terminal alkynes

2.8.2.1. 4,4',4''-$Me_3SiC{\equiv}CC_6H_4C{\equiv}CC_6H_4C{\equiv}CC_6H_4NO_2{\cdot}0.5MeOH$ (3)

4,4'-$HC{\equiv}CC_6H_4C{\equiv}CC_6H_4NO_2$ (**2**) (100 mg, 0.31 mmol), 4-$Me_3SiC{\equiv}CC_6H_4I$ (113 mg, 0.38 mmol) and $[Pd(PPh_3)_4]$ (15 mg) were heated in refluxing triethylamine (50 mL) overnight. The solution was filtered through a silica plug and the solvent removed under reduced pressure to yield the pale yellow product which was recrystallized from methanol / dichloromethane (74 mg, 56 %). Anal. Calcd for $C_{27.5}H_{23}NO_{2.5}Si$: C 75.84, H 5.32, N 3.22 %. Found: C 76.07, H 5.27, N 3.25 %. IR: (CH_2Cl_2) $\nu(Me_3SiC{\equiv})$ 2157 cm^{-1}, $\nu(C{\equiv}C)$ 2217 cm^{-1}. UV-Vis: λ (thf) 346 nm, ε 25 300

M^{-1} cm^{-1}. ^1H NMR: (δ, 300 MHz, $CDCl_3$); 0.24 (s, 9H, $SiMe_3$), 3.47 (s, 1.5H, MeOH), 7.44 (s, 4H, H_4, H_5), 7.52 (s, 4H, H_{10}, H_{11}), 7.65 (d, 2H, J_{HH} = 9 Hz, H_{16}), 8.21 (d, 2H, J_{HH} = 9 Hz, H_{17}). ^{13}C NMR: (δ, 75 MHz, $CDCl_3$); -0.2 CH_3, 89.2, 90.6, 91.4, 94.1 (C_7, C_8, C_{13}, C_{14}), 96.5 (C_2), 104.4 (C_1), 121.8, 122.7, 123.2, 123.8 (C_3, C_6, C_9, C_{12}), 123.6 (C_{17}), 129.8 (C_{15}), 131.3, 131.6, 131.7, 131.8, 132.2 (C_4, C_5, C_{10}, C_{11}, C_{16}), 146.9 (C_{17}). SI MS; *m/z* (fragment, relative intensity): 419 ($[M]^+$, 100), 404 ($[M - Me]^+$, 90), 389 ($[M - 2Me]^+$, 10), 358, ($[M - 3Me - O]^+$, 20). HRMS calcd for $C_{27}H_{21}NO_2Si$ *m/e* 419.1343, found 419.1342.

2.8.2.2. 4,4',4''-HC≡CC$_6$H$_4$C≡CC$_6$H$_4$C≡CC$_6$H$_4$NO$_2$ (4)

4,4',4''-$Me_3SiC{\equiv}CC_6H_4C{\equiv}CC_6H_4C{\equiv}CC_6H_4NO_2$ (**3**) (74 mg, 0.18 mmol) was dissolved in CH_2Cl_2 (20 mL) and NBu^n_4F (1.0 mL, 1 M in thf) was added. The solution was stirred for 1 h. and the solution was filtered through an alumina plug. Petroleum spirit (25 mL) was added, and removal of the solvent under reduced pressure yielded the pale yellow product (55 mg, 83%). Anal. Calcd for $C_{24}H_{13}NO_2$: C 82.98, H 3.77, N 4.03 %. Found: C 82.62, H 3.97, N 4.07 %. IR: (CH_2Cl_2) ν(HC≡) 3301 cm^{-1}, ν(C≡C) 2218 cm^{-1}, ν(HC≡C) 2109 cm^{-1}. UV-Vis: λ (thf) 351 nm, ε 52 200 M^{-1} cm^{-1}. ^1H NMR: (δ, 300 MHz, $CDCl_3$); 3.17 (s, 1H, HC≡C), 7.44 (s, 4H, H_4, H_5), 7.52 (s, 4H, H_{10}, H_{11}), 7.65 (d, 2H, J_{HH} = 9 Hz, H_{16}), 8.22 (d, 2H, J_{HH} = 9 Hz, H_{17}). ^{13}C NMR: (δ, 75 MHz, $CDCl_3$); 79.1 (C_1), 83.1 (C_2), 89.3, 91.2, 94.1, 96.5 (C_7, C_8, C_{13}, C_{14}), 122.0, 122.2, 123.2, 123.8 (C_3, C_6, C_9, C_{12}), 123.6 (C_{17}), 131.4, 131.6, 131.7, 132.0, 132.2 (C_4, C_5, C_{10}, C_{11}, C_{16}), 147.0 (C_{17}). SI MS; *m/z* (fragment, relative intensity): 347 ($[M]^+$, 100), 317 ($[M - 2Me]^+$, 5), 300 ($[M - NO_2 - H]^+$, 25). HRMS calcd for $C_{24}H_{13}NO_2$ *m/e* 347.0943, found 347.0946.

2.8.3 Synthesis of ruthenium complexes

2.8.3.1. trans-[Ru(4-C=CHC$_6$H$_4$C≡CPh)Cl(dppm)$_2$]PF$_6$ (7)

cis-[RuCl$_2$(dppm)$_2$] (400 mg, 0.43 mmol), NH_4PF_6 (140 mg, 0.86 mmol) and 4-HC≡CC$_6$H$_4$C≡CPh (174 mg, 0.86 mmol) were added to dichloromethane (25 mL) and refluxed for 2 h. The solution was allowed to cool and petroleum ether (50 mL) was added. The resulting precipitate was collected and washed with diethyl ether to afford the pale red solid identified as **7** (409 mg, 76 %). Anal. Calcd for $C_{66}H_{54}ClF_6P_5Ru$: C 63.29, H 4.34 %. Found: C 63.33, H 4.66 %. IR: (KBr) ν(C≡C) 2064 cm^{-1}, ν(PF) 837 cm^{-1}. UV-Vis: λ (thf) 381 nm, ε 21 500 M^{-1} cm^{-1}. ^{1}H NMR: (δ, 300 MHz, $CDCl_3$); 3.05 (m, H_2), 5.12 (m, 2H, PCH_2P), 5.32 (m, 2H, PCH_2P), 5.45 (d, J_{HH} = 8 Hz, 2H, H_4), 6.02 (d, J_{HH} = 8 Hz, 2H, H_5), 6.77 (d, J_{HH} = 8 Hz, 2H, H_{10}), 7.10 - 7.60 (m, 45H, Ph). ^{13}C NMR: (δ, 75 MHz, $CDCl_3$); 45.9 (m, J_{CP} = 14 Hz, PCH_2P), 110.2 (C_2), 119.6 (C_3), 122.3 (C_9), 126.2, 127.3 (C_4, C_5), 129.1 (d, J_{CP} = 47 Hz, C_m), 130.9 (d, J_{CP} = 17 Hz, C_o), 131.6, 132.1 (C_{10}, C_{11}), 132.9 (C_p), 360.2 (m, C_1). ^{31}P NMR: (δ, 121 MHz, $CDCl_3$); -15.6. SI MS; *m/z* (fragment, relative intensity): 1107 ([M - PF_6]$^+$, 60), 904 ([RuCl(dppm)$_2$]$^+$, 100), 869 ([Ru(dppm)$_2$ - H]$^+$, 80).

2.8.3.2. trans-[Ru(4-C≡CC$_6$H$_4$C≡CPh)Cl(dppm)$_2$]·0.5 CH_2Cl_2 (8)

trans-[Ru(4-C=CHC$_6$H$_4$C≡CPh)Cl(dppm)$_2$]PF_6 (**7**) (200 mg 0.17 mmol) was added to dichloromethane (25 mL) and triethylamine (1.0 mL) and stirred for 10 min at room temperature. The mixture was passed through an alumina plug, petroleum ether (50 mL) was added, and the resulting precipitate was collected and washed with petroleum ether to yield the yellow product **8** (156 mg, 83 %). Anal. Calcd for $C_{66.5}H_{54}Cl_2P_4Ru$: C 69.51, H 4.47, %. Found: C 69.63, H 4.28 %. IR: (CH_2Cl_2) ν(C≡C) 2066 cm^{-1}. UV-Vis: λ (thf) 380 nm, ε 29 400 M^{-1} cm^{-1}. ^{1}H NMR: (δ, 300 MHz, $CDCl_3$); 4.89 (m, 4H, PCH_2P), 5.28 (s, 1H, CH_2Cl_2), 5.97 (d, J_{HH} = 8 Hz, 2H, H_4), 7.00 - 7.60

(m, 47H, Ph). ^{13}C NMR: (δ, 75 MHz, $CDCl_3$); 50.2 (m, J_{CP} = 14 Hz, PCH_2P), 113.0, 115.7 (C_7, C_8), 123.9 (C_3), 127.39 (C_p), 128.1, 129.8, 130.1, 131.2 (C_4, C_5, C_{10}, C_{11}), 129.0 (d, J_{CP} = 15 Hz, C_m), 133.3 (d, J_{CP} = 26 Hz, C_o), 134.7 (m, C_i). ^{31}P NMR: (δ, 121 MHz, $CDCl_3$); -6.0. SI MS; *m/z* (fragment, relative intensity): 1106 ($[M]^+$, 100), 905 ($[RuCl(dppm)_2]^+$, 25), 869 ($[Ru(dppm)_2 - H]^+$, 40), 486 ($[Ru(dppm)]^+$, 30).

*2.8.3.3. trans-[Ru(4,4'-C=CHC$_6$H$_4$C≡CC$_6$H$_4$NO$_2$)Cl(dppm)$_2$]PF$_6$ (**11**)*

cis-$[RuCl_2(dppm)_2]$ (400 mg, 0.43 mmol), NH_4PF_6 (140 mg, 0.86 mmol) and 4,4'-$HC{\equiv}CC_6H_4C{\equiv}CC_6H_4NO_2$ (**2**) (213 mg, 0.86 mmol) were added to dichloromethane (25 mL), and refluxed for 2 h. The solution was cooled, petroleum ether (50 mL) was added, and the resulting precipitate was collected and washed with diethyl ether to yield the yellow-orange product **11** (441 mg, 79 %). Anal. Calcd for $C_{66}H_{53}ClF_6NO_2P_5Ru$: C 61.10, H 4.11, N 1.08 %. Found: C 61.68, H 4.48, N 1.34 %. IR: (KBr) ν(C≡C) 2069 cm^{-1}, ν(PF) 836 cm^{-1}. UV-Vis: λ (thf) 461 nm, ε 12 300 M^{-1} cm^{-1}. ^1H NMR: (δ, 300 MHz, $CDCl_3$); 3.08 (m, 1H, =CH), 5.15 (m, 2H, PCH_2P), 5.34 (m, 2H, PCH_2P), 5.50 (d, J_{HH} = 8 Hz, 2H, H_4), 6.89 (d, J_{HH} = 8 Hz, 2H, H_5), 7.10 - 7.50 (m, 44H, Ph), 7.64 (d, J_{HH} = 9 Hz, 2H, H_{10}), 8.20 (d, J_{HH} = 9 Hz, 2H, H_{11}). ^{13}C NMR: (δ, 75 MHz, $CDCl_3$); 45.5 (m, J_{CP} = 10 Hz, PCH_2P), 88.9, 94.6 (C_7, C_8), 109.8 (C_2), 118.8, (C_6), 123.4, 126.6 (C_4, C_5), 128.6 (d, J_{CP} = 46 Hz, C_m), 131.2 (C_p), 131.5, 132.0 (C_{10}, C_{11}), 132.7 (d, J_{CP} = 70 Hz, C_o), 146.7 (C_{12}). ^{31}P NMR: (δ, 121 MHz, $CDCl_3$); -15.8. SI MS; *m/z* (fragment, relative intensity): 1152 ($[M - PF_6]^+$, 20), 905 ($[RuCl(dppm)_2]^+$, 45), 869 ($[Ru(dppm)_2 - H]^+$, 60), 485 ($[Ru(dppm) - H]^+$, 40).

*2.8.3.4. trans-[Ru(4,4'-C≡CC$_6$H$_4$C≡CC$_6$H$_4$NO$_2$)Cl(dppm)$_2$] (**12**)*

trans-$[Ru(4,4'\text{-}C{=}CHC_6H_4C{\equiv}CC_6H_4NO_2)Cl(dppm)_2]PF_6$ (**11**) (200 mg, 0.15 mmol) was added to dichloromethane (25 mL) and triethylamine (1.0 mL) and stirred for 10 min at room temperature. The mixture was passed through an alumina plug,

petroleum ether (50 mL) was added, and the resulting precipitate was collected and washed with petroleum ether to yield the deep red product **12** (143 mg, 83 %). Anal. Calcd for $C_{66}H_{52}ClNO_2P_4Ru$: C 68.84, H 4.55, N 1.21 %. Found: C 68.14, H 4.62, N 1.21 %. IR: (KBr) ν(C≡C) 2064, 2059 cm^{-1}. UV-Vis: λ (thf) 468 nm, ε 23 000 M^{-1} cm^{-1}, 344 nm, ε 22 600 M^{-1} cm^{-1}. ^1H NMR: (δ, 300 MHz, $CDCl_3$); 4.90 (m, 4H, PCH_2P), 5.97 (d, J_{HH} = 8 Hz, 2H, H_4), 7.00 - 7.50 (m, 42H, Ph), 7.57 (d, J_{HH} = 9 Hz, 2H, H_{10}), 8.18 (d, J_{HH} = 9 Hz, 2H, H_{11}). ^{13}C NMR: (δ, 75 MHz, $CDCl_3$); 50.0 (m, PCH_2P), 87.8, 96.5 (C_7, C_8), 109.8 (C_2), 118.8 (C_3), 123.5, 126.7 (C_4, C_5), 127.3 (C_p), 129.0 (d, J_{CP} = 20 Hz, C_m), 129.8, 130.4, (C_{10}), (C_{11}), 133.5 (d, J_{CP} = 13 Hz, C_o), 146.1 (C_{12}). ^{31}P NMR: (δ, 121 MHz, $CDCl_3$); -5.8. SI MS; *m/z* (fragment, relative intensity): 1151 ($[M]^+$, 100), 905 ($[RuCl(dppm)_2]^+$, 20), 869 ($[Ru(dppm)_2 - H]^+$, 60), 486 ($[Ru(dppm)]^+$, 30).

*2.8.3.5. trans-[Ru(4,4',4''-C=CHC$_6$H$_4$C≡CC$_6$H$_4$C≡CC$_6$H$_4$NO$_2$)Cl(dppm)$_2$]PF$_6$· 0.5CH$_2$Cl$_2$ (**13**)*

cis-$[RuCl_2(dppm)_2]$ (100 mg, 0.11 mmol), NH_4PF_6 (36 mg, 0.22 mmol) and 4,4',4''-HC≡CC_6H_4C≡CC_6H_4C≡$CC_6H_4NO_2$ (**13**) (44 mg, 0.13 mmol) were stirred in dichloromethane (25 mL) for 3 h. The solution was filtered, petroleum spirit (50 mL) was added, and the resulting precipitate was collected and washed with diethyl ether to yield the red product **13** (108 mg, 73 %), Anal. Calcd for $C_{74.5}H_{58}Cl_2F_6NO_2P_5Ru$: C 62.14, H 4.06, N 0.97 %. Found: C 62.39 H 4.67, N 1.05 %. IR: (KBr) ν(PF) 836 cm^{-1}, ν(C≡C) 2211 cm^{-1}, 2065 cm^{-1}. UV-Vis: λ (thf) 427 nm, ε 14 300 M^{-1} cm^{-1}. ^1H NMR: (δ, 300 MHz, $CDCl_3$); 3.05 (m, H_2, =CH), 5.13, (m, 2H, PCH_2P), 5.28 (s, 1H, CH_2Cl_2), 5.34 (m, 2H, PCH_2P), 5.48 (d, J_{HH} = 8 Hz, 2H, H_4), 6.90 - 7.55 (m, 46H, Ph), 7.65 (d, J_{HH} = 9 Hz, 2H, H_{10}), 8.21 (d, J_{HH} = 9 Hz, 2H, H_{11}). ^{31}P NMR: (δ, 121 MHz, $CDCl_3$); -15.9. SI MS; *m/z* (fragment, relative intensity): 1252 ($[M - PF_6]^+$, 15), 905 ($[RuCl(dppm)_2]^+$, 90), 871 ($[Ru(dppm)_2 + H]^+$, 100).

*2.8.3.6. trans-[Ru(4,4',4''-C≡CC$_6$H$_4$C≡CC$_6$H$_4$C≡CC$_6$H$_4$NO$_2$)Cl(dppm)$_2$]·CH$_2$Cl$_2$ (**14**)*

trans-[Ru(4,4',4''-C=CHC$_6$H$_4$C≡CC$_6$H$_4$C≡CC$_6$H$_4$NO$_2$)Cl(dppm)$_2$]PF$_6$ (**13**) (150 mg, 0.11 mmol) and triethylamine (1.0 mL) were added to dichloromethane (25 mL) and stirred for 10 min at room temperature. The solution was passed through an alumina plug, petroleum spirit (50 mL) was added, and the resulting precipitate was collected and washed with petroleum spirit to yield the red product **14** (110 mg, 82 %). Anal. Calcd for $C_{75}H_{58}Cl_3NO_2P_4Ru$: C 67.40, H 4.37, N 1.05 %. Found: C 67.71, H 4.68, N 1.25 %. IR: (CH_2Cl_2) ν(C≡C) 2205, 2070 cm^{-1}. UV-Vis: λ (thf) 439 nm, ε 19 800 M^{-1} cm^{-1}, 359 nm, ε 35 700 M^{-1} cm^{-1}. ^{1}H NMR: (δ, 300 MHz, $CDCl_3$); 4.90 (m, 4H, PCH_2P), 5.28 (s, 2H, CH_2Cl_2), 5.97 (d, J_{HH} = 8 Hz, 2H, H_4), 7.00 - 7.50 (m, 46H, Ph), 7.65 (d, J_{HH} = 8 Hz, 2H, H_{16}), 8.22 (d, J_{HH} = 9 Hz, 2H, H_{17}). ^{13}C NMR: (δ, 75 MHz, $CDCl_3$); 50.2 (m, PCH_2P), 88.9 93.6, 94.5, 96.1 (C_7, C_8, C_{13}, C_{14}), 113.3 (C_2), 115.3, 120.9, 124.9 (C_3, C_6, C_9), 123.6 (C_{17}), 127.4 (C_p), 129.1 (d, J_{CP} = 18 Hz, C_m), 129.9, 130.2, 131.2, 131.6, 132.1 (C_4, C_5, C_{10}, C_{11}, C_{16}), 130.0 (C_{15}), 133.4 (d, J_{CP} = 26 Hz, C_o), 134.3 (m, J_{CP} = 64 Hz, C_i), 146.8 (C_{18}). ^{31}P NMR: (δ, 121 MHz, $CDCl_3$); -6.0. SI MS; *m/z* (fragment, relative intensity): 1252 ([M + H]$^+$, 100), 869 ([Ru(dppm)$_2$ - H]$^+$, 90), 485 ([Ru(dppm) - H]$^+$, 90).

2.9. References

[1] Kanis, D.R., Ratner, M.A., Marks, T.J., *Chem. Rev.*, **1994**, *94*, 195.

[2] Hermann, J.P., Ducuing, J., *J. Appl. Phys.*, **1974**, *45*, 5100.

[3] Bosshard, C., Spreiter, R., Gunter, P., Tykwinkski, R.R., Schreiber, M., Diederich, F., *Adv. Mater.*, **1996**, *8*, 231.

[4] Samuel, I.D.W., Ledoux, I., Delporte, C., Pearson, D.L., Tour, J.M., *Chem. Mater.*, **1996**, *8*, 819.

[5] Ghosal, S., Samoc, M., Prasad, P.N., Tufariello, J.T., *J. Phys. Chem.*, **1990**, *133*, 244.

[6] Morley, J.O., Pugh, D., *Spec. Publ. - R. Soc. Chem.*, **1989**, *69*, 28.

[7] Morley, J.O., *Int. J. Quantum Chem.*, **1993**, *46*, 19.

[8] Jain, M., Chandrasekhar, J., *J. Phys. Chem.*, **1993**, *97*, 4044.

[9] Dehu, C., Meyers, F., Bredas, J., *J. Am. Chem. Soc.*, **1993**, *115*, 6198.

[10] Barzoukas, M., Fort, A., Servutoviez, C., Oswald, L., Nicoud, J.F., *Chem. Phys.*, **1991**, *164*, 457.

[11] Cheng, L.-T., Tam, W., Stevenson, S.H., Meredith, G.R., Rikken, G., Marder, S.R., *J. Phys. Chem.*, **1991**, *95*, 10643.

[12] Whittall, I.R., Humphrey, M.G., Houbrechts, S., Persoons, A., Hockless, D.C.R., *Organometallics*, **1996**, *15*, 5738.

[13] Ooba, N., Tomaru, S., Kurihara, T., Kaino, T., Yamada, W., Takagi, M., Yamamoto, T., *Jpn J. Appl. Phys.,* **1995**, *34*, 3139.

[14] Wautelet, P., Moroni, M., Oswald, L., LeMoigne, J., Pham, A., Bigot, J.Y., Luzzati, S., *Macromolecules,* **1996**, *29*, 446.

[15] Rumi, M., Zerbi, G., Mullen, K., Muller, G., Rehahn, M., *J. Chem. Phys.,* **1997**, *106*, 24.

[16] Tykwinski, R.R., Gubler, U., Martin, R.E., Diederich, F., Bosshard, C., Gunter, P., *J. Phys. Chem. B,* **1998**, *102*, 4451.

[17] Bredas, J.L., Adant, C., Beljonne, D., Meyers, F., Shuai, Z., *Synth. Met.,* **1993**, *55*, 3933.

[18] Whittall, I.R., Humphrey, M.G., Samoc, M., Luther-Davies., B., *Angew. Chem., Int. Ed. Engl.,* **1997**, *36*, 370.

[19] Frazier, C.C., Guha, S., Chen, W.P., Cockerham, M.P., Porter, P.L., Chauchard, E.A., Lee, C.H., *Polymer,* **1987**, *28*, 553.

[20] McDonagh, A.M., Cifuentes, M.P., Whittall, I.R., Humphrey, M.G., Samoc, M., Luther-Davies, B., Hockless, D.C.R., *J. Organomet. Chem.,* **1996**, *526*, 99.

[21] McDonagh, A.M., Whittall, I.R., Humphrey, M.G., Hockless, D.C.R., Skelton, B.W., White, A.H., *J. Organomet. Chem.,* **1996**, *523*, 33.

[22] McDonagh, A.M., Cifuentes, M.P., Lucas, N.T., Humphrey, M.G., Houbrechts, S., Persoons, A., *J. Organomet. Chem.,* **2000**, *605*, 184.

[23] McDonagh, A.M., Lucas, N.T., Cifuentes, M.P., Humphrey, M.G., Houbrechts, S., Persoons, A., *J. Organomet. Chem.,* **2000**, *605*, 193.

[24] Naulty, R.H., McDonagh, A.M., Whittall, I.R., Cifuentes, M.P., Humphrey, M.G., Houbrechts, S., Maes, J., Persoons, A., Heath, G.A., Hockless, D.C.R., *J. Organomet. Chem.,* **1998**, *563*, 137.

[25] Whittall, I.R., Humphrey, M.G., Houbrechts, S., Maes, J., Persoons, A., Schmid, S., Hockless, D.C.R., *J. Organomet. Chem.,* **1997**, *544*, 277.

[26] Touchard, D., Haquette, P., Guesmi, S., Pinchon, L.L., Daridor, A., Toupet, L., Dixneuf, P.H., *Organometallics,* **1997**, *16*, 3640.

[27] Whittall, I.R., Cifuentes, M.P., Costigan, M.J., Humphrey, M.G., Goh, S.C., Skelton, B.W., White, A.H., *J. Organomet. Chem.,* **1994**, *471*, 193.

[28] Fischer, H., Podschadly, O., Roth, G., Herminghaus, S., Klewitz, S., Heck, J., Houbrechts, S., Meyer, T., *J. Organomet. Chem.,* **1997**, *541*, 321.

[29] Cifuentes, M.P., Driver, J., Humphrey, M.G., Asselberghs, I., Persoons, A., Samoc, M., Luther-Davies, B., *J. Organomet. Chem.,* **2000**, *607*, 72.

[30] Cadierno, V., Conejero, S., Gamasa, M.P., Gimeno, J., Asselberghs, I., Houbrechts, S., Clays, K., Persoons, A., Borge, J., Garcia-Granda, S., *Organometallics,* **1999**, *18*, 582.

[31] Calabrese, J.C., Cheng, L.T., Green, J.C., Marder, S.R., Tam, W., *J. Am. Chem. Soc.,* **1991**, *113*, 7227.

[32] Lavastre, O., Cabioch, S., Dixneuf, P.H., Vohlidal, J., *Tetrahedron,* **1997**, *53*, 7595.

[33] Takahashi, S., Kuroyama, Y., Sonogashira, K., Hagihara, N., *Synthesis,* **1980**, 627.

[34] Touchard, D., Haquette, P., Pirio, N., Toupet, L., Dixneuf, P.H., *Organometallics,* **1993**, *12*, 3132.

[35] Whittall, I.R., Cifuentes, M.P., Humphrey, M.G., Luther-Davies, B., Samoc, M., Houbrechts, S., Persoons, A., Heath, G.A., Hockless, D.C.R., *J. Organomet. Chem.,* **1997**, *549*, 127.

[36] Younus, M., Long, N.J., Raithby, P.R., Lewis, J., Page, N.A., White, A.J.P., Williams, D.J., Colbert, M.C.B., Hodge, A.J., Khan, M.S., Parker, D.G., *J. Organomet. Chem.,* **1999**, *578*, 198.

[37] Colbert, M.C.B., Lewis, J., Long, N.J., Raithby, P.R., White, A.J.P., Williams, D.J., *J. Chem. Soc., Dalton Trans.,* **1997**, 99.

[38] Jones, N.D., Wolf, M.O., Giaquinta, D.M., *Organometallics,* **1997**, *16*, 1352.

[39] Lebreton, C., Touchard, D., Le Pichon, L., Daridor, A., Toupet, L., Dixneuf, P.H., *Inorg. Chim. Acta,* **1998**, *272*, 188.

[40] Choi, M.Y., Chan, M.C.W., Zhang, S.B., Cheung, K.K., Che, C.M., Wong, K.Y., *Organometallics,* **1999**, *18*, 2074.

[41] Bianchini, C., Meli, A., Peruzzini, M., Zanobini, F., Zanello, P., *Organometallics,* **1990**, *9*, 241.

[42] McDonagh, A.M., Whittall, I.R., Humphrey, M.G., Skelton, B.W., White, A.H., *J. Organomet. Chem.,* **1996**, *519*, 229.

[43] Hurst, S.K., Cifuentes, M.P., Morrall, J.P.L., Lucas, N.T., Whittall, I.R., Humphrey, M.G., Asselberghs, I., Persoons, A., Samoc, M., Luther-Davies, B., Willis, A.C., *Organometallics,* **2001**, In press.

[44] Cheng, L.-T., Tam, W., Stevenson, S.H., Meredith, G.R., Rikken, G., Marder, S.R., *J. Phys. Chem.,* **1991**, *95*, 10631.

[45] Chaudret, B., Commenges, G., Poilblanc, R., *J. Chem. Soc., Dalton Trans.,* **1984**, 1635.

[46] Hsung, R.P., Chidsey, C.E.D., Sita, L.R., *Organometallics,* **1995**, *14*, 4808.

[47] Hodge, A.J., Ingham, S.L., Kakkar, A.K., Khan, M.S., Lewis, J., Long, N.J., Parker, D.G., Raithby, P.R., *J. Organomet. Chem.,* **1995**, *488*, 205.

Chapter 3

Some dipolar metal complexes and their nonlinear optical properties

---

Contents

Chapter 3

Some dipolar metal complexes and their nonlinear optical properties

---

3.1. Introduction

As outlined in Chapter 1, much research has been undertaken over the last decade on designing and synthesizing molecular compounds for nonlinear optics. A common methodology for producing a compound with a large second-order response is to employ a "push-pull" design. These complexes use strong electron-withdrawing groups such as nitro substituents to induce electron delocalization across a π-conjugated backbone from an electron-rich donor. Although this approach has produced materials with large second-order responses, use of strongly polarized donor/acceptor groups often leads to centrosymmetric packing of the molecule, and consequently low values of χ^2. In addition, commonly used donor/acceptor groups such as $-NMe_2$ and $-NO_2$ are difficult to functionalize synthetically, preventing useful modification of the complex. Repetitive synthesis using a simple linkable organometallic complex may potentially lead to large modular complexes with larger NLO responses than traditional donor-acceptor systems.

One of the most versatile functional groups for synthesis is the aryl aldehyde moiety. Scheme 3.1. outlines a few of the available derivitizations. Additionally, *ortho*, *meta*, *para* or multiple formyl substitution around the aromatic ring allows even greater design flexibility. Previous work[1] has shown that replacement of C=N or (Z)-C=C

bonds with (*E*)-C=C bonds results in a significant increase in second-order response exhibited by gold acetylides. The Wadsworth-Horner-Emmons protocol can be used to synthesize (*E*)-C=C-linked organometallic complexes, with large second-order responses, from aryl aldehyde-containing precursors which have only modest second-order responses. Previously, ferrocene monocarboxaldehyde[2] and (concurrently with the studies described in this Thesis) ferrocene dicarboxaldehyde[3] have served as the precursor for a large number of organometallics. Ferrocenyl-containing complexes, however, possess absorption bands close to the second-harmonic frequency, which is undesirable for second-order NLO materials.

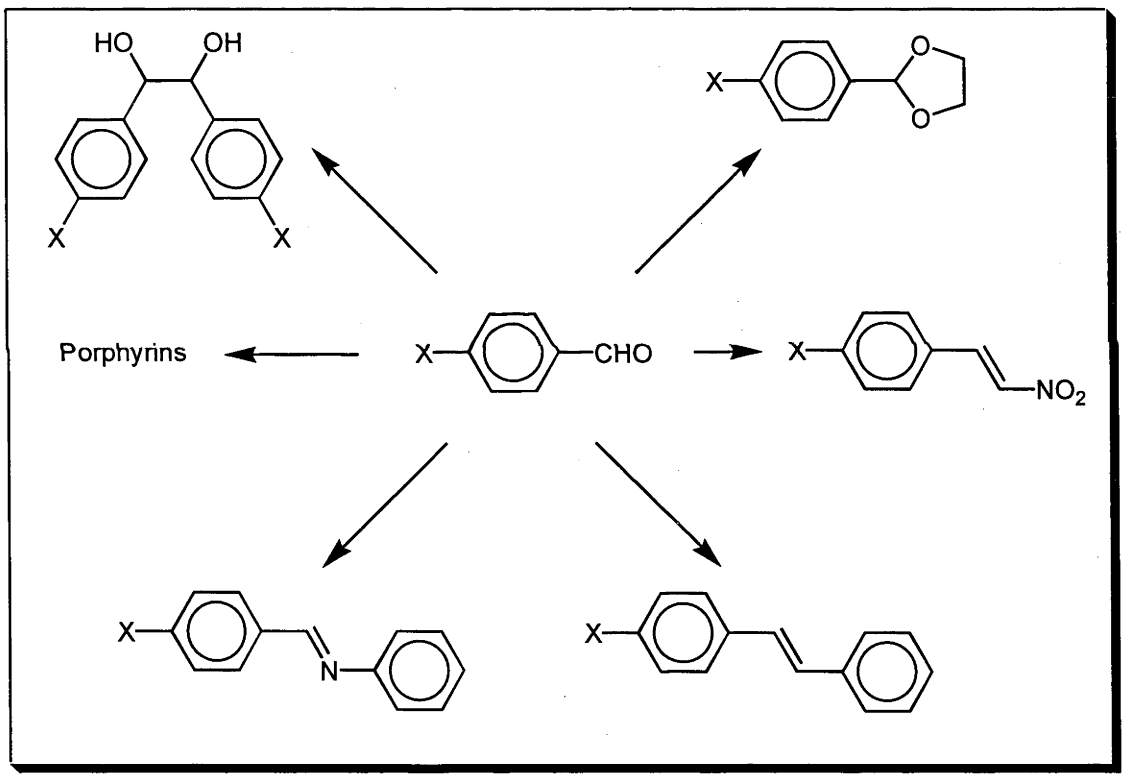

Scheme 3.1. Potential derivitizations utilizing aryl aldehydes.

Other organometallic aldehydes have received less attention either as NLO-active complexes themselves or as sub-units of larger systems, possibly because of the intermediate electron-acceptor strength of the formyl moiety. Hansch *et al.*[4] have reported that the susceptibilities for ferrocenyl derivatives are largest for molecules

containing the strongest electron acceptors, with NO_2 > CHO ≈ CN. The two-level model (Equation 3.1.) attempts to quantify the effect on β of these traditional "push-pull" NLO systems, by taking into account the difference between the ground and excited state dipole moments (μ_{ee} - μ_{gg}), the transition dipole moment (μ_{ge}) and the energy gap between the ground and excited state (E_{ge}). This model presumes that the second-order response is due to a single charge-transfer excitation along the conjugated axis of the molecule. A consequence of this model is that a decrease in the energy gap between the ground and excited states should lead to an increase in β. In addition, a large difference between the ground and excited state dipole moments is expected to increase β. The ordering NO_2 > CHO ≈ CN is therefore consistent with the two-level model, where strong electron-accepting groups lead to an increase in λ_{max} and consequently β. Studies of -NO_2 and related unsubstituted complexes have been undertaken, but similar studies embracing substitution with a moderate acceptor group and the consequent effect on second- and third-order NLO response are comparatively rare. Kanis *et al.*[5] have summarized the effect on β of different substituents in ferrocenyl and (arene)chromium tricarbonyl derivatives (Table 3.1.), but this work did not extend to complexes containing the metal centre in the plane of the electron polarization.

$$\beta_{CT} \propto \frac{(\mu_{ee} - \mu_{gg})(\mu_{ge}^2)}{E_{ge}^2}$$

Equation 3.1. The two-level model.

The aims of the studies described in this Chapter are to synthesize and assess the NLO properties of some aryl aldehyde-functionalized organometallic complexes. The preparation and characterization of ruthenium vinylidene and acetylide complexes and gold acetylide complexes are presented in this Chapter, together with their second- and third-order NLO data.

Table 3.1. Experimental β values for systematically varied ferrocenyl complexes.[a]

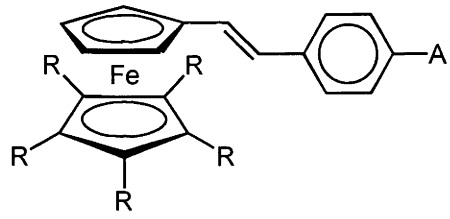

A	R	Isomer	β_{vec}
CN	H	*E*	10
CHO	H	*E*	12
NO_2	H	*E*	31
NO_2	Me	*E*	40
NO_2	H	*Z*	13

[a] Units of 10^{-30} cm^5 esu^{-1}; measured at 1.91 μm.

3.2. Synthesis of terminal alkynes

Aryl acetylenes with a protected formyl group were required for the subsequent preparation of alkynyl complexes. 4-HC≡$CC_6H_4CH\{OC(O)Me\}_2$ (**2**) was prepared by extending the method of Kochar *et al.*,[6] stirring 4-HC≡CC_6H_4CHO (**1**) in acetic anhydride with a catalytic amount of $FeCl_3$ (Scheme 3.2.). The formyl group can also be protected by conversion into a 1,3-dioxane moiety. This was accomplished by stirring 4-HC≡CC_6H_4CHO in a mixture of dichloromethane and 1,3-propanediol with a catalytic amount of 4-toluenesulfonic acid monohydrate, to give **18** in good yield (Scheme 3.2.). While the current research was in progress, a synthesis of **18** was reported by acetalizing 4-Me_3SiC≡CC_6H_4CHO with 1,3-propanediol, and desilylating the intermediate with K_2CO_3 / methanol, although the yield of this procedure was not specified.[7] The identities of **2** and **18** were confirmed by IR, UV-vis and ^1H NMR spectroscopy, mass spectrometry (including accurate mass determinations of the molecular ion signal), and satisfactory microanalyses.

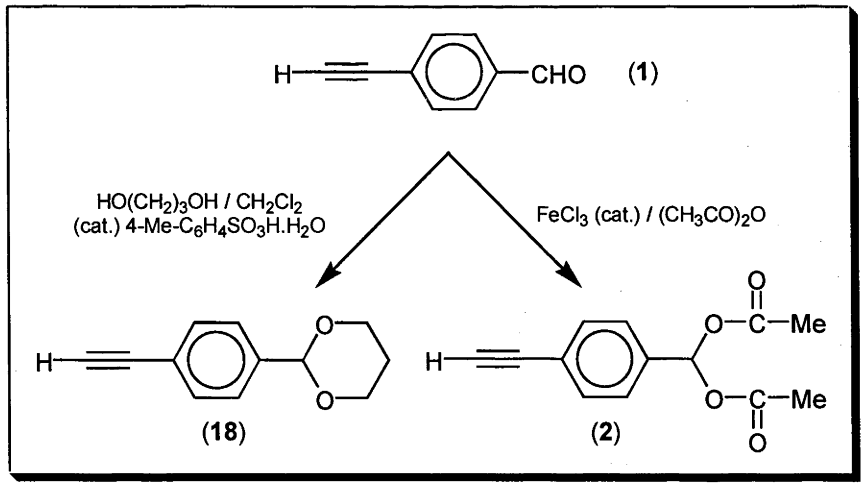

Scheme 3.2. Syntheses of protected aryl aldehydes

3.3. Synthesis of metal complexes

3.3.1. Gold acetylide complexes

The gold acetylide complexes were prepared by extending the method of Naulty *et al.*[8] The room temperature reaction of the terminal alkynes with the ligated gold centres in a methanol / dichloromethane solution with sodium methoxide for 18 hours led to the formation of the gold complexes in good yield (Scheme 3.3.). The new acetylide complexes were characterized by SI mass spectrometry, satisfactory microanalyses, UV-vis and IR spectroscopy, ^{1}H, ^{31}P and ^{13}C NMR spectroscopy.

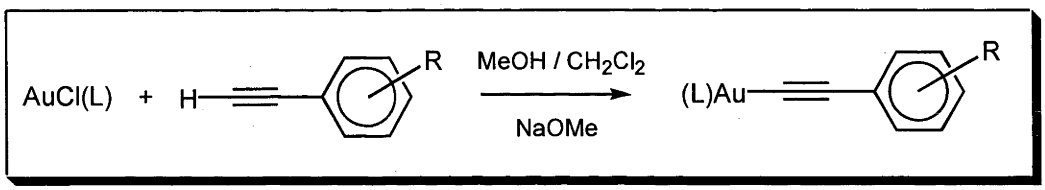

L	R	Complex
PPh_3	4-CHO	**5**
PMe_3	4-CHO	**6**
PPh_3	3-CHO	**13**
PMe_3	3-CHO	**14**
PPh_3	4-$\overline{CHO(CH_2)_3O}$	**21**
PMe_3	4-$\overline{CHO(CH_2)_3O}$	**22**

Scheme 3.3. Synthesis of (phosphine)gold alkynyl complexes

3.3.2. Ruthenium complexes

The synthetic methodologies employed for the preparation of the new complexes are adaptations of those successfully utilized for the preparation of the corresponding phenylacetylides. The bis(bidentate phosphine)ruthenium complexes were prepared by extending the method of Touchard *et al.*,[9] a procedure which also permits isolation of the stable vinylidene intermediates (Scheme 3.4.). The behaviour of the 2-formylphenylvinylidene complex **17** was markedly different, attempted deprotonation resulting in decomposition. Unlike the analogous *trans*-[Ru(4-C≡CC_6H_4CHO)Cl$(dppm)_2$], it did not prove possible to prepare [Ru(4-C≡CC_6H_4CHO)$(PPh_3)_2(\eta\text{-}C_5H_5)$] by the most direct route, namely reaction of [RuCl$(PPh_3)_2(\eta\text{-}C_5H_5)$] with 4-HC≡C$C_6H_4$CHO followed by basic work-up; only decomposition products were observed. Access to the 4-formylphenylethynyl complex necessitated preparation of a complex with a protected formyl group. The (cyclopentadienyl)bis(triphenylphosphine)ruthenium acetylide complex **3**, containing a protected formyl group, was prepared in good yield by reaction of **2** with [RuCl$(PPh_3)_2(\eta\text{-}C_5H_5)$] and deprotonation of the intermediate vinylidene complex. Deprotection of **3** by extended treatment with base gave the formylphenylethynyl complex **4** in good yield (Scheme 3.5.). The new complexes were characterized by FAB mass spectrometry, satisfactory microanalyses, UV-vis and IR spectroscopy, ^{1}H, ^{31}P and ^{13}C NMR spectroscopy.

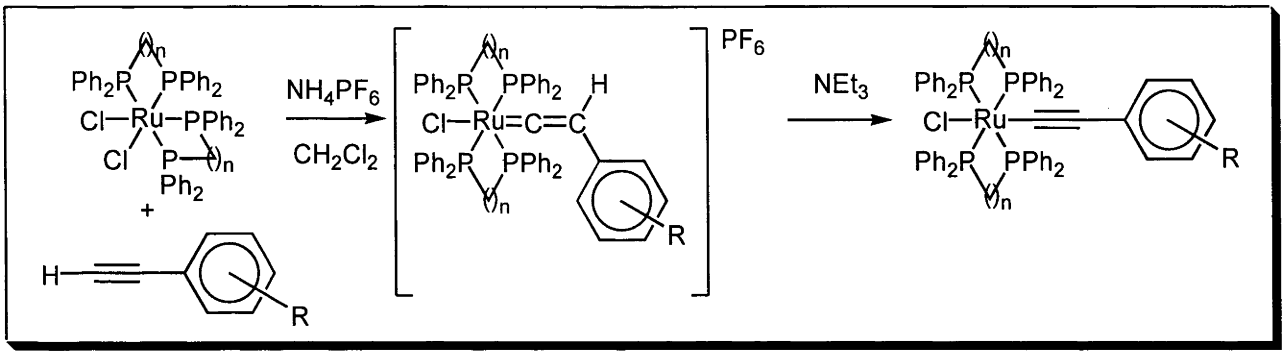

n	R	Vinylidene Complex	n	R	Alkynyl Complex
1	4-CHO	**5**	1	4-CHO	**6**
2	4-CHO	**7**	2	4-CHO	**8**
1	3-CHO	**12**	1	3-CHO	**13**
1	2-CHO	**17**	1	4-$\overline{\text{CHO(CH}_2)_3\text{O}}$	**20**
1	4-$\overline{\text{CHO(CH}_2)_3\text{O}}$	**19**			

Scheme 3.4. Syntheses of *trans*-bis(bidentate phosphine)chlororuthenium acetylide and vinylidene complexes

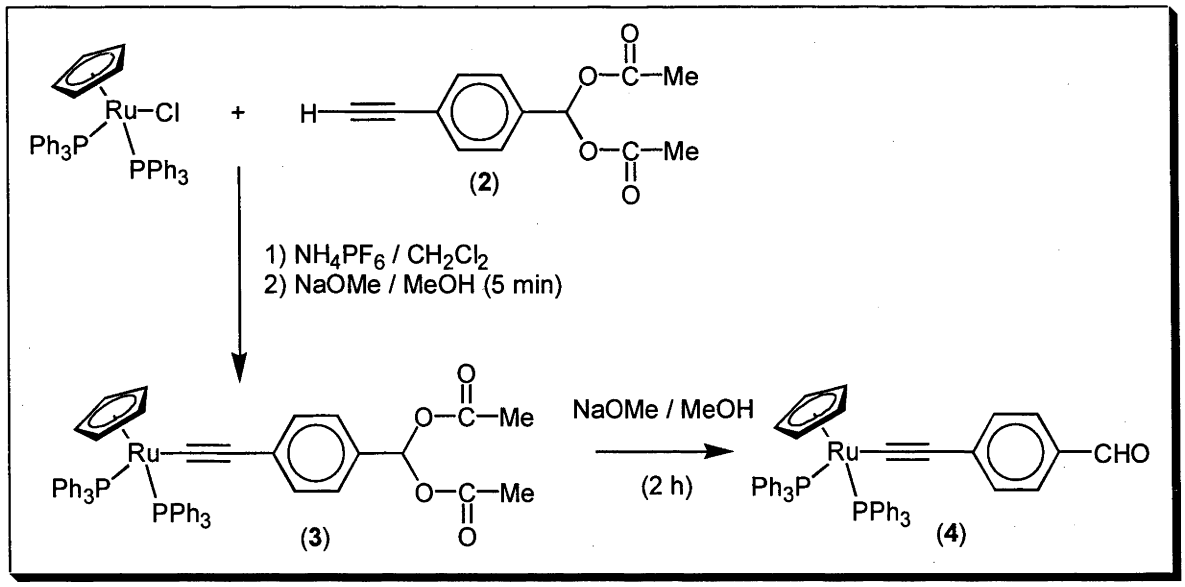

Scheme 3.5. Synthesis of **3** and **4**

3.3.3. Comparison of characterization data

Selected ^{1}H NMR data for compounds **1** - **22** are listed in Table 3.2. and the NMR numbering scheme is displayed in Figure 3.1. Compound **17** is discussed separately because of its unusual characteristics. The terminal alkynes **1**, **2**, **11** and **18** all have resonances for the acetylenic proton in the range of 3.05 to 3.28 ppm, as expected. The *ortho* substituted acetylene **16** has the acetylenic proton resonance shifted to a higher frequency of 3.44 ppm due to the close proximity of the deshielding carbonyl group. The resonance of the formyl proton is also shifted upfield to 10.52 ppm by the anisotropic effects of the alkyne and carbonyl groups. For the gold acetylide complexes, the position of the H_9 proton is shifted to higher frequencies compared with the ruthenium complexes, probably because of the poorer electron-donating capacity of the ligated gold centre. In the vinylidene complexes, the resonances of the H_4 protons are shifted upfield from those of the terminal acetylenes. For example, the resonances for the H_4 protons on **19** are located at 5.48 ppm; in comparison, the parent acetylene **18** has the same protons resonating at 7.42 ppm. The corresponding acetylide complexes have smaller chemical shift differences for the H_4 protons compared to those of the precursor acetylene.

The ^{31}P NMR spectra of complexes **1** - **16** and **18** - **22** are unremarkable, with similar shifts observed for complexes with a given phosphine ligand irrespective of functional group substitution.

Table 3.3. contains IR and UV-vis data for complexes **1** – **22**. The IR $\nu(C\equiv C)$ bands occur in the range 2047 – 2118 cm^{-1}. The gold acetylide complexes have similar $\nu(C\equiv C)$ values to the terminal acetylenes, with the bands occurring between 2111 and 2118 cm^{-1}. Substitution of gold with a ruthenium centre leads to a low frequency shift for the $\nu(C\equiv C)$ band, but there appears to be no clear relationship between $\nu(C\equiv C)$ and

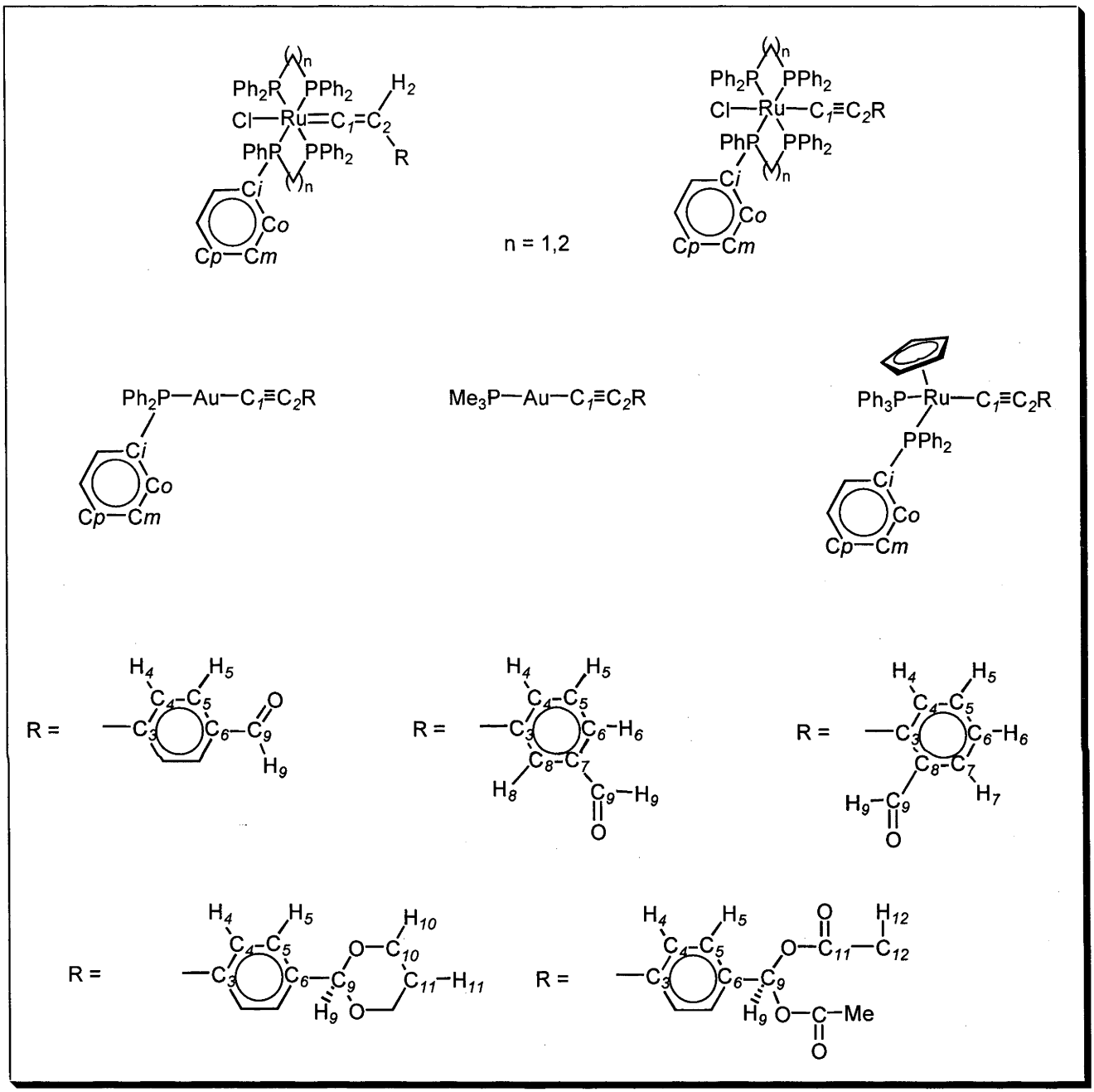

Figure 3.1. NMR numbering scheme

the nature of the aryl substituent. The UV-vis spectra for the terminal acetylenes show absorption at short wavelengths, with λ_{max} below 300 nm. Introduction of a ligated gold centre shifts the λ_{max} values to slightly longer wavelengths, but use of a 18-electron ruthenium centre results in a consistently larger red-shift. Proceeding from a *para*

Table 3.2. Selected ^{1}H NMR data [ppm (J_{HH}, Hz)].

Compound	H_1	H_4	H_5	Ph	$P(CH_2)_nP$	H_9
4-HC≡CC_6H_4CHO (**1**)	3.28	7.62 (8)	7.82 (9)	--	--	9.99
4-HC≡CC_6H_4CH{OC(O)Me}$_2$ (**2**)	3.10	7.45 (9)	7.51 (9)	--	--	7.64
[Ru(4-C≡CC_6H_4CH{OC(O)Me}$_2$)(PPh_3)$_2$(η-C_5H_5)] (**3**)	--	[a]	[a]	7.10 – 7.50	--	7.61
[Ru(4-C≡CC_6H_4CHO)(PPh_3)$_2$(η-C_5H_5)] (**4**)	--	[a]	[a]	7.30 – 7.80	--	9.85
trans-[Ru(4-C=CHC_6H_4CHO)Cl(dppm)$_2$]PF_6 (**5**)	--	5.62 (8)	[a]	7.10 – 7.55	5.25, 5.62	9.75
trans-[Ru(4-C≡CC_6H_4CHO)Cl(dppm)$_2$] (**6**)	--	6.03 (8)	[a]	7.00 – 7.60	4.92	9.75
trans-[Ru(4-C=CHC_6H_4CHO)Cl(dppe)$_2$]PF_6 (**7**)	--	5.81 (8)	[a]	6.90 – 7.40	2.90	9.64
trans-[Ru(4-C≡CC_6H_4CHO)Cl(dppe)$_2$] (**8**)	--	6.57 (8)	7.57 (8)	6.90 – 7.40	2.67	9.75
[Au(4-C≡CC_6H_4CHO)(PPh_3)] (**9**)	--	[a]	[a]	7.30 – 7.80	--	9.94
[Au(4-C≡CC_6H_4CHO)(PMe_3)] (**10**)	--	7.54 (8)	7.72 (8)	--	--	9.92
3-HC≡CC_6H_4CHO (**11**)	3.15	7.71	7.48	7.25 – 8.20	--	9.97
trans-[Ru(3-C=CHC_6H_4CHO)Cl(dppm)$_2$]PF_6 (**12**)	--	[b]	[b]	7.10 – 7.60	5.12, 5.32	9.54
trans-[Ru(3-C≡CC_6H_4CHO)Cl(dppm)$_2$] (**13**)	--	[b]	[b]	7.05 – 7.60	4.89	9.69
[Au(3-C≡CC_6H_4CHO)(PPh_3)] (**14**)	--	[a]	[a]	7.35 – 7.80	--	9.93
[Au(3-C≡CC_6H_4CHO)(PMe_3)] (**15**)	--	[b]	[b]	--	--	9.92

2-HC≡CC_6H_4CHO (**16**)	3.44	[b]	[b]	--	--	10.52
trans-[Ru(2-C=CHC_6H_4CHO)Cl(dppm)$_2$]PF_6 (**17**)	--	[a]	[a]	6.80 – 7.60	5.25, 5.39	8.53
4-HC≡CC_6H_4{$\overline{CHO(CH_2)_3O}$} (**18**)	3.05	7.42 (8)	7.48 (9)	--	--	5.47
trans-[Ru{4-C=$CHC_6H_4\overline{CHO(CH_2)_3O}$}Cl(dppm)$_2$]$PF_6$ (**19**)	--	5.48 (8)	6.85 (8)	7.10 – 7.50	5.07, 5.30	5.35
trans-[Ru{4-C≡$CC_6H_4\overline{CHO(CH_2)_3O}$}Cl(dppm)$_2$] (**20**)	--	6.04 (8)	[a]	6.90 – 7.50	4.88	5.35
[Au{4-C≡$CC_6H_4\overline{CHO(CH_2)_3O}$}($PPh_3$)] (**21**)	--	7.35 (8)	[a]	7.38 – 7.60	--	5.45
[Au{4-C≡$CC_6H_4\overline{CHO(CH_2)_3O}$}($PMe_3$)] (**22**)	--	7.33 (8)	7.44 (8)	--	--	5.44

[a] Obscured by other resonances. [b] Not assigned.

Table 3.3. IR[a] and UV-vis[b] data for complexes **1-22**.

Compound	ν(C≡C) (cm^{-1})	λ_{max} (nm) [ε (10^4 M^{-1} cm^{-1})]
4-HC≡CC_6H_4CHO (**1**)	2114	271 [2.5]
4-HC≡$CC_6H_4CH\{OC(O)Me\}_2$ (**2**)	2111	252 [2.3]
[Ru(4-C≡$CC_6H_4CH\{OC(O)Me\}_2$)(PPh_3)$_2$(η-C_5H_5)] (**3**)	2066	326 [2.4]
[Ru(4-C≡CC_6H_4CHO)(PPh_3)$_2$(η-C_5H_5)] (**4**)	2053	400 [2.3]
trans-[Ru(4-C=CHC_6H_4CHO)Cl(dppm)$_2$]PF_6 (**5**)	--	403 [1.9]
trans-[Ru(4-C≡CC_6H_4CHO)Cl(dppm)$_2$] (**6**)	2059	405 [6.0]
trans-[Ru(4-C=CHC_6H_4CHO)Cl(dppe)$_2$]PF_6 (**7**)	--	412 [2.0]
trans-[Ru(4-C≡CC_6H_4CHO)Cl(dppe)$_2$] (**8**)	2047	413 [2.8]
[Au(4-C≡CC_6H_4CHO)(PPh_3)] (**9**)	2115	322 [5.0]
[Au(4-C≡CC_6H_4CHO)(PMe_3)] (**10**)	2112	322 [5.0]
3-HC≡CC_6H_4CHO (**11**)	2111	332 [0.1]
trans-[Ru(3-C=CHC_6H_4CHO)Cl(dppm)$_2$]PF_6 (**12**)	--	320 [1.1]
trans-[Ru(3-C≡CC_6H_4CHO)Cl(dppm)$_2$] (**13**)	2075	321 [0.9]
[Au(3-C≡CC_6H_4CHO)(PPh_3)] (**14**)	2120	286 [1.8]

[Au(3-C≡CC_6H_4CHO)(PMe_3)] (**15**)	2116	282 [1.6]
trans-[Ru(2-C=CHC_6H_4CHO)Cl(dppm)$_2$]PF_6 (**17**)	2097	555 [0.2]
4-HC≡CC_6H_4  (**18**)	2112	250 [1.9]
trans-[Ru 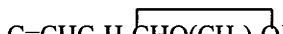 Cl(dppm)$_2$]PF_6 (**19**)	--	317 [1.3]
trans-[Ru 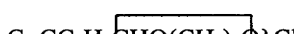 Cl(dppm)$_2$] (**20**)	2081	320 [1.2]
[Au 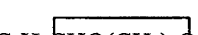 (PPh_3)] (**21**)	2117	296 [1.7]
[Au 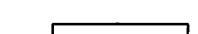 (PMe_3)] (**22**)	2118	292 [0.8]

[a] In dichloromethane. [b] In THF.

substituted terminal group to *meta* substitution leads to a decrease in λ_{max} and ε because there is no longer a conjugated path between donor and acceptor groups in the molecule.

Selected ^{13}C NMR spectra of complexes **1** – **22** are presented in Table 3.4. The vinylidene complexes **5**, **7**, **12** and **20** all show the strongly deshielded C_1 atom at 353 – 364 ppm which is not observed in the corresponding acetylides. Formyl groups display little variation in the chemical shift of the C_9 atom, with the exception of **17** which occurs at 170.2 ppm due to anisotropic effects.

Complex **17** was unusual in several other respects. The formyl proton which was found at 10.52 ppm in the parent acetylene and 9.54 ppm for the analogous *ortho* substituted complex, was found to be shifted upfield to 8.53 ppm, while the vinylidene proton which occurs at 3.13 ppm in the *meta* substituted analogue **12** has also been shifted upfield to 2.12 ppm. The ^{31}P NMR resonance occurs at -7.6 ppm in **17**, compared with -15.9 ppm for **12** and -16.1 ppm for **5**. The complex has a deep purple colouration, and a low intensity absorption band in the UV-vis spectrum at 555 nm, compared to **12** which has a λ_{max} of 320 nm and a shoulder at 400 nm and which is pale yellow in colour. Figure 3.2. represents a possible reason for these differing properties - a hydrogen bonding interaction between the formyl group and the vinylidene proton results in a more strongly stabilized intermediate.

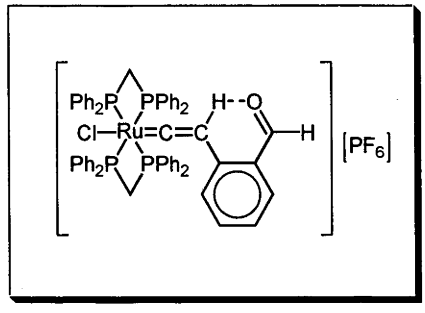

Figure 3.2. Suggested hydrogen-bonding interaction in **17**

Table 3.4. Selected ^{13}C NMR data (ppm)

Compound	C_1	C_2	C_3	C_9	C_{10}	C_{11}
4-HC≡CC_6H_4CHO (**1**)	81.0	82.5	128.2	191.3	--	--
4-HC≡$CC_6H_4CH\{OC(O)Me\}_2$ (**2**)	78.2	82.6	123.3	88.9	168.4	20.6
[Ru(4-C≡$CC_6H_4CH\{OC(O)Me\}_2$)$(PPh_3)_2(\eta\text{-}C_5H_5)$] (**3**)	122	114.9	129.9 or 132.7	90.7	169.5	21.7
[Ru(4-C≡CC_6H_4CHO)$(PPh_3)_2(\eta\text{-}C_5H_5)$] (**4**)	[a]	116.8	130.8	191.2	--	--
trans-[Ru(4-C=CHC_6H_4CHO)$Cl(dppm)_2$]PF_6 (**5**)	353.2	109.7	[a]	191.0	--	--
trans-[Ru(4-C≡CC_6H_4CHO)$Cl(dppm)_2$] (**6**)	[a]	115.0	130.2	191.4	--	--
trans-[Ru(4-C=CHC_6H_4CHO)$Cl(dppe)_2$]PF_6 (**7**)	353.8	109.2	[a]	191.2	--	--
trans-[Ru(4-C≡CC_6H_4CHO)$Cl(dppe)_2$] (**8**)	[b]	115.9	132.2	191.3	--	--
[Au(4-C≡CC_6H_4CHO)(PPh_3)] (**9**)	[b]	103.1	129.5 or 131.2	191.3	--	--
[Au(4-C≡CC_6H_4CHO)(PMe_3)] (**10**)	[b]	103.8	131.4 or 133.8	191.4	--	--
3-HC≡CC_6H_4CHO (**11**)	78.8	82.0	123.2	191.3	--	--
trans-[Ru(3-C=CHC_6H_4CHO)$Cl(dppm)_2$]PF_6 (**12**)	363.8	109.3	[a]	191.9	--	--
trans-[Ru(3-C≡CC_6H_4CHO)$Cl(dppm)_2$] (**13**)	[a]	111.1	122.5	192.8	--	--
[Au(3-C≡CC_6H_4CHO)(PPh_3)] (**14**)	[a]	[a]	125.5	192.0	--	--
[Au(3-C≡CC_6H_4CHO)(PMe_3)] (**15**)	[a]	102.9	125.9	191.9	--	--

2-HC≡CC_6H_4CHO (**16**)	79.0	84.2	125.3	191.3	--	--
trans-[Ru(2-C=CHC_6H_4CHO)Cl(dppm)$_2$]PF_6 (**17**)		[a]	123.5	170.2	--	--
4-HC≡CC_6H_4{$\overline{CHO(CH_2)_3O}$} (**18**)	[a]	83.3	122.2	100.7	67.2	25.5
trans-[Ru{4-C≡$CC_6H_4\overline{CHO(CH_2)_3O}$}Cl(dppm)$_2$]$PF_6$ (**19**)	356.7	109.6	[a]	100.9	67.2	25.5
trans-[Ru{4-C≡$CC_6H_4\overline{CHO(CH_2)_3O}$}Cl(dppm)$_2$] (**20**)	[a]	112.1	124.1	101.9	67.1	25.5
[Au{4-C≡$CC_6H_4\overline{CHO(CH_2)_3O}$}($PPh_3$)] (**21**)	[a]	[a]	125.1	101.3	67.2	25.6
[Au{4-C≡$CC_6H_4\overline{CHO(CH_2)_3O}$}($PMe_3$)] (**22**)	[a]	108.1	125.2	101.2	67.2	25.6

[a] Obscured by other resonances. [b] Not observed.

3.3.4. Electrochemical studies.

The results of cyclic voltammetric investigations into the new ruthenium vinylidene and acetylide complexes are summarized in Table 3.5. together with previously reported data for related complexes. All new complexes show an anodic wave assigned to the $Ru^{II/III}$ oxidation process. The tabulated data are consistent with several broad trends. Alkynylruthenium complexes exhibit reversible or quasi-reversible processes (in the range of 0.51 - 0.68 V for the new complexes), whereas the vinylidene complexes exhibit irreversible complexes at a considerably more positive potential (the latter as expected for cationic complexes). The 2-formylphenylvinylidene complex **15** has an anomalously low oxidation potential (in this regard, its very low energy UV-vis transition and lack of facile deprotonation to the corresponding alkynyl complex can also be regarded as non-conforming: see section 3.3.3.). Oxidation potentials vary on phenyl substituent variation as 4-H < 4-CH{OC(O)Me}$_2$ < 4-CHO < 4-NO_2, the increasingly stronger electron-withdrawing groups resulting in increasing difficulty in oxidation. Oxidation potentials vary on phenyl substituents location as 3-CHO < 4-CHO, the former out of conjugation, the latter in conjugation with the metal. These results are consistent with the arylalkynyl bridge providing an efficient conduit for electronic communication.

Table 3.5. Cyclic voltammetry data for ruthenium complexes

Complex	$E°_{Ru}{}^{II/III}$	ΔE	i_{pc}/i_{pa}*	Ref.
trans-[Ru{4-C=CHC$_6$H$_4$CHO(CH$_2$)$_3$O}Cl(dppm)$_2$]PF$_6$ (**19**)	1.48	--	NR	This work
trans-[Ru(2-C=CHC$_6$H$_4$CHO)Cl(dppm)$_2$]PF$_6$ (**17**)	1.23	--	NR	This work
trans-[Ru(3-C=CHC$_6$H$_4$CHO)Cl(dppm)$_2$]PF$_6$ (**12**)	1.34	--	NR	This work
trans-[Ru(4-C=CHC$_6$H$_4$CHO)Cl(dppm)$_2$]PF$_6$ (**5**)	1.50	0.15	NR	This work
trans-[Ru(C≡CPh)Cl(dppm)$_2$]	0.55	0.07	1.0	8
trans-[Ru{4-C≡CC$_6$H$_4$CHO(CH$_2$)$_3$O}Cl(dppm)$_2$] (**20**)	0.51	0.08	1.0	This work
trans-[Ru(3-C≡CC$_6$H$_4$CHO)Cl(dppm)$_2$] (**13**)	0.60	0.07	0.9	This work
trans-[Ru(4-C≡CC$_6$H$_4$CHO)Cl(dppm)$_2$] (**6**)	0.64	0.09	1.0	This work
trans-[Ru(4-C≡CC$_6$H$_4$NO$_2$)Cl(dppm)$_2$]	0.72	0.08	0.9	8
trans-[Ru(4-C=CHC$_6$H$_4$CHO)Cl(dppe)$_2$]PF$_6$ (**7**)	1.48	0.14	NR	This work
trans-[Ru(C≡CPh)Cl(dppe)$_2$]	0.55	0.06	1.0	This work
trans-[Ru(4-C≡CC$_6$H$_4$CHO)Cl(dppe)$_2$] (**8**)	0.68	0.08	1.0	This work
trans-[Ru(4-C≡CC$_6$H$_4$NO$_2$)Cl(dppe)$_2$]	0.74	0.08	0.9	This work
[Ru(C≡CPh)(PPh$_3$)$_2$(η-C$_5$H$_5$)]	0.54	--	0.5	10
[Ru(4-C≡CC$_6$H$_4$CH{OC(O)Me}$_2$)(PPh$_3$)$_2$(η-C$_5$H$_5$)] (**3**)	0.59	0.08	1.0	This work

[Ru(4-C≡CC$_6$H$_4$CHO)(PPh$_3$)$_2$(η-C$_5$H$_5$)] (**8**)	0.67	0.08	0.9	This work
[Ru(4-C≡CC$_6$H$_4$NO$_2$)(PPh$_3$)$_2$(η-C$_5$H$_5$)]	0.73	--	1.0	10

* NR signifies a nonreversible process under standard conditions (scan rate 100 mV s^{-1}, 25 °C)

3.4. X-ray structural study of some metal acetylides

3.4.1. X-ray structural study of trans-[Ru(4-C≡CC$_6$H$_4$CHO)Cl(dppe)$_2$]·1.75CH$_2$Cl$_2$ (8)

A single-crystal X-ray diffraction study of *trans*-[Ru(4-C≡CC$_6$H$_4$CHO)Cl(dppe)$_2$] (**8**) has been performed by collaborators at the Australian National University. An ORTEP plot of the complex is displayed in Figure 3.3. and selected bond lengths and angles are gathered in Table 3.6. A comparison of selected bond lengths and angles with those of related complexes appears in Table 3.7.

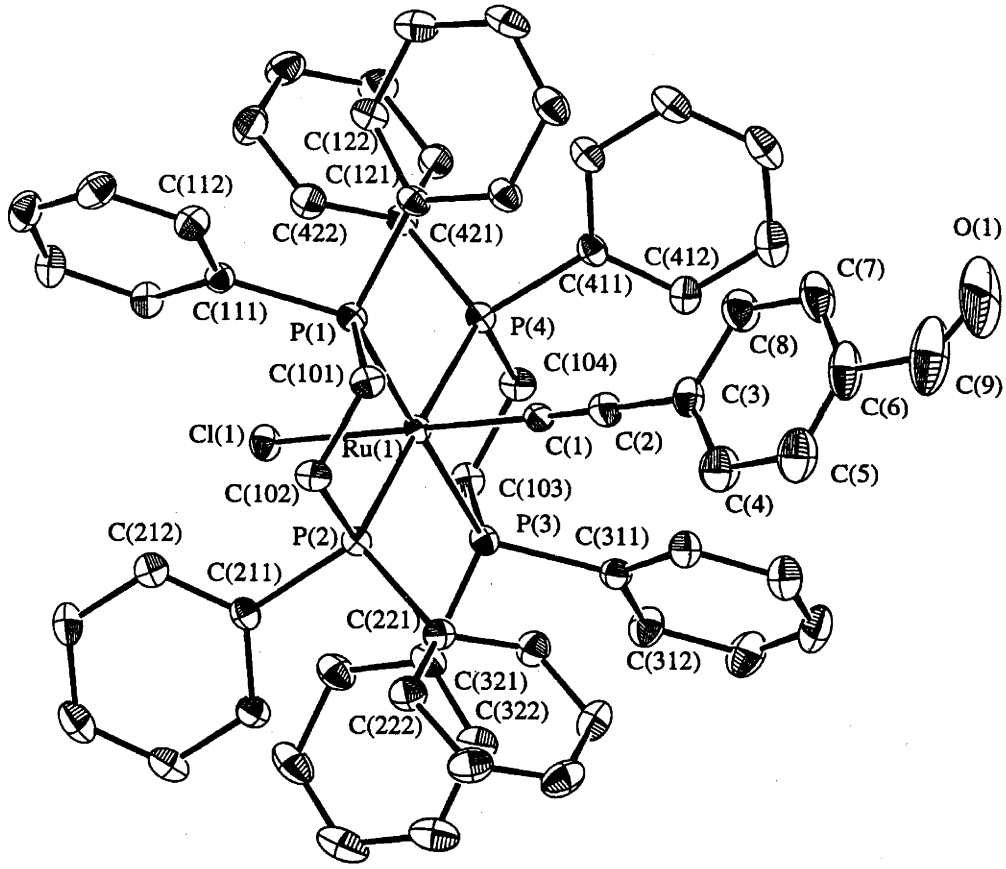

Figure 3.3. Molecular geometry and atomic labeling scheme for *trans*-[Ru(4-C≡CC$_6$H$_4$CHO)Cl(dppe)$_2$] (**8**). 20% thermal ellipsoids are shown for the non-hydrogen atoms. Hydrogen atoms are omitted for clarity. (Crystal structure provided by A.C. Willis and I.R. Whittall).

The structural study of **8** confirms the octahedral geometry at ruthenium and *trans*-disposed chloride and acetylide ligands. Important bond lengths about the metal centre are similar to those of the related, structurally characterized complexes *trans*-[Ru(C≡CPh)Cl(dppe)$_2$],[11] *trans*-[Ru(4-C≡CC$_6$H$_4$NO$_2$)Cl(dppe)$_2$][12] and *trans*-[Ru{(*E*)-4,4'-C≡CC$_6$H$_4$CH=CHC$_6$H$_4$NO$_2$}Cl(dppe)$_2$][13] (see Table 3.7.). The Cl-Ru-C(1) and Ru-C(1)-C(2) angles deviate slightly from the idealized 180°, presumably a result of packing effects. Distances and angles within the diphosphine ligands are unexceptional.

Table 3.6. Selected bond distances (Å) and angles (deg) for *trans*-[Ru(4-C≡CC_6H_4CHO)Cl(dppe)$_2$]·1.75CH_2Cl_2 (**8**)

Ru - Cl	2.507(1)	Ru - P(1)	2.388(1)
Ru - P(2)	2.365(1)	Ru - P(3)	2.384(1)
Ru - P(4)	2.370(1)	Ru - C(1)	2.012(4)
P(1) - C(101)	1.844(4)	C(101) - C(102)	1.519(5)
P(2) - C(102)	1.857(4)	P(3) - C(103)	1.840(4)
C(103) - C(104)	1.517(5)	P(4) - C(104)	1.866(4)
C(1) - C(2)	1.158(5)	C(2) - C(3)	1.457(6)
C(3) - C(4)	1.393(7)	C(3) - C(8)	1.396(6)
C(4) - C(5)	1.377(7)	C(7) - C(8)	1.371(7)
C(5) - C(6)	1.361(8)	C(6) - C(7)	1.389(8)
C(6) - C(9)	1.488(9)	C(9) - O(1)	1.08(1)
Cl(1) - Ru(1) - P(1)	98.52(4)	Cl(1) - Ru(1) - P(2)	92.29(4)
Cl(1) - Ru(1) - P(3)	82.58(4)	Cl(1) - Ru(1) - P(4)	88.70(4)
Cl(1) - Ru(1) - C(1)	179.1(1)	P(1) - Ru(1) - P(2)	81.93(4)
P(1) - Ru(1) - P(3)	178.89(4)	P(1) - Ru(1) - P(4)	98.73(4)
P(2) - Ru(1) - P(3)	97.87(4)	P(2) - Ru(1) - P(4)	178.72(4)
P(3) - Ru(1) - P(4)	81.45(4)	Ru(1) - P(1) - C(101)	103.4(1)
P(1) - C(101) - C(102)	107.0(3)	C(101) - C(102) - P(2)	110.0(3)
C(102) - P(2) - Ru(1)	108.9(1)	Ru(1) - P(3) - C(103)	104.1(1)
P(3) - C(103) - C(104)	106.8(3)	C(103) - C(104) - P(4)	111.5(3)
C(104) - P(4) - Ru(1)	108.6(1)	Ru(1) - C(1) - C(2)	176.5(4)
C(1) - C(2) - C(3)	178.2(5)	C(2) - C(3) - C(4)	121.4(4)
C(2) - C(3) - C(8)	120.8(4)	C(3) - C(4) - C(5)	120.8(5)
C(3) - C(8) - C(7)	120.8(5)	C(4) - C(5) - C(6)	120.8(6)
C(8) - C(7) - C(6)	120.4(5)	C(5) - C(6) - C(7)	119.3(5)
C(5) - C(6) - C(9)	120.9(9)	C(7) - C(6) - C(9)	119.7(9)
C(6) - C(9) - O(1)	133(2)		

Table 3.7. Comparison of selected bond lengths and angles in **8** with those of related complexes

Compound	Ru-C(1)	C(1)-C(2)	C(2)-C(3)	Cl-Ru-C(1)	Ru-C(1)-C(2)	C(1)-C(2)-C(3)	Reference
trans-[Ru(4-C≡CC_6H_4CHO)Cl(dppe)$_2$] (**8**)	2.009(3)	1.190(8)	1.428(8)	179.1(1)	176.5(4)	178.2(5)	This work
trans-[Ru(C≡CPh)Cl(dppe)$_2$]	2.007(5)	1.198(7)	1.445(8)	175.72(14)	174.1(5)	--	11
trans-[Ru(4-C≡C$C_6H_4NO_2$)Cl(dppe)$_2$]	1.986(5)	1.206(7)	1.442(7)	176.20(13)	175.3(4)	174.4(5)	12
trans-[Ru{(*E*)4,4'-C≡CC_6H_4CH=C$H C_6H_4NO_2$}Cl(dppe)$_2$]	1.996(4)	1.205(7)	1.434(7)	171.8(1)	177.4(4)	174.4(5)	13

3.4.2. X-ray structural study of [Au{4-C≡CC$_6$H$_4$CHO(CH$_2$)$_3$O}(PPh$_3$)] (21)

A single-crystal X-ray diffraction study of [Au{4-C≡CC$_6$H$_4$CHO(CH$_2$)$_3$O}(PPh$_3$)] (**21**) has been performed by collaborators at the Australian National University. An ORTEP plot is displayed in Figure 3.4. and selected bond lengths and angles are gathered in Table 3.8. A comparison of selected bond lengths and angles with those of related complexes appears in Table 3.9..

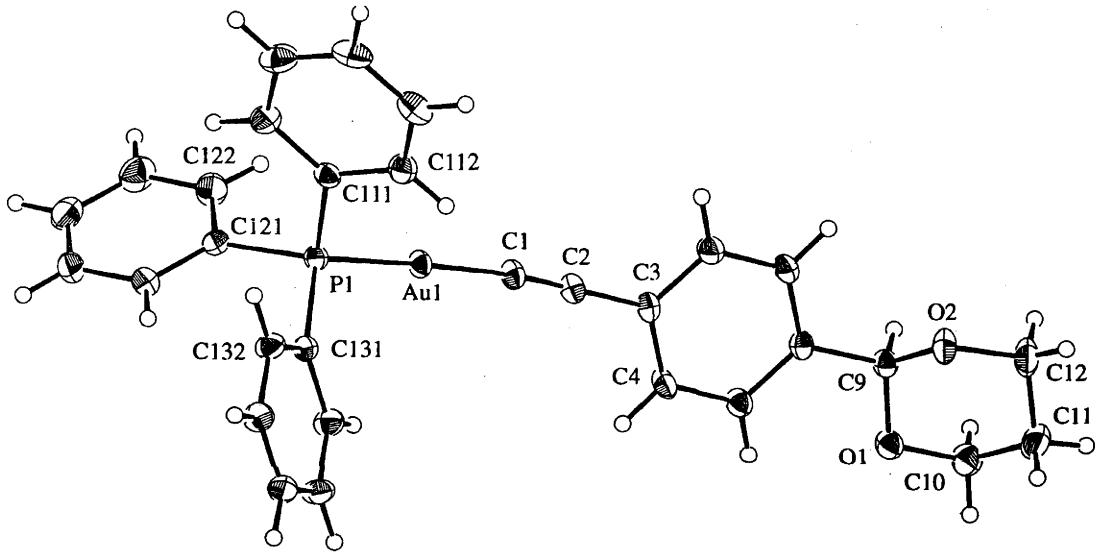

Figure 3.4. Molecular geometry and atomic labeling scheme for [Au{4-C≡CC$_6$H$_4$CHO(CH$_2$)$_3$O}(PPh$_3$)] (**21**). 30% thermal ellipsoids are shown for the non-hydrogen atoms. Hydrogen atoms are drawn as circles. (Crystal structure provided by A.C. Willis and N.T. Lucas).

The structural study of **21** confirms the approximately linear geometry about the gold. The Au - P, Au - C(1) and C(1) - C(2) bond distances are within the range of previously observed values for (phosphine)gold acetylide complexes.[14-16] Angles about the P - Au - C(1) - C(2) moiety are close to linearity, with any deviations likely to be the result of crystal packing forces. Intraphosphine bond lengths and angles in **21** are not unusual. Distances within the phenyl and 1,3-dioxane components of the alkynyl ligand are not unexpected. Gold complexes have attracted significant interest as many show aurophilic Au···Au interactions in the solid state. In the present case, however, Au···Au contacts are all greater than 5 Å.

Table 3.8. Selected bond distances (Å) and angles (deg) for [Au{4-C≡CC$_6$H$_4$CHO(CH$_2$)$_3$O}(PPh$_3$)] (**21**)

Au - P	2.2726(7)	P - C(111)	1.821(3)
P - C(121)	1.812(3)	P - C(131)	1.816(3)
Au - C(1)	2.006(3)	C(1) - C(2)	1.194(4)
C(2) - C(3)	1.440(4)	C(3) - C(4)	1.398(4)
C(4) - C(5)	1.381(4)	C(5) - C(6)	1.389(4)
C(6) - C(7)	1.386(4)	C(7) - C(8)	1.382(4)
C(3) - C(8)	1.391(4)	C(6) - C(9)	1.505(4)
C(9) - O(1)	1.408(4)	O(1) - C(10)	1.439(4)
C(10) - C(11)	1.500(6)	C(11) - C(12)	1.513(6)
C(12) - O(2)	1.450(4)	C(9) - O(2)	1.408(4)
C(9) - H(9)	0.95		
P - Au - C(1)	177.5(1)	Au - P - C(111)	113.1(1)
Au - P - C(121)	112.6(1)	Au - P - C(131)	114.0(1)
Au - C(1) - C(2)	170.9(3)	C(1) - C(2) - C(3)	174.5(3)
C(2) - C(3) - C(4)	121.7(3)	C(3) - C(4) - C(5)	121.2(3)
C(4) - C(5) - C(6)	120.6(3)	C(5) - C(6) - C(7)	118.6(3)
C(6) - C(7) - C(8)	120.8(3)	C(2) - C(3) - C(8)	120.7(3)
C(3) - C(8) - C(7)	121.2(3)	C(5) - C(6) - C(9)	122.5(3)
C(7) - C(6) - C(9)	118.9(3)	C(6) - C(9) - O(1)	109.8(2)
C(6) - C(9) - O(2)	108.0(3)	C(9) - O(1) - C(10)	110.1(3)
O(1) - C(9) - O(2)	111.2(3)	O(1) - C(10) - C(11)	109.7(3)
C(10) - C(11) - C(12)	110.0(3)	C(12) - O(2) - C(9)	110.0(3)

Table 3.9. Comparison of selected bond lengths and angles in **21** with those of analogous complexes

Compound	Au-C(1)	C(1)-C(2)	C(2)-C(3)	P-Au-C(1)	Au-C(1)-C(2)	C(1)-C(2)-C(3)	Reference
[Au{4-C≡CC$_6$H$_4$CHO(CH$_2$)$_3$O}(PPh$_3$)] (**21**)	2.006(3)	1.194(4)	1.440(4)	177.5(1)	170.9(3)	174.5(3)	This work
[Au(4-C≡CC$_6$H$_4$NO$_2$)(PPh$_3$)]	1.973(5)	1.206(6)	1.446(6)	178.1(2)	175.1(5)	179.8(6)	16
[Au(C≡CPh)(PPh$_3$)]	2.02(2)	1.16(2)	1.47(2)	173.8(5)	170.8(19)	174.0(20)	15
[Au(C≡CC$_6$F$_5$)(PPh$_3$)]	1.993(14)	1.197(16)	1.442(20)	177.9(3)	175.4(10)	178.4(12)	14

3.5. *Nonlinear optical investigations*

3.5.1. Results of second-order nonlinear optical investigations

Measurements of the second-order nonlinearities of the new metal complexes and some of their organic precursors were performed at 1064 nm using the hyper-Rayleigh scattering technique by collaborators at the University of Leuven, Belgium. The results are presented in Table 3.10. together with the two-level-corrected values β_0. The potential inadequacies of the two-state model have been discussed previously.[10] The low-energy band for these complexes is MLCT in character; higher-energy bands involve transitions with other ligands, which result in little change in dipole moment between ground and excited states, and hence little contribution to nonlinearity, so it is probable that the two-level-corrected values have some significance as an indicator of zero-frequency nonlinearity. Table 3.11. shows a comparison with previously reported values for related organometallic complexes. The tabulated data reveal that phenyl substituent variation results in β values increasing as 4-H < 4-CH{OC(O)Me}$_2$, 4-$\overline{\text{CHO(CH}_2)_3\text{O}}$ < 4-CHO < 4-NO_2, the expected trend for increasing acceptor strength in these dipolar molecules. In most instances, nonlinearities increase significantly on proceeding from precursor acetylene to product vinylidene or acetylide complex. Nonlinearities for gold complexes are significantly less than those for their ruthenium analogues, a result noted previously for related pairs of complexes.[1] Replacing PPh_3 by PMe_3 in proceeding from **21** to **22** results in a three-fold increase in β_{exp} and β_0, the opposite result to that seen in an earlier study of 5-nitro-2-pyridylalkynyl complexes;[8] PMe_3 is a more basic phosphine, resulting in a more electron-rich gold donor, but PPh_3 provides for more extensive π-delocalization, and it is not immediately apparent which is the more important factor influencing the magnitude of β in these complexes. Phenyl substituent location affects β, in replacing 3-CHO by 4-CHO (proceeding from **13** to **6**), with the magnitude increasing upon formal conjugation of the metal centre with the

Table 3.10. Second-order NLO results.

Compound	λ_{max} (nm) [ε (10^4) M^{-1} cm^{-1}]	β_{HRS} [a]	β_0 [a,b]
4-HC≡CC_6H_4CHO (**1**)	271 [2.5]	7	4
4-HC≡$CC_6H_4CH\{OC(O)Me\}_2$ (**2**)	252 [2.3]	11	7
[Ru(4-C≡$CC_6H_4CH\{OC(O)Me\}_2$)(PPh_3)$_2$(η-C_5H_5)] (**3**)	326 [2.4]	68	38
[Ru(4-C≡CC_6H_4CHO)(PPh_3)$_2$(η-C_5H_5)] (**4**)	400 [2.3]	120	45
trans-[Ru(4-C=CHC_6H_4CHO)Cl(dppm)$_2$]PF_6 (**5**)	403 [1.9]	108	39
trans-[Ru(4-C≡CC_6H_4CHO)Cl(dppm)$_2$] (**6**)	405 [6.0]	106	38
trans-[Ru(4-C=CHC_6H_4CHO)Cl(dppe)$_2$]PF_6 (**7**)	412 [2.0]	181	61
trans-[Ru(4-C≡CC_6H_4CHO)Cl(dppe)$_2$] (**8**)	413 [2.8]	120	40
[Au(4-C≡CC_6H_4CHO)(PPh_3)] (**9**)	322 [5.0]	14	8
[Au(4-C≡CC_6H_4CHO)(PMe_3)] (**10**)	322 [5.0]	[c]	--
3-HC≡CC_6H_4CHO (**11**)	332 [0.1]	21	12
trans-[Ru(3-C=CHC_6H_4CHO)Cl(dppm)$_2$]PF_6 (**12**)	320 [1.1]	45	26
trans-[Ru(3-C≡CC_6H_4CHO)Cl(dppm)$_2$] (**13**)	321 [0.9]	58	34
[Au(3-C≡CC_6H_4CHO)(PPh_3)] (**14**)	286 [1.8]	[c]	--
[Au(3-C≡CC_6H_4CHO)(PMe_3)] (**15**)	282 [1.6]	[c]	--
trans-[Ru(2-C=CHC_6H_4CHO)Cl(dppm)$_2$]PF_6 (**17**)	555 [0.2]	27	2
4-HC≡CC_6H_4CHO$(CH_2)_3$O (**18**)	250 [1.9]	27	20
trans-[Ru{4-C≡CC_6H_4CHO$(CH_2)_3$O}Cl(dppm)$_2$]PF_6 (**19**)	317 [1.3]	64	38
trans-[Ru{4-C≡CC_6H_4CHO$(CH_2)_3$O}Cl(dppm)$_2$] (**20**)	320 [1.2]	61	35
[Au{4-C≡CC_6H_4CHO$(CH_2)_3$O}(PPh_3)] (**21**)	296 [1.7]	15	4
[Au{4-C≡CC_6H_4CHO$(CH_2)_3$O}(PMe_3)] (**22**)	292 [0.8]	48	13

[a] Units of 10^{-30} esu. [b] HRS at 1064 nm corrected for resonance enhancement at 532 nm using the two-level model with $\beta_0 = \beta[1-(2\lambda_{max}/1064)^2][1-\lambda_{max}/1064)^2]$; damping factors not included. [c] Too low to measure.

acceptor formyl unit; however, this result does not translate to increased corrected nonlinearities, experimentally indistinguishable β_0 values being observed. Vinylidene and acetylide complex pairs {(**5**, **6**), (**12**, **13**) and (**19**, **20**)} have very similar nonlinearities.

Table 3.11. Comparison of second-order NLO data.

Compound	λ_{max} (nm) [ε (x 10^4) M^{-1} cm^{-1}]	β_{HRS} [a] (10^{-30} esu)	β_0 [a,b] (10^{-30} esu)	Ref.
trans-[Ru(4-C=CHC$_6$H$_4$R)Cl(dppm)$_2$]PF$_6$				
R = H	264 [2.5]	24	16	This work
R = $\overline{\text{CHO(CH}_2)_3\text{O}}$ (**19**)	317 [1.3]	64	38	This work
R = CHO (**5**)	403 [1.9]	108	39	This work
R = NO_2	471 [1.1]	721	127	This work
trans-[Ru(4-C≡CC$_6$H$_4$R)Cl(dppm)$_2$]				
R = H	308 [1.7]	20	12	8
R = $\overline{\text{CHO(CH}_2)_3\text{O}}$ (**20**)	320 [1.2]	61	35	This work
R = CHO (**6**)	405 [6.0]	106	38	This work
R = NO_2	473 [1.8]	767	129	8
trans-[Ru(4-C≡CC$_6$H$_4$R)Cl(dppe)$_2$]				
R = H	319 [1.8]	6	3	17
R = CHO (**8**)	413 [2.8]	120	40	This work
R = NO_2	477 [2.0]	351	55	17
[Ru(4-C≡CC$_6$H$_4$R)(PPh$_3$)$_2$(η-C$_5$H$_5$)]				
R = H	310 [2.0]	16	10	10
R = CH{OC(O)Me}$_2$ (**3**)	326 [2.4]	68	38	This work
R = CHO (**4**)	400 [2.3]	120	45	This work
R = NO_2	460 [1.1]	468	96	10
[Au(4-C≡CC$_6$H$_4$R)(PPh$_3$)]				
R = H	296 [1.3]	6	4	16
R = $\overline{\text{CHO(CH}_2)_3\text{O}}$ (**21**)	296 [1.7]	15	4	This work
R = CHO (**9**)	322 [5.0]	14	8	This work
R = NO_2	338 [2.5]	22	12	16

[a] Units of 10^{-30} esu. [b] HRS at 1064 nm corrected for resonance enhancement at 532 nm using the two-level model with $\beta_0 = \beta[1-(2\lambda_{max}/1064)^2][1-\lambda_{max}/1064)^2]$; damping factors not included.

3.5.3. Results of third-order nonlinear optical studies

Measurements of third-order optical nonlinearities were performed by the author with assistance from Dr M. Samoc using the Z-scan technique (see Section 1.3.5.) at 800 nm. The results are presented in Table 3.12. Table 3.13. shows a comparison of the data for the new complexes with previously reported values for related organometallic complexes.

3.5.4. Discussion of third-order nonlinear optical results

An electronic origin for cubic nonlinearities in related metal acetylide complexes has been demonstrated previously by degenerate four-wave mixing measurements,[18] and nonlinearities for the present series of compounds are therefore likely to be electronic in origin. Nonlinearities for the new compounds are low, with large error margins in many instances, rendering extraction of structure-property relationships difficult. Nevertheless, several points may be noted. Introduction of ligated gold in proceeding from **18** to **21** and replacing PMe_3 by PPh_3 in proceeding from **10** to **9** both result in increased γ_{real} and $|\gamma|$, and the γ_{real} and $|\gamma|$ values for **17** are larger than those of the 3- and 4-formylphenylvinylidene complex analogues.

Table 3.12. Third-order NLO results measured by Z-scan at 800 nm .[a]

Compound	γ_{real} (10^{-36} esu)	γ_{imag} (10^{-36} esu)	$\lvert\gamma\rvert$ (10^{-36} esu)
4-HC≡CC_6H_4CHO (**1**)	17 ± 8	0	17 ± 8
4-HC≡$CC_6H_4CH\{OC(O)Me\}_2$ (**2**)	-180 ± 80	5 ± 5	180 ± 80
[Ru(4-C≡$CC_6H_4CH\{OC(O)Me\}_2$)$(PPh_3)_2(\eta\text{-}C_5H_5)$] (**3**)	100 ± 100	0	100 ± 100
[Ru(4-C≡CC_6H_4CHO)$(PPh_3)_2(\eta\text{-}C_5H_5)$] (**4**)	-75 ± 50	210 ± 50	220 ± 60
trans-[Ru(4-C=CHC_6H_4CHO)Cl$(dppm)_2$]PF_6 (**5**)	25 ± 25	10 ± 10	30 ± 30
trans-[Ru(4-C≡CC_6H_4CHO)Cl$(dppm)_2$] (**6**)	60 ± 60	210 ± 60	220 ± 70
trans-[Ru(4-C=CHC_6H_4CHO)Cl$(dppe)_2$]PF_6 (**7**)	130 ± 130	0	130 ± 130
trans-[Ru(4-C≡CC_6H_4CHO)Cl$(dppe)_2$] (**8**)	-300 ± 500	100 ± 100	320 ± 510
[Au(4-C≡CC_6H_4CHO)(PPh_3)] (**9**)	300 ± 150	0	300 ± 150
[Au(4-C≡CC_6H_4CHO)(PMe_3)] (**10**)	35 ± 20	45 ± 30	60 ± 40
trans-[Ru(3-C=CHC_6H_4CHO)Cl$(dppm)_2$]PF_6 (**12**)	200 ± 200	0	200 ± 200
trans-[Ru(3-C≡CC_6H_4CHO)Cl$(dppm)_2$] (**13**)	150 ± 150	0	150 ± 150
[Au(3-C≡CC_6H_4CHO)(PPh_3)] (**14**)	[b]	--	--
[Au(3-C≡CC_6H_4CHO)(PMe_3)] (**15**)	[b]	--	--
trans-[Ru(2-C=CHC_6H_4CHO)Cl$(dppm)_2$]PF_6 (**17**)	450 ± 150	150 ± 60	470 ± 160
4-HC≡$CC_6H_4\overline{CHO(CH_2)_3O}\}$ (**18**)	15 ± 7	3 ± 3	15 ± 7
trans-[Ru{4-C≡$CC_6H_4\overline{CHO(CH_2)_3O}\}Cl(dppm)_2$]$PF_6$ (**19**)	75 ± 75	0	75 ± 75
trans-[Ru{4-C≡$CC_6H_4\overline{CHO(CH_2)_3O}\}Cl(dppm)_2$] (**20**)	50 ± 50	0	50 ± 50
[Au{4-C≡$CC_6H_4\overline{CHO(CH_2)_3O}\}(PPh_3)$] (**21**)	210 ± 100	0	210 ± 100

[a] All complexes are optically transparent at the fundamental frequency corresponding to the wavelength of 800 nm. Measured in THF. Results are referenced to the nonlinear refractive index of silica $n_2 = 3 \times 10^{-16}$ cm^2 W^{-1}.
[b] Not sufficiently soluble.

Table 3.13. Comparison of third-order NLO data.

Compound	γ_{real} (10^{-36} esu)	γ_{imag} (10^{-36} esu)	$\|\gamma\|$ (10^{-36} esu)	Ref.
trans-[Ru(4-C=CHC$_6$H$_4$R)Cl(dppm)$_2$]PF$_6$				
R = H	220 ± 220	0	220 ± 220	17
R = CHO(CH$_2$)$_3$O (**19**)	75 ± 75	0	75 ± 75	This work
R = CHO (**5**)	50 ± 50	0	50 ± 50	This work
R = NO$_2$	25 ± 25	3 ± 3	25 ± 25	17
trans-[Ru(4-C≡CC$_6$H$_4$R)Cl(dppm)$_2$]				
R = H	60 ± 60	0	60 ± 60	17
R = CHO(CH$_2$)$_3$O (**20**)	50 ± 50	0	50 ± 50	This work
R = CHO (**6**)	60 ± 60	210 ± 60	220 ± 70	This work
R = NO$_2$	170 ± 34	230 ± 46	286 ± 57	19
trans-[Ru(4-C≡CC$_6$H$_4$R)Cl(dppe)$_2$]				
R = H	-170 ± 40	71 ± 20	200 ± 50	20
R = CHO (**8**)	-300 ± 500	100 ± 100	316 ± 506	This work
R = NO$_2$	[a]	[a]	320 ± 55	13
[Ru(4-C≡CC$_6$H$_4$R)(PPh$_3$)$_2$(η-C$_5$H$_5$)]				
R = H	75 ± 75		75 ± 75	10
R = CH{OC(O)Me}$_2$ (**3**)	100 ± 100	0	100 ± 100	This work
R = CHO (**4**)	-75 ± 50	210 ± 50	220 ± 60	This work
R = NO$_2$	-210 ± 50	5 ± 5	210 ± 50	10
[Au(4-C≡CC$_6$H$_4$R)(PPh$_3$)]				
R = H	39 ± 20	0	39 ± 20	16
R = CHO(CH$_2$)$_3$O (**21**)	210 ± 100	0	210 ± 100	This work
R = CHO (**9**)	300 ± 150	0	300 ± 150	This work
R = NO$_2$	120 ± 40	20 ± 15	122 ± 42	16

[a] Not specified.

3.6. Conclusions

The acetylenes 4-HC≡CC$_6$H$_4$R [R = CH{OC(O)Me}$_2$ (**2**), $\overline{\text{CHO(CH}_2)_3\text{O}}$ (**18**)], ruthenium complexes [Ru(n-C≡CC$_6$H$_4$R)(PPh$_3$)$_2$(η-C$_5$H$_5$)] [R = CH{OC(O)Me}$_2$ (**3**), CHO (**4**)], [Ru(n-C=CHC$_6$H$_4$R)Cl(L$_2$)$_2$]PF$_6$ [L = dppm, n = 4, R = $\overline{\text{CHO(CH}_2)_3\text{O}}$ (**19**), R = CHO, n = 3 (**12**), 2 (**17**); L = dppe, n = 4, R = CHO (**7**)] and [Ru(n-C≡CC$_6$H$_4$R)Cl(L$_2$)$_2$] [L = dppm, n = 4, R = $\overline{\text{CHO(CH}_2)_3\text{O}}$ (**20**), n = 3, R = CHO (**13**); L = dppe, n = 4, R = CHO (**8**)] and gold complexes [Au(n-C≡CC$_6$H$_4$R)(L)] [n = 4, R = CHO, L = PPh$_3$ (**9**), PMe$_3$ (**10**); n = 4, R = $\overline{\text{CHO(CH}_2)_3\text{O}}$, L = PPh$_3$ (**21**), PMe$_3$ (**22**); n = 3, R = CHO, L = PPh$_3$ (**14**), PMe$_3$ (**15**)] have been prepared, and **8** and **21** characterized by a single-crystal X-ray diffraction study. Electrochemical data for the ruthenium complexes reveal reversible or quasi-reversible (alkynyl complexes) or irreversible (vinylidene complexes) processes assigned to the $Ru^{II/III}$ couple; the effect on $E_{1/2}$ values of the various structural modifications across **8**, **12**, **13**, **17**, **19** and **20** have been examined, with increasingly stronger electron-withdrawing groups resulting in increasing difficulty in oxidation, and the out-of-conjugation 3-CHO complexes easier to oxidize than their in-conjugation 4-CHO analogues. Those results are consistent with the arylalkynyl bridge providing an efficient conduit for electronic communication. The molecular quadratic and cubic optical nonlinearities of **1 – 10**, **12 - 15** and **17 - 22** have been determined by the hyper-Rayleigh scattering technique at 1064 nm and the Z-scan technique at 800 nm, respectively; β values increase on increasing acceptor strength, proceeding from 3-acceptor-substituted to 4-acceptor-substituted arylalkynyl ligand, and increasing phosphine donor strength, whereas γ values increase on increasing number of phosphine aryl groups (i.e. increasing delocalization) proceeding from PMe$_3$ to PPh$_3$-containing complex.

3.7. Experimental

3.7.1 General Conditions, Reagents and Instruments

General Conditions

All reactions were performed under a nitrogen atmosphere with the use of standard Schlenk techniques unless otherwise stated. Dichloromethane and triethylamine were dried by distilling over calcium hydride, diethyl ether and THF were dried by distilling over sodium / benzophenone, and other solvents were used as received. "Petroleum spirit" refers to a fraction of petroleum ether of boiling range 60-80 °C. Chromatography was on silica gel (230-400 mesh ASTM) or basic ungraded alumina.

The following reagents were prepared by the literature procedures: *cis*-$[RuCl_2(dppm)_2]$ and *cis*-$[RuCl_2(dppe)_2]$,[21] $[AuCl(PPh_3)]$,[22] $[AuCl(PMe_3)]$,[14] 4-$HC{\equiv}CC_6H_4CHO$, 3-$HC{\equiv}CC_6H_4CHO$ and 2-$HC{\equiv}CC_6H_4CHO$.[23] Ammonium hexafluorophosphate (Aldrich), 4-$MeC_6H_4SO_3H.H_2O$ (Aldrich), 1,3-propanediol (Aldrich), $FeCl_3$ (Ajax) and acetic anhydride (Aldrich) were used as received.

EI (electron impact) mass spectra (both unit resolution and high resolution (HR)) were recorded using a VG Autospec instrument (70 eV electron energy, 8 kV accelerating potential) and secondary ion mass spectra (SI MS) were recorded using a VG ZAB 2SEQ instrument (30 kV Cs^+ ions, current 1 mA, accelerating potential 8 kV, 3-nitrobenzyl alcohol matrix) at the Research School of Chemistry, Australian National University; peaks are reported as *m/z* (assignment, relative intensity). Microanalyses were carried out at the Research School of Chemistry, Australian National University. Infrared spectra were recorded either as 1% KBr discs or dichloromethane solutions using a Perkin-Elmer System 2000 FT-IR. ^1H, ^{31}P, and ^{13}C NMR spectra were recorded using a Varian Gemini-300 FT NMR spectrometer and are referenced to residual

chloroform (7.24 ppm), *d*-chloroform (77.0 ppm) or external 85% H_3PO_4 (0.0 ppm), respectively. The assignments follow the numbering scheme shown in Figure 3.1. UV-vis spectra of solutions were recorded in tetrahydrofuran in 1 cm quartz cells using a Cary 5 spectrophotometer. Electrochemical measurements were recorded using a MacLab 400 interface and MacLab potentiostat from ADInstruments. The supporting electrolyte was 0.1 M $(NBu^n_4)PF_6$ in distilled, deoxygenated CH_2Cl_2. Solutions containing *ca* 1 x 10^{-3} M complex were maintained under argon. Measurements were carried out at room temperature using platinum disc working-, Pt wire auxiliary- and Ag/AgCl reference- electrodes, such that the ferrocene/ferrocenium redox couple was located at 0.56 V (peak separation around 0.09 V). Scan rates were typically 100 mV s^{-1}.

3.7.2. Synthesis of terminal acetylenes

3.7.2.1. 4-HC≡CC$_6$H$_4$CH{OC(O)Me}$_2$ (1)

4-HC≡CC$_6$H$_4$CHO (1.00 g, 7.69 mmol) was stirred in acetic anhydride (6 mL) for 15 min, and then 0.1 g of anhydrous ferric chloride was added. After stirring a further 20 min, the reaction mixture was poured into 50 mL of hexane and 10 mL of water. The aqueous phase was washed with hexane (3 x 30 mL), and the combined organic extracts were washed with water (3 x 30 mL). The organic phase was dried and concentrated to give the white product (690 mg, 39 %). Anal. Calcd for $C_{13}H_{12}O_4$: C 67.23, H 5.21 %. Found: C 66.45, H 5.31 %. IR: (CH_2Cl_2) ν(HC≡) 3297 cm^{-1}, (C≡C) 2111 cm^{-1}. UV-Vis: λ (thf) 252 nm, ε 17 000 M^{-1} cm^{-1}. ^{1}H NMR: (δ, 300 MHz, $CDCl_3$); 2.11 (s, 6H, H_{11}), 3.10 (s, 1H, H_1), 7.45 (d, J_{HH} = 9 Hz, 2H, H_4), 7.51 (d, J_{HH} = 9 Hz, 2H, H_5), 7.64 (s, 1H, H_9). SI MS; 232 ([M]$^+$, 20), 189 ([M - C(O)Me]$^+$, 25), 173 ([M - OC(O)Me]$^+$, 20), 129 ([M] - MeC(O)OC(O)Me - H]$^+$, 100), 101 ([M] - CH{OC(O)Me}$_2$]$^+$, 40). HR MS calcd for $C_{13}H_{12}O_4$ *m/z* 232.0737, found 232.0735.

3.7.2.2. *4-HC≡CC$_6$H$_4$CHO(CH$_2$)$_3$O (18)*

4-HC≡CC$_6$H$_4$CHO (200 mg, 1.54 mmol), 4-MeC$_6$H$_4$SO$_3$H·H$_2$O (40 mg, 0.21 mmol) and HO(CH$_2$)$_3$OH (140 mg, 1.85 mmol) were stirred in dichloromethane (25 mL) for 8 h. The solution was neutralized with saturated sodium hydrogen carbonate solution, washed with water and dried with MgSO$_4$. The solvent was removed under reduced pressure to obtain the off-white product (204 mg, 69 %). Anal. Calcd for C$_{12}$H$_{12}$O$_2$: C 76.57, H 6.43 %. Found: C 75.89, H 5.93 %. IR: (CH$_2$Cl$_2$) ν(C≡C) 2112 cm^{-1}. UV-Vis: λ (thf) 250 nm, ε 18 900 M^{-1} cm^{-1}. ^{1}H NMR: (δ, 300 MHz, CDCl$_3$); 1.44 (m, 1H, H$_{11}$), 2.10 – 2.30 (m, 1H, H$_{11}$), 3.05 (s, 1H, H$_1$), 3.90 - 4.05 (m, 2H, H$_{10}$), 4.20 - 4.30 (m, 2H, H$_{10}$), 5.47 (s, 1H, H$_9$), 7.42 (d, J_{HH} = 9 Hz, 2H, H$_4$), 7.48 (d, J_{HH} = 9 Hz, 2H, H$_5$). EI MS; 188 ([M]$^+$, 100), 129 ([M - H - (CH$_2$)$_3$O]$^+$, 95). HR MS calcd for C$_{12}$H$_{12}$O$_2$ *m/z* 188.0837, found 188.0836.

3.7.3. Synthesis of metal complexes

3.7.3.1. *[Ru(4-C≡CC$_6$H$_4$CH{OC(O)Me}$_2$)(PPh$_3$)$_2$(η-C$_5$H$_5$)] (3)*

[RuCl(PPh$_3$)$_2$(η-C$_5$H$_5$)] (300 mg, 0.41 mmol), NH$_4$PF$_6$ (101 mg, 0.62 mmol) and 4-HC≡CC$_6$H$_4$CH{OC(O)Me}$_2$ (**1**) (115 mg, 0.50 mmol) were added to methanol (25 mL), and the resultant mixture refluxed with stirring for 1 h, and then allowed to cool. A solution of sodium methoxide in methanol (1 M, 5 mL) was added, the mixture was stirred for 5 min, and then the solvent removed under reduced pressure. Column chromatography with 1:1 petroleum spirit / dichloromethane yielded the orange product (235 mg, 62 %). Anal. Calcd for C$_{54}$H$_{46}$O$_4$P$_2$Ru: C 70.35, H 5.03 %. Found: C 70.19, H 5.40 %. IR: (CH$_2$Cl$_2$) ν(C≡C) 2066 cm^{-1}. UV-Vis: λ (thf) 327 nm, ε 22 600 M^{-1} cm^{-1}. ^{1}H NMR: (δ, 300 MHz, CDCl$_3$); 2.10 (m, 6H, Me), 4.29 (s, 5H, C$_5$H$_5$), 7.10 - 7.50 (m, 30H, Ph), 7.64 (s, 1H, H$_9$). ^{31}P NMR: (δ, 121 MHz, CDCl$_3$); 51.3. SI MS; 922 ([M]$^+$,

40), 863 ([M - OC(O)Me]$^+$, 5), 660 ([M – PPh_3]$^+$, 10), 429 ([M – PPh_3 - $C{\equiv}CC_6H_4CH\{OC(O)Me\}_2$]$^+$, 100).

3.7.3.2. [Ru(4-C≡CC$_6$H$_4$CHO)(PPh$_3$)$_2$(η-C$_5$H$_5$)] (4)

[Ru(4-C≡CC$_6$H$_4$CH{OC(O)Me}$_2$)(PPh$_3$)$_2$(η-C$_5$H$_5$)] (**3**) (300 mg, 0.33 mmol) was dissolved in methanol (15 mL) and a solution of sodium methoxide in methanol (1 M, 5 mL) was added. The mixture was stirred at room temperature for 2 h and then the solvent reduced, yielding the orange-red product (221 mg, 73 %). Anal. Calcd for $C_{50}H_{40}OP_2Ru$: C 73.25, H 4.92 %. Found: C 72.32, H 5.32 %. IR: (CH_2Cl_2) ν(C≡C) 2053 cm^{-1}. UV-Vis: λ (thf) 400 nm, ε 23 000 M^{-1} cm^{-1}. ^{1}H NMR: (δ, 300 MHz, $CDCl_3$); 4.33 (s, 5H, C_5H_5), 6.90 - 7.60 (m, 32H, Ph), 9.85 (s, 1H, H_9). ^{31}P NMR: (δ, 121 MHz, $CDCl_3$); 51.0. SI MS; 820 ([M]$^+$, 100), 691 ([M - C≡CC$_6$H$_4$CHO]$^+$, 25), 558 ([M - PPh_3 - H]$^+$, 20), 429 ([Ru(PPh_3)(η-C$_5$H$_5$)]$^+$, 45).

3.7.3.3. trans-[Ru(4-C=CHC$_6$H$_4$CHO)Cl(dppm)$_2$]PF$_6$ (5)

cis-[$RuCl_2$(dppm)$_2$] (300 mg, 0.32 mmol), NH_4PF_6 (105 mg, 0.64 mmol) and 4-HC≡CC$_6$H$_4$CHO (83 mg, 0.64 mmol) were added to dichloromethane (25 mL), and the mixture stirred for 6 h. The cooled reaction mixture was passed through a sintered glass funnel to remove NH_4Cl and excess NH_4PF_6. The solvent was removed under reduced pressure and the resulting residue was washed with diethyl ether, affording the orange-yellow product (240 mg, 73 %). Anal. Calcd for $C_{59}H_{50}ClF_6OP_5Ru$: C, 60.03; H, 4.27 %. Found: C, 60.34; H, 4.33 %. IR: (KBr) ν(PF) 838 cm^{-1}. UV-Vis: λ 403 nm, ε 19 000 M^{-1} cm^{-1}. ^{1}H NMR: (δ, 300 MHz, $CDCl_3$); 3.17 (m, H_2, =CH), 5.12 (m, 2H, PCH_2), 5.30 (m, 2H, PCH_2), 5.62 (d, J_{HH} = 8 Hz, 2H, H_4), 7.10 - 7.55 (m, 42H, H_5 + Ph), 9.75 (s, 1H, H_9). ^{31}P NMR: (δ, 121 MHz, $CDCl_3$); -16.1. SI MS: 1035 ([M – PF_6]$^+$, 95), 999 ([M - PF_6 - HCl]$^+$, 20), 905 ([M – PF_6 - C≡CHC$_6$H$_4$CHO]$^+$, 90), 869 ([Ru(dppm)$_2$ - H]$^+$, 100), 485 ([Ru(dppm) - H]$^+$, 55).

3.7.3.4. *trans-[Ru(4-C≡CC$_6$H$_4$CHO)Cl(dppm)$_2$]·0.75CH$_2$Cl$_2$ (6)*

cis-[RuCl$_2$(dppm)$_2$] (300 mg, 0.32 mmol), NH_4PF_6 (105 mg, 0.64 mmol) and 4-HC≡CC$_6$H$_4$CHO (83 mg, 0.64 mmol) were added to dichloromethane (25 mL), and the mixture stirred for 6 h. Triethylamine (0.5 mL) and petroleum spirit (10 mL) were added and the mixture passed through a silica plug. The solvents were removed under reduced pressure and the resulting residue purified by column chromatography on alumina using 1:1 dichloromethane/petroleum spirit as eluant. The major, yellow, band was collected and the solvent removed to afford the yellow product (220 mg, 66 %). Anal. Calcd for $C_{59.75}H_{49.5}Cl_{1.5}OP_4Ru$: C, 65.35; H, 4.64 %. Found: C, 65.27; H 4.91 %. IR: ν(C≡C) 2059 cm^{-1}. UV-Vis: λ 405 nm, ε 60 000 M^{-1} cm^{-1}. ^{1}H NMR: (δ, 300 MHz, $CDCl_3$); 4.92 (m, 4H, PCH_2), 5.28 (s, 1.5H, CH_2Cl_2), 6.03 (d, J_{HH} = 8 Hz, 2H, H_4), 7.00-7.60 (m, 42H, H_5 + Ph), 9.75 (s, 1H, H_9). ^{31}P NMR: (δ, 121 MHz, $CDCl_3$); -5.9. SI MS: 1034 ([M]$^+$, 100), 999 ([M - Cl]$^+$, 12), 905 ([M - C≡CC$_6$H$_4$CHO]$^+$, 6), 869 ([Ru(dppm)$_2$ - H]$^+$, 12), 486 ([Ru(dppm)]$^+$, 75).

3.7.3.5. *trans-[Ru(4-C=CHC$_6$H$_4$CHO)Cl(dppe)$_2$]PF$_6$ (7)*

A mixture of *cis*-[RuCl$_2$(dppe)$_2$] (300 mg, 0.31 mmol), NH_4PF_6 (101 mg, 0.62 mmol) and HC≡CC$_6$H$_4$CHO (**7**, 83 mg, 0.64 mmol) in dichloromethane (25 mL) was stirred for 6 h and was then filtered to remove NH_4Cl and excess NH_4PF_6. The solvent was removed under reduced pressure and the resulting residue was washed with diethyl ether to afford the yellow product (375 mg, 78 %). Anal. Calcd for $C_{61}H_{54}ClF_6OP_5Ru$: C, 60.63; H, 4.50 %. Found: C, 60.43; H 4.77 %. IR: (KBr) ν(PF) 836 cm^{-1}. UV-Vis: λ 413 nm, ε 20 000 M^{-1} cm^{-1}. ^{1}H NMR: (δ, 300 MHz, $CDCl_3$); 2.90 (m, 8H, PCH_2), 4.47 (m, 1H, =CH), 5.70 (d, 2H, J_{HH} = 8 Hz, H_4), 6.90 - 7.40 (m, 42H, H_5 + Ph), 9.64 (s, 1H, H_9). ^{31}P NMR: (δ, 121 MHz, $CDCl_3$); 35.9. SI MS: 1063 ([M – PF_6]$^+$, 100), 1027 ([M – PF_6 - HCl]$^+$, 30), 933 ([M – PF_6 – C=CHC$_6$H$_4$CHO]$^+$, 40), 897 ([Ru(dppe)$_2$ - H]$^+$, 45), 498 ([Ru(dppe) - 2H]$^+$, 98).

3.7.3.6. *trans-[Ru(4-C≡CC$_6$H$_4$CHO)Cl(dppe)$_2$]·1.75CH$_2$Cl$_2$ (**8**)*

A mixture of *cis*-[RuCl$_2$(dppe)$_2$] (300 mg, 0.31 mmol), NH_4PF_6 (101 mg, 0.64 mmol) and HC≡CC$_6$H$_4$CHO (81 mg, 0.64 mmol) in dichloromethane (25 mL) was stirred for 6 h. Triethylamine (0.5 mL) and petroleum spirit (10 mL) were then added and the mixture passed through an alumina plug. The solvent was removed from the filtrate under reduced pressure and the resulting residue washed with diethyl ether (50 mL), taken up in dichloromethane and purified by column chromatography using 1:1 dichloromethane / petroleum spirit as eluant. The major yellow band was collected and taken to dryness to afford **8** as a yellow solid (230 mg, 70 %). Recrystallization by solvent diffusion of methanol into a dichloromethane solution afforded yellow crystals suitable for the X-ray study. Anal. Calcd for $C_{62.75}H_{56.5}Cl_{4.5}OP_4Ru$: C, 62.23; H, 4.70 %. Found: C, 62.60; H 4.53 %. IR: ν(C≡C) 2047 cm^{-1}. UV-Vis: λ 413 nm, ε 28 000 M^{-1} cm^{-1}. ^{1}H NMR: (δ, 300 MHz, $CDCl_3$); 2.67 (m, 8H, PCH_2), 5.28 (s, 3.5H, CH_2Cl_2), 6.57 (d, 2H, J_{HH} = 8 Hz, H_4), 6.90 - 7.40 (m, 40H, Ph), 7.57 (d, 2H, J_{HH} = 8 Hz, H_5), 9.75 (s, 1H, H_9). ^{31}P NMR: (δ, 121 MHz, $CDCl_3$); 49.6. SI MS: 1062 ([M]$^+$, 100), 1027 ([M - Cl]$^+$, 45), 933 ([M - C≡CC$_6$H$_4$CHO]$^+$, 8), 897 ([Ru(dppe)$_2$ - H]$^+$, 35), 498 ([Ru(dppe) - 2H]$^+$, 25).

3.7.3.7. *[Au(4-C≡CC$_6$H$_4$CHO)(PPh$_3$)] (**9**)*

[AuCl(PPh$_3$)] (200 mg, 0.40 mmol) and 4-HC≡CC$_6$H$_4$CHO (57 mg, 0.44 mmol) were stirred in a solution of sodium methoxide in methanol (0.1 M, 15 mL) for 16 h. After this time, a solid had precipitated and was collected by filtration to yield the yellow product (135 mg, 57 %). Anal. Calcd for $C_{27}H_{20}AuOP$: C 55.12, H 3.43 %. Found: C 54.62, H 3.39 %. IR: (CH_2Cl_2) ν(C≡C) 2115 cm^{-1}. UV-Vis: λ (thf) 322 nm, ε 50 000 M^{-1} cm^{-1}. ^{1}H NMR: (δ, 300 MHz, $CDCl_3$); 7.30 - 7.80 (m, 19H, Ph), 9.94 (s, 1H, H_9). ^{31}P NMR: (δ, 121 MHz, $CDCl_3$); 42.8. SI MS; 1047 ([M + Au(PPh$_3$)]$^+$, 75), 721 ([Au(PPh$_3$)$_2$]$^+$, 20), 589 ([M]$^+$, 30), 459 ([Au(PPh$_3$)]$^+$, 100).

3.7.3.8. *[Au(4-C≡CC$_6$H$_4$CHO)(PMe$_3$)] (**10**)*

[AuCl(PMe$_3$)] (154 mg, 0.50 mmol) and 4-HC≡CC$_6$H$_4$CHO (72 mg, 0.55 mmol) were stirred in a solution of sodium methoxide in methanol (0.1 M, 15 mL) for 16 h. After this time, a solid had precipitated and was collected by filtration to yield the pale-yellow product (156 mg, 78 %). Anal. Calcd for $C_{12}H_{14}AuOP$: C 35.84, H 3.51 %. Found: C 36.87, H 3.71 %. IR: (CH_2Cl_2) ν(C≡C) 2112 cm^{-1}. UV-Vis: λ (thf) 322 nm, ε 49 800 M^{-1} cm^{-1}. ^{1}H NMR: (δ, 300 MHz, $CDCl_3$); 1.51 (d, J_{HP} = 10 Hz, 9H, Me), 7.54 (d, J_{HH} = 8 Hz, 2H, C$_6$H$_4$), 7.72 (d, J_{HH} = 8 Hz, 2H, C$_6$H$_4$), 9.92 (s, H$_9$). ^{31}P NMR: (δ, 121 MHz, $CDCl_3$); 1.6. SI MS; 675 ([M + Au(PMe$_3$) - 2H]$^+$, 40), 403 ([M]$^+$, 60), 349 ([Au(PMe$_3$)$_2$]$^+$, 45), 273 ([Au(PMe$_3$)]$^+$, 80).

3.7.3.9. *trans-[Ru(3-C=CHC$_6$H$_4$CHO)Cl(dppm)$_2$]PF$_6$ (**12**)*

cis-[RuCl$_2$(dppm)$_2$] (400 mg, 0.43 mmol), NH_4PF_6 (140 mg, 0.86 mmol) and 3-HC≡CC$_6$H$_4$CHO (174 mg, 0.86 mmol) were added to dichloromethane (25 mL), and the resultant mixture refluxed for 2 h. Petroleum spirit (50 mL) was added, and the resulting precipitate was collected and washed with diethyl ether (30 mL) to afford the pale red solid (409 mg, 76 %). Anal. Calcd for $C_{59}H_{50}ClF_6OP_5Ru$: C 60.03, H 4.27 %. Found: C 59.67, H 4.44 %. IR: (KBr) ν(PF) 839 cm^{-1}. UV-Vis: λ (thf) 320 nm, ε 10 900 M^{-1} cm^{-1}. ^{1}H NMR: (δ, 300 MHz, $CDCl_3$); 3.13 (m, H$_2$, =CH), 5.12 (m, 2H, PCH$_2$P), 5.32 (m, 2H, PCH$_2$P), 5.75 - 6.90 (4H, H$_4$, H$_5$), 7.10 - 7.60 (m, 40H, Ph), 9.54 (s, H$_9$). ^{31}P NMR: (δ, 121 MHz, $CDCl_3$); -15.9. SI MS; 1035 ([M – PF$_6$]$^+$, 40), 999 ([M - Cl – PF$_6$]$^+$, 10), 904 ([RuCl(dppm)$_2$]$^+$, 70), 869 ([Ru(dppm)$_2$ - H]$^+$, 100).

3.7.3.10. *trans-[Ru(3-C≡CC$_6$H$_4$CHO)Cl(dppm)$_2$] (**13**)*

cis-[RuCl$_2$(dppm)$_2$] (300 mg, 0.32 mmol), NH_4PF_6 (104 mg, 0.64 mmol) and 3-HC≡CC$_6$H$_4$CHO (90 mg, 0.69 mmol) were added to dichloromethane (25 mL), and the resultant mixture stirred for 4 h. Triethylamine (1.0 mL) and petroleum spirit (20 mL)

were then added, and the solution filtered through an alumina plug. The solvent was removed under vacuum, and the solid was then triturated with petroleum spirit and filtered to afford the yellow product (156 mg, 83%). Anal. Calcd for $C_{59}H_{49}ClOP_4Ru$: C 68.50, H 4.77 %. Found: C 68.06, H 4.75 %. IR: (CH_2Cl_2) ν(C≡C) 2075 cm^{-1}. UV-Vis: λ (thf) 321 nm, ε 9 500 M^{-1} cm^{-1}, 260 nm, ε 32 300 M^{-1} cm^{-1}. ^1H NMR: (δ, 300 MHz, $CDCl_3$); 4.89 (m, 4H, PCH_2P), 6.28 (d, J_{HH} = 8 Hz, 1H, H_4 or H_6), 6.39 (s, 1H, H_8), 7.05 - 7.60 (m, 40H, Ph + H_5 + H_4 or H_6), 9.54 (s, 1H, H_9). ^{31}P NMR: (δ, 121 MHz, $CDCl_3$); -6.0. SI MS; 1034 ($[M - H]^+$, 100), 999 ($[M - Cl]^+$, 20), 905 ($[RuCl(dppm)_2]^+$, 25), 869 ($[Ru(dppm)_2 - H]^+$, 60), 485 ($[Ru(dppm) - H]^+$, 35).

3.7.3.11. [Au(3-C≡CC$_6$H$_4$CHO)(PPh$_3$)] (14)

[AuCl(PPh_3)] (200 mg, 0.404 mmol) and 3-HC≡CC_6H_4CHO (63 mg, 0.49 mmol) were stirred in a solution of sodium methoxide in methanol (0.1 M, 15 mL) for 16 h. After this time, a solid product had precipitated which was washed with petroleum spirit and was collected by filtration to yield the pale-yellow solid (136 mg, 57 %). Anal. Calcd for $C_{27}H_{20}AuOP$: C 55.11, H 3.43 %. Found: C 54.43, H 3.53 %. IR: (CH_2Cl_2) ν(C≡C) 2120 cm^{-1}. UV-Vis: λ (thf) 318 nm, ε 4 700 M^{-1} cm^{-1}, 286 nm, 18 400 M^{-1} cm^{-1}. ^1H NMR: (δ, 300 MHz, $CDCl_3$); 7.30 - 7.80 (m, 19H, Ph), 9.93 (s, 1H, H_9). ^{31}P NMR: (δ, 121 MHz, $CDCl_3$); 42.9. SI MS; 721 ($[Au(PPh_3)_2]^+$, 50), 589 ($[M]^+$, 5), 459 ($[Au(PPh_3)]^+$, 100).

3.7.3.12. [Au(3-C≡CC$_6$H$_4$CHO)(PMe$_3$)]·2C$_6$H$_6$ (15)

[AuCl(PMe_3)] (200 mg, 0.65 mmol) and 3-HC≡CC_6H_4CHO (101 mg, 0.78 mmol) were stirred in a solution of sodium methoxide in methanol (0.1 M, 15 mL) for 16 h. After this time, a solid material had precipitated, which was collected by filtration and washed with petroleum spirit to yield the off-white product which was recrystallized from benzene (167 mg, 64 %). $C_{24}H_{38}AuOP$: C 51.62, H 4.69 %. Found:

C 50.75, H 3.95 %. IR: (CH_2Cl_2) ν(C≡C) 2116 cm^{-1}. UV-Vis: λ (thf) 322 nm, ε 1 000 M^{-1} cm^{-1}. ^1H NMR: (δ, 300 MHz, $CDCl_3$); 1.54 (br s, 9H, Me), 7.32 (s, 12H, C_6H_6), 7.35 – 8.00 (m, 4H, C_6H_4), 9.92 (s, 1H, H_9). ^{31}P NMR: (δ, 121 MHz, $CDCl_3$); 1.6. SI MS; 675 ($[M + Au(PMe_3) - 2H]^+$, 15), 403 ($[M]^+$, 5), 349 ($[Au(PMe_3)_2]^+$, 100), 273 ($[Au(PMe_3)]^+$, 60).

3.7.3.13. *trans-[Ru(2-C=CHC$_6$H$_4$CHO)Cl(dppm)$_2$]PF$_6$ (17)*

cis-[$RuCl_2$(dppm)$_2$] (300 mg, 0.32 mmol), NH_4PF_6 (104 mg, 0.64 mmol) and 2-HC≡CC_6H_4CHO (90 mg, 0.69 mmol) were added to dichloromethane (25 mL), and the resultant mixture stirred for 4 h. The solution was filtered, petroleum spirit (20 mL) was added, and the solvent removed under vacuum. The solid was triturated with diethyl ether and the purple solid was collected by filtration (305 mg, 81 %). Anal. Calcd for $C_{59}H_{50}ClF_6OP_5Ru$: C 60.03, H 4.27 %. Found: C 59.95, H 4.69 %. IR: (KBr) ν(PF) 841 cm^{-1}. UV-Vis: λ (thf) 555 nm, ε 2 000 M^{-1} cm^{-1}, 355 nm, ε 7 400 M^{-1} cm^{-1}. ^1H NMR: (δ, 300 MHz, $CDCl_3$); 5.25 (m, 2H, PCH_2P), 5.39 (m, 2H, PCH_2P), 5.67 (d, J_{HH} = 9 Hz, H_7), 6.40 (m, 1H, H_2), 6.80 - 7.60 (m, 43H, Ph + C_6H_4), 8.53 (s, 1H, H_9). ^{31}P NMR: (δ, 121 MHz, $CDCl_3$); -7.6. SI MS; 1059 ($[M - PF_6 + Na]^+$, 100), 869 ($[Ru(dppm)_2 - H]^+$, 35).

3.7.3.14. *trans-[Ru{4-C=CHC$_6$H$_4$CHO(CH$_2$)$_3$O}Cl(dppm)$_2$]PF$_6$ (19)*

cis-[$RuCl_2$(dppm)$_2$] (200 mg, 0.21 mmol), NH_4PF_6 (70 mg, 0.43 mmol) and **18** (48 mg, 0.26 mmol) were added to dichloromethane (25 mL), and the resultant mixture stirred for 4 h. Petroleum spirit (50 mL) was added, and the solvent removed under vacuum. The solid material was triturated with ether and then filtered to yield the pale red product (220 mg, 84 %). Anal. Calcd for $C_{62}H_{56}ClF_6O_2P_5Ru$: C 60.13, H 4.56 %. Found: C 59.99, H 4.78 %. IR: (KBr) ν(PF) 839 cm^{-1}. UV-Vis: λ (thf) 317 nm, ε 13 400 M^{-1} cm^{-1}. ^1H NMR: (δ, 300 MHz, $CDCl_3$); 1.40 (m, 1H, H_{11}), 2.10 - 2.20 (m, 1H, H_{11}),

2.95 (m, 1H, H_2), 3.85 - 4.25 (m, 4H, H_{10}), 5.06 (m, 2H, PCH_2P), 5.30 (m, 2H, PCH_2P), 5.35 (s, 1H, H_9), 5.48 (d, J_{HH} = 8 Hz, 2H, H_4), 6.85 (d, J_{HH} = 8 Hz, 2H, H_5), 7.10 - 7.50 (m, 40H, Ph). ^{31}P NMR: (δ, 121 MHz, $CDCl_3$); -15.5. SI MS; 1092 ($[M - PF_6]^+$, 15), 905 $[RuCl(dppm)_2]^+$, 90), 869 ($[Ru(dppm)_2 - H]^+$, 100), 485 ($[Ru(dppm)]^+ - H$, 90).

*3.7.3.15. trans-[Ru{4-C≡CC$_6$H$_4$CHO(CH$_2$)$_3$O}Cl(dppm)$_2$]·0.5CH$_2$Cl$_2$ (**20**)*

trans-[Ru{4-C=CHC$_6$H$_4$CHO(CH$_2$)$_3$O}Cl(dppm)$_2$]PF_6 (**7**) (200 mg, 0.16 mmol) was added to dichloromethane (25 mL) and triethylamine (1.0 mL) and the resultant mixture stirred for 10 min at room temperature. The mixture was passed through an alumina plug, petroleum spirit (50 mL) was added, and the resulting precipitate was collected and washed with petroleum spirit yielding the pale red product (153 mg, 87 %). Anal. Calcd for $C_{62.5}H_{56}Cl_2O_2P_4Ru$: C 66.14, H 4.97 %. Found: C 66.85, H 5.09 %. IR: (CH_2Cl_2) ν(C≡C) 2081 cm^{-1}. UV-Vis: λ (thf) 320 nm, ε 11 600 M^{-1} cm^{-1}. ^1H NMR: (δ, 300 MHz, $CDCl_3$); 1.40 (m, 1H, H_{11}), 2.20 - 2.40 (m, 1H, H_{11}), 3.80 - 4.00 (m, 2H, H_{10}), 4.20 - 4.30 (m, 2H, H_{10}), 4.88 (m, 4H, PCH_2P), 5.27 (s, 1H, CH_2Cl_2), 5.35 (s, H_9), 5.97 (d, J_{HH} = 8 Hz, 2H, H_4), 6.90 - 7.50 (m, 42H, Ph + H_5). ^{31}P NMR: (δ, 121 MHz, $CDCl_3$); -6.1. SI MS; 1092 ($[M]^+$, 100), 905 ($[RuCl(dppm)_2]^+$, 15), 869 ($[Ru(dppm)_2 - H]^+$, 50), 483 ($[Ru(dppm)]^+$, 30).

*3.7.3.16. [Au{4-C≡CC$_6$H$_4$CHO(CH$_2$)$_3$O}(PPh$_3$)] (**21**)*

[AuCl(PPh_3)] (100 mg, 0.20 mmol) and **18** (46 mg, 0.24 mmol) were stirred in a solution of sodium methoxide in methanol (0.1 M, 15 mL) for 16 h. After this time, a solid product had precipitated and was collected by filtration to yield the pale yellow product (121 mg, 93 %). Anal. Calcd for $C_{30}H_{26}AuO_2P$: C 54.88, H 4.46 %. Found: C 54.66, H 4.32 %. IR: (CH_2Cl_2) ν(C≡C) 2117 cm^{-1}. UV-Vis: λ (thf) 296 nm, ε 16 600 M^{-1} cm^{-1}, 288 nm, ε 30 600 M^{-1} cm^{-1}. ^1H NMR: (δ, 300 MHz, $CDCl_3$); 1.43 (m, 1H, H_{11}), 2.10 - 2.30 (m, 1H, H_{11}), 3.90 - 4.00 (m, 2H, H_{10}), 4.20 - 4.30 (m, 2H, H_{10}), 5.45 (s, 1H,

H_9), 7.35 (d, J_{HH} = 8 Hz, 2H, H_4), 7.38 - 7.60 (m, 17H, Ph + H_5). ^{31}P NMR: (δ, 121 MHz, $CDCl_3$); 42.8. SI MS; 721 ($[Au(PPh_3)_2]^+$, 20), 647 ($[M]^+$, 30), 459 ($[Au(PPh_3)]^+$, 100).

3.7.3.17. [Au{4-C≡CC$_6$H$_4$CHO(CH$_2$)$_3$O}(PMe$_3$)]·1EtOH (22)

[AuCl(PMe_3)] (100 mg, 0.324 mmol) and **18** (80 mg, 0.40 mmol) were stirred in a solution of sodium methoxide in methanol (0.1 M, 15 mL) for 16 h. After this time, a solid product had precipitated and was collected by filtration to yield the pale yellow product which was recrystallized from ethanol/dichloromethane (108 mg, 72 %). Anal. Calcd for $C_{17}H_{26}AuO_3P$: C 40.33, H 5.18 %. Found: C 40.43, H 4.28 %. IR: (CH_2Cl_2) ν(C≡C) 2118 cm^{-1}. UV-Vis: λ (thf) 292 nm, ε 7 600 M^{-1} cm^{-1}, 285 nm, ε 23 200 M^{-1} cm^{-1}. ^1H NMR: (δ, 300 MHz, $CDCl_3$); 1.20 (t, J_{HH} = 5 Hz, 3H, Me), 1.42 (br s, 1H, H_{11}), 1.52 (br s, 9H, Me), 2.10 - 2.30 (m, 1H, H_{11}), 3.67 (q, J_{HH} = 5 Hz, 2H, CH_2), 3.80 - 4.00 (m, 2H, H_{10}), 4.15 - 4.30 (m, 2H, H_{10}), 5.44 (s, 1H, H_9), 7.33 (d, J_{HH} = 8 Hz, 2H, H_4), 7.44 (d, J_{HH} = 8 Hz, 2H, H_5). ^{31}P NMR: (δ, 121 MHz, $CDCl_3$); 1.7. SI MS; 459 ($[M + Au(PMe_3)]^+$, 10), 459 ($[M - H]^+$, 100).

3.8. References

[1] Whittall, I.R., Cifuentes, M.P., Humphrey, M.G., Luther-Davies, B., Samoc, M., Houbrechts, S., Persoons, A., Heath, G.A., Bogsanyi, D., *Organometallics,* **1997**, *16*, 2631.

[2] Rodriguez, J.G., Gayo, M., Fonseca, I., *J. Organomet. Chem.,* **1997**, *534*, 35.

[3] Turrin, C.-O., Chiffre, J., Montauzon, D., Daran, J.-C., Caminade, M., Manoury, E., Balavoine, G., Majorla, J.-P., *Macromolecules,* **2000**, *33*, 7328.

[4] Hansch, C., Leo, A., Taft, R.W., *Chem. Rev.,* **1991**, *91*, 165.

[5] Kanis, D.R., Ratner, M.A., Marks, T.J., *J. Am. Chem. Soc.,* **1992**, *114*, 10338.

[6] Kochar, K.S., Bal, B.S., Deshpande, R.P., Rajadhyaksha, S.N., Pinnick, H.W., *J. Org. Chem.,* **1983**, *48*, 1765.

[7] Thorand, S., Vogtle, F., Krause, N., *Angew. Chem., Int. Ed. Engl.,* **1999**, *38*, 3721.

[8] Naulty, R.H., McDonagh, A.M., Whittall, I.R., Cifuentes, M.P., Humphrey, M.G., Houbrechts, S., Maes, J., Persoons, A., Heath, G.A., Hockless, D.C.R., *J. Organomet. Chem.,* **1998**, *563*, 137.

[9] Touchard, D., Haquette, P., Pirio, N., Toupet, L., Dixneuf, P.H., *Organometallics,* **1993**, *12*, 3132.

[10] Whittall, I.R., Cifuentes, M.P., Humphrey, M.G., Luther-Davies, B., Samoc, M., Houbrechts, S., Persoons, A., Heath, G.A., Hockless, D.C.R., *J. Organomet. Chem.,* **1997**, *549*, 127.

[11] Faulkner, C.W., Ingham, S.L., Khan, M.S., Lewis, J., Long, N.J., Raithby, P.R., *J. Organomet. Chem.,* **1994**, *482*, 139.

[12] Younus, M., Long, N.J., Raithby, P.R., Lewis, J., Page, N.A., White, A.J.P., Williams, D.J., Colbert, M.C.B., Hodge, A.J., Khan, M.S., Parker, D.G., *J. Organomet. Chem.,* **1999**, *578*, 198.

[13] Hurst, S.K., Cifuentes, M.P., Morrall, J.P.L., Lucas, N.T., Whittall, I.R., Humphrey, M.G., Asselberghs, I., Persoons, A., Samoc, M., Luther-Davies, B., Willis, A.C., *Organometallics,* **2001**, In press.

[14] Bruce, M.I., Horn, E., Matisons, J.G., Snow, M.R., *Aust. J. Chem.,* **1984**, *37*, 1163.

[15] Bruce, M.I., Duffy, D.N., *Aust. J. Chem.,* **1986**, *39*, 1697.

[16] Whittall, I.R., Humphrey, M.G., Houbrechts, S., Persoons, A., Hockless, D.C.R., *Organometallics,* **1996**, *15*, 5738.

[17] Hurst, S.K., Lucas, N.T., Cifuentes, M.P., Humphrey, M.G., Samoc, M., Luther-Davies, B., Asselberghs, I., Persoons, A., *J. Organomet. Chem.,* **2001**, In press.

[18] Whittall, I.R., Humphrey, M.G., Samoc, M., Swiatkiewicz, J., Luther-Davies, B., *Organometallics,* **1995**, *14*, 5493.

[19] McDonagh, A.M., Cifuentes, M.P., Whittall, I.R., Humphrey, M.G., Samoc, M., Luther-Davies, B., Hockless, D.C.R., *J. Organomet. Chem.,* **1996**, *526*, 99.

[20] McDonagh, A.M., Humphrey, M.G., Samoc, M., Luther-Davies, B., Houbrechts, S., Wada, T., Sasabe, H., Persoons, A., *J. Am. Chem. Soc.,* **1999**, *121*, 1405.

[21] Chaudret, B., Commenges, G., Poilblanc, R., *J. Chem. Soc., Dalton Trans.,* **1984**, 1635.

[22] McAuliffe, C.A., Parish, R.V., Randall, P.D., *J. Chem. Soc., Dalton Trans.*, **1979**, 1730.

[23] Austin, W.B., Bilow, N., Kelleghan, W.J., Lau, K.S.Y., *J. Org. Chem.*, **1981**, *46*, 2280.

Chapter 4

Polymetallic complexes and some of their nonlinear optical properties

---

Contents

Chapter 4

Polymetallic complexes and some of their nonlinear optical properties

4.1. Introduction

Materials of interest for nonlinear optics which contain more than one metal centre may place the metal centres in the bridge or a donor/acceptor group. Employing the metal centres in the donor/acceptor groups is of interest since variations in the bridging unit can be used to elucidate mechanisms for interaction between the two metals which may prove useful for technological applications. Additional data can be obtained through variation of the peripheral metal centres, ligand environment or coordination geometry. Research using a metal-bridge-metal system has been extensive, with a large number of different ligated metal centres and a diverse assortment of conjugated bridging units being employed.[1-3] Organic spacers which have been commonly used are carbon-rich groups including alkynes,[4] alkenes,[5] or arenes.[6]

The use of bridges with extensive π-electron delocalization is useful when seeking to enhance molecular hyperpolarizability. Several studies of the NLO properties of bimetallic compounds have been undertaken and the area of organometallics for second-order nonlinearities has been reviewed.[7] Heck and co-workers[8,9] have studied the molecular first hyperpolarizabilities of bimetallic sesquifulvalenes, while McCleverty and co-workers[10,11] have investigated the bulk NLO responses of molybdenum and tungsten nitrosyl units linked to ferrocene. Some examples of bimetallic complexes with measured β values are given in Table 4.1., reflecting the large proportion of research undertaken on ferrocenyl-based compounds. Other authors[12,13] have investigated the

third-order NLO properties of organometallic compounds, and this area has also been recently reviewed.[14]

Table 4.1. Molecular second-order NLO measurements for some bimetallic complexes.

Compound	λ_{max} (nm)	Fund. (μm)	β_{exp} [a,b]	β_0 [a]	Ref.
$[FcC{\equiv}C(\eta^7\text{-}C_7H_6)Cr(CO)_3]$	600	1.06	570	105	15
$[Fc\text{-}(E)\text{-}CH{=}CH(\eta^7\text{-}C_7H_6)Cr(CO)_3]$	670	1.06	320	113	15
$[Fc\text{-}(E)\text{-}CH{=}CHB(mes)_2]$	336	1.91	-24	-	16
$[Ru\{C{\equiv}NW(CO)_5\}(PPh_3)_2(\eta^5\text{-indenyl})]$	392	1.06	40	15	17
$[Ru(\eta\text{-}C_5H_5)(\eta\text{-}C_5H_4\text{-}(E)\text{-}CH{=}CH\text{-}\eta^7\text{-}C_7H_6)Ru(\eta\text{-}C_5H_5)](PF_6)_2$	549	1.06	358	17	9
$[Mo\{C{\equiv}NRu(NH_3)_5\}(CO)_5](PF_6)_2$	693	1.06	225	90	18

[a] Units = 10^{-30} esu. [b] Uncertainty of ±10%.

Bimetallic compounds which have been investigated for their third-order NLO properties include metallocene derivatives, acetylenic polymers and organometallic films. Some bimetallic compounds and their third-order NLO results are presented in Table 4.2. Few studies, however, have been undertaken on the third-order properties of bimetallic transition metal acetylides despite large third-order values having been reported for monometallic acetylides.[19]

Electrochemical studies have also been undertaken[20,21] and provide a useful method for examining the degree of electronic interaction between metal centres. Not only can different metal combinations and bridging units be investigated, but the effect of having two similar metals possessing different oxidation states can be examined.[22]

Bimetallic molecules are a useful way of systematically assessing the relative merits of individual bridging units and ligated metal centres for electronic communication and thereby allow the development of design criteria for the creation of technologically useful materials. Bis-acetylenic bridges have frequently been employed as a linker

unit,[23,24] and are often used in combination with an arene spacer to permit greater variation in bridge design. Bridge design is an important consideration since different bridging components may have varying resistance to electron delocalization. Levanda *et al.*[25] established that [FcC≡CFc] possesses moderate electronic communication (ΔE_0 = 100-130 mV), whereas [Fc-4-C_6H_4Fc] has none.[6]

Table 4.2. Molecular third order NLO measurements of some bimetallic complexes.

Compound	Technique	γ	Fund. (μm)	Ref.
[FcCH=CH-4-C_6H_4CH=CHFc]	DFWM	504 x 10^{-36} esu	0.60	13
[FcC≡CC≡CC≡CC≡CFc]	THG	110 x 10^{-36} esu	1.91	26
[{$ZrCl(\eta$-$C_5H_5)_2$}$_2${μ-(*E*)-CH=CHC_6H_4-4-(*E*)-CH=CH}]	THG	154 x 10^{-36} esu	1.91	27
trans-[{$PtCl(PBu^n_3)_2$}$_2$(μ-C≡CC_6H_4-4-C≡C)]	DFWM	350 x 10^{-36} esu	0.63	28

The role of the metal centre is equally important as outlined in Table 4.3. Lavastre *et al.*[29] reported communication (ΔE_0 = 360 mV) between two *trans*-[$RuCl(dppe)_2$] centres linked via a *para*-substituted diethynylbenzene. Replacement of the *trans*-[$RuCl(dppe)_2$] moieties with ferrocene units resulted in a single large oxidation wave, suggesting that communication was either small or non-existent. Modification of the ferrocenyl bridging unit does not give rise to communication except in the case of the thiophene-linked adduct (ΔE_0 = 150 mV). Use of similar aryl-alkyne bridges with *trans*-[$RuCl(dppm)_2$] metal centres all result in compounds with moderate metal-metal communication belonging to the Robin-Day class II weakly-coupled category.

The aims of the studies in this Chapter are to determine the degree of electronic communication between novel bimetallic species and to provide additional information about the third-order properties of symmetrical bimetallic derivatives. To this end, the preparation and characterization of [Fe{η-C_5H_4-(*E*)-4-CH=CHC_6H_4C≡CH}$_2$] and

derivative ruthenium and gold acetylide complexes are presented in this Chapter together with electrochemistry and third-order NLO data.

Table 4.3. Effect of variation in donor unit and bridging unit on ΔE_0

Compound	ΔE_0 (mV)	Ref.
trans,trans-[{RuCl(dppe)$_2$}$_2$(μ-4-C≡CC$_6$H$_4$C≡C)]	360	29
trans,trans-[{RuCl(dppm)$_2$}$_2$(μ-4-C≡CC$_6$H$_4$C≡C)]	300	30
trans,trans-[{RuCl(dppm)$_2$}$_2$(μ-3-C≡CC$_6$H$_4$C≡C)]	190	30
trans,trans-[{RuCl(dppm)$_2$}$_2$(μ-2,5-C≡CC$_4$H$_2$SC≡C)]	360	30
[(Fc)$_2$(μ-4-C≡CC$_6$H$_4$C≡C)]	0	29
[(Fc)$_2$(μ-2,5-C≡CC$_4$H$_2$SC≡C)]	0	31
[(Fc)$_2$(μ-2,5-(*E*)-CH=CHC$_4$H$_2$S-(*E*)-CH=CH)]	0	31
[(Fc)$_2$(μ-1,4-C$_6$H$_4$)]	0	6
[(Fc)$_2$(μ-2,5-C$_4$H$_2$S)]	150	6

4.2. Synthesis of [Fe{η-C_5H_4-(E)-4-CH=$CHC_6H_4C{\equiv}CH$}$_2$]

Thomas *et al.*[32] have previously reported the synthesis of [Fe{η-C_5H_4-(*E*)-4-CH=CHC_6H_4I}$_2$] (**12**). The iodo substituents can be functionalized; thus, Sonogashira coupling with trimethylsilylacetylene affords the protected alkyne **13**, which can be deprotected with base to give the terminal acetylene **14** (Scheme 4.1.). The new acetylenes were characterized by EI and HR mass spectrometry, satisfactory microanalyses, UV-vis, IR and ^{1}H-NMR spectroscopy, and the identity of **13** was confirmed by a single-crystal X-ray diffraction study.

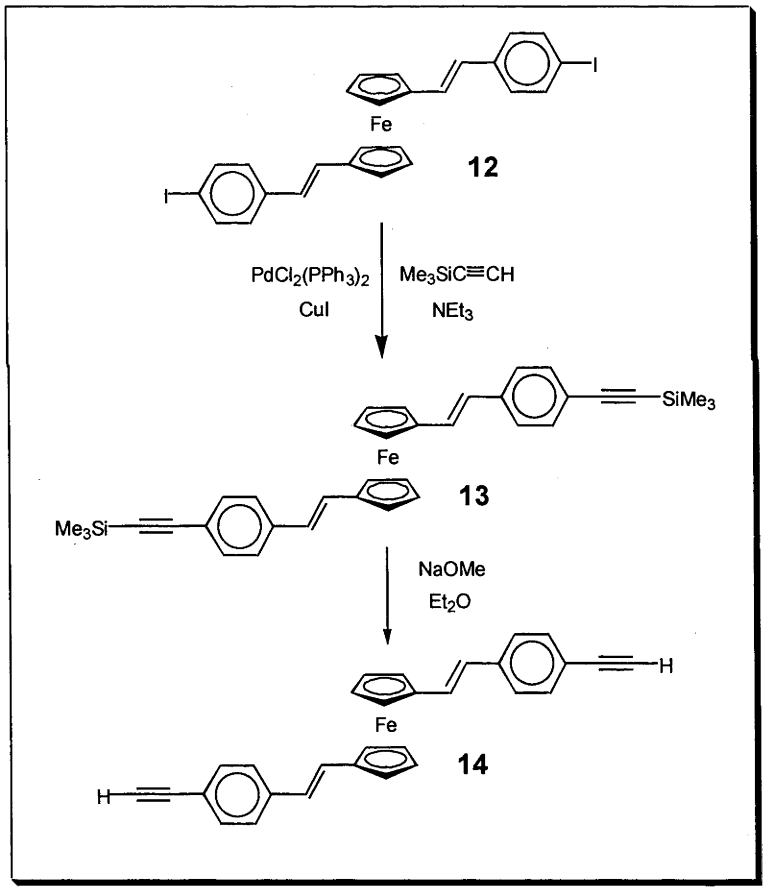

Scheme 4.1. Synthesis of [Fe{η-C_5H_4-(*E*)-4-CH=$CHC_6H_4C{\equiv}CH$}$_2$] (**14**)

4.3. X-ray structural study of [Fe{η-C_5H_4-(E)-4-CH=CHC_6H_4C≡CSiMe_3}$_2$]

A single-crystal X-ray diffraction study of [Fe{η-C_5H_4-(*E*)-4-CH=CHC_6H_4C≡CSiMe_3}$_2$] (**13**) has been performed by collaborators at the Australian National University. ORTEP plots are displayed in Figures 4.1. and 4.2., and selected bond lengths and angles are gathered in Table 4.4. A comparison of selected bond lengths and angles with those of related complexes appears in Table 4.5.

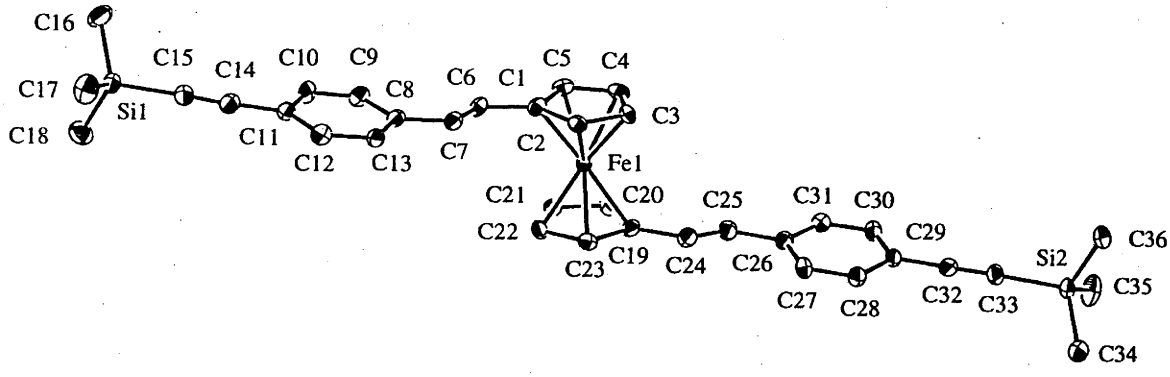

Figure 4.1. Thermal ellipsoid diagram of [Fe{η-C_5H_5-(*E*)-4-CH=CHC_6H_4C≡CSiMe_3}$_2$] (**13**). Ellipsoids show 30% probability levels. Hydrogen atoms have been omitted for clarity (crystal structure provided by A.C. Willis).

The structural study of **13** confirms the approximately planar geometry of the CH=CHC_6H_4C≡CSiMe_3 ligands. The Fe - C(1), C(1) - C(6) and C(6) - C(7) bond distances are within the range of previously observed values for (*E*)-ene linked ferrocenyl complexes.[31,33,34] The C(1) - C(6) - C(7) - C(8) moiety is approximately planar, with deviations likely to be the result of crystal packing forces. Intra-ferrocenyl bond lengths and angles in **13** are not unusual. Distances within the arylalkyne components are not unexpected.

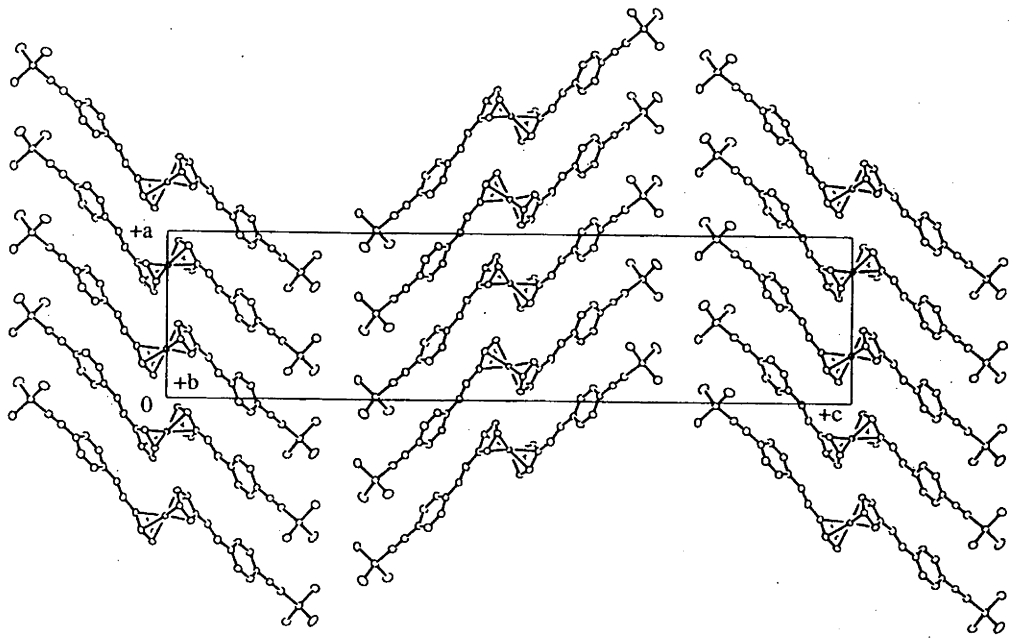

Figure 4.2. Unit cell diagram of [Fe{η-C_5H_4-(*E*)-4-CH=$CHC_6H_4C{\equiv}CSiMe_3$}$_2$] (**13**) projected down the *b* axis. Ellipsoids show 30% probability levels. Hydrogen atoms have been omitted for clarity (crystal structure provided by A.C. Willis).

Table 4.4. Selected bond distances (Å) and angles (deg) for [Fe{η-C_5H_4-(*E*)-4-CH=$CHC_6H_4C{\equiv}CSiMe_3$}$_2$] (**13**)

Fe(1) – C(1)	2.069(5)	Fe(1) – C(1) – C(6)	128.4(4)
Fe(1) – C(2)	2.044(5)	C(1) – C(6) – C(7)	125.2(4)
Fe(1) – C(3)	2.042(5)	C(6) – C(7) – C(8)	126.2(4)
Fe(1) – C(4)	2.050(4)	C(7) – C(8) – C(9)	123.2(4)
Fe(1) – C(5)	2.049(4)	C(8) – C(9) – C(10)	121.4(4)
C(1) – C(6)	1.467(7)	C(9) – C(10) – C(11)	122.2(4)
C(6) – C(7)	1.342(7)	C(10) – C(11) – C(14)	118.4(4)
C(7) – C(8)	1.459(7)	C(11) – C(14) – C(15)	177.2(5)
C(8) – C(9)	1.385(7)	C(14) – C(15) – Si(1)	169.3(5)
C(9) – C(10)	1.356(7)	C(11) – C(14)	1.435(7)
C(10) – C(11)	1.407(7)	C(14) – C(15)	1.190(7)

Table 4.5. Comparison of selected bond lengths and angles in **13** with those of analogous complexes.

Complex	C(1) - C(6)	C(6) - C(7)	C(7) - C(8)	Fe(1) - C(1) - C(6)	C(1) - C(6) - C(7)	C(6) - C(7) - C(8)	Ref.
[Fe{η-C_5H_4-(*E*)-4-CH=$CHC_6H_4C{\equiv}CSiMe_3$}$_2$] (**13**)	1.467(7)	1.342(7)	1.459(7)	128.4(4)	125.2(4)	126.2(4)	This work
[Fc-(*E*)-4-CH=CHC_6H_4I]	1.422(15)	1.332(16)	1.479(15)	--	127(1)	127(1)	33
[Fc-(*E*)-4-CH=CHC_6H_4-2,5-C_4H_2SPtBr(PPh_3)$_2$]	1.42(2)	1.26(2)	1.47(2)	124.2(11)	129(2)	129(2)	31
[Fc-(*E,E*)-4-CH=CHC_6H_4CH=CHFc]	1.471(4)	1.327(4)	1.476(4)	122.9(2)	128.9(3)	125.8(3)	34

4.4. Syntheses of metal acetylide complexes

4.4.1. Gold complexes

The preparation of the gold acetylides complexes followed the method of Whittall *et al.*[35] The room temperature reactions of the terminal alkynes with the chloro(phosphine)gold(I) complexes in a mixture of sodium methoxide solution and dichloromethane lead to the formation of the gold complexes in good yield (Schemes 4.2. and 4.3.). The new acetylide complexes were characterized by SI mass spectrometry, satisfactory microanalyses, UV-vis and IR spectroscopy, ^{1}H and ^{31}P NMR spectroscopy.

4.4.2. Ruthenium complexes

The synthetic methodologies employed for the preparation of the new complexes are adaptations of those successfully utilized for the preparation of the corresponding phenylacetylides. The bis{bis(diphenylphosphino)alkane}ruthenium complexes were prepared by extending the method of Touchard *et al.*,[36] a procedure which also permits isolation of the stable vinylidene intermediates (Scheme 4.4.). A mixture of either *cis*-$[RuCl_2(dppm)_2]$ or *cis*-$[RuCl_2(dppe)_2]$ was reacted with an excess of terminal acetylene in the presence of ammonium hexafluorophosphate. In the case of the reaction using *cis*-$[RuCl_2(dppe)_2]$, excess acetylene was removed before deprotonation to avoid the formation of the bis-alkynyl product. The intermediate vinylidene complex was deprotonated via the addition of base (triethylamine) to afford the corresponding acetylide. The new complexes were characterized by SI mass spectrometry, satisfactory microanalyses, UV-vis and IR spectroscopy, ^{1}H and ^{31}P NMR spectroscopy.

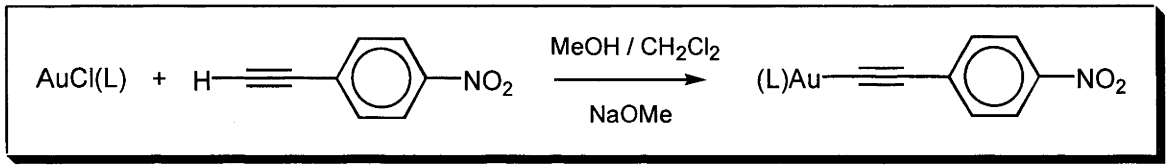

L	Complex
PCy_3	**1**
PPh_3	**2**
PMe_3	**3**

Scheme 4.2. Syntheses of 4-nitrophenylalkynylgold complexes **1 - 3**

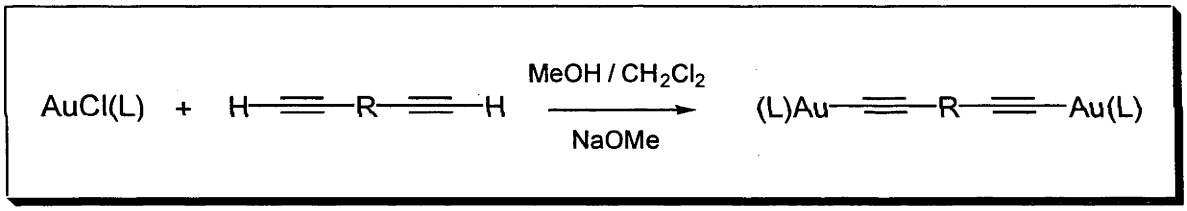

R	L	Complex
4-C_6H_4	PCy_3	**4**
4-C_6H_4	PPh_3	**5**
4-C_6H_4	PMe_3	**6**
4,4′-$C_6H_4C_6H_4$	PCy_3	**7**
4,4′-$C_6H_4C_6H_4$	PPh_3	**8**
4,4′-$C_6H_4C_6H_4$	PMe_3	**9**
[Fe{η-C_5H_4-(*E*)-CH=CH-4-C_6H_4}$_2$]	PCy_3	**15**
[Fe{η-C_5H_4-(*E*)-CH=CH-4-C_6H_4}$_2$]	PPh_3	**16**
[Fe{η-C_5H_4-(*E*)-CH=CH-4-C_6H_4}$_2$]	PMe_3	**17**

Scheme 4.3. Syntheses of alkynylbis{(phosphine)gold} complexes **4 - 9** and **15 - 17**

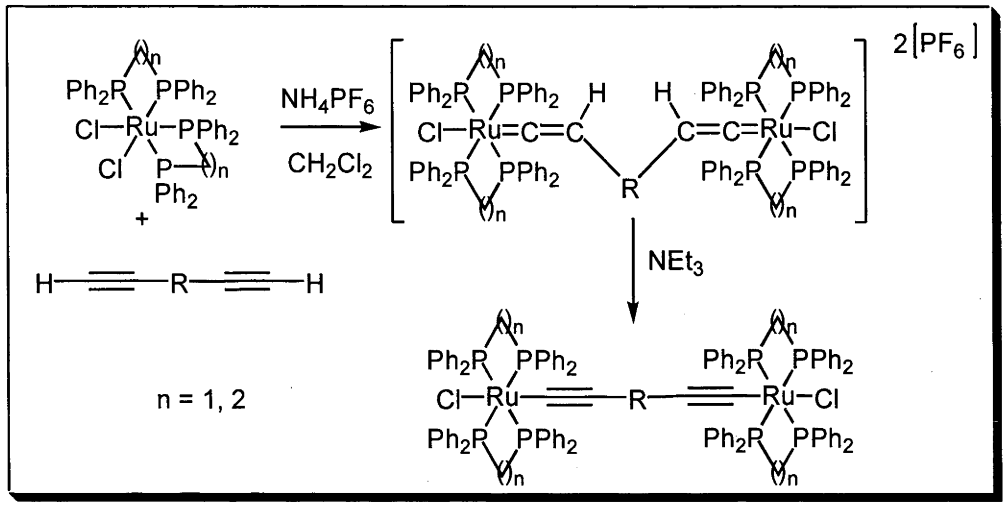

R	n	Complex
4-C_6H_4	1	**10**
4,4′-$C_6H_4C_6H_4$	1	**11**
[Fc{(*E*)-4-CH=CHC_6H_4}$_2$]	1	**18**
[Fc{(*E*)-4-CH=CHC_6H_4}$_2$]	1	**19**
[Fc{(*E*)-4-CH=CHC_6H_4}$_2$]	2	**20**

Scheme 4.4. Syntheses of alkynyl bis[bis{bis(diphenylphosphino)-alkane}chlororuthenium] complexes **10** - **11** and **18** - **20**

4.4.3. Comparison of characterization data

Selected ^{1}H NMR data for compounds **1** - **20** are listed in Table 4.6. and the numbering scheme is displayed in Figure 4.3. ^{1}H NMR spectra of complexes **1** and **3** show the expected AB quartet of the *p*-nitrophenylacetylide ligand, with similar chemical shifts. Complexes **4** and **6** containing the 1,4-diethynylbenzene linker show a single peak corresponding to the H_4/H_5 protons indicating that these protons are equivalent. The ^{1}H NMR spectra of complexes **7** and **9** (which contain the 4,4′-biphenyl linker)

Table 4.6. Selected ^{1}H NMR data (ppm (J_{HH}, Hz))

Compound	H_4	H_5	H_7	H_8	Ph	$P(CH_2)_nP$
[Au(4-C≡CC$_6$H$_4$NO$_2$)(PCy$_3$)] (**1**)	7.55 (9)	8.08 (9)	--	--	--	--
[Au(4-C≡CC$_6$H$_4$NO$_2$)(PPh$_3$)] (**2**)	[a]	8.10 (9)	--	--	7.40 – 7.60	--
[Au(4-C≡CC$_6$H$_4$NO$_2$)(PMe$_3$)] (**3**)	7.52 (9)	8.08 (9)	--	--	--	--
[(PCy$_3$)Au-4-C≡CC$_6$H$_4$C≡CAu(PCy$_3$)] (**4**)	7.31		--	--	--	--
[(PPh$_3$)Au-4-C≡CC$_6$H$_4$C≡CAu(PPh$_3$)] (**5**)	7.36		--	--	7.40 – 7.60	--
[(PMe$_3$)Au-4-C≡CC$_6$H$_4$C≡CAu(PMe$_3$)] (**6**)	7.31		--	--	--	--
[(PCy$_3$)Au-4,4′-C≡CC$_6$H$_4$C$_6$H$_4$C≡CAu(PCy$_3$)] (**7**)	7.31		--	--	--	--
[(PPh$_3$)Au-4,4′-C≡CC$_6$H$_4$C$_6$H$_4$C≡CAu(PPh$_3$)] (**8**)	[a]		--	--	7.35 – 7.60	--
[(PMe$_3$)Au-4,4′-C≡CC$_6$H$_4$C$_6$H$_4$C≡CAu(PMe$_3$)] (**9**)	7.44 (8)	7.49 (8)	--	--	--	--
trans,trans-[RuCl(dppm)$_2$(μ-4-C≡CC$_6$H$_4$C≡C)RuCl(dppm)$_2$] (**10**)	5.95		--	--	6.95 – 7.60	4.88
trans,trans-[RuCl(dppm)$_2$(μ-4,4′-C≡CC$_6$H$_4$C$_6$H$_4$C≡C)RuCl(dppm)$_2$] (**11**)	6.10	[a]	--	--	7.00 – 7.60	4.90
[Fe{η-C$_5$H$_4$-(*E*)-4-CH=CHC$_6$H$_4$I}$_2$] (**12**)	6.94 (8)	7.48 (8)	6.43 (16)	6.63 (16)	--	--
[Fe{η-C$_5$H$_4$-(*E*)-4-CH=CHC$_6$H$_4$C≡CSiMe$_3$}$_2$] (**13**)	7.20 (8)	7.34 (8)	6.56 (16)	6.78 (16)	--	--
[Fe{η-C$_5$H$_4$-(*E*)-4-CH=CHC$_6$H$_4$C≡CH}$_2$] (**14**)	7.17 (8)	7.32 (8)	6.54 (16)	6.72 (16)	--	--
[Fe{η-C$_5$H$_4$-(*E*)-4-CH=CHC$_6$H$_4$C≡CAu(PCy$_3$)}$_2$] (**15**)	7.21 (8)	7.42 (8)	6.59 (16)	6.78 (16)	--	--

[Fe{η-C_5H_4-(*E*)-4-CH=$CHC_6H_4C{\equiv}CAu(PPh_3)\}_2$] (**16**)	7.26 (8)	[a]	6.60 (16)	6.82 (16)	7.30 – 7.60	--
[Fe{η-C_5H_4-(*E*)-4-CH=$CHC_6H_4C{\equiv}CAu(PMe_3)\}_2$] (**17**)	7.24 (8)	7.40 (8)	6.59 (16)	6.79 (16)	--	--
[Fe{η-C_5H_4-(*E*)-4-CH=$CHC_6H_4CH{=}CRuCl(dppm)_2\}_2](PF_6)_2$ (**18**)	[a]	[a]	[a]	[a]	6.50 – 7.55	5.12, 5.34
[Fe{η-C_5H_4-(*E*)-4-CH=$CHC_6H_4C{\equiv}CRuCl(dppm)_2\}_2$] (**19**)	6.99 (8)	[a]	6.57 (16)	6.67 (16)	7.03 – 7.60	4.88
[Fe{η-C_5H_4-(*E*)-4-CH=$CHC_6H_4C{\equiv}CRuCl(dppe)_2\}_2$] (**20**)	[a]	[a]	[a]	[a]	6.90 – 7.60	2.65

[a] Obscured by other resonances.

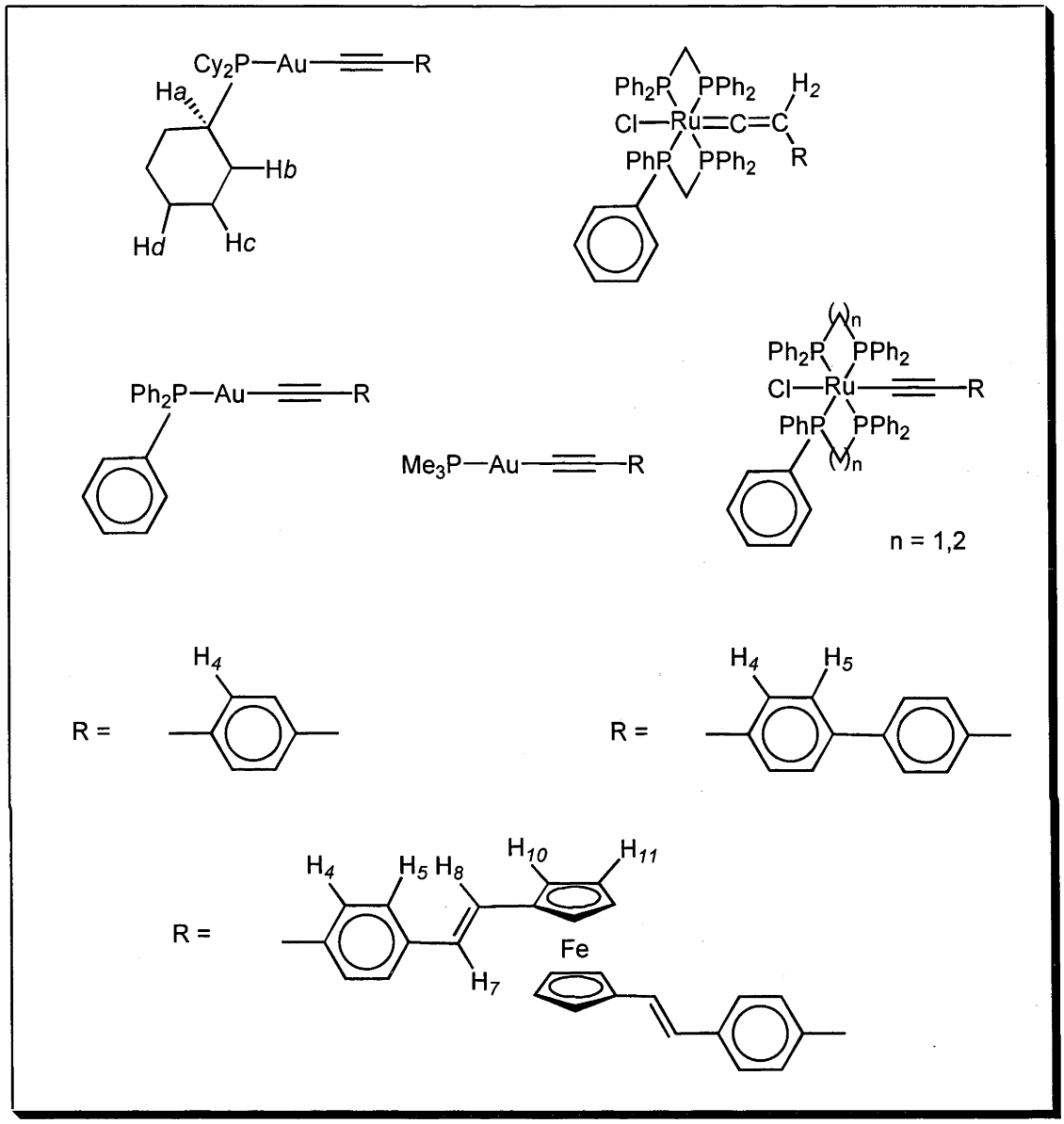

Figure 4.3. NMR numbering scheme

reveal a pair of doublet signals corresponding to the linker unit. Comparison of the chemical shifts of the phenyl resonances on the linker group between complexes **7** and **9** shows little variation between different ligated metal centres. For complexes **2**, **5**, **8**, **10** and **11**, which contain [Au(PPh_3)] or *trans*-[RuCl(dppm)$_2$] ligated metal centres, the proton resonances for the linker phenyl groups are partially or wholly obscured.

Complexes **12** - **20** contain the novel [Fe{η-C_5H_4-(*E*)-4-CH=CHC_6H_4}$_2$] linker system. The protons on individual cyclopentadienyl rings are inequivalent and give rise to two singlets whose chemical shifts are relatively invariant upon coordination of the acetylene linkers to the ligated metal substituents. The stereoselectivity of the Wadsworth-Horner-Emmons reaction for synthesis of the pure (*E*)-ene isomer was confirmed by an AB quartet signal centered around 6.6 ppm with a coupling constant of *ca* 16 Hz. The chemical shift of the (*E*)-ene linkage in the ^{1}H NMR is also relatively invariant to the terminal substituents on the acetylene. The ^{31}P NMR spectra for all complexes are unremarkable, with similar shifts for comparable ligated metal centres.

Table 4.7. contains selected IR and UV-vis data for complexes **1** - **20**. The position of the ν(C≡C) bands in the IR spectra are generally dependent upon the terminal substituent. There is a shift of about 7 cm^{-1} between the mono-metallic gold nitrophenylacetylide complexes and the equivalent linked bimetallic acetylide complexes. However, there is minimal difference in ν(C≡C) between the linked alkynylarene and corresponding ferrocenyl-containing complexes. Substitution of gold with a ruthenium centre leads to a low frequency shift for the ν(C≡C) band. Certain trends are apparent in the UV-vis data. Irrespective of the acetylide linker, the [Au(PPh_3)] and [Au(PCy_3)] complexes had similar extinction coefficients and λ_{max} values, whilst [Au(PMe_3)] complexes had similar λ_{max} but consistently lower extinction coefficients. Ligated gold centres connected by the biphenyl linker also had systematically higher extinction coefficients than the phenyl linker. The ferrocene-linked complexes have a relatively small absorption band at approximately 463-9 nm which is attributed to ligand field "d – d" excitations.[37] A stronger metal-to-ligand charge-transfer band occurs at shorter wavelengths in the metallated complexes, λ_{max} for which varies with the nature of the terminal substituent. In the case of the ligated ruthenium centres, this strong absorption band obscures the weaker ferrocenyl ligand field-related band.

Table 4.7. IR[a] and UV-vis[b] data for complexes **1-20**.

Compound	ν(C≡C) (cm^{-1})	λ_{max} (nm) [ε (10^4 M^{-1} cm^{-1})]
[Au(4-C≡C$C_6H_4NO_2$)(PCy_3)] (**1**)	2113	342 [2.2]
[Au(4-C≡C$C_6H_4NO_2$)(PPh_3)] (**2**)	2116	338 [2.5]
[Au(4-C≡C$C_6H_4NO_2$)(PMe_3)] (**3**)	2115	339 [1.3]
[(PCy_3)Au-4-C≡CC_6H_4C≡CAu(PCy_3)] (**4**)	2106	325 [5.6]
[(PPh_3)Au-4-C≡CC_6H_4C≡CAu(PPh_3)] (**5**)	2108	329 [5.4]
[(PMe_3)Au-4-C≡CC_6H_4C≡CAu(PMe_3)] (**6**)	2108	324 [3.5]
[(PCy_3)Au-4,4′-C≡C$C_6H_4C_6H_4$C≡CAu(PCy_3)] (**7**)	2112	324 [6.5]
[(PPh_3)Au-4,4′-C≡C$C_6H_4C_6H_4$C≡CAu(PPh_3)] (**8**)	2106	325 [6.6]
[(PMe_3)Au-4,4′-C≡C$C_6H_4C_6H_4$C≡CAu(PMe_3)] (**9**)	2111	325 [4.8]
trans,trans-[RuCl(dppm)$_2$(4-C≡CC_6H_4C≡C)RuCl(dppm)$_2$] (**10**)	2075	354 [4.2]
trans,trans-[RuCl(dppm)$_2$(μ-4,4′-C≡C$C_6H_4C_6H_4$C≡C)RuCl(dppm)$_2$] (**11**)	2077	360 [9.0]
[Fe{η-C_5H_4-(*E*)-4-CH=CHC_6H_4I}$_2$] (**12**)	--	468 [0.6], 336 [8.1]
[Fe{η-C_5H_4-(*E*)-4-CH=CHC_6H_4C≡C$SiMe_3$}$_2$] (**13**)	2066	468 [0.5], 317 [6.4]
[Fe{η-C_5H_4-(*E*)-4-CH=CHC_6H_4C≡CH}$_2$] (**14**)	2106	469 [0.3], 311 [3.8]
[Fe{η-C_5H_4-(*E*)-4-CH=CHC_6H_4C≡CAu(PCy_3)}$_2$] (**15**)	2110	467 [0.4], 355 [6.4]
[Fe{η-C_5H_4-(*E*)-4-CH=CHC_6H_4C≡CAu(PPh_3)}$_2$] (**16**)	2106	465 [0.5], 333 [7.7]
[Fe{η-C_5H_4-(*E*)-4-CH=CHC_6H_4C≡CAu(PMe_3)}$_2$] (**17**)	2107	463 [0.3], 331 [4.4]
[Fe{η-C_5H_4-(*E*)-4-CH=CHC_6H_4CH=CRuCl(dppm)$_2$}$_2$](PF_6)$_2$ (**18**)	--	383 [3.1]
[Fe{η-C_5H_4-(*E*)-4-CH=CHC_6H_4C≡CRuCl(dppm)$_2$}$_2$] (**19**)	2073	396 [7.4]
[Fe{η-C_5H_4-(*E*)-4-CH=CHC_6H_4C≡CRuCl(dppe)$_2$}$_2$] (**20**)	2065	388 [5.2]

[a] In dichloromethane. [b] In thf.

4.4.4. Electrochemistry

Cyclic voltammetry data for complexes **10** - **20** are gathered in Table 4.8. Complex **10** and **12** have been examined previously by cyclic voltammetry by Colbert *et al.*[38] and Thomas *et al.*,[32] respectively; these data are also included in Table 4.8., and are experimentally similar to data collected under our own experimental conditions. Complexes **10**, **11** and **19** are of interest as they correspond to a range of potentially π-delocalizable bridging units coupling two *trans*-[Ru(dppm)$_2$Cl] groups. The $Ru^{II/III}$ couples of **10**, **11** and **19** are essentially reversible, so an assessment of electronic communication by considering the difference in $Ru^{II/III}$ couples ($\Delta E_{½}$) is appropriate. McDonagh *et al.* have previously noted that *trans*-disposed phenylalkynyl ligands behave electronically as pseudo-halides in complexes of this type,[39] so the progression in $\Delta E_{½}$ data should reflect changes in the nature of the bridging unit. Several studies assessing electronic communication between metal centres in binuclear acetylide complexes have been reported recently;[29,30,40-42] the present data affords the possibility of assessing the effect of bridge lengthening on electronic communication. Extending the length of the π-delocalizable bridge in proceeding from **10** to **11** and then **19** results in a decrease in electronic communication, as assessed by $\Delta E_{½}$. The comproportionation constants K_{com} for these complexes have been calculated and are listed in Table 4.8. Following the Robin and Day classification,[43] **19** is a Class I binuclear complex, in which the metal centres are not interacting, **11** is a borderline Class I / Class II example, and **10** belongs to Class II, in which metal centres are weakly interacting.

Complexes **12** - **17** exhibit a single reversible oxidation wave corresponding to the ferrocenyl unit in the bridging linker. The potential for this ferrocene/ferrocenium couple is similar to that observed for free ferrocene/ferrocenium, the most significant shift in potential for this process being observed on proceeding to the alkynyl complexes **19** and **20**. Cyclic voltammograms for the ruthenium-containing complexes

Table 4.8. Cyclic voltammetric data for **10** – **20**. [a]

Complex	$E_{½}$ $Fe^{II/III}$ (V)	$[i_{pc}/i_{pa}]$	$E_{½}$ $Ru^{II/III}$ (V)	K_{com}	$[i_{pc}/i_{pa}]$	Ref.
trans,trans-[RuCl(dppm)$_2$(4-C≡CC$_6$H$_4$C≡C)RuCl(dppm)$_2$] (**10**)	--	--	0.22, 0.54	2.6×10^5	1.0, 1.0	This work
	--	--	0.26, 0.56	1.2×10^5	[b]	30
trans,trans-[RuCl(dppm)$_2$(μ-4,4′-C≡CC$_6$H$_4$C$_6$H$_4$C≡C)RuCl(dppm)$_2$] (**11**)	--	--	0.41, 0.51	4.9 x 10	1.0, 1.0	This work
[Fe{η-C$_5$H$_4$-(*E*)-4-CH=CHC$_6$H$_4$I}$_2$] (**12**)	0.54	1.0	--	--	--	This work
	0.56	[b]	--	--	--	32
[Fe{η-C$_5$H$_4$-(*E*)-4-CH=CHC$_6$H$_4$C≡CSiMe$_3$}$_2$] (**13**)	0.55	1.0	--	--	--	This work
[Fe{η-C$_5$H$_4$-(*E*)-4-CH=CHC$_6$H$_4$C≡CH}]$_2$] (**14**)	0.55	1.0	--	--	--	This work
[Fe{η-C$_5$H$_4$-(*E*)-4-CH=CHC$_6$H$_4$C≡CAu(PCy$_3$)}$_2$] (**15**)	0.54	1.0	--	--	--	This work
[Fe{η-C$_5$H$_4$-(*E*)-4-CH=CHC$_6$H$_4$C≡CAu(PPh$_3$)}$_2$] (**16**)	0.54	1.0	--	--	--	This work
[Fe{η-C$_5$H$_4$-(*E*)-4-CH=CHC$_6$H$_4$C≡CAu(PMe$_3$)}$_2$] (**17**)	0.52	1.0	--	--	--	This work
[Fe{η-C$_5$H$_4$-(*E*)-4-CH=CHC$_6$H$_4$CH=CRuCl(dppm)$_2$}$_2$](PF$_6$)$_2$ (**18**)[c]	0.52	1.0	1.25	0	[d]	This work
[Fe{η-C$_5$H$_4$-(*E*)-4-CH=CHC$_6$H$_4$C≡CRuCl(dppm)$_2$}$_2$] (**19**)	0.61	1.0	0.44	0	1.0	This work
[Fe{η-C$_5$H$_4$-(*E*)-4-CH=CHC$_6$H$_4$C≡CRuCl(dppe)$_2$}$_2$] (**20**)	0.63	1.0	0.49	0	1.0	This work

[a] Ferrocene/ferrocenium couple (0.56 V) as an internal standard except where specified. [b] Not specified. [c] [Ru(NCMe)$_2$(acac)$_2$]/[Ru(NCMe)$_2$(acac)$_2$]$^+$ (0.25 V) as an internal standard. [d] Not reversible.

18 – **20** also show reversible (**19**, **20**) or nonreversible (**18**) processes attributable to Ru-centered oxidation, at potentials similar to those of monoruthenium alkynyl or vinylidene complexes, respectively.[44]

4.5. Nonlinear optical investigations

4.5.1. Results of third-order nonlinear optical studies

Measurements of third-order optical nonlinearities were carried out by the author with assistance from Dr M. Samoc using the Z-scan technique (see Section 1.3.5.) at 800 nm. Results for **1**, **3**, **4**, **7**, and **10** - **20** are collected in Table 4.9; complexes **5**, **6**, **8**, and **9** were insufficiently soluble in CH_2Cl_2 or thf to acquire useful data.

4.5.2. Discussion of third-order nonlinear optical results

An electronic origin for cubic nonlinearities in related metal acetylide complexes has been demonstrated previously by degenerate four-wave mixing measurements,[45] and nonlinearities for the present series of compounds are therefore likely to be electronic in origin. The effect on refractive nonlinearity γ_{real} of phosphine ligand replacement in the dipolar series **1** – **3** is negligible, all γ_{real} data being equivalent within the error margins; unlike **2**, no detectable γ_{imag} component is present for **1** and **3**. The binuclear gold complexes **4** and **7** have very small cubic nonlinearities. Molecular second hyperpolarizabilities for the binuclear ruthenium complexes **10** and **11** are significantly larger; thus, replacing [Au(PCy_3)] with *trans*-[RuCl(dppm)$_2$] in proceeding from **4** to **10** or **7** to **11** results in a dramatic increase in $|\gamma|$.

The real components γ_{real} of the nonlinearities for most of the ferrocenyl complexes **12** - **17** are negative, and the imaginary components γ_{imag} for most are significant, consistent with two-photon absorption contributions to the observed molecular nonlinearities $|\gamma|$; comment on the effect of structural variation on the magnitude of $|\gamma|$ is therefore cautious, particularly in the light of the significant error margins. Nonlinearities for the ferrocenyl complexes **12**, **13** and **14** are low. Introduction of terminal (phosphine)gold units in proceeding from **14** to **15** – **17** results in little change in the linear optical

Table 4.9. Results of Z-scan experiments at 800 nm.[a]

Compound	λ_{max} (nm) [ε (x10^4 M^{-1} cm^{-1})]	γ_{real} (10^{-36} esu)	γ_{imag} (10^{-36} esu)	$\lvert\gamma\rvert$ (10^{-36} esu)	Ref.
[Au(4-C≡C$C_6H_4NO_2$)(PCy_3)] (**1**)	342 [2.2]	100 ± 50	0 ± 0	100 ± 50	This work
[Au(4-C≡C$C_6H_4NO_2$)(PPh_3)] (**2**)	338 [2.5]	120 ± 40	20 ± 15	120 ± 40	46
[Au(4-C≡C$C_6H_4NO_2$)(PMe_3)] (**3**)	339 [1.3]	150 ± 50	0 ± 0	150 ± 50	This work
[(PCy_3)Au-4-C≡CC_6H_4C≡CAu(PCy_3)] (**4**)	325 [5.6]	0 ± 250	0 ± 50	0 ± 0	This work
[(PCy_3)Au-4,4′-C≡C$C_6H_4C_6H_4$C≡CAu(PCy_3)] (**7**)	324 [6.5]	-300 ± 200	0 ± 30	300 ± 200	This work
trans,trans-[RuCl(dppm)$_2$(4-C≡CC_6H_4C≡C)RuCl(dppm)$_2$] (**10**)	354 [4.2]	-3200 ± 500	1400 ± 300	3500 ± 600	This work
trans-[Ru(4-C≡C$C_6H_4NO_2$)Cl(dppm)$_2$]	466 [1.6]	170 ± 34	230 ± 46	290 ± 60	19
trans,trans-[RuCl(dppm)$_2$(4,4′-C≡C$C_6H_4C_6H_4$C≡C)RuCl(dppm)$_2$] (**11**)	360 [9.0]	-1100 ± 800	3300 ± 1500	1100 ± 300	This work
trans-[Ru(4,4′-C≡C$C_6H_4C_6H_4NO_2$)Cl(dppm)$_2$]	448 [1.8]	140 ± 28	64 ± 13	150 ± 30	19
[Fe{η-C_5H_4-(*E*)-4-CH=CHC_6H_4I}$_2$] (**12**)	468 [0.6], 336 [8.1]	-200 ± 50	100 ± 20	220 ± 50	This work
[Fe{η-C_5H_4-(*E*)-4-CH=CHC_6H_4C≡C$SiMe_3$}$_2$] (**13**)	468 [0.5], 317 [6.4]	0 ± 50	200 ± 40	200 ± 40	This work
[Fe{η-C_5H_4-(*E*)-4-CH=CHC_6H_4C≡CH}]$_2$] (**14**)	469 [0.3], 311 [3.8]	-400 ± 250	200 ± 40	450 ± 240	This work
[Fe{η-C_5H_4-(*E*)-4-CH=CHC_6H_4C≡CAu(PCy_3)}$_2$] (**15**)	467 [0.4], 355 [6.4]	-400 ± 500	500 ± 100	640 ± 390	This work

$[Fe\{\eta\text{-}C_5H_4\text{-}(E)\text{-}4\text{-}CH{=}CHC_6H_4C{\equiv}CAu(PPh_3)\}_2]$ (**16**)	465 [0.5], 333 [7.7]	-1100 ± 300	300 ± 60	1140 ± 310	This work
$[Fe\{\eta\text{-}C_5H_4\text{-}(E)\text{-}4\text{-}CH{=}CHC_6H_4C{\equiv}CAu(PMe_3)\}_2]$ (**17**)	463 [0.3], 331 [4.4]	200 ± 150	0 ± 30	200 ± 150	This work
$[Fe\{\eta\text{-}C_5H_4\text{-}(E)\text{-}4\text{-}CH{=}CHC_6H_4CH{=}CRuCl(dppm)_2\}_2](PF_6)_2$ (**18**)	383 [3.1]	-3000 ± 1200	2300 ± 800	3780 ± 1440	This work
$[Fe\{\eta\text{-}C_5H_4\text{-}(E)\text{-}4\text{-}CH{=}CHC_6H_4C{\equiv}CRuCl(dppm)_2\}_2]$ (**19**)	396 [7.4]	-7100 ± 3000	10600 ± 2000	12760 ± 3330	This work
$[Fe\{\eta\text{-}C_5H_4\text{-}(E)\text{-}4\text{-}CH{=}CHC_6H_4C{\equiv}CRuCl(dppe)_2\}_2]$ (**20**)	388 [5.2]	-2500 ± 400	2600 ± 200	3610 ± 420	This work

[a] In dichloromethane.

absorption spectra and does not result in a significant increase in nonlinearity. In contrast, introduction of the ligated ruthenium centre (in proceeding to **18 - 20**) results in intense transitions in the UV-vis spectra close to the second-harmonic wavelength of our Ti-sapphire laser (400 nm) and, as a consequence, complexes **18 – 20** possess large negative γ_{real} and large γ_{imag} values.

Comparison with previous work indicates that replacing NO_2 in the dipolar examples with *trans*-[(C≡C)RuCl(dppm)$_2$] to afford **10** or **11** results in significant increases in $|\gamma|$, the presence of the second electron-rich metal centre being more important than dipolar composition in enhancing cubic NLO merit. These data suggest that extending π-delocalization is the critical factor, consistent with experience with organic compounds. Significant extension of the π-system, in proceeding from **10**, **11** to **19**, results in a further considerable increase in $|\gamma|$.

4.6. Conclusions

The complexes [Au(4-C≡C$C_6H_4NO_2$)(L)] [L = PCy_3 (**1**), PMe_3 (**2**)], [(L)Au(μ-4-C≡CRC≡C)Au(L)] [R = C_6H_4, L = PCy_3 (**4**), PPh_3 (**5**); R = C_6H_4-4-C_6H_4 , L = PCy_3 (**7**), PPh_3 (**8**)], *trans,trans*-[RuCl(dppm)$_2$(μ-4,4′-C≡C$C_6H_4C_6H_4$C≡C)RuCl(dppm)$_2$] (**11**), [Fe{η-C_5H_4-(*E*)-4-CH=CHC_6H_4R}$_2$] [R = C≡C$SiMe_3$ (**13**), C≡CH (**14**), C≡CAu(PCy_3) (**15**), C≡CAu(PPh_3) (**16**), C≡CAu(PMe_3) (**17**), CH=CRuCl(dppm)$_2^+$ (**18**) as its PF_6^- salt, C≡CRuCl(dppm)$_2$ (**19**), C≡CRuCl(dppe)$_2$ (**20**)] have been prepared and their electrochemical (Ru complexes) and NLO properties assessed. Electronic communication between the metal centres diminishes in the order of *trans,trans*-[RuCl(dppm)$_2$(μ-4-C≡CC_6H_4C≡C)RuCl(dppm)$_2$] (**10**) > **11** > **15** as the π-delocalizable bridge between the *trans*-[RuCl(dppm)$_2$] centers is lengthened. Measured cubic molecular hyperpolarizabilities at 800 nm are small for the gold complexes and much larger for the ruthenium examples which may have a significant two-photon contribution. The presence of the ferrocenyl sub-unit may allow for electrochemical modulation of the cubic hyperpolarizability.

4.7. Experimental

4.7.1 General Conditions, Reagents and Instruments

General Conditions

All reactions were performed under a nitrogen atmosphere with the use of standard Schlenk techniques unless otherwise stated. Dichloromethane and triethylamine were dried by distilling over calcium hydride, diethyl ether and tetrahydrofuran were dried by distilling over sodium / benzophenone; other solvents were used as received. "Petroleum spirit" refers to a fraction of petroleum ether of boiling range 60-80 °C. Chromatography was on silica gel (230-400 mesh ASTM) or basic ungraded alumina.

Reagents

The following reagents were prepared by the literature procedures: [Fe{η-C_5H_4-(*E*)-4-$CH{=}CHC_6H_4I$}$_2$],[32] [AuCl(PPh_3)],[47] [AuCl(PMe_3)],[48] [AuCl(PCy_3)],[49] 4-$HC{\equiv}CC_6H_4C{\equiv}CH$, 4,4′-$HC{\equiv}CC_6H_4C_6H_4C{\equiv}CH$ and 4-$HC{\equiv}CC_6H_4NO_2$,[50] *cis*-[$RuCl_2$(dppm)$_2$] and *cis*-[$RuCl_2$(dppe)$_2$],[51] [Au(4-$C{\equiv}CC_6H_4NO_2$)(PPh_3)] (**2**),[35] *trans,trans*-[(dppm)$_2$ClRu(μ-4-$C{\equiv}CC_6H_4C{\equiv}C$)RuCl(dppm)$_2$] (**10**),[30] [($PMe_3$)Au(4-$C{\equiv}CC_6H_4C{\equiv}C$)Au($PMe_3$)] (**6**) and [($PMe_3$)Au(4,4′-$C{\equiv}CC_6H_4C_6H_4C{\equiv}C$)Au($PMe_3$)] (**9**).[52] NH_4PF_6 (Aldrich), NaOMe (Aldrich), $Me_3SiC{\equiv}CH$ (Aldrich), CuI (Unilab), [$PdCl_2$(PPh_3)$_2$] (PMO) were used as received.

Instruments

EI (electron impact) mass spectra (both unit resolution and high resolution (HR)) were recorded using a VG Autospec instrument (70 eV electron energy, 8 kV accelerating potential) and secondary ion mass spectra were recorded using a VG ZAB 2SEQ instrument (30 kV Cs^+ ions, current 1 mA, accelerating potential 8 kV, 3-nitrobenzyl

alcohol matrix) at the Research School of Chemistry, Australian National University; peaks are reported as *m/z* (assignment, relative intensity). Microanalyses were carried out at the Research School of Chemistry, Australian National University. Infrared spectra were recorded either as 1% KBr discs or dichloromethane solutions using a Perkin-Elmer System 2000 FT-IR. ^{1}H and ^{31}P NMR spectra were recorded using a Varian Gemini-300 FT NMR spectrometer and are referenced to residual chloroform (7.24 ppm) or external 85% H_3PO_4 (0.0 ppm), respectively. The assignments follow the numbering scheme shown in Figure 4.3. UV-vis spectra of solutions in tetrahydrofuran in 1 cm quartz cells were obtained using a Cary 5 spectrophotometer. Electrochemical measurements were recorded using a MacLab 400 interface and MacLab potentiostat from ADInstruments. The supporting electrolyte was 0.1 M $(NBu^{n}_4)PF_6$ in distilled, deoxygenated CH_2Cl_2. Solutions containing *ca* 1 x 10^{-3} M complex were maintained under argon. Measurements were carried out at room temperature using platinum disc working-, Pt wire auxiliary- and Ag/AgCl reference- electrodes, such that the ferrocene/ferrocenium redox couple was located at 0.56 V (peak separation around 0.09 V). Scan rates were typically 100 mV s^{-1}.

4.7.2. Synthesis of metal complexes

4.7.2.1. [Au(4-C≡CC$_6$H$_4$NO$_2$)(PCy$_3$)] (1)

[AuCl(PCy$_3$)] (200 mg, 0.39 mmol), 4-HC≡CC$_6$H$_4$NO$_2$ (69 mg, 0.47 mmol) and CuI (5 mg) were stirred in a solution of sodium methoxide in methanol (0.1 M, 15 mL) for 12 h. Dichloromethane (100 mL) was added and the solution filtered through a plug of silica. The solvent was removed under vacuum; the residue was then triturated under petroleum spirit to yield the pale yellow product (201 mg, 82 %). Anal. Calcd for $C_{26}H_{37}AuNO_2P$: C 50.08, H 5.98, N 2.25 %. Found: C 49.95, H 6.15, N 2.05 %. IR: (CH_2Cl_2) ν(C≡C) 2113 cm^{-1}. UV-Vis: λ (thf) 342 nm, ε 21 700 M^{-1} cm^{-1}. ^{1}H NMR: (δ, 300 MHz, $CDCl_3$); 1.10 – 2.10 (m, 33H, Cy), 7.55 (d, 2H, J_{HH} = 9 Hz, H_4), 8.08 (d, 2H,

J_{HH} = 9 Hz, H_5). ^{31}P NMR: (δ, 121 MHz, $CDCl_3$); 56.8. SI MS; 1100 ($[M + PCy_3]^+$, 25), 624 ($[M]^+$, 50), 477 $[Au(PCy_3)]^+$, 100).

4.7.2.2. [Au(4-C≡CC$_6$H$_4$NO$_2$)(PMe$_3$)] (3)

[AuCl(PMe_3)] (180 mg, 0.58 mmol) and 4-HC≡C$C_6H_4NO_2$ (103 mg, 0.70 mmol) were stirred in a solution of sodium methoxide in methanol (0.1 M, 15 mL) for 16 h. After this time, a solid yellow product precipitated which was collected by filtration (198 mg, 81 %). Anal. Calcd for $C_{11}H_{13}AuNO_2P$: C 31.52, H 3.13, N 3.34 %. Found: C 31.09, H 3.21, N 3.28 %. IR: (CH_2Cl_2) ν(C≡C) 2115 cm^{-1}. UV-Vis: λ (thf) 339 nm, ε 13 500 M^{-1} cm^{-1}. ^1H NMR: (δ, 300 MHz, $CDCl_3$); 1.51 (m, 9H, Me), 7.52 (d, 2H, J_{HH} = 9 Hz, H_4), 8.08 (d, 2H, J_{HH} = 9 Hz, H_5). ^{31}P NMR: (δ, 121 MHz, $CDCl_3$); 1.4. SI MS; 349 $[Au(PMe_3)_2]^+$, 100), 273 ($[Au(PMe_3)]^+$, 25).

4.7.2.3. [(PCy$_3$)Au(μ-4-C≡CC$_6$H$_4$C≡C)Au(PCy$_3$)] (4)

[AuCl(PCy_3)] (200 mg, 0.39 mmol), 4-HC≡CC_6H_4C≡CH (24 mg, 0.19 mmol) and CuI (5 mg) were stirred in a solution of sodium methoxide in methanol (0.1 M, 15 mL) for 12 h. Dichloromethane (50 mL) was added and the solution filtered through a plug of silica. The solvent was removed under vacuum to yield the pale yellow product (183 mg, 87 %). Anal. Calcd for $C_{46}H_{70}Au_2P_2$: C 51.21, H 6.54 %. Found: C 51.30, H 6.45 %. IR: (CH_2Cl_2) ν(C≡C) 2115 cm^{-1}. UV-Vis: λ (thf) 325 nm, ε 56 000 M^{-1} cm^{-1}, 306 nm, ε 40 400 M^{-1} cm^{-1}. ^1H NMR: (δ, 300 MHz, $CDCl_3$); 1.20 - 2.00 (m, 66H, Cy), 7.31 (s, 4H, C_6H_4). ^{31}P NMR: (δ, 121 MHz, $CDCl_3$); 56.8. SI MS; 1079 ($[M]^+$, 15), 757 ($[Au(PCy_3)_2]^+$, 100), 477 ($[PCy_3]^+$, 100).

4.7.2.4. [(PPh$_3$)Au(μ-4-C≡CC$_6$H$_4$C≡C)Au(PPh$_3$)] (5)

[AuCl(PPh_3)] (230 mg, 0.46 mmol), 4-HC≡CC_6H_4C≡CH (29 mg, 0.23 mmol) and CuI (5 mg) were stirred in a solution of sodium methoxide in methanol (0.1 M, 15

mL) for 12 h. Dichloromethane (80 mL) was added and the solution filtered through a plug of silica. The solvent was removed under vacuum to yield the pale yellow product (183 mg, 87 %). Anal. Calcd for $C_{46}H_{34}Au_2P_2$: C 52.99, H 3.29 %. Found: C 52.46, H 3.39 %. IR: (CH_2Cl_2) ν(C≡C) 2108 cm^{-1}. UV-Vis: λ (thf) 329 nm, ε 53 800 M^{-1} cm^{-1}, 309 nm, ε 37 700 M^{-1} cm^{-1}. ^1H NMR: (δ, 300 MHz, $CDCl_3$); 7.36 (s, 4H, H_4, H_5), 7.40 – 7.60 (m, 30H, Ph). ^{31}P NMR: (δ, 121 MHz, $CDCl_3$); 42.8. SI MS; 1042 ($[M]^+$, 5), 721 ($[Au(PPh_3)_2]^+$ 10), 459 ($[AuPPh_3]^+$, 65).

4.7.2.5. [(PCy$_3$)Au(μ-4,4′-C≡CC$_6$H$_4$C$_6$H$_4$C≡C)Au(PCy$_3$)] (7)

[AuCl(PCy$_3$)] (200 mg, 0.39 mmol), 4,4′-HC≡CC$_6$H$_4$C$_6$H$_4$C≡CH (39 mg, 0.19 mmol) and CuI (5 mg) were stirred in a solution of sodium methoxide in methanol (0.1 M, 15 mL) for 16 h. After this time, a precipitate had formed which was collected by filtration, washed with methanol and then with petroleum spirit, affording the white product (253 mg, 56 %). Anal. Calcd for $C_{52}H_{74}Au_2P_2$: C 54.07, H 6.46 %. Found: C 53.33, H 6.38 %. IR: (CH_2Cl_2) ν(C≡C) 2115 cm^{-1}. UV-Vis: λ (thf) 325 nm, ε 56 000 M^{-1} cm^{-1}, 306 nm, ε 40 400 M^{-1} cm^{-1}. ^1H NMR: (δ, 300 MHz, $CDCl_3$); 1.20 - 2.00 (m, 66H, Cy), 7.31 (s, 4H, C_6H_4). ^{31}P NMR: (δ, 121 MHz, $CDCl_3$); 56.8. SI MS; 477 ($[Au(PCy)_3]^+$, 100).

4.7.2.6. [(PPh$_3$)Au(μ-4,4′-C≡CC$_6$H$_4$C$_6$H$_4$C≡C)Au(PPh$_3$)] (8)

[AuCl(PPh$_3$)] (150 mg, 0.30 mmol), 4,4′-HC≡CC$_6$H$_4$C$_6$H$_4$C≡CH (28 mg, 0.14 mmol) and CuI (5 mg) were stirred in a solution of sodium methoxide in methanol (0.1 M, 15 mL) for 16 h. After this time, a precipitate had formed which was collected by filtration, washed with methanol and then with petroleum spirit, to afford the white product (118 mg, 76 %). Anal. Calcd for $C_{52}H_{38}Au_2P_2$: C 55.83, H 3.42 %. Found: C 54.87, H 3.53 %. IR: (CH_2Cl_2) ν(C≡C) 2106 cm^{-1}. UV-Vis: λ (thf) 325 nm, ε 65 600 M^{-1} cm^{-1}. ^1H NMR: (δ, 300 MHz, $CDCl_3$); 7.35 - 7.60 (m, 38H, Ph + C_6H_4). ^{31}P NMR: (δ,

121 MHz, $CDCl_3$); 42.8. SI MS; 1119 ($[M]^+$, 10), 757 ($[Au(PPh_3)_2]^+$, 35), 459 ($[Au(PPh_3)]^+$, 100).

4.7.2.7. trans,trans-[RuCl(dppm)$_2$(μ-4,4′-C≡CC$_6$H$_4$C$_6$H$_4$C≡C)RuCl(dppm)$_2$] ·H$_2$O (11)

cis-$[RuCl_2(dppm)_2]$ (200 mg, 0.22 mmol), 4,4′-HC≡CC$_6$H$_4$C$_6$H$_4$C≡CH (21 mg, 0.11 mmol) and NH_4PF_6 (69 mg, 0.42 mmol) were heated in refluxing dichloromethane (25 mL) for 9 h. The solution was filtered and the solvent removed from the filtrate under reduced pressure. The residue was triturated with diethyl ether and the resultant solid was then redissolved in dichloromethane (15 mL). Triethylamine (1 mL) was added with stirring and the solution eluted through an alumina plug with dichloromethane. Removal of the solvent under reduced pressure yielded the yellow product (145 mg, 68 %). Anal. Calcd for $C_{116}H_{98}OP_8Ru_2$: C 68.67, H 4.87 %. Found: C 67.85, H 5.04 %. IR: (CH_2Cl_2) ν(C≡C) 2077 cm^{-1}. UV-Vis: λ (thf) 360 nm, ε 90 400 M^{-1} cm^{-1}. ^1H NMR: (δ, 300 MHz, $CDCl_3$); 1.55 (s, 2H, H_2O), 4.90 (m, 8H, PCH_2P), 6.10 (m, 4H, H_4), 7.00 - 7.60 (m, 84H, Ph + H_5). ^{31}P NMR: (δ, 121 MHz, $CDCl_3$); -5.9. SI MS; 2012 ($[M + 2H]^+$, 5), 905 ($[RuCl(dppm)_2]^+$, 85), 870 ($[Ru(dppm)_2]^+$, 100).

4.7.2.8. [Fe{η-C$_5$H$_4$-(E)-4-CH=CHC$_6$H$_4$C≡CSiMe$_3$}$_2$] (12)

$[Fe\{\eta\text{-}C_5H_4\text{-}(E)\text{-}4\text{-}CH{=}CHC_6H_4I\}_2]$ (540 mg, 0.84 mmol), $Me_3SiC{\equiv}CH$ (0.48 mL, 3.36 mmol), $[PdCl_2(PPh_3)_2]$ (25 mg) and CuI (10 mg) were stirred together in triethylamine (80 mL) for 8 h. The solution was then filtered through a silica plug and the solvent was reduced under vacuum to yield the red product (402 mg, 82 %). Anal. Calcd for $C_{36}H_{38}FeSi_2$: C 74.20, H 6.57 %. Found: C 73.62, H 6.16 %. IR: (CH_2Cl_2) ν(C≡C) 2153 cm^{-1}. UV-Vis: λ (thf) 468 nm, ε 4 700 M^{-1} cm^{-1}, 345 nm, ε 52 600 M^{-1} cm^{-1}. ^1H NMR: (δ, 300 MHz, $CDCl_3$); 0.25 (s, 18H, Me), 4.26 (s, 4H, C_5H_4), 4.39 (s, 4H, C_5H_4), 6.56 (d, 2H, J_{HH} = 16 Hz, H_7), 6.78 (d, 2H, J_{HH} = 16 Hz, H_8), 7.20 (d, 4H,

J_{HH} = 8 Hz, H_4), 7.34 (d, 4H, J_{HH} = 8 Hz, H_5). SI MS; 582 ($[M]^+$, 100), 567 ($[M - Me]^+$, 5), 319 ($[M - (C_5H_4CH{=}CHC_6H_4C{\equiv}CSiMe_3)]^+$, 40).

*4.7.2.9. [Fe{η-C$_5$H$_4$-(E)-4-CH=CHC$_6$H$_4$C≡CH}$_2$]·H$_2$O (**14**)*

[Fe{η-C_5H_4-(*E*)-4-CH=$CHC_6H_4C{\equiv}CSiMe_3$}$_2$] (**13**) (400 mg, 0.69 mmol) and NBu^n_4F (1.0 mL, 1 M solution in thf) were stirred together in dichloromethane (40 mL) for 2 h. The solution was then filtered through an alumina plug and the solvent was reduced under vacuum to yield the red product (256 mg, 85 %). Anal. Calcd for $C_{30}H_{24}FeO$: C 78.96, H 5.30 %. Found: C 78.72, H 6.16 %. IR: (CH_2Cl_2) ν(C≡C) 2106 cm^{-1}, ν(≡CH) 3297 cm^{-1}. UV-Vis: λ (thf) 469 nm, ε 2 600 M^{-1} cm^{-1}, 341 nm, ε 30 400 M^{-1} cm^{-1}. ^{1}H NMR: (δ, 300 MHz, $CDCl_3$); 1.55 (s, 2H, H_2O), 3.11 (s, 2H, H_1), 4.26 (s, 4H, C_5H_4), 4.41 (s, 4H, C_5H_4), 6.54 (d, 2H, J_{HH} = 16 Hz, H_7), 6.72 (d, 2H, J_{HH} = 16 Hz, H_8), 7.17 (d, 4H, J_{HH} = 8 Hz, H_4), 7.32 (d, 4H, J_{HH} = 8 Hz, H_5). SI MS; 438 ($[M]^+$, 100), 247 ($[M - (C_5H_4CH{=}CHC_6H_4C{\equiv}CH)]^+$, 55).

*4.7.2.10. [Fe{η-C$_5$H$_4$-(E)-4-CH=CHC$_6$H$_4$C≡CAu(PCy$_3$)}$_2$] (**15**)*

[AuCl(PCy_3)] (200 mg, 0.42 mmol), [Fe{η-C_5H_4-(*E*)-4-CH=$CHC_6H_4C{\equiv}CH$}$_2$] (**2**) (92 mg, 0.21 mmol) and CuI (5 mg) were stirred in a solution of sodium methoxide in methanol (0.1 M, 15 mL) and dichloromethane (15 mL) for 12 h. Dichloromethane (50 mL) was added and the solution filtered through a silica plug. The solvent was reduced under vacuum to yield the red product (184 mg, 63 %). Anal. Calcd for $C_{66}H_{86}Au_2FeP_2$: C 56.98, H 6.23 %. Found: C 56.47, H 5.84 %. IR: (CH_2Cl_2) ν(C≡C) 2109 cm^{-1}. UV-Vis: λ (thf) 468 nm, ε 4 200 M^{-1} cm^{-1}, 355 nm, ε 63 600 M^{-1} cm^{-1}. ^{1}H NMR: (δ, 300 MHz, $CDCl_3$); 1.15 - 2.10 (m, 66H, Cy), 4.22 (s, 4H, C_5H_4), 4.34 (s, 4H, C_5H_4), 6.59 (d, 2H, J_{HH} = 16 Hz, H_7), 6.78 (d, 2H, J_{HH} = 16 Hz, H_8), 7.21 (d, 4H, J_{HH} = 8 Hz, H_4), 7.42 (d, 4H, J_{HH} = 8 Hz, H_5). ^{31}P NMR: (δ, 121 MHz, $CDCl_3$); 56.9. SI MS; 1391 ($[M]^+$, 15), 914 ($[M - Au(PCy_3)]^+$, 100), 477 ($[Au(PCy_3)]^+$, 100).

4.7.2.11. [Fe{η-C_5H_4-(E)-4-CH=CHC_6H_4C≡CAu(PPh_3)}$_2$] (16)

[AuCl(PPh_3)] (200 mg, 0.40 mmol), [Fe{η-C_5H_4-(*E*)-4-CH=CHC_6H_4C≡CH}$_2$] (**2**) (87 mg, 0.20 mmol) and CuI (5 mg) were stirred in a solution of sodium methoxide in methanol (0.1 M, 15 mL) and dichloromethane (15 mL) for 12 h. Dichloromethane (50 mL) was added and the solution filtered through a silica plug. The solvent was reduced under vacuum to yield the red product (183 mg, 87 %). Anal. Calcd for $C_{66}H_{50}Au_2FeP_2$: C 58.51, H 3.72 %. Found: C 58.25, H 3.90 %. IR: (CH_2Cl_2) ν(C≡C) 2107 cm^{-1}. UV-Vis: λ (thf) 465 nm, ε 5 100 M^{-1} cm^{-1}, 352 nm, ε 72 600 M^{-1} cm^{-1}. ^1H NMR: (δ, 300 MHz, $CDCl_3$); 4.23 (s, 4H, C_5H_4), 4.35 (s, 4H, C_5H_4), 6.60 (d, 2H, J_{HH} = 16 Hz, H_7), 6.82 (d, 2H, J_{HH} = 16 Hz, H_8), 7.26 (d, 4H, J_{HH} = 9 Hz, H_4), 7.30 – 7.60 (m, 34H, Ph + H_5). ^{31}P NMR: (δ, 121 MHz, $CDCl_3$); 42.8. SI MS; 1355 ($[M]^+$, 5), 721 ($[Au(PPh_3)_2]^+$, 35), 459 ($[AuPPh_3]^+$, 45).

4.7.2.12. [Fe{η-C_5H_4-(E)-4-CH=CHC_6H_4C≡CAu(PMe_3)}$_2$]·1.5CH_2Cl_2 (17)

[AuCl(PMe_3)] (200 mg, 0.65 mmol), [Fe{η-C_5H_4-(*E*)-4-CH=CHC_6H_4C≡CH}$_2$] (**2**) (142 mg, 0.32 mmol) and CuI (5 mg) were stirred in a solution of sodium methoxide in methanol (0.1 M, 15 mL) and dichloromethane (15 mL) for 12 h. Dichloromethane (60 mL) was added and the solution filtered through a silica plug. The solvent was reduced under vacuum to yield the red product, which was recrystalized from diffusion of a dichloromethane solution into methanol (172 mg, 54 %). Anal. Calcd for $C_{37.5}H_{41}Au_2Cl_3FeP_2$: C 40.58, H 3.72 %. Found: C 40.58, H 4.40 %. IR: (CH_2Cl_2) ν(C≡C) 2107 cm^{-1}. UV-Vis: λ (thf) 463 nm, ε 3 200 M^{-1} cm^{-1}, 350 nm, ε 43 100 M^{-1} cm^{-1}. ^1H NMR: (δ, 300 MHz, $CDCl_3$); 1.51 (d, J_{HH} = 10 Hz, 18H, Me), 4.22 (s, 4H, C_5H_4), 4.34 (s, 4H, C_5H_4), 5.27 (s, 3H, CH_2Cl_2), 6.59 (d, 2H, J_{HH} = 16 Hz, H_7), 6.79 (d, 2H, J_{HH} = 16 Hz, H_8), 7.24 (d, 4H, J_{HH} = 8 Hz, H_4), 7.40 (d, 4H, J_{HH} = 8 Hz, H_5). ^{31}P NMR: (δ, 121 MHz, $CDCl_3$); 1.7. SI MS; 349 ($[Au(PMe_3)_2]^+$, 10), 273 ($[Au(PMe_3)]^+$, 100).

4.7.2.13. [Fe{η-C_5H_4-(E)-4-CH=CHC_6H_4CH=CRuCl(dppm)$_2$}$_2$](PF$_6$)$_2$·CH_2Cl_2 (18)

cis-[$RuCl_2$(dppm)$_2$] (255 mg, 0.27 mmol), [Fe{η-C_5H_4-(*E*)-4-CH=CH-$C_6H_4C{\equiv}CH$}$_2$] (**2**) (59 mg, 0.14 mmol) and NH_4PF_6 (88 mg) were stirred in refluxing dichloromethane (35 mL) for 12 h. The mixture was cooled, petroleum spirit (50 mL) was added, and the precipitate was collected on a sintered-glass funnel and washed with diethyl ether (100 mL) to give the pale red product (248 mg, 72 %). Anal. Calcd for $C_{131}H_{112}Cl_2F_{12}FeP_{10}Ru_2$: C 59.97, H 4.30 %. Found: C 59.42, H 4.09 %. IR: (KBr) ν(PF) 838 cm^{-1}. UV-Vis: λ (thf) 383 nm, ε 31 400 M^{-1} cm^{-1}. ^{1}H NMR: (δ, 300 MHz, $CDCl_3$); 3.10 (m, 2H, H_2), 4.20 (s, 4H, C_5H_4), 4.35 (s, 4H, C_5H_4), 5.12 (m, 4H, PCH_2P), 5.27 (s, 2H, CH_2Cl_2), 5.34 (m, 2H, PCH_2P), 7.35 - 7.60 (m, 92H, Ph + H_7 + H_8 + C_6H_4). ^{31}P NMR: (δ, 121 MHz, $CDCl_3$); -14.4. SI MS; 2393 ([M – PF_6]$^+$, 40), 2247 ([M - H - 2PF_6]$^+$, 20), 1342 ([M – RuCl(dppm)$_2$]$^+$, 80), 869 ([Ru(dppm)$_2$ - H]$^+$, 100).

4.7.2.14. [Fe{η-C_5H_4-(E)-4-CH=$CHC_6H_4C{\equiv}$CRuCl(dppm)$_2$}$_2$]·CH_2Cl_2 (19)

[Fe{η-C_5H_4-(*E*)-4-CH=CHC_6H_4CH=CRuCl(dppm)$_2$}$_2$](PF$_6$)$_2$ (**18**) (205 mg, 0.081 mmol) and triethylamine (1 mL) were stirred in dichloromethane (25 mL) for 2 h. The solution was filtered through an alumina plug eluting with dichloromethane. The solvent was reduced in volume under reduced pressure to yield the red product (169 mg, 93 %). Anal. Calcd for $C_{131}H_{110}Cl_2FeP_8Ru_2$: C 67.47, H 4.75 %. Found: C 67.92, H 5.19 %. IR: (CH_2Cl_2) ν(C≡C) 2073 cm^{-1}. UV-Vis: λ (thf) 397 nm, ε 74 500 M^{-1} cm^{-1}. ^{1}H NMR: (δ, 300 MHz, $CDCl_3$); 4.21 (s, 4H, C_5H_4), 4.32 (s, 4H, C_5H_4), 4.88 (m, 8H, PCH_2P), 5.27 (s, 2H, CH_2Cl_2), 6.06 (d, 4H, J_{HH} = 8 Hz, H_4), 6.57 (d, 2H, J_{HH} = 16 Hz, H_7), 6.67 (d, 2H, J_{HH} = 16 Hz, H_8), 6.99 (d, 4H, J_{HH} = 8 Hz, H_5), 7.03 – 7.60 (m, 80H, Ph). ^{31}P NMR: (δ, 121 MHz, $CDCl_3$); -5.9. SI MS; 2248 ([M + H]$^+$, 40), 905 ([RuCl(dppm)$_2$]$^+$, 50), 869 ([Ru(dppm)$_2$ - H]$^+$, 100).

*4.7.2.15. [Fe{η-C_5H_4-(E)-4-CH=CHC_6H_4C≡$CRuCl(dppe)_2$}$_2$] (**20**)*

cis-[$RuCl_2(dppe)_2$] (300 mg, 0.31 mmol), [Fe{η-C_5H_4-(*E*)-4-CH=CHC_6H_4C≡CH}$_2$] (**2**) (68 mg, 0.15 mmol) and NH_4PF_6 (101 mg) were stirred in refluxing dichloromethane (40 mL) for 6 h. The solution was cooled, triethylamine (1 mL) was added and stirring continued for 10 min. Petroleum spirit (50 mL) was added and the precipitated material was adsorbed onto an alumina column. Diethyl ether (300 mL) was used to remove *trans*-[$RuCl_2(dppe)_2$], and the deep red product was eluted with dichloromethane (200 mL) (275 mg, 77 %). Anal. Calcd for $C_{134}H_{116}Cl_2FeP_8Ru_2$: C 69.88, H 5.08 %. Found: C 69.32, H 5.29 %. IR: (CH_2Cl_2) ν(C≡C) 2065 cm^{-1}. UV-Vis: λ (thf) 388 nm, ε 52 300 M^{-1} cm^{-1}. ^{1}H NMR: (δ, 300 MHz, $CDCl_3$); 2.65 (m, 16H, PCH_2), 4.28 (s, 4H, C_5H_4), 4.40 (s, 4H, C_5H_4), 6.60 - 6.80 (m, 8H, H_4 + H_7 + H_8), 6.90 - 7.60 (m, 84 H, Ph + H_5). ^{31}P NMR: (δ, 121 MHz, $CDCl_3$); 50.1. SI MS; 2267 ([M - Cl]$^+$, 5), 1368 ([M - RuCl(dppe)$_2$]$^+$, 5), 896 ([Ru(dppe)$_2$]$^+$, 100).

4.8. References

[1] Fyfe, H.B., Mlekuz, M., Zargarian, D., Taylor, N.J., Marder, T.B., *J. Chem. Soc. Chem. Commun.*, **1991**, 188.

[2] Yam, V.W.W., Choi, S.W.K., *J. Chem. Soc., Dalton Trans.*, **1996**, 4227.

[3] Davies, S.J., Johnson, B.F.G., Lewis, J., Khan, M.S., *J. Organomet. Chem.*, **1991**, *401*, C43.

[4] Fraysse, S., Coudret, C., Launay, J.P., *Tetrahedron Lett.*, **1998**, *39*, 7873.

[5] Briel, O., Fehn, A., Beck, W., *J. Organomet. Chem.*, **1999**, *578*, 247.

[6] Iyoda, M., Kondo, T., Okabe, T., Matsuyama, H., Sasaki, S., Kuwatani, Y., *Chem. Lett.*, **1997**, 35.

[7] Whittall, I.R., McDonagh, A.M., Humphrey, M.G., Samoc, M., *Adv. Organomet. Chem.*, **1998**, *42*, 291.

[8] Wong, H., Meyer-Friedrichsen, T., Farrell, T., Mecker, C., Heck, J., *Eur. J. Inorg. Chem.*, **2000**, 631.

[9] Heck, J., Dabek, S., Meyer-Friedrichsen, T., Wong, H., *Coord. Chem. Rev.*, **1999**, *192*, 1217.

[10] Coe, B.J., Jones, C.J., McCleverty, J.A., Bloor, D., Cross, G., *J. Organomet. Chem.*, **1994**, *464*, 225.

[11] Coe, B.J., Hamor, T.A., Jones, C.J., McCleverty, J.A., Bloor, D., Cross, G.H., Axon, T.L., *J. Chem. Soc., Dalton Trans.*, **1995**, 673.

[12] Page, H., Blau, W., Davey, A.P., Lou, X., Cardin, D.J., *Synth. Met.*, **1994**, *63*, 179.

[13] Ghosal, S., Samoc, M., Prasad, P.N., Tufariello, J.J., *J. Phys. Chem.,* **1990**, *94*, 2847.

[14] Whittall, I.R., McDonagh, A.M., Humphrey, M.G., Samoc, M., *Adv. Organomet. Chem.,* **1999**, *43*, 349.

[15] Behrens, U., Brussaard, H., Hagenau, U., Heck, J., Hendrickx, E., Kornich, J., van der Linden, J.G.M., Persoons, A., Spek, A.L., Veldman, N., Voss, B., Wong, H., *Chem. Eur. J.,* **1996**, *2*, 98.

[16] Yuan, Z., Taylor, N.J., Sun, Y., Marder, T.B., *J. Organomet. Chem.,* **1993**, *449*, 27.

[17] Cadierno, V., Conejero, S., Gamasa, M.P., Gimeno, J., Asselberghs, I., Houbrechts, S., Clays, K., Persoons, A., Borge, J., Garcia-Granda, S., *Organometallics,* **1999**, *18*, 582.

[18] Laidlaw, W.M., Denning, R.G., Verbiest, T., Chauchard, E., Persoons, A., *Proc. SPIE-Int. Soc. Opt. Eng.*, **1994**, *2143*, 14.

[19] McDonagh, A.M., Cifuentes, M.P., Whittall, I.R., Humphrey, M.G., Samoc, M., Luther-Davies, B., Hockless, D.C.R., *J. Organomet. Chem.,* **1996**, *526*, 99.

[20] Osella, D., Milone, L., Nervi, C., Ravera, M., *J. Organomet. Chem.,* **1995**, *488*, 1.

[21] Long, N.J., Martin, A.J., de Biani, F.F., Zanello, P., *J. Chem. Soc., Dalton Trans.,* **1998**, 2017.

[22] Hendrickx, E., Persoons, A., Samson, S., Stephenson, G.R., *J. Organomet. Chem.,* **1997**, *542*, 295.

[23] Khan, M.S., Kakkar, A.K., Ingham, S.L., Raithby, P.R., Lewis, J., Spencer, B., Wittmann, F., Friend, R.H., *J. Organomet. Chem.,* **1994**, *472*, 247.

[24] Viola, E., Losterzo, C., Crescenzi, R., Frachey, G., *J. Organomet. Chem.*, **1995**, *493*, C9.

[25] Levanda, C., Bechgaard, K., Cowan, D.O., *J. Org. Chem.*, **1976**, *41*, 2700.

[26] Yuan, Z., Stringer, G., Jobe, I.R., Kreller, D., Scott, K., Koch, L., Taylor, N.J., Marder, T.B., *J. Organomet. Chem.*, **1993**, *452*, 115.

[27] Myers, L.K., Langhoff, C., Thompson, M.E., *J. Am. Chem. Soc.*, **1992**, *114*, 7560.

[28] Frazier, C.C., Chauchard, E.A., Cockerham, M.P., Porter, P.L., *Mater. Res. Soc, Symp. Proc.*, **1988**, *109*, 323.

[29] Lavastre, O., Plass, J., Bachmann, P., Guesmi, S., Moinet, C., Dixneuf, P.H., *Organometallics,* **1997**, *16*, 184.

[30] Colbert, M.C.B., Lewis, J., Long, N.J., Raithby, P.R., Younus, M., White, A.J.P., Williams, D.J., Payne, N.N., Yellowlees, L., Beljonne, D., Chawdhury, N., Friend, R.H., *Organometallics,* **1998**, *17*, 3034.

[31] Thomas, K.R.J., Lin, J.T., Wen, Y.S., *Organometallics,* **2000**, *19*, 1008.

[32] Thomas, K.R.J., Lin, J.T., Lin, K.J., *Organometallics,* **1999**, *18*, 5285.

[33] Rodriguez, J.G., Gayo, M., Fonseca, I., *J. Organomet. Chem.*, **1997**, *534*, 35.

[34] Hradsky, A., Bildstein, B., Schuler, N., Schottenberger, H., Jaitner, P., Ongania, K.H., Wurst, K., Launay, J.P., *Organometallics,* **1997**, *16*, 392.

[35] Whittall, I.R., Humphrey, M.G., Houbrechts, S., Persoons, A., Hockless, D.C.R., *Organometallics,* **1996**, *15*, 5738.

[36] Touchard, D., Haquette, P., Pirio, N., Toupet, L., Dixneuf, P.H., *Organometallics,* **1993**, *12*, 3132.

[37] Kanis, D.R., Ratner, M.A., Marks, T.J., *J. Am. Chem. Soc.,* **1992**, *114*, 10338.

[38] Colbert, M.C.B., Lewis, J., Long, N.J., Raithby, P.R., White, A.J.P., Williams, D.J., *J. Chem. Soc., Dalton Trans.,* **1997**, 99.

[39] McDonagh, A.M., Humphrey, M.G., Samoc, M., Luther-Davies, B., Houbrechts, S., Wada, T., Sasabe, H., Persoons, A., *J. Am. Chem. Soc.,* **1999**, *121*, 1405.

[40] Lebreton, C., Touchard, D., Le Pichon, L., Daridor, A., Toupet, L., Dixneuf, P.H., *Inorg. Chim. Acta,* **1998**, *272*, 188.

[41] Jones, N.D., Wolf, M.O., Giaquinta, D.M., *Organometallics,* **1997**, *16*, 1352.

[42] Zhu, Y.B., Clot, O., Wolf, M.O., Yap, G.P.A., *J. Am. Chem. Soc.,* **1998**, *120*, 1812.

[43] Zanello, P., Tamburini, S., Vigato, P.A., Mazzocchin, G.A., *Coord. Chem. Rev.,* **1987**, *77*, 165 .

[44] Hurst, S.K., Cifuentes, M.P., Morrall, J.P.L., Lucas, N.T., Whittall, I.R., Humphrey, M.G., Asselberghs, I., Persoons, A., Samoc, M., Luther-Davies, B., Willis, A.C., *Organometallics,* **2001**, In press.

[45] Whittall, I.R., Humphrey, M.G., Samoc, M., Swiatkiewicz, J., Luther-Davies, B., *Organometallics,* **1995**, *14*, 5493.

[46] Whittall, I.R., Humphrey, M.G., Samoc, M., Luther-Davies., B., *Angew. Chem., Int. Ed. Engl.,* **1997**, *36*, 370.

[47] McAuliffe, C.A., Parish, R.V., Randall, P.D., *J. Chem. Soc., Dalton Trans.,* **1979**, 1730.

[48] Bruce, M.I., Horn, E., Matisons, J.G., Snow, M.R., *Aust. J. Chem.,* **1984**, *37*, 1163.

[49] Bailey, J., *J. Inorg. Nucl. Chem.,* **1973**, *35*, 1921.

[50] Takahashi, S., Kuroyama, Y., Sonogashira, K., Hagihara, N., *Synthesis,* **1980**, 627.

[51] Chaudret, B., Commenges, G., Poilblanc, R., *J. Chem. Soc., Dalton Trans.,* **1984**, 1635.

[52] Jia, G.C., Puddephatt, R.J., Scott, J.D., Vittal, J.J., *Organometallics,* **1993**, *12*, 3565.

Chapter 5

Branched transition metal complexes and some of their nonlinear optical properties

---

Contents

Chapter 5

Branched transition metal complexes and some of their nonlinear optical properties

5.1. Introduction

Traditional approaches to the construction of materials for nonlinear optical applications have been to synthesize dipolar materials which possess a long, easily delocalized π-bonded backbone connecting a strong electron donor to a strong electron acceptor. While this approach has led to materials with very large nonlinearities, it has several drawbacks. Lengthening the π-bonded backbone leads to an increase in NLO merit, but also causes a loss of transparency over useful wavelengths. The use of strongly electron donating and withdrawing groups may cause the molecule to adopt centrosymmetric packing in the solid state where $\chi^{(2)} = 0$. An additional drawback of this type of chromophore is the presence of small off-diagonal components of their hyperpolarizability tensor β.

To overcome these drawbacks, it has been proposed that future NLO materials should be based on octopolar chromophores. Investigations by Zyss and coworkers[1] established that octopolar molecules may have zero net dipole moment, and yet still have finite β. Anti-symmetric alignment of polarized donor and acceptor groups could therefore be avoided. Subsequent computational[2-5] and synthetic work[6-9] has demonstrated that octopolar materials also have improved transparency/NLO trade-off and larger quadratic hyperpolarizabilities in comparison with their dipolar analogues.

Certain branched octopolar compounds are referred to as "dendrimers". The term "dendrimer" (from the Greek *dendros* = tree and *meros* = part) reflects the branching nature of this type of molecule. Dendrimers differ from polymers by being monodisperse and possessing a well defined molecular structure. The regular branched nature, large size and orderly internal cavities of dendrimers suggests that they may be employed in diverse technological applications such as light-harvesting arrays,[10-12] complexation agents[13] and homogeneous catalysts.[14,15] Metal-containing dendrimers have been reported previously,[16,17] and have advantages of organic systems including

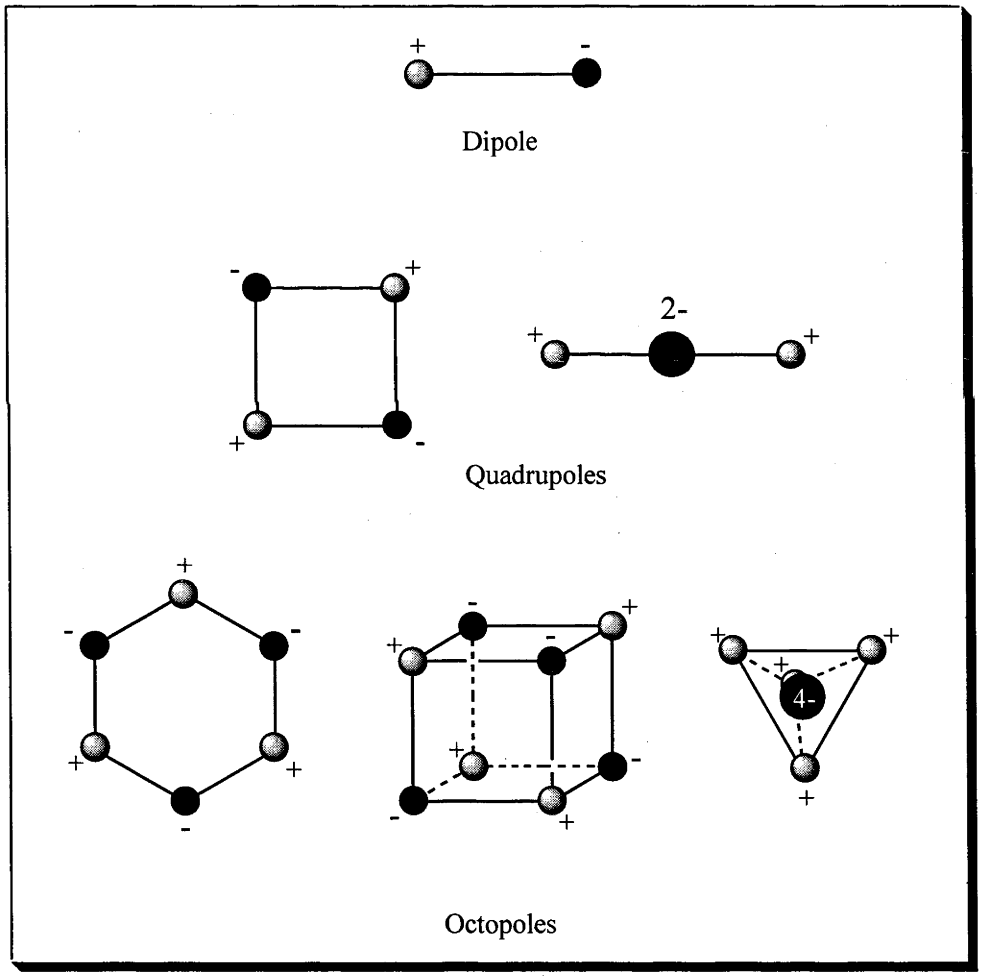

Figure 5.1. Donor-acceptor arrangement in dipolar and octopolar systems

good processability as well as permitting greater architectural flexibility. The majority of these compounds accommodate the metal centre only as a peripheral group,[18-21] and incorporation of metal centres into each generational layer of a dendrimer has only recently begun to be addressed.[22-24]

Dendrimeric compounds have also been considered as materials for nonlinear optics.[25-27] Although many compounds have been tested for their NLO merit, most of these materials have been dipolar donor-acceptor systems (See Figure 5.1). In addition, the majority of the work has considered optimization of the quadratic hyperpolarizability, with only a few studies examining third-order properties.[28-30] Previous work[31] has

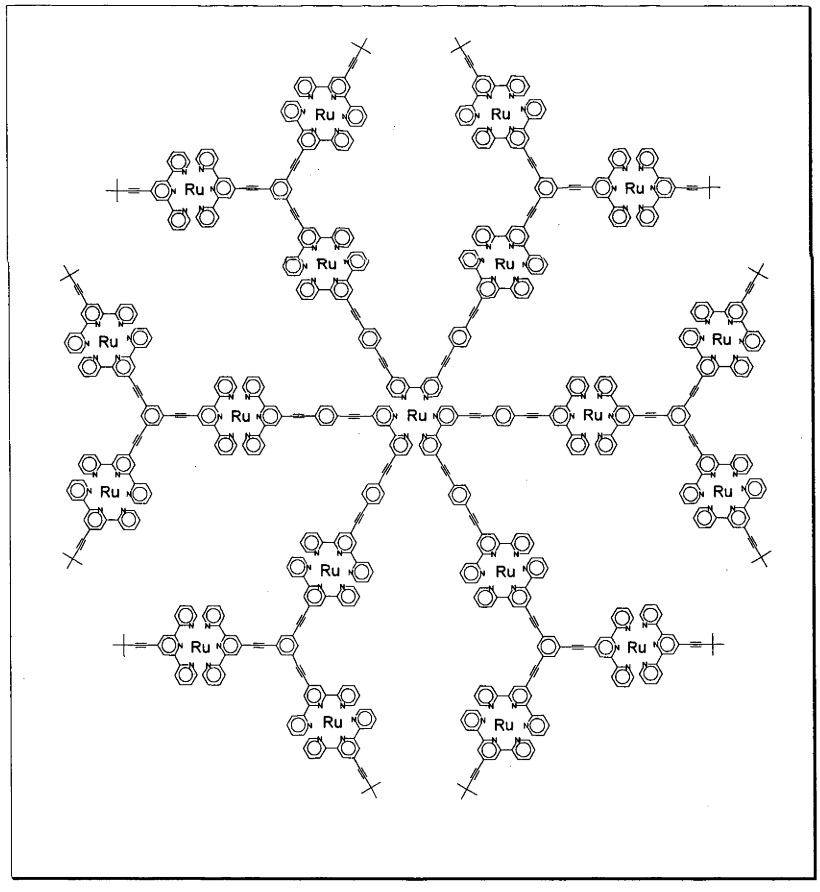

Figure 5.2. Large ruthenium-containing dendrimer of Osawa *et al.*[16]

enabled the elucidation of various structure-property relationships for optimization of molecular third-order nonlinearities, which suggests that replacement of yne linkages by (*E*)-ene linkages should give enhanced nonlinearities. Recently Cho *et al.*[32] demonstrated that in octopolar compounds, β and β_0 were both strongly enhanced upon replacing yne linkages with (*E*)-ene linkages, but no analogous study has been undertaken on third-order nonlinearities of octopolar complexes.

The aims of this Chapter are to compare the NLO properties of dipolar and octopolar systems and to examine the effect of changes in structure upon the molecular third-order properties. To this end, the preparation and characterization of a systematically varied series of dipolar and octopolar ruthenium and gold acetylide complexes are presented in this Chapter, along with their third-order NLO data.

5.2. *Syntheses of terminal alkynes*

Allred *et al.*[33] have previously reported the synthesis of (*E*)-4-IC_6H_4CH=CHPh. The iodo substituent can be functionalized; thus, Sonogashira coupling with trimethylsilylacetylene affords the protected alkyne **1**, which can be deprotected with base to give the terminal acetylene **2** (Scheme 5.1.). The new acetylenes were characterized by EI and HR mass spectrometry, satisfactory microanalyses, UV-vis, IR and ^{1}H-NMR spectroscopy. While the current research was in progress, an alternate synthesis of **2** was reported by reacting 4-ethynylbenzaldehyde and diethylphenylmethanephosphonate, but the yield via this procedure was lower (49%).[34]

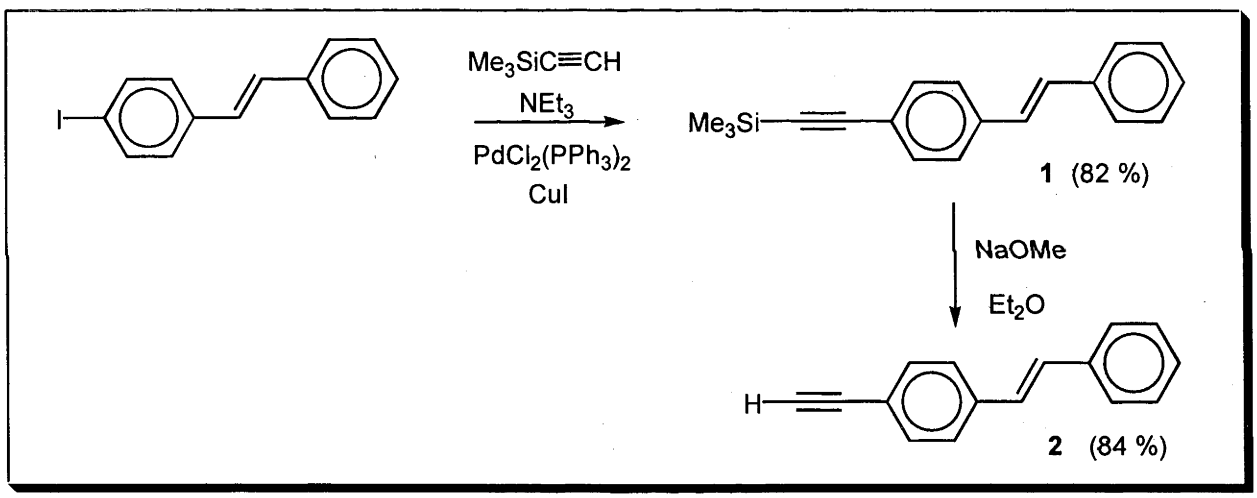

Scheme 5.1. Synthesis of compounds **1** and **2**

The synthetic pathway in Scheme 5.1. used for the synthesis of the linear acetylenes was also used for the synthesis of the branched acetylenes (Scheme 5.2.). Reaction of excess 4-IC_6H_4CHO with 1,3,5-$C_6H_3\{CH_2P(O)(OEt)_2\}_3$ in the presence of *t*-BuOK gave the new trisubstituted compound 1,3,5-$\{(E)$-4-IC_6H_4CH=$CH\}_3C_6H_3$ (**3**). Reaction of **3** with trimethylsilylacetylene under Sonogashira conditions gave the protected acetylene **4** which could be deprotected with base to yield the terminal acetylene **5**. Attempts to form either 1,3 or 1,4-bis(4-iodophenylethenyl)benzene via similar Wadsworth-Horner-

Emmons conditions were not successful. The new complexes **3** – **5** were characterized by EI and HR mass spectrometry, satisfactory microanalyses, UV-vis and IR spectroscopy and ^{1}H spectroscopy.

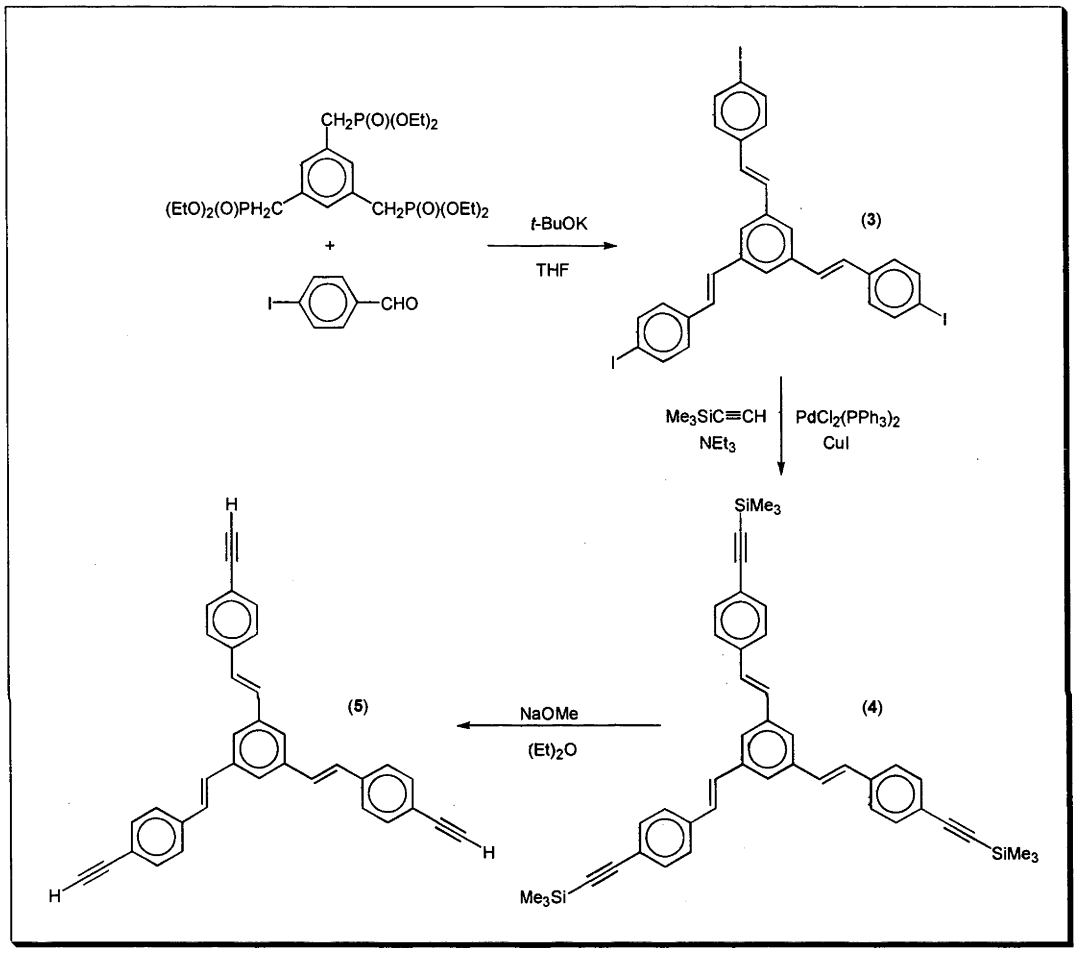

Scheme 5.2. Synthesis of branched compounds **3** - **5**

5.3. *Synthesis of metal complexes*

5.3.1. Gold acetylide complexes

The preparation of the gold acetylides complexes followed the method of Whittall *et al.*[35] The room temperature reaction of the terminal alkynes with the chloro(phosphine)gold complexes in a mixture of sodium methoxide solution and dichloromethane for 18 hours lead to the formation of the gold complexes in good yield (Scheme 5.3.). The octopolar complex **10** was synthesized in the same manner (Figure 5.3). The new acetylide complexes **6** – **10** were characterized by SI mass spectrometry, satisfactory microanalyses, UV-vis and IR spectroscopy, ^{1}H and ^{31}P NMR spectroscopy.

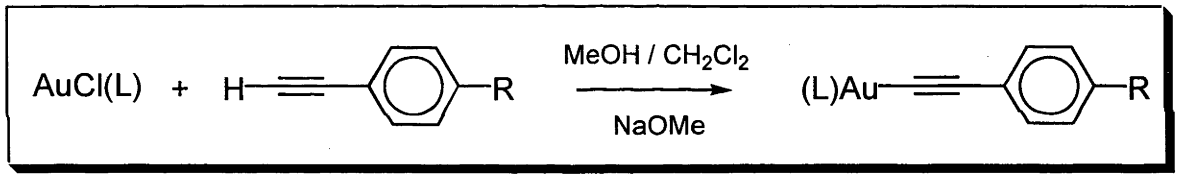

L	R	Complex
PPh_3	(*E*)-CH=CHPh	**6**
PMe_3	(*E*)-CH=CHPh	**7**
PPh_3	C≡CPh	**8**
PMe_3	C≡CPh	**9**

Scheme 5.3. Syntheses of linear alkynyl{(phosphine)gold} complexes **6 - 9**

5.3.2. Ruthenium complexes

The synthetic methodologies employed for the preparation of the new complexes are adaptations of those successfully utilized for the preparation of the corresponding phenylacetylides. The bis{bis(diphenylphosphino)alkane}ruthenium complexes were prepared by extending the method of Touchard *et al.*,[36] a procedure which also permits isolation of the stable vinylidene intermediates (Scheme 5.4.). A mixture of either *cis*-$[RuCl_2(dppm)_2]$ or *cis*-$[RuCl_2(dppe)_2]$ was stirred with ammonium hexafluorophosphate and an excess of terminal acetylene. In the case of the reaction using *cis*-$[RuCl_2(dppe)_2]$, excess acetylene was removed before deprotonation to avoid the formation of the bis-alkynyl product. The intermediate vinylidene complex could be deprotected via the addition of base (triethylamine) to give the corresponding acetylide. The octopolar complexes **14 - 17** were synthesized analogously (Figure 5.3.).The new complexes were characterized by SI mass spectrometry, satisfactory microanalyses, UV-vis and IR spectroscopy, ^1H and ^{31}P NMR spectroscopy.

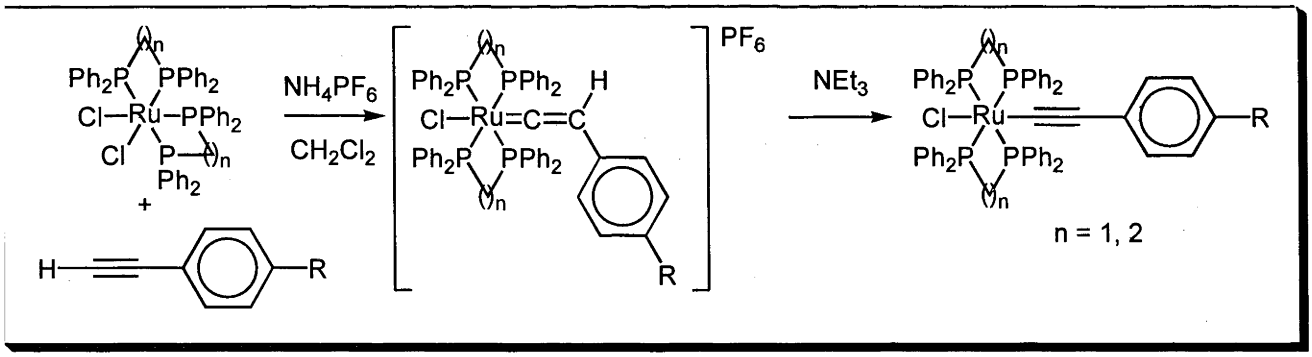

R	Vinylidene Complex	Alkynyl Complex	n
(*E*)-CH=CHPh	**11**	**12**	1
(*E*)-CH=CHPh	--	**13**	2

Scheme 5.4. Syntheses of linear *trans*-bis{bis(diphenylphosphino)alkane}chlororuthenium acetylide and vinylidene complexes

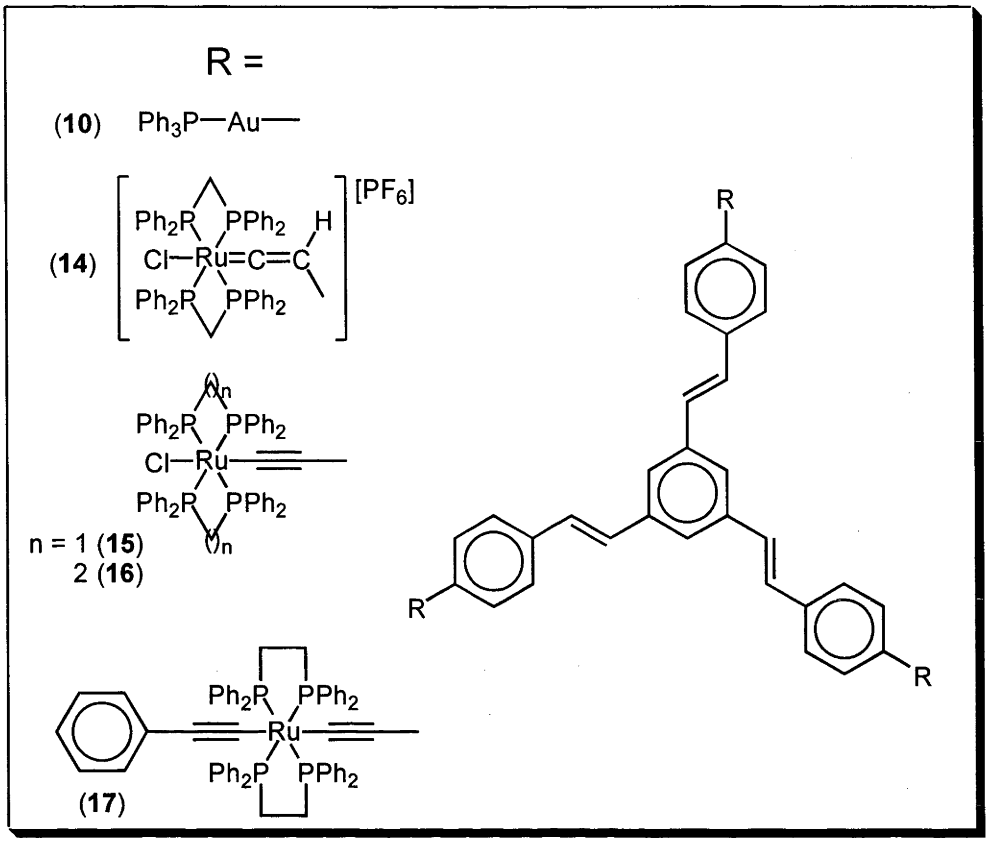

R	Complex	n
[(PPh$_3$)AuC≡C-]	**10**	--
trans-[(dppm)$_2$ClRu(C=CH-)][PF$_6$]	**14**	1
trans-[(dppm)$_2$ClRu(C≡C-)]	**15**	1
trans-[(dppe)$_2$ClRu(C≡C-)]	**16**	2
trans-[(dppe)$_2$(PhC≡C)Ru(C≡C-)]	**17**	2

Figure 5.3. Octopolar complexes **10, 14 - 17**

5.3.3. Branched ruthenium complexes

The preparation of the branched metal complexes utilized a new methodology developed over the course of this research (Scheme 5.5.). Previous research by Whittall *et al.*[37] demonstrated that, due to steric crowding, only two equivalents of *cis*-$[RuCl_2(dppm)_2]$ could be coupled to a core of 1,3,5-$(HC{\equiv}C)_3C_6H_3$. Coupling of *cis*-$[RuCl_2(dppe)_2]$ to 1,3,5-$(HC{\equiv}C)_3C_6H_3$ in dichloromethane with ammonium hexafluorophosphate also gave the exclusively di-substituted complex **18**. This complex could then be coupled with HC≡CPh to produce the bis-substituted product **19**. Treatment of complex **19** with a Cu(I) catalyst under Cadiot/Chodkiewicz conditions gave the homo-coupled product **22** (Scheme 5.5.). Coupling the unreacted acetylene functionality in **19** with excess 4-$IC_6H_4C{\equiv}CSiMe_3$ using $[Pd(PPh_3)_4]$ in a rigorously degassed mixture of triethylamine and dichloromethane led to the formation of the new complex **20** (Scheme 5.6.). Deprotection of the trimethylsilyl protecting group could be accomplished through the use of sodium methoxide solution or NBu^n_4F to give **21** in good yield. Complex **21** could be coupled to 1,3,5-triiodobenzene under palladium-catalyzed conditions to give the dendritic complex **23** (Scheme 5.6.). The new complexes were characterized by SI mass spectrometry, satisfactory microanalyses, UV-vis and IR spectroscopy, ^1H and ^{31}P NMR spectroscopy.

5.3.4. Comparison of characterization data

Selected ^1H NMR data for compounds **1** - **17** and **18** – **23** are listed in Tables 5.1. and 5.2., respectively. The NMR numbering scheme for complexes **1** – **17** and **18** – **23** are displayed in Figures 5.4. and 5.5., respectively. The terminal alkynes **2** and **5** have resonances for the acetylenic proton at 3.12 and 3.13 ppm respectively, as expected. Complexes **18**, **19** and **21** also exhibit singlet resonances at 3.01, 3.01 and 3.18 ppm, respectively, corresponding to the unreacted acetylene functionality. In the complexes

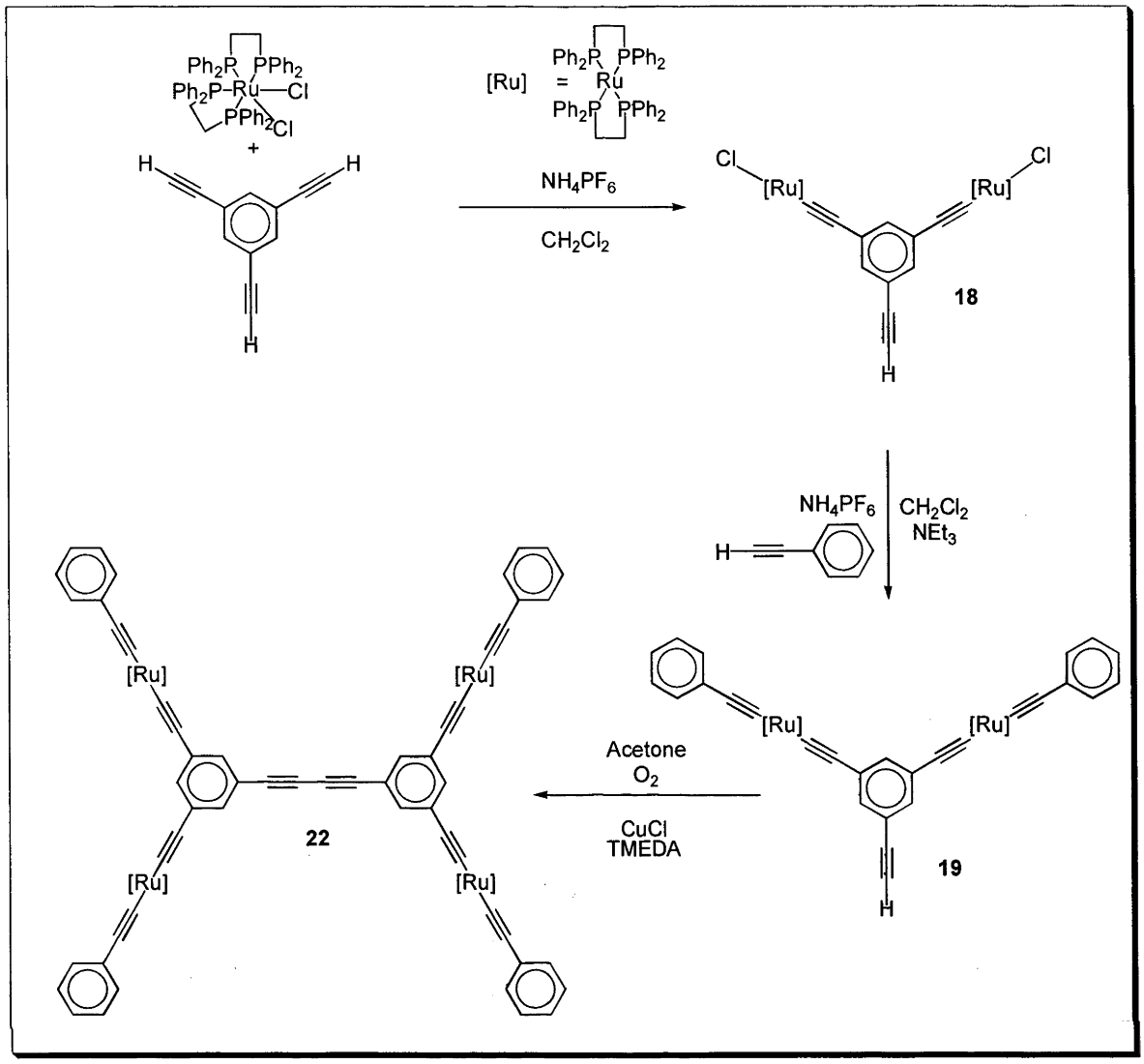

Scheme 5.5. Syntheses of complexes **18**, **19** and **22**

containing an (*E*)-ene linkage, stereoselectivity about the double bond was confirmed by the presence of a pair of doublets centered around 7.08 ppm with a coupling constant of *ca* 16 Hz, which is characteristic of the (*E*)-ene double bond. None of the (*Z*)-ene isomer could be detected by NMR. The ^{31}P NMR spectra for all complexes were unremarkable with similar shifts for comparable ligated metal centres.

Table 5.3. contains IR and UV-vis data for complexes **1** – **25**. The IR ν(C≡C) bands for the protected acetylenes (**1**, **4**) are at 2154 cm^{-1} and the free acetylenes (**2**, **5**) occur at

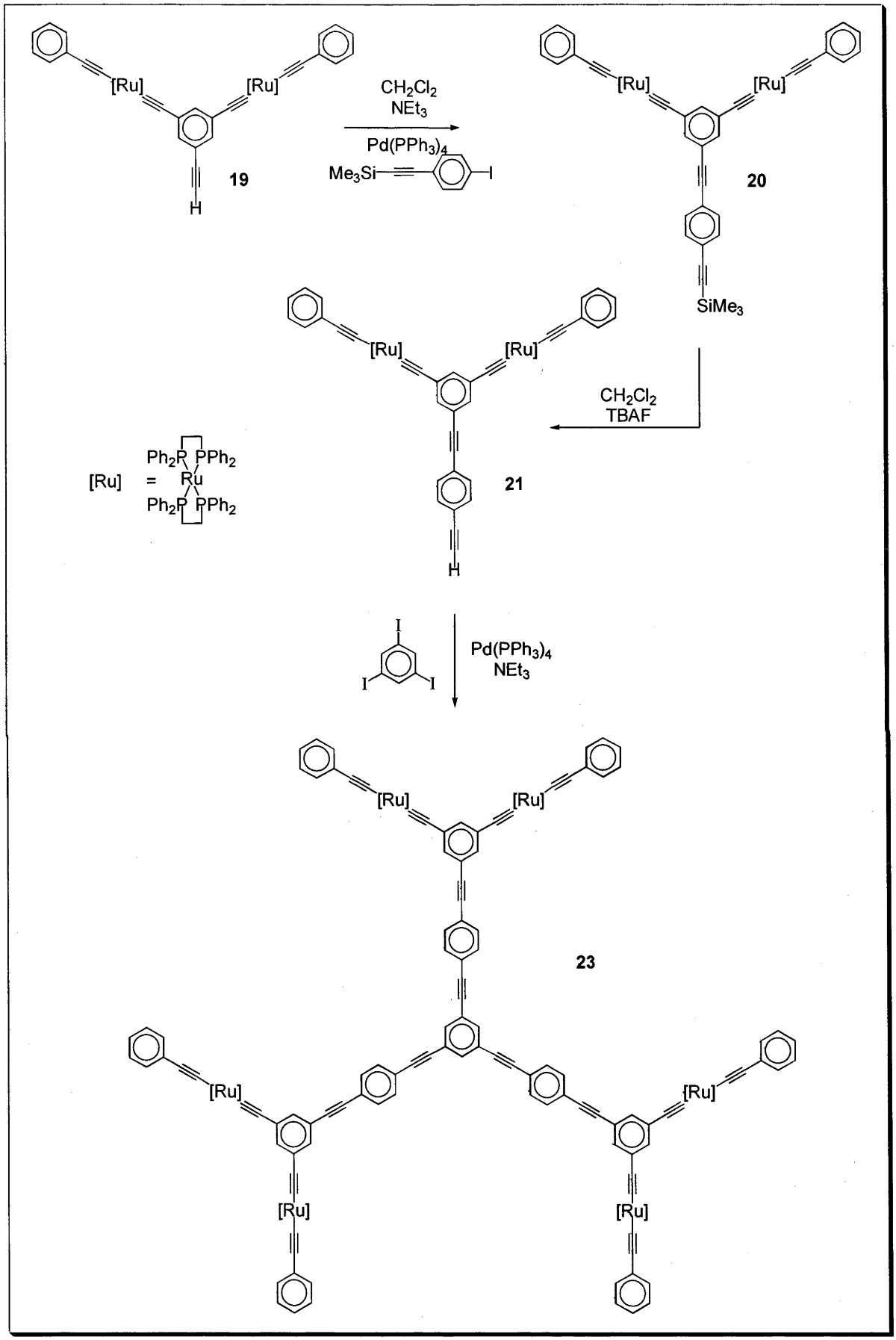

Scheme 5.6. Synthesis of complexes **20**, **21** and **23**

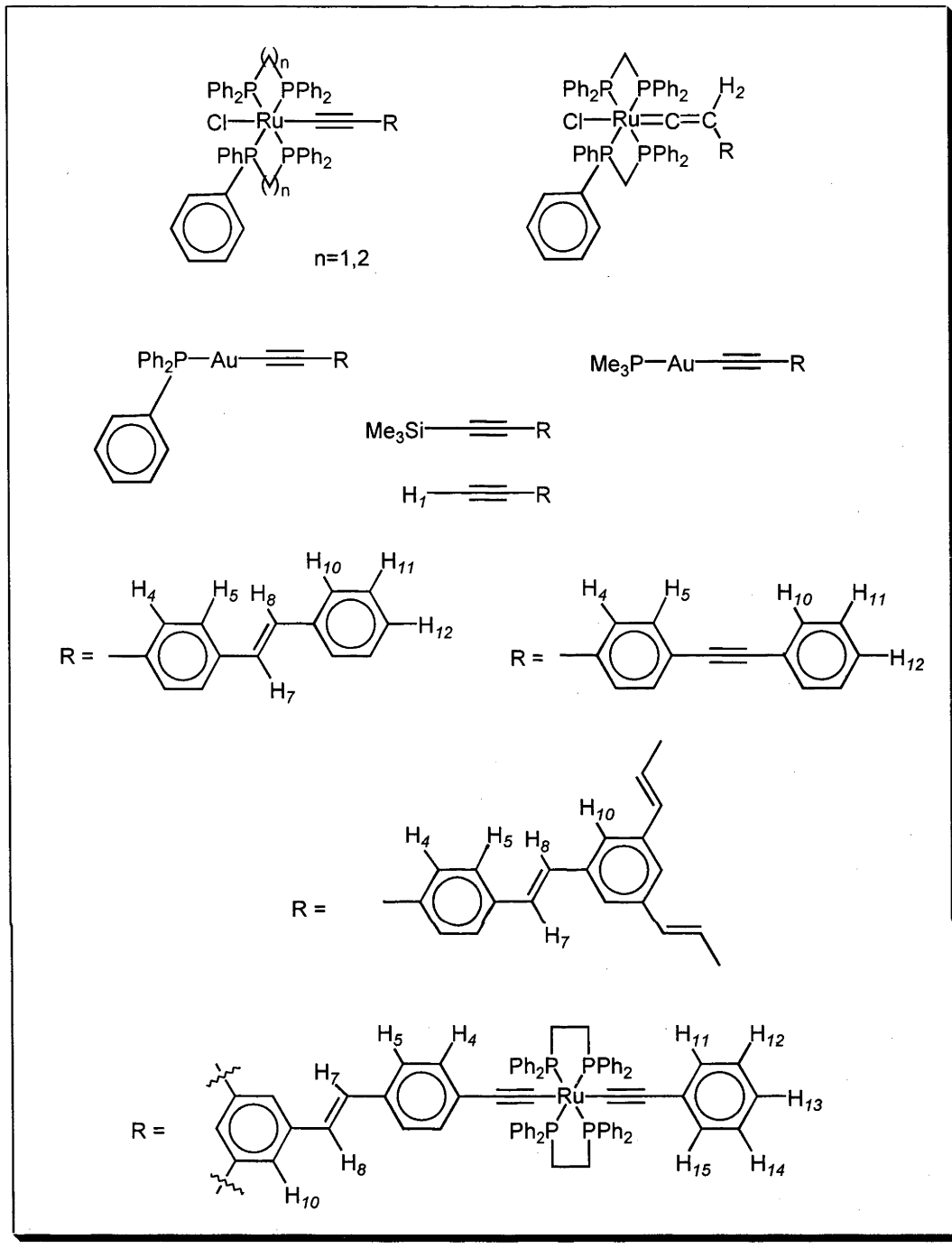

Figure 5.4. NMR numbering scheme for complexes **1 - 17**

approximately 2107 cm^{-1}. The gold acetylide complexes have similar ν(C≡C) values to the terminal acetylenes, with the bands occurring between 2108 and 2112 cm^{-1}. Substitution of gold with a ruthenium centre leads to a low frequency shift for the ν(C≡C) band. The UV-vis spectra for the terminal acetylenes and the ligated gold complexes all have $\lambda_{max} < 400$ nm. Replacement of PPh_3 by PMe_3 has little effect on

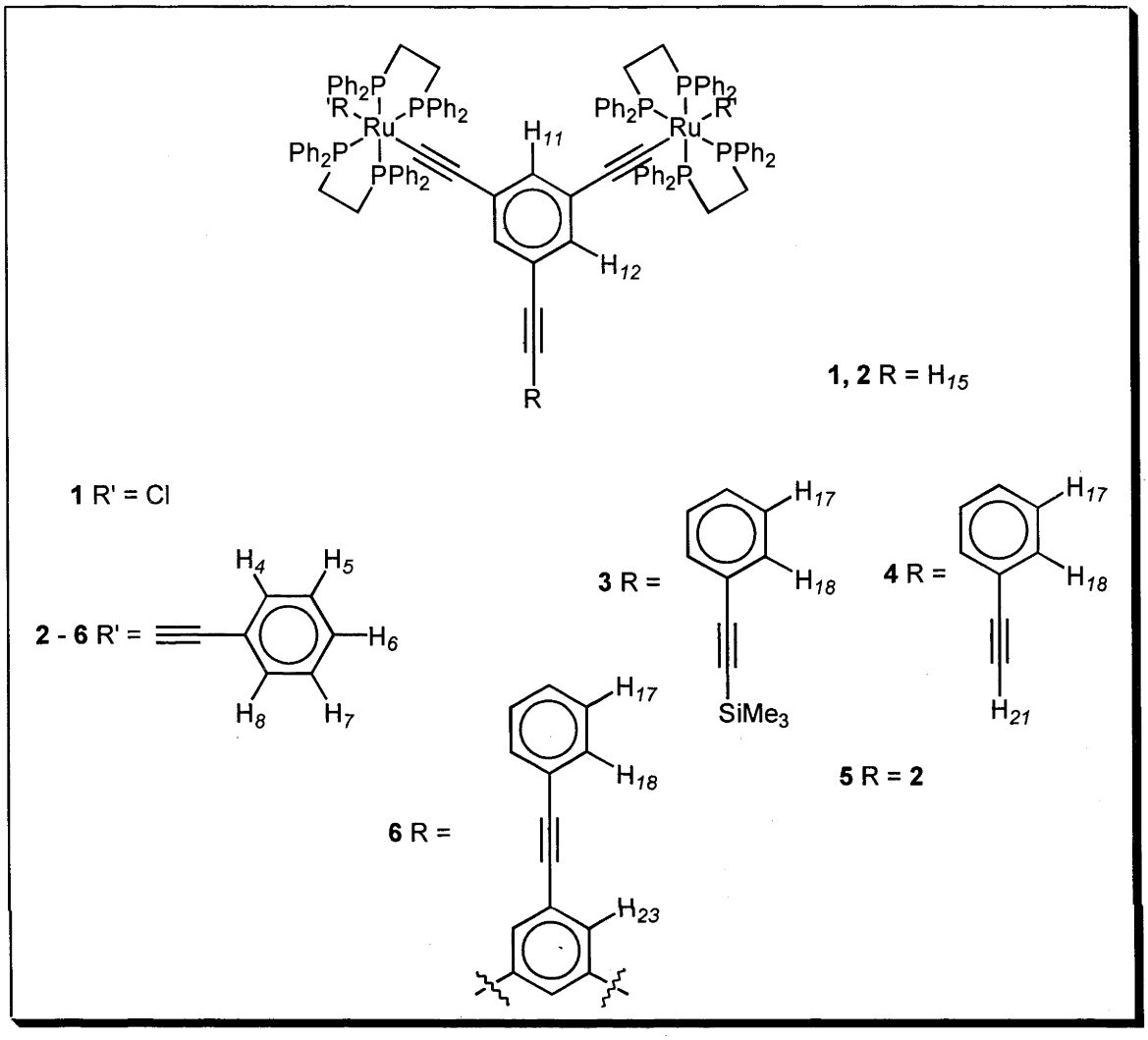

Figure 5.5. ^{1}H NMR numbering scheme for complexes **18** – **22**

either λ_{max} or extinction coefficient. Introduction of a *trans*-[RuCl(dppm)$_2$] or *trans*-[RuCl(dppe)$_2$] centre shifts the λ_{max} to higher wavelengths, with the acetylide complexes being more red-shifted than their analogous vinylidene complexes. The tris-substituted complexes **14** – **16** have λ_{max} only slightly greater than their linear analogues, although the tris-substituted complexes have larger extinction coefficients. Complexes **18** - **23** have λ_{max} in the region of 330 - 339 nm which are higher in energy than the analogous 1,4-substituted system *trans,trans*-[(dppm)$_2$ClRu(μ-4-C≡CC$_6$H$_4$C≡C)RuCl(dppm)$_2$] (354 nm). Progressing from a mono-acetylide (**18**) to a bis-acetylide (**19**) results in a

Table 5.1. Selected ^{1}H NMR data for complexes **1** - **17** (ppm)

Compound	H_4	H_5	H_7	H_8	Ph	$P(CH_2)_nP$
(*E*)-4-$Me_3SiC{\equiv}CC_6H_4CH{=}CHPh$ (**1**)	[a]	[a]	7.04	7.11	7.15 – 7.55	--
(*E*)-4-$HC{\equiv}CC_6H_4CH{=}CHPh$ (**2**)	[a]	[a]	7.05	7.12	7.20 – 7.60	--
1,3,5-{(*E*)-4-$IC_6H_4CH{=}CH\}_3C_6H_3$ (**3**)	7.26	7.68	7.06	7.13	--	--
1,3,5-{(*E*)-4-$Me_3SiC{\equiv}CC_6H_4CH{=}CH\}_3C_6H_3$ (**4**)		7.49		7.15	--	--
1,3,5-{(*E*)-4-$HC{\equiv}CC_6H_4CH{=}CH\}_3C_6H_3$ (**5**)		7.49		7.15	--	--
[Au{(*E*)-4-$C{\equiv}CC_6H_4CH{=}CHPh\}(PPh_3)$] (**6**)	[a]	[a]		7.06	7.30 – 7.60	--
[Au{(*E*)-4-$C{\equiv}CC_6H_4CH{=}CHPh\}(PMe_3)$] (**7**)	[a]	[a]		7.04	7.20 – 7.55	--
[Au(4-$C{\equiv}CC_6H_4C{\equiv}CPh)(PPh_3)$] (**8**)	[a]	[a]	--	--	7.25 – 7.60	--
[Au(4-$C{\equiv}CC_6H_4C{\equiv}CPh)(PMe_3)$] (**9**)	[a]	[a]	--	--	7.25 – 7.55	--
1,3,5-[(Ph_3P)Au{(*E*)-4-$C{\equiv}CC_6H_4CH{=}CH\}]_3C_6H_3$ (**10**)	[a]	[a]	7.11	7.15	7.40 – 7.60	--
trans-[Ru{(*E*)-4-$C{=}CHC_6H_4CH{=}CHPh\}Cl(dppm)_2]PF_6$ (**11**)	5.50	6.88	[a]	[a]	7.10 – 7.60	5.10, 5.32
trans-[Ru{(*E*)-4-$C{\equiv}CC_6H_4CH{=}CHPh\}Cl(dppm)_2$] (**12**)	6.21	[a]	[a]	[a]	7.10 – 7.60	4.89
trans-[Ru{(*E*)-4-$C{\equiv}CC_6H_4CH{=}CHPh\}Cl(dppe)_2$] (**13**)	[a]	[a]	[a]	[a]	7.10 – 7.60	2.67
[1,3,5-(*trans*-[$(dppm)_2$ClRu{(*E*)-4-$C{=}CHC_6H_4CH{=}CH\}])_3C_6H_3(PF_6)_3$] (**14**)	5.51	6.98	[a]	[a]	7.10 – 7.60	5.10, 5.26
1,3,5-(*trans*-[$(dppm)_2$ClRu{(*E*)-4-$C{\equiv}CC_6H_4CH{=}CH\}])_3C_6H_3$ (**15**)	6.07	[a]	[a]	[a]	6.90 – 7.60	4.91
1,3,5-(*trans*-[$(dppe)_2$ClRu{(*E*)-4-$C{\equiv}CC_6H_4CH{=}CH\}])_3C_6H_3$ (**16**)	6.66	[a]	[a]	[a]	6.90 – 7.60	2.70
1,3,5-(*trans*-[$(dppe)_2(PhC{\equiv}C)$Ru{(*E*)-4-$C{\equiv}CC_6H_4CH{=}CH\}])_3C_6H_3$ (**17**)	[a]	[a]	[a]	[a]	6.70 – 7.60	2.63

[a] Obscured by other resonances.

Table 5.2. Selected ^{1}H NMR data for complexes **18 - 23** (ppm)

Compound	H_{15}	H_{11}	H_{12}	Ph	$P(CH_2)_nP$
1,3-{*trans*-[(dppe)$_2$ClRuC≡C]}$_2$-5-HC≡CC$_6$H$_3$ (**18**)	3.01	6.55	6.41	6.80 – 7.70	2.68
1,3-{*trans*-[(dppe)$_2$(PhC≡C)RuC≡C]}$_2$-5-HC≡CC$_6$H$_3$ (**19**)	3.02	6.55	6.41	6.80 – 7.70	2.64
1,3-{*trans*-[(dppe)$_2$(PhC≡C)RuC≡C]}$_2$-5-(Me$_3$SiC≡C-4-C$_6$H$_4$C≡C)C$_6$H$_3$ (**20**)	--	6.55	6.41	6.80 – 7.70	2.67
1,3-{*trans*-[(dppe)$_2$(PhC≡C)RuC≡C]}$_2$-5-(HC≡C-4-C$_6$H$_4$C≡C)C$_6$H$_3$ (**21**)	--	6.70	6.40	6.80 – 7.70	2.66
{3,5-(*trans*-[(dppe)$_2$(PhC≡C)RuC≡C])$_2$C$_6$H$_3$C≡C}$_2$ (**22**)	--	[a]	[a]	6.85 – 7.60	2.63
1,3,5-{3,5-(*trans*-[(dppe)$_2$(PhC≡C)RuC≡C])$_2$C$_6$H$_3$C≡CC$_6$H$_4$-4-C≡C}$_3$C$_6$H$_3$ (**23**)	--	[a]	[a]	6.50 - 7.75	2.65

[a] Obscured by other resonances.

Table 5.3. IR[a] and UV-vis[b] data for complexes **1 - 25**

Compound	ν(C≡C) (cm^{-1})	λ_{max} (nm) [ε (10^4 M^{-1} cm^{-1})]
(*E*)-4-$Me_3SiC{\equiv}CC_6H_4CH{=}CHPh$ (**1**)	2154	346 [1.7]
(*E*)-4-$HC{\equiv}CC_6H_4CH{=}CHPh$ (**2**)	2107	339 [2.2]
1,3,5-{(*E*)-4-$IC_6H_4CH{=}CH\}_3C_6H_3$ (**3**)	--	340 [6.1]
1,3,5-{(*E*)-4-$Me_3SiC{\equiv}CC_6H_4CH{=}CH\}_3C_6H_3$ (**4**)	2154	354 [11.2]
1,3,5-{(*E*)-4-$HC{\equiv}CC_6H_4CH{=}CH\}_3C_6H_3$ (**5**)	2108	348 [9.0]
[Au{(*E*)-4-$C{\equiv}CC_6H_4CH{=}CHPh\}(PPh_3)$] (**6**)	2111	338 [1.7]
[Au{(*E*)-4-$C{\equiv}CC_6H_4CH{=}CHPh\}(PMe_3)$] (**7**)	2108	339 [1.9]
[Au(4-$C{\equiv}CC_6H_4C{\equiv}CPh)(PPh_3)$] (**8**)	2112	336 [6.5]
[Au(4-$C{\equiv}CC_6H_4C{\equiv}CPh)(PMe_3)$] (**9**)	2112	335 [5.5]
1,3,5-[(Ph_3P)Au{(*E*)-4-$C{\equiv}CC_6H_4CH{=}CH\}]_3C_6H_3$ (**10**)	2108	336 [9.6]
trans-[Ru{(*E*)-4-$C{=}CHC_6H_4CH{=}CHPh\}Cl(dppm)_2]PF_6$ (**11**)	--	360 [1.5]
trans-[Ru{(*E*)-4-$C{\equiv}CC_6H_4CH{=}CHPh\}Cl(dppm)_2$] (**12**)	2073	397 [2.3]
trans-[Ru{(*E*)-4-$C{\equiv}CC_6H_4CH{=}CHPh\}Cl(dppe)_2$] (**13**)	2066	404 [2.9]
[1,3,5-(*trans*-[$(dppm)_2$ClRu{(*E*)-4-$C{=}CHC_6H_4CH{=}CH\}])_3C_6H_3(PF_6)_3$] (**14**)	--	396 [2.0]
1,3,5-(*trans*-[$(dppm)_2$ClRu{(*E*)-4-$C{\equiv}CC_6H_4CH{=}CH\}])_3C_6H_3$ (**15**)	2073	415 [4.9]
1,3,5-(*trans*-[$(dppe)_2$ClRu{(*E*)-4-$C{\equiv}CC_6H_4CH{=}CH\}])_3C_6H_3$ (**16**)	2062	426 [8.7]
1,3,5-(*trans*-[$(dppe)_2(PhC{\equiv}C)$Ru{(*E*)-4-$C{\equiv}CC_6H_4CH{=}CH\}])_3C_6H_3$ (**17**)	2057	421 [13.0]
1,3-{*trans*-[$(dppe)_2$ClRu$C{\equiv}C]\}_2$-5-$HC{\equiv}CC_6H_3$ (**18**)	2059	334 [3.8]
1,3-{*trans*-[$(dppe)_2(PhC{\equiv}C)$Ru$C{\equiv}C]\}_2$-5-$HC{\equiv}CC_6H_3$ (**19**)	2055	335 [8.0]
1,3-{*trans*-[$(dppe)_2(PhC{\equiv}C)$Ru$C{\equiv}C]\}_2$-5-($Me_3SiC{\equiv}C$-4-$C_6H_4C{\equiv}C)C_6H_3$ (**20**)	2056, 2155	335 [9.5]
1,3-{*trans*-[$(dppe)_2(PhC{\equiv}C)$Ru$C{\equiv}C]\}_2$-5-($HC{\equiv}C$-4-$C_6H_4C{\equiv}C)C_6H_3$ (**21**)	2056	330 [9.9]
{3,5-(*trans*-[$(dppe)_2(PhC{\equiv}C)$Ru$C{\equiv}C])_2C_6H_3C{\equiv}C\}_2$ (**22**)	2056	335 [14.1]
1,3,5-{3,5-(*trans*-[$(dppe)_2(PhC{\equiv}C)$Ru$C{\equiv}C])_2C_6H_3C{\equiv}CC_6H_4$-4-$C{\equiv}C\}_3C_6H_3$ (**23**)	2057	339 [34.2]

[a] In dichloromethane. [b] In thf.

significant increase in extinction coefficient, lengthening the π-conjugated system also resulting in an increase in extinction coefficient. The modest λ_{max} values for complexes **18 - 23** may be due to the non-conjugated π-delocalized pathway introduced by the 1,3-substitution.

5.3.5 Electrochemistry

The results of cyclic voltammetric investigations into the new ruthenium complexes are summarized in Table 5.4. together with previously reported data for related complexes. All new complexes show an anodic wave assigned to the $Ru^{II/III}$ oxidation process. The tabulated data are consistent with several broad trends. Alkynylruthenium complexes exhibit reversible or quasi-reversible processes (in the range of 0.46 - 0.72 V for the new complexes), whereas the vinylidene complexes exhibit irreversible processes at a considerably more positive potential (the latter as expected for cationic complexes). The tris-substituted complexes **14 – 17** exhibit a single oxidation wave indicating that the three ruthenium centres are equivalent, with the π-delocalized framework preventing communication.

Complexes **18 – 23** exhibit electronic communication between the ruthenium centres. These results are consistent with the short 1,3-substituted arylalkynyl bridge providing an efficient conduit for electronic communication. Previous work on *trans,trans*-$[(dppm)_2ClRu(\mu\text{-}3\text{-}C{\equiv}CC_6H_4C{\equiv}C)RuCl(dppm)_2]$[38] gives similar K_{com} values to **18**, with the shift in $E_{½}$ possibly due to the differences between the ligated ruthenium units and the presence of the terminal acetylene functionality in **18**; the 1,3-substituted system results in less electronic communication than the analogous 1,4-substituted system. The tabulated K_{com} values are consistent with all examples behaving as Robin and Day Class II weakly interacting complexes.

Table 5.4. Cyclic voltammetric data for **11 - 23** [a]

Complex	$E_{½}$ $Ru^{II/III}$ (V)	$[i_{pc}/i_{pa}]$	K_{com}	Ref.
trans-[Ru{(*E*)-4-C=CHC$_6$H$_4$CH=CHPh}Cl(dppm)$_2$]PF$_6$ (**11**)	1.38	[b]	--	This work
trans-[Ru{(*E*)-4-C≡CC$_6$H$_4$CH=CHPh}Cl(dppm)$_2$] (**12**)	0.46	[0.9]	--	This work
trans-[Ru{(*E*)-4-C≡CC$_6$H$_4$CH=CHPh}Cl(dppe)$_2$] (**13**)	0.51	[1.0]	--	This work
[1,3,5-(*trans*-[(dppm)$_2$ClRu{(*E*)-4-C=CHC$_6$H$_4$CH=CH}])$_3$C$_6$H$_3$(PF$_6$)$_3$] (**14**)	1.45	[b]	--	This work
1,3,5-(*trans*-[(dppm)$_2$ClRu{(*E*)-4-C≡CC$_6$H$_4$CH=CH}])$_3$C$_6$H$_3$ (**15**)	0.68	[1.0]	--	This work
1,3,5-(*trans*-[(dppe)$_2$ClRu{(*E*)-4-C≡CC$_6$H$_4$CH=CH}])$_3$C$_6$H$_3$ (**16**)	0.51	[0.9]	--	This work
1,3,5-(*trans*-[(dppe)$_2$(PhC≡C)Ru{(*E*)-4-C≡CC$_6$H$_4$CH=CH}])$_3$C$_6$H$_3$ (**17**)	0.49	[1.0]	--	This work
1,3-{*trans*-[(dppe)$_2$ClRuC≡C]}$_2$-5-HC≡CC$_6$H$_3$ (**18**)	0.53, 0.72	1.0, 1.0	1.6×10^3	This work
trans,trans-[(dppm)$_2$ClRu(μ-3-C≡CC$_6$H$_4$C≡C)RuCl(dppm)$_2$]	0.44, 0.63	1.0, 1.0	1.6×10^3	38
trans,trans-[(dppm)$_2$ClRu(μ-4-C≡CC$_6$H$_4$C≡C)RuCl(dppm)$_2$]	0.26, 0.56	1.0, 1.0	1.2×10^5	38
1,3-{*trans*-[(dppe)$_2$(PhC≡C)RuC≡C]}$_2$-5-HC≡CC$_6$H$_3$ (**19**)	0.47, 0.60	1.0, 1.0	1.57×10^2	This work
1,3-{*trans*-[(dppe)$_2$(PhC≡C)RuC≡C]}$_2$-5-(Me$_3$SiC≡C-4-C$_6$H$_4$C≡C)C$_6$H$_3$ (**20**)	0.49, 0.61	1.0, 1.0	1.07×10^2	This work
1,3-{*trans*-[(dppe)$_2$(PhC≡C)RuC≡C]}$_2$-5-(HC≡C-4-C$_6$H$_4$C≡C)C$_6$H$_3$ (**21**)	0.50, 0.62	1.0, 1.0	1.07×10^2	This work
{3,5-(*trans*-[(dppe)$_2$(PhC≡C)RuC≡C])$_2$C$_6$H$_3$C≡C}$_2$ (**22**)	0.50, 0.62	1.0, 1.0	1.07×10^2	This work
1,3,5-{3,5-(*trans*-[(dppe)$_2$(PhC≡C)RuC≡C])$_2$C$_6$H$_3$C≡CC$_6$H$_4$-4-C≡C}$_3$C$_6$H$_3$ (**23**)	0.48, 0.59	1.0, 1.0	72	This work

[a] Ferrocene/ferrocenium couple (0.56 V) as an internal standard except where specified. [b] Not reversible.

5.4. X-ray structural study of [Au{(E)-4-C≡CC$_6$H$_4$CH=CHPh}(PPh$_3$)] (6)

A single-crystal X-ray diffraction study of [Au{(*E*)-4-C≡CC$_6$H$_4$CH=CHPh}(PPh$_3$)] (**6**) has been performed by collaborators at the Australian National University. An ORTEP plot is displayed in Figure 5.6. and a cell-packing diagram in Figure 5.7., and selected bond lengths and angles are gathered in Table 5.5. A comparison of important bond lengths and angles with those of related complexes appears in Table 5.6.

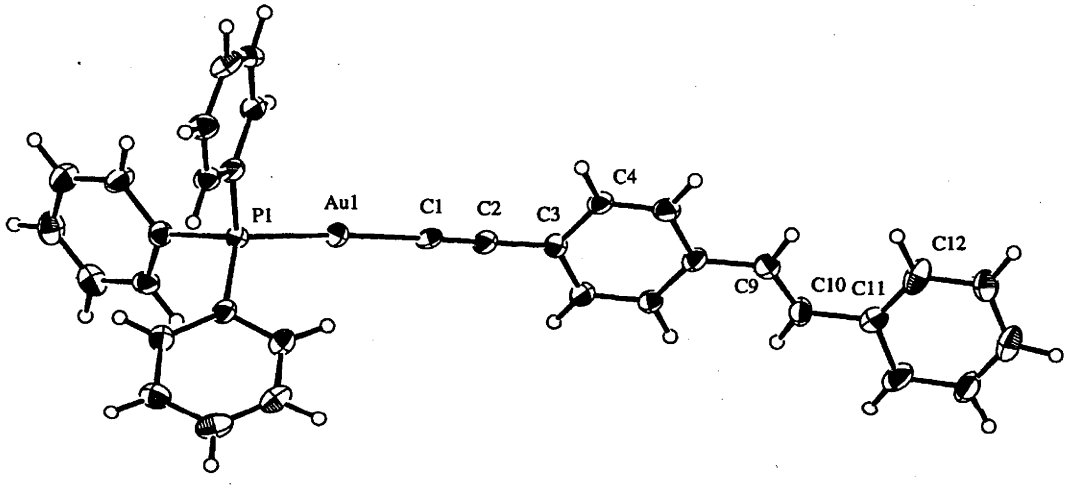

Figure 5.6. Molecular geometry and atomic labeling scheme for [Au{(*E*)-4-C≡CC$_6$H$_4$CH=CHPh}(PPh$_3$)] (**6**). 30% thermal ellipsoids are shown for the non-hydrogen atoms. Hydrogen atoms are drawn as circles (crystal structure provided by N.T. Lucas).

The structural study of **6** confirms the approximately linear geometry about the gold. Due to crystal packing forces, distances and angles within the phenyl rings and the (*E*)-ene components of the alkynyl ligand are slightly distorted. The Au - P, Au - C(1) and C(1) - C(2) bond distances are slightly shorter in comparison with previously observed values for (phosphine)gold acetylide complexes.[35,39,40] The angles about the P - Au - C(1) - C(2) moiety are close to linearity, with deviations likely to be the result of crystal packing forces. Intraphosphine bond lengths and angles in **6** are not unusual. Gold complexes have attracted significant interest as many show aurophilic Au···Au interactions in the solid state. In the present case, however, Au···Au contacts are all greater than 5 Å.

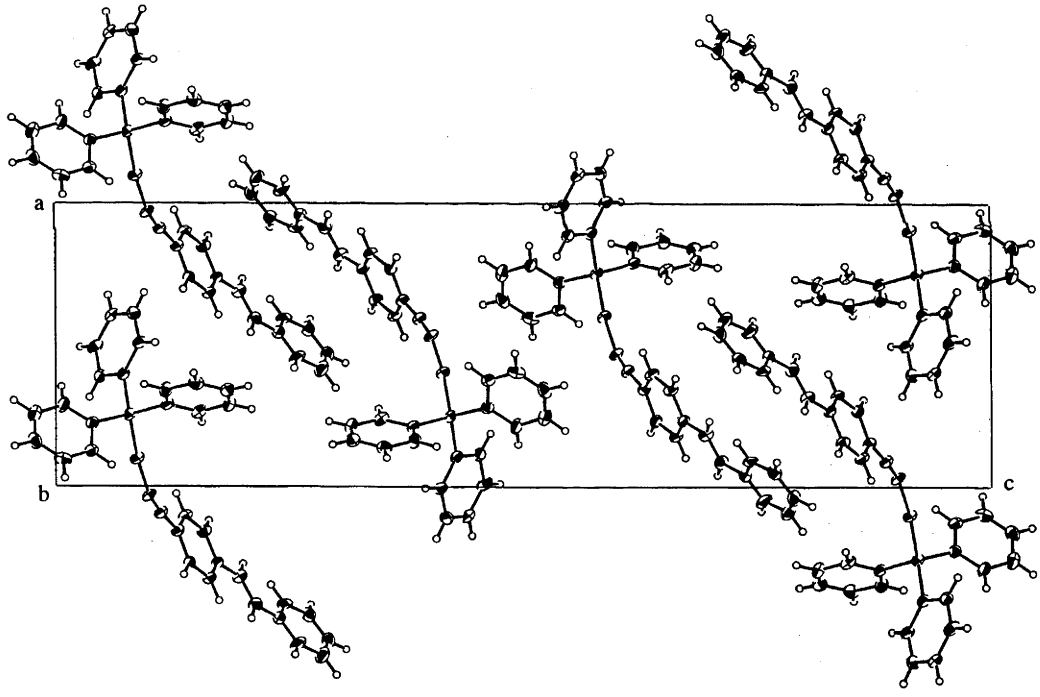

Figure 5.7. Unit cell diagram of [Au{(*E*)-4-C≡CC$_6$H$_4$CH=CHPh}(PPh$_3$)] (**6**) projected down the *b* axis. Ellipsoids show 30% probability levels (crystal structure provided by N.T. Lucas).

Table 5.5. Selected bond distances (Å) and angles (deg) for [Au{(*E*)-4-C≡CC$_6$H$_4$CH=CHPh}(PPh$_3$)] (**6**)

Au - P	2.236(2)	P - C(111)	1.861(9)
P - C(121)	1.862(9)	P - C(131)	1.809(9)
Au - C(1)	1.989(9)	C(1) - C(2)	1.12(1)
C(2) - C(3)	1.38(1)	C(3) - C(4)	1.42(1)
C(4) - C(5)	1.31(1)	C(5) - C(6)	1.35(1)
C(6) - C(7)	1.41(1)	C(7) - C(8)	1.35(1)
C(3) - C(8)	1.36(1)	C(6) - C(9)	1.42(1)
C(9) - C(10)	1.25(1)	C(10) - C(11)	1.44(1)
C(11) - C(12)	1.36(1)	C(12) - C(13)	1.36(1)
C(13) - C(14)	1.32(1)	C(14) - C(15)	1.36(1)
C(15) - C(16)	1.38(1)		
P - Au - C(1)	174.1(3)	Au - P - C(111)	115.2(3)
Au - P - C(121)	110.7(3)	Au - P - C(131)	112.3(3)
Au - C(1) - C(2)	167.2(9)	C(1) - C(2) - C(3)	173(1)
C(2) - C(3) - C(4)	122.1(8)	C(3) - C(4) - C(5)	123.1(8)
C(4) - C(5) - C(6)	119.3(9)	C(5) - C(6) - C(7)	118.2(8)
C(6) - C(7) - C(8)	123.5(7)	C(2) - C(3) - C(8)	118.8(8)
C(3) - C(8) - C(7)	116.9(8)	C(5) - C(6) - C(9)	115.4(9)
C(7) - C(6) - C(9)	126.3(7)	C(6) - C(9) - C(10)	123.1(9)
C(9) - C(10) - C(11)	123.0(9)	C(10) - C(11) - C(12)	125.6(8)

Table 5.6. Comparison of important bond lengths and angles in **6** with those of analogous complexes

Compound	Au-C(1)	C(1)-C(2)	C(2)-C(3)	P-Au-C(1)	Au-C(1)-C(2)	C(1)-C(2)-C(3)	Reference
[Au{(*E*)-4-C≡CC_6H_4CH=CHPh}(PPh_3)] (**6**)	1.989(9)	1.12(1)	1.38(1)	174.1(3)	167.2(9)	173(1)	This work
[Au(4-C≡C$C_6H_4NO_2$)(PPh_3)]	1.973(5)	1.206(6)	1.446(6)	178.1(2)	175.1(5)	179.8(6)	35
[Au(C≡CPh)(PPh_3)]	2.02(2)	1.16(2)	1.47(2)	173.8(5)	170.8(19)	174.0(20)	40
[Au(C≡CC_6F_5)(PPh_3)]	1.993(14)	1.197(16)	1.442(20)	177.9(3)	175.4(10)	178.4(12)	39

5.5. *Nonlinear optical investigations*

5.5.1. Results of third-order nonlinear optical studies

Measurements of third-order optical nonlinearities were by the author with assistance from Dr M. Samoc using the Z-scan technique (see Section 1.3.5.) at 800 nm and 660 nm. The results are presented in Table 5.7. and 5.8. Table 5.9. contains one and two-photon absorption cross-sections for complexes **16** - **23** and analogous complexes, together with these parameters divided by the molecular weight.

5.5.2. Discussion of third-order nonlinear optical results

An electronic origin for cubic nonlinearities in related metal acetylide complexes has been demonstrated previously by degenerate four-wave mixing measurements,[41] and nonlinearities for the present series of compounds are therefore likely to be electronic in origin. Nonlinearities for the organic compounds are low. Introduction of terminal (phosphine)gold units in proceeding from **2** to **6** and **5** to **10** results in little change in the linear optical absorption spectra and does not result in a significant increase in nonlinearity. Introduction of ligated ruthenium in proceeding from **2** to **11** - **13** and from **5** to **14** - **17** both result in increased γ_{real} and $|\gamma|$. The ruthenium vinylidene complexes have smaller γ_{real} and γ_{imag} values than their alkynyl analogues, which may be due to decreased electron density about the ruthenium centre. The γ_{real} and γ_{imag} values for the dendrimeric complexes are significantly greater than for their linear analogues.

Comparison of complexes **16** and **17** with the analogous complexes of McDonagh *et al.*[28] demonstrates enhancement of third-order NLO properties by replacement of acetylene linkages with (*E*)-ene linkages. Comparison between **6** {(*E*)-ene linkage} and **8** {yne linkage} is difficult, because of the large error margins. The small nonlinearities for **6** and **8** are presumably due to the poor electron-donating capability of the gold

Table 5.7. Results of Z-scan experiments at 800 nm[a]

Compound	λ_{max} (nm) [ε (10^4 M^{-1} cm^{-1})]	γ_{real} (10^{-36} esu)	γ_{imag} (10^{-36} esu)	$\lvert\gamma\rvert$ (10^{-36} esu)	Ref.
(*E*)-4-$Me_3SiC{\equiv}CC_6H_4CH{=}CHPh$ (**1**)	346 [1.7]	300 ± 200	0 ± 20	300 ± 200	This work
(*E*)-4-$HC{\equiv}CC_6H_4CH{=}CHPh$ (**2**)	339 [2.2]	100 ± 60	0 ± 20	100 ± 60	This work
1,3,5-{(*E*)-4-$IC_6H_4CH{=}CH\}_3C_6H_3$ (**3**)	340 [6.1]	--	--	--	This work
1,3,5-{(*E*)-4-$Me_3SiC{\equiv}CC_6H_4CH{=}CH\}_3C_6H_3$ (**4**)	354 [11.2]	0 ± 120	0 ± 40	--	This work
1,3,5-{(*E*)-4-$HC{\equiv}CC_6H_4CH{=}CH\}_3C_6H_3$ (**5**)	348 [9.0]	330 ± 150	95 ± 50	340 ± 160	This work
[Au{(*E*)-4-$C{\equiv}CC_6H_4CH{=}CHPh\}(PPh_3)$] (**6**)	338 [1.7]	0 ± 300	0 ± 50	--	This work
[Au{(*E*)-4-$C{\equiv}CC_6H_4CH{=}CHPh\}(PMe_3)$] (**7**)	339 [1.9]	--	--	--	This work
[Au(4-$C{\equiv}CC_6H_4C{\equiv}CPh)(PPh_3)$] (**8**)	336 [6.5]	-900 ± 400	0 ± 100	900 ± 400	This work
[Au(4-$C{\equiv}CC_6H_4C{\equiv}CPh)(PMe_3)$] (**9**)	335 [5.5]	-200 ± 150	0 ± 50	200 ± 150	This work
1,3,5-[(Ph_3P)Au{(*E*)-4-$C{\equiv}CC_6H_4CH{=}CH\}]_3C_6H_3$ (**10**)	336 [9.6]	< 500	0 ± 0	--	This work
trans-[Ru{(*E*)-4-$C{=}CHC_6H_4CH{=}CHPh\}Cl(dppm)_2]PF_6$ (**11**)	360 [1.5]	< 200	90 ± 50	--	This work
trans-[Ru{(*E*)-4-$C{\equiv}CC_6H_4CH{=}CHPh\}Cl(dppm)_2$] (**12**)	397 [2.3]	-600 ± 400	700 ± 400	920 ± 560	This work
trans-[Ru{(*E*)-4-$C{\equiv}CC_6H_4CH{=}CHPh\}Cl(dppe)_2$] (**13**)	404 [2.9]	300 ± 400	300 ± 100	420 ± 350	This work
[1,3,5-(*trans*-[$(dppm)_2$ClRu{(*E*)-4-$C{=}CHC_6H_4CH{=}CH\}])_3C_6H_3(PF_6)_3$] (**14**)	396 [2.0]	-900 ± 500	700 ± 400	1140 ± 640	This work

1,3,5-(*trans*-[(dppm)$_2$ClRu{(*E*)-4-C≡CC$_6$H$_4$CH=CH}])$_3$C$_6$H$_3$ (**15**)	415 [4.9]	-640 ± 500	2000 ± 500	2100 ± 630	This work
1,3,5-(*trans*-[(dppe)$_2$ClRu{(*E*)-4-C≡CC$_6$H$_4$CH=CH}])$_3$C$_6$H$_3$ (**16**)	426 [8.7]	-4600 ± 2000	4200 ± 800	6230 ± 2020	This work
1,3,5-(*trans*-[(dppe)$_2$ClRu{4-C≡CC$_6$H$_4$C≡C)])$_3$C$_6$H$_3$	414 [10.0]	-330 ± 100	2200 ± 500	2200 ± 600	29
1,3,5-(*trans*-[(dppe)$_2$(PhC≡C)Ru{(*E*)-4-C≡CC$_6$H$_4$CH=CH}])$_3$C$_6$H$_3$ (**17**)	421 [13.0]	11200 ± 3000	8600 ± 2000	14120 ± 3600	This work
1,3,5-(*trans*-[(dppe)$_2$(PhC≡C)Ru(4-C≡CC$_6$H$_4$C≡C)])$_3$C$_6$H$_3$	411 [11.6]	-600 ± 200	2900 ± 500	3000 ± 600	29
1,3-{*trans*-[(dppe)$_2$ClRuC≡C]}$_2$-5-HC≡CC$_6$H$_3$ (**18**)	334 [3.8]	-900 ± 500	0 ± 100	900 ± 500	This work
1,3-{*trans*-[(dppe)$_2$(PhC≡C)RuC≡C]}$_2$-5-HC≡CC$_6$H$_3$ (**19**)	335 [8.0]	500 ± 400	200 ± 100	540 ± 410	This work
1,3-{*trans*-[(dppe)$_2$(PhC≡C)RuC≡C]}$_2$-5-(Me$_3$SiC≡C-4-C$_6$H$_4$C≡C)C$_6$H$_3$ (**20**)	335 [9.5]	700 ± 1200	0 ± 0	700 ± 1200	This work
1,3-{*trans*-[(dppe)$_2$(PhC≡C)RuC≡C]}$_2$-5-(HC≡C-4-C$_6$H$_4$C≡C)C$_6$H$_3$ (**21**)	330 [9.9]	1700 ± 500	0 ± 0	1700 ± 500	This work
1,3,5-{3,5-(*trans*-[(dppe)$_2$(PhC≡C)RuC≡C])$_2$C$_6$H$_3$C≡CC$_6$H$_4$-4-C≡C}$_3$C$_6$H$_3$ (**23**)	339 [34.2]	-1600 ± 2400	0 ± 0	1600 ± 2400	This work

[a] In thf.

Table 5.8. Results of Z-scan experiments at 660 nm[a]

Compound	λ_{max} (nm) [ε (10^4 M^{-1} cm^{-1})]	γ_{real} (10^{-36} esu)	γ_{imag} (10^{-36} esu)	$\lvert\gamma\rvert$ (10^{-36} esu)
1,3-{*trans*-[(dppe)$_2$ClRuC≡C]}$_2$-5-HC≡CC_6H_3 (**18**)	334 [3.8]	-300 ± 150	180 ± 50	350 ± 180
1,3-{*trans*-[(dppe)$_2$(PhC≡C)RuC≡C]}$_2$-5-HC≡CC_6H_3 (**19**)	335 [8.0]	-200 ± 500	0 ± 30	200 ± 500
1,3-{*trans*-[(dppe)$_2$(PhC≡C)RuC≡C]}$_2$-5-(Me_3SiC≡C-4-C_6H_4C≡C)C_6H_3 (**20**)	335 [9.5]	-910 ± 700	330 ± 60	970 ± 680
1,3-{*trans*-[(dppe)$_2$(PhC≡C)RuC≡C]}$_2$-5-(HC≡C-4-C_6H_4C≡C)C_6H_3 (**21**)	330 [9.9]	-250 ± 400	250 ± 50	350 ± 320
{3,5-(*trans*-[(dppe)$_2$(PhC≡C)RuC≡C])$_2$$C_6H_3$C≡C}$_2$ (**22**)	335 [14.1]	-400 ± 600	160 ± 60	430 ± 580
		200 ± 600	120 ± 100	460 ± 350
1,3,5-{3,5-(*trans*-[(dppe)$_2$(PhC≡C)RuC≡C])$_2$$C_6H_3$C≡C$C_6H_4$-4-C≡C}$_3$$C_6H_3$ (**23**)	339 [34.2]	-3100 ± 600	2000 ± 400	3690 ± 720

[a] In thf.

Table 5.9. One and two-photon absorption cross-sections for selected complexes.

Compound	ε (10^4 M^{-1} cm^{-1})	σ [a] (10^{-17} cm^2)	σ / MWT (10^{-20} cm^2 mole g^{-1})	σ_2 (10^{-50} cm^4 s)	σ_2 / MWT (10^{-51} cm^4 s mole g^{-1})	Ref
1,3,5-(*trans*-[(dppe)$_2$ClRu{(*E*)-4-C≡CC_6H_4CH=CH}])$_3C_6H_3$ (**16**)	8.7	14.5	4.4	1000	3.1	This work
1,3,5-(*trans*-[(dppe)$_2$(PhC≡C)Ru{(*E*)-4-C≡CC_6H_4CH=CH}])$_3C_6H_3$ (**17**)	13.0	21.6	6.3	2050	5.9	This work
1,3,5-*trans*-[(dppe)$_2$(PhC≡C)Ru(4-C≡CC_6H_4C≡C)]$_3C_6H_3$	11.6	19.3	5.5	700	2.0	29
1,3-{*trans*-[(dppe)$_2$ClRuC≡C]}$_2$-5-HC≡CC_6H_3 (**18**)	3.8	6.3	3.1	--	--	This work
1,3-{*trans*-[(dppe)$_2$(PhC≡C)RuC≡C]}$_2$-5-HC≡CC_6H_3 (**19**)	8.0	13.3	6.2	--	--	This work
1,3-{*trans*-[(dppe)$_2$(PhC≡C)RuC≡C]}$_2$-5-(Me_3SiC≡C-4-C_6H_4C≡C)C_6H_3 (**20**)	9.5	15.8	6.8	--	--	This work
1,3-{*trans*-[(dppe)$_2$(PhC≡C)RuC≡C]}$_2$-5-(HC≡C-4-C_6H_4C≡C)C_6H_3 (**21**)	9.9	16.5	7.3	--	--	This work
{3,5-(*trans*-[(dppe)$_2$(PhC≡C)RuC≡C])$_2C_6H_3$C≡C}$_2$ (**22**)	14.1	23.5	5.5	--	--	This work
1,3,5-{3,5-(*trans*-[(dppe)$_2$(PhC≡C)RuC≡C])$_2C_6H_3$C≡CC_6H_4-4-C≡C}$_3C_6H_3$ (**23**)	34.2	57.0	8.4	480	0.7	This work
1,3,5-{3,5-(*trans*-[C≡C-4-C_6H_4C≡CRu(C≡CPh)(dppe)$_2$])$_2C_6H_3$[*trans*-C≡CRuC≡CC_6H_4-4-C≡C(dppe)$_2$]}$_3C_6H_3$	42.1	70	6.9	4800	4.7	29

[a] σ = ε x (1/6 x 10^{-20} cm^2)

centre.

The cubic nonlinearities of complexes **18** - **23** were measured at both 800 and 660 nm, the latter being of interest because the second-harmonic corresponding to 660 nm (330 nm) is essentially coincident with λ_{max} for these complexes, and hence two-photon effects may be expected.

The importance of long, linear π-conjugation upon third-order properties has been demonstrated previously;[42] the significant enhancement in γ_{real} upon progressing from **22** to **23** can be attributed to the large extended π-delocalized framework. The similarities in γ_{imag} between the two measurement wavelengths for **18** - **22** suggests that (suprisingly) there is minimal two-photon enhancement for these complexes and that their cubic nonlinearities are low. Complex **23**, however, exhibits no γ_{imag} component at 800 nm, which suggests that the large γ_{imag} value at 660 nm has a significant TPA contribution.

The one-photon absorption cross-sections σ (which are simply the extinction coefficients ε expressed in terms of area) have the ordering of **18** < **19** < **20** ≈ **21** < **23** and **16** < **17**. Thus, the most important factor affecting σ/MWT is the extent of π-delocalized, including through the ruthenium centre, mono-acetylides having smaller values than the corresponding bis-acetylides. Replacing C≡CPh with the extended ligand 4-C≡CC_6H_4C≡CPh should lead to a significant increase in ε and hence σ, but this has not been pursued in the current studies.

The two-photon absorption coefficient σ_2 was too small to be calculated for **18** – **21**, calculated σ_2 and σ_2/MWT following the ordering of **17** > **16** >> **23**. Comparison of σ_2/MWT values in Table 5.9. shows that, despite the large σ_2 value for 1,3,5-{3,5-(*trans*-[C≡C-4-C_6H_4C≡CRu(C≡CPh)(dppe)$_2$])$_2C_6H_3$[*trans*-C≡CRuC≡CC_6H_4-4-C≡C(dppe)$_2$]}$_3C_6H_3$, the smaller complex **17** is more efficient, suggesting that there is

an optimum ratio of conjugation length to metal centre. Comparison of σ_2 values also suggests that (*E*)-ene groups are more efficient than yne linkages. 1,3,5-{3,5-(*trans*-[C≡C-4-C_6H_4C≡CRu(C≡CPh)(dppe)$_2$])$_2C_6H_3$[*trans*-C≡CRuC≡CC_6H_4-4-C≡C(dppe)$_2$]}$_3C_6H_3$ has greater linear π-conjugation through the ruthenium centre than **23** but similar σ/MWT, which suggests that replacing C≡CPh with 4-C≡CC_6H_4C≡CPh in the present series of complexes should produce a complex with a significant σ_2/MWT value.

5.6. Conclusions

The complexes (*E*)-4-XC≡CC$_6$H$_4$CH=CHPh [X = SiMe$_3$ (**1**), H (**2**)], 1,3,5-{(*E*)-4-XC$_6$H$_4$CH=CH}$_3$C$_6$H$_3$ [X = I (**3**), C≡CSiMe$_3$ (**4**), C≡CH (**5**)], [Au{(*E*)-4-C≡CC$_6$H$_4$CH=CHPh}(L)] [L = PPh$_3$ (**6**), PMe$_3$ (**7**)], [Au(4-C≡CC$_6$H$_4$C≡CPh)(L)] [L = PPh$_3$ (**8**), PMe$_3$ (**9**)], 1,3,5-[(Ph$_3$P)Au{(*E*)-4-C≡CC$_6$H$_4$CH=CH}]$_3$C$_6$H$_3$ (**10**), *trans*-[Ru{(*E*)-4-C=CHC$_6$H$_4$CH=CHPh}Cl(dppm)$_2$]PF$_6$ (**11**), *trans*-[Ru{(*E*)-4-C≡CC$_6$H$_4$CH=CHPh}Cl(L$_2$)$_2$] [L = dppm (**12**), dppe (**13**)], [1,3,5-(*trans*-[(dppm)$_2$ClRu{(*E*)-4-C=CHC$_6$H$_4$CH=CH}])$_3$C$_6$H$_3$(PF$_6$)$_3$] (**14**), 1,3,5-(*trans*-[(L$_2$)$_2$ClRu{(*E*)-4-C≡CC$_6$H$_4$CH=CH}])$_3$C$_6$H$_3$ [L = dppm (**15**), dppe (**16**)], 1,3,5-*trans*-[(dppe)$_2$(PhC≡C)Ru{(*E*)-4-C≡CC$_6$H$_4$CH=CH}])$_3$C$_6$H$_3$ (**17**), 1,3-{*trans*-[(dppe)$_2$XRuC≡C]}$_2$-5-HC≡CC$_6$H$_3$ [X = Cl (**18**), C≡CPh (**19**)], 1,3-{*trans*-[(dppe)$_2$(PhC≡C)RuC≡C]}$_2$-5-(XC≡C-4-C$_6$H$_4$C≡C)C$_6$H$_3$ [X = SiMe$_3$ (**20**), H (**21**)], (3,5-{*trans*-[(dppe)$_2$(PhC≡C)RuC≡C]}$_2$C$_6$H$_3$C≡C)$_2$ (**22**), and 1,3,5-(3,5-{*trans*-[(dppe)$_2$(PhC≡C)RuC≡C]}$_2$C$_6$H$_3$C≡CC$_6$H$_4$-4-C≡C)$_3$C$_6$H$_3$ (**23**) have been prepared and their electrochemical (Ru complexes) and NLO properties assessed. The ruthenium complexes **11** – **17** display reversible or nonreversible processes attributable to Ru-centred oxidation, at potentials similar to those of previously investigated monoruthenium alkynyl or vinylidene complexes. Complexes **18** – **23** have two reversible oxidations assigned to $Ru^{II/III}$ processes at ruthenium atoms separated by 1,3-diethynylbenzene units, with comproportionation constants indicative of weakly-interacting Robin and Day Class II behaviour. Measured cubic molecular hyperpolarizabilities at 800 nm values for the organic compounds and gold complexes are low. The cubic nonlinearities for the octopolar ruthenium examples are significantly larger than their linear analogues, with increased π-conjugation having a positive effect upon $|\gamma|$. Replacement of yne linkages with (*E*)-ene linkages also leads to a significant enhancement of the cubic nonlinearity. The organometallic dendrons **18** – **21** were

synthesized via a novel, sterically-controlled methodology, affording access to the nanometre-sized π-delocalized quadrupolar (**22**) and octopolar complexes (**23**). Further lengthening of the π-delocalized framework within these complexes should lead to considerably enhanced cubic nonlinearities.

5.7. Experimental

5.7.1 General Conditions, Reagents and Instruments

General Conditions

All reactions were performed under a nitrogen atmosphere with the use of standard Schlenk techniques unless otherwise stated. Dichloromethane and triethylamine were dried by distilling over calcium hydride, diethyl ether and tetrahydrofuran were dried by distilling over sodium / benzophenone, and other solvents were used as received. "Petroleum spirit" refers to a fraction of petroleum ether of boiling range 60-80 °C. Chromatography was on silica gel (230-400 mesh ASTM) or basic ungraded alumina.

Reagents

The following reagents were prepared by the literature procedures: *cis*-$[RuCl_2(dppm)_2]$ and *cis*-$[RuCl_2(dppe)_2]$,[43] 4-$IC_6H_4C{\equiv}CSiMe_3$,[44] 1,3,5-$(HC{\equiv}C)_3C_6H_3$,[45] (*E*)-4-$IC_6H_4CH{=}CHPh$,[33] 4-$HC{\equiv}CC_6H_4C{\equiv}CPh$,[46] (*E*)-$HC{\equiv}CC_6H_4CH{=}CHPh$ (**2**),[34] $[AuCl(PPh_3)]$,[47] $[AuCl(PMe_3)]$,[39] 1,3,5-$C_6H_3\{CH_2P(O)(OEt)_2\}_3$.[48] NH_4PF_6 (Aldrich), NaOMe (Aldrich), $Me_3SiC{\equiv}CH$ (Aldrich), $PhC{\equiv}CH$ (Aldrich), NBu^n_4F (Aldrich), $[PdCl_2(PPh_3)_2]$ (PMO), CuI (Aldrich), and 4-IC_6H_4CHO (Karl Industries) were used as received. $[Pd(PPh_3)_4]$ was a gift from Dr B.L. Flynn.

Instruments

EI (electron impact) mass spectra [both unit resolution and high resolution (HR)] were recorded using a VG Autospec instrument (70 eV electron energy, 8 kV accelerating potential) and secondary ion mass spectra (SI MS) were recorded using a VG ZAB 2SEQ instrument (30 kV Cs^+ ions, current 1 mA, accelerating potential 8 kV, 3-nitrobenzyl alcohol matrix) at the Research School of Chemistry, Australian National

University; peaks are reported as *m/z* (assignment, relative intensity). Microanalyses were carried out at the Research School of Chemistry, Australian National University. Infrared spectra were recorded either as 1% KBr discs or dichloromethane solutions using a Perkin-Elmer System 2000 FT-IR. ^{1}H- and ^{31}P-NMR spectra were recorded using a Varian Gemini-300 FT NMR spectrometer and are referenced to residual chloroform (7.24 ppm) or external 85% H_3PO_4 (0.0 ppm), respectively. The assignments follow the numbering schemes shown in Figures 5.4. and 5.5. UV-Vis spectra of solutions were recorded in tetrahydrofuran in 1 cm quartz cells using a Cary 5 spectrophotometer. Electrochemical measurements were recorded using a MacLab 400 interface and MacLab potentiostat from ADInstruments. The supporting electrolyte was 0.1 M $(NBu^n_4)PF_6$ in distilled, deoxygenated CH_2Cl_2. Solutions containing *ca* 1 x 10^{-3} M complex were maintained under argon. Measurements were carried out at room temperature using platinum disc working-, Pt wire auxiliary- and Ag/AgCl reference-electrodes, such that the ferrocene/ferrocenium redox couple was located at 0.56 V (peak separation around 0.09 V). Scan rates were typically 100 mV s^{-1}.

5.7.2. Synthesis of organic precursors

5.7.2.1. (E)-4-$Me_3SiC{\equiv}CC_6H_4CH{=}CHPh$ (1)

(*E*)-4-$IC_6H_4CH{=}CHPh$ (250 mg, 0.82 mmol), $Me_3SiC{\equiv}CH$ (96 mg, 0.98 mmol), $[PdCl_2(PPh_3)_2]$ (10 mg) and CuI (4 mg) were stirred in triethylamine (40 mL) for 2 h at 40 °C. The solution was filtered through a silica plug and the solvent volume reduced under reduced pressure to afford the pale white product (185 mg, 82 %). Anal. Calcd for $C_{19}H_{20}Si$: C 82.55, H 7.29 %. Found: C 82.20, H 7.28 %. IR: (CH_2Cl_2) ν(C≡C) 2154 cm^{-1}. UV-Vis: λ (thf) 346 nm, ε 16 800 M^{-1} cm^{-1}, 330 nm, ε 25 200 M^{-1} cm^{-1}. ^{1}H NMR: (δ, 300 MHz, $CDCl_3$); 0.24 (s, 9H, Me), 7.04 (d, 1H, J_{HH} = 16 Hz, H_7), 7.11 (d, 1H, J_{HH} = 16 Hz, H_8), 7.15 – 7.55 (m, 9H, Ph). EI MS; *m/z* (fragment, relative intensity): 276

([M]$^+$, 50), 261 ([M - Me]$^+$, 60), 179 ([M – Me_3Si]$^+$, 100). HR MS calcd for $C_{19}H_{20}Si$ *m/e* 276.1335, found 276.1334.

5.7.2.2. 1,3,5-{(E)-4-IC_6H_4CH=CH}$_3C_6H_3$·H_2O (3)

4-IC_6H_4CHO (145 mg, 0.63 mmol), 1,3,5-C_6H_3{$CH_2P(O)(OEt)_2$}$_3$ (100 mg, 0.19 mmol) and *t*-BuOK (67 mg, 0.60 mmol) were stirred in thf (30 mL) overnight. HCl (1.0 mL, 0.5 M) was then added and the solution filtered through an alumina plug. The solvent was reduced in volume under vacuum to afford the white product (104 mg, 72 %). Anal. Calcd for $C_{30}H_{23}I_3O$: C 46.18, H 2.97 %. Found: C 45.96, H 3.08 %. UV-Vis: λ (thf) 340 nm, ε 60 800 M^{-1} cm^{-1}, 326 nm, ε 82 400 M^{-1} cm^{-1}. ^{1}H NMR: (δ, 300 MHz, $CDCl_3$); 1.55 (s, 2H, H_2O), 7.06 (d, 3H, J_{HH} = 16 Hz, H_8), 7.13 (d, 3H, J_{HH} = 16 Hz, H_7), 7.26 (d, 6H, J_{HH} = 9 Hz, H_4), 7.52 (s, 3H, H_{10}), 7.68 (d, 6H, J_{HH} = 9 Hz, H_5). EI MS; *m/z* (fragment, relative intensity): 762 ([M]$^+$, 100), 636 ([M - I]$^+$, 30), 506 ([M – 2I]$^+$, 10). HR MS calcd for $C_{30}H_{21}I_3$ *m/e* 761.8771, found 761.8778.

5.7.2.3. 1,3,5-{(E)-4-Me_3SiC≡CC_6H_4CH=CH}$_3C_6H_3$ (4)

1,3,5-{(*E*)-4-IC_6H_4CH=CH}$_3C_6H_3$ (**3**) (200 mg, 0.26 mmol), Me_3SiC≡CH (103 mg, 1.05 mmol), [$PdCl_2(PPh_3)_2$] (10 mg) and CuI (4 mg) were stirred in triethylamine (40 mL) for 2 h at 40 °C. The solution was filtered through a silica plug and the solvent reduced in volume under reduced pressure to afford the pale white product (145 mg, 82 %). Anal. Calcd for $C_{45}H_{48}Si_3$: C 80.30, H 7.19 %. Found: C 79.33, H 7.24 %. IR: (CH_2Cl_2) ν(C≡C) 2154 cm^{-1}. UV-Vis: λ (thf) 354 nm, ε 112 200 M^{-1} cm^{-1}, 339 nm, ε 136 500 M^{-1} cm^{-1}. ^{1}H NMR: (δ, 300 MHz, $CDCl_3$); 0.24 (s, 27H, Me), 7.15 (s, 6H, H_7, H_8), 7.49 (s, 12H, H_4, H_5), 7.55 (s, 3H, H_{10}). EI MS; *m/z* (fragment, relative intensity): 672 ([M]$^+$, 35), 576 ([M – C≡$CSiMe_3$]$^+$, 20). HR MS calcd for $C_{45}H_{48}Si_3$ *m/e* 672.3057, found 672.3064.

5.7.2.4. 1,3,5-{(E)-4-HC≡*CC_6H_4CH=CH}$_3C_6H_3$·H_2O (5)*

1,3,5-{(*E*)-4-$Me_3SiC{\equiv}CC_6H_4CH{=}CH\}_3C_6H_3$ (**4**) (250 mg, 0.37 mmol), and NBu^n_4F (1.0 mL, 1 M in thf) were stirred in dichloromethane (15 mL) for 1 h. The solvent was removed under reduced pressure, the material was redissolved in petroleum spirit and the solution was filtered through a silica plug eluting with petroleum spirit. The solvent was reduced in volume under reduced pressure to afford the white product (137 mg, 81 %). Anal. Calcd for $C_{36}H_{26}O$: C 91.11, H 5.52 %. Found: C 92.02, H 5.52 %. IR: (CH_2Cl_2) ν(C≡C) 2108 cm^{-1}. UV-Vis: λ (thf) 348 nm, ε 90 000 M^{-1} cm^{-1}, 332 nm, ε 116 800 M^{-1} cm^{-1}. ^1H NMR: (δ, 300 MHz, $CDCl_3$); 1.55 (s, 2H, H_2O), 3.13 (s, 3H, H_1), 7.15 (s, 6H, H_7, H_8), 7.49 (s, 12H, H_4, H_5), 7.55 (s, 3H, H_{10}). EI MS; *m/z* (fragment, relative intensity): 456 ($[M]^+$, 35). HR MS calcd for $C_{36}H_{24}$ *m/e* 456.1879, found 456.1878.

5.7.3. Synthesis of metal complexes

5.7.3.1. [Au{(E)-4-C≡CC$_6$H$_4$CH=CHPh}(PPh$_3$)] (6)

[$AuCl(PPh_3)$] (100 mg, 0.20 mmol) and (*E*)-4-HC≡CC_6H_4CH=CHPh (**2**) (45 mg, 0.22 mmol) were stirred together in a solution of sodium methoxide in methanol (20 mL, 0.1 M) for 18 h. Dichloromethane (20 mL) was added and the solution passed through a silica plug. The solvent was removed under reduced pressure and the material triturated with petroleum spirit. The solid was collected on a sintered-glass funnel, and washed with more petroleum spirit to yield a pale yellow material (98 mg, 73 %). Anal. Calcd for $C_{34}H_{26}AuP$: C 61.64, H 3.96 %. Found: C 61.61, H 4.33 %. IR: (CH_2Cl_2) ν(C≡C) 2111 cm^{-1}. UV-Vis: λ (thf) 338 nm, ε 16 500 M^{-1} cm^{-1}, 324 nm, ε 25 300 M^{-1} cm^{-1}. ^1H NMR: (δ, 300 MHz, $CDCl_3$); 7.06 (s, 2H, H_7, H_8), 7.30 - 7.60 (m, 24H, Ph). ^{31}P NMR: (δ, 121 MHz, $CDCl_3$); 42.8. SI MS; *m/z* (fragment, relative intensity): 721 ($[Au(PPh_3)_2]^+$, 20), 459 ($[Au(PPh_3)]^+$, 100).

5.7.3.2. [Au{(E)-4-C≡CC$_6$H$_4$CH=CHPh}(PMe$_3$)] (7)

[AuCl(PMe_3)] (100 mg, 0.32 mmol) and (*E*)-4-HC≡CC_6H_4CH=CHPh (**2**) (73 mg, 0.36 mmol) were stirred together in a solution of sodium methoxide in methanol (20 mL, 1 M) for 18 h. Dichloromethane (10 mL) was added and the solution passed through a silica plug. The solvent was removed under reduced pressure and the material triturated with petroleum spirit. The solid was collected on a sintered-glass funnel, and washed with more petroleum spirit to yield the off-white material (90 mg, 58 %). Anal. Calcd for $C_{19}H_{20}AuP$: C 47.91, H 4.23 %. Found: C 48.53, H 4.63 %. IR: (CH_2Cl_2) ν(C≡C) 2108 cm^{-1}. UV-Vis: λ (thf) 339 nm, ε 18 800 M^{-1} cm^{-1}, 323 nm, ε 28 600 M^{-1} cm^{-1}. ^{1}H NMR: (δ, 300 MHz, $CDCl_3$); 1.51 (d, 9H, J_{HP} = 11 Hz, Me), 7.04 (s, 2H, H_7, H_8), 7.20 - 7.55 (m, 9H, Ph). ^{31}P NMR: (δ, 121 MHz, $CDCl_3$); 1.7. SI MS; *m/z* (fragment, relative intensity): 533 ($[Au_2(PMe_3)_3]^+$, 15), 349 ($[Au(PMe_3)_2]^+$, 95), 273 ($[Au(PMe_3)]^+$, 100).

*5.7.3.3. [Au(4-C≡CC_6H_4C≡CPh)(PPh_3)] (**8**)*

[AuCl(PPh_3)] (100 mg, 0.20 mmol) and 4-HC≡CC_6H_4C≡CPh (45 mg, 0.22 mmol) were stirred in a solution of sodium methoxide in methanol (15 mL, 0.1 M) for 16 h. Dichloromethane (15 mL) was added and the solution passed through a silica plug. The solvent was removed under reduced pressure to give the yellow product (113 mg, 85 %). Anal. Calcd for $C_{34}H_{24}AuP$: C 61.83, H 3.66 %. Found: C 61.22, H 4.59 %. IR: (CH_2Cl_2) ν(C≡C) 2112 cm^{-1}. UV-Vis: λ (thf) 336 nm, ε 65 000 M^{-1} cm^{-1}. ^{1}H NMR: (δ, 300 MHz, $CDCl_3$); 7.25 - 7.60 (m, 24H, Ph). ^{31}P NMR: (δ, 121 MHz, $CDCl_3$); 42.7. SI MS; *m/z* (fragment, relative intensity): 721 ($[Au(PPh_3)_2]^+$, 40), 660 ($[M]^+$, 5), 459 ($[Au(PPh_3)]^+$, 100).

*5.7.3.4. [Au(4-C≡CC_6H_4C≡CPh)(PMe_3)] (**9**)*

[AuCl(PMe_3)] (100 mg, 0.32 mmol) and 4-HC≡CC_6H_4C≡CPh (72 mg, 0.36 mmol) were stirred in a solution of sodium methoxide in methanol (20 mL, 0.1 M)

for 16 h. Dichloromethane (10 mL) was added and the solution passed through a silica plug. The solvent was removed under reduced pressure to give the yellow product (105 mg, 68 %). Anal. Calcd for $C_{19}H_{18}AuP$: C 48.12, H 3.83 %. Found: C 48.52, H 4.16 %. IR: (CH_2Cl_2) ν(C≡C) 2112 cm^{-1}. UV-Vis: λ (thf) 335 nm, ε 55 000 M^{-1} cm^{-1}. ^1H NMR: (δ, 300 MHz, $CDCl_3$); 1.56 (d, 9H, J_{HP} = 15 Hz, Me), 7.25 - 7.55 (m, 9H, Ph). ^{31}P NMR: (δ, 121 MHz, $CDCl_3$); 1.7. SI MS; *m/z* (fragment, relative intensity): 474 ($[M]^+$, 10), 349 ($[Au(PMe_3)_2]^+$, 75), 273 ($[Au(PMe_3)]^+$, 100).

*5.7.3.5. 1,3,5-[(Ph$_3$P)Au{(E)-4-C≡CC$_6$H$_4$CH=CH}]$_3$C$_6$H$_3$ (**10**)*

[AuCl(PPh_3)] (162 mg, 0.33 mmol) and 1,3,5-{(*E*)-4-HC≡CC_6H_4CH=CH}$_3C_6H_3$ (**5**) (50 mg, 0.11 mmol) were stirred in a solution of sodium methoxide in methanol (0.1 M, 15 mL) for 16 h. Dichloromethane (25 mL) was added, the solution was passed through a silica plug and the solvent removed under vacuum to yield the solid white product (158 mg, 79 %). Anal. Calcd for $C_{90}H_{66}Au_3P_3$: C 59.03, H 3.63 %. Found: C 58.83, H 4.04 %. IR: (CH_2Cl_2) ν(C≡C) 2108 cm^{-1}. UV-Vis: λ (thf) 366 nm, ε 96 100 M^{-1} cm^{-1}, 350 nm, ε 131 700 M^{-1} cm^{-1}. ^1H NMR: (δ, 300 MHz, $CDCl_3$); 7.11 (s, 6H, H_7, H_8), 7.40 - 7.60 (m, 60H, Ph). ^{31}P NMR: (δ, 121 MHz, $CDCl_3$); 42.8. SI MS; *m/z* (fragment, relative intensity): 1834 ($[M + 3H]^+$, 15), 1375 ($[M - Au(PPh_3) + 3H]^+$, 60), 722 ($[Au(PPh_3)_2 + H]^+$, 100).

*5.7.3.6. trans-[Ru{(E)-4-C=CHC$_6$H$_4$CH=CHPh}Cl(dppm)$_2$]PF$_6$ (**11**)*

cis-[$RuCl_2$(dppm)$_2$] (200 mg, 0.21 mmol), (*E*)-4-HC≡CC_6H_4CH=CHPh (**3**) (52 mg, 0.26 mmol) and NH_4PF_6 (69 mg, 0.42 mmol) were stirred together in dichloromethane (25 mL) at room temperature for 24 h. Petroleum spirit (50 mL) was added and the resulting precipitate was collected and washed with diethyl ether (50 mL) to afford the pale yellow product (208 mg, 78 %). Anal. Calcd for $C_{66}H_{56}ClF_6P_5Ru$: C 63.19, H 4.50 %. Found: C 62.32, H 4.73 %. IR: (KBr) ν(PF) 837 cm^{-1}. UV-Vis: λ (thf)

360 nm, ε 14 600 M^{-1} cm^{-1}. ^1H NMR: (δ, 300 MHz, $CDCl_3$); 3.05 (m, 1H, =CH), 5.10 (m, 2H, PCH_2P), 5.32 (m, 2H, PCH_2P), 5.50 (d, J_{HH} = 8 Hz, 2H, H_4), 6.88 (d, J_{HH} = 8 Hz, 2H, H_5), 7.10 - 7.60 (m, 47H, Ph + H_7 + H_8). ^{31}P NMR: (δ, 121 MHz, $CDCl_3$); -15.6. SI MS; *m/z* (fragment, relative intensity): 1109 ($[M - PF_6]^+$, 100), 905 ($[RuCl(dppm)_2]^+$, 40), 869 ($[Ru(dppm)_2 - H]^+$, 100).

5.7.3.7. trans-[Ru{(E)-4-C≡CC$_6$H$_4$CH=CHPh}Cl(dppm)$_2$]·0.5CH$_2$Cl$_2$ (12)

trans-[Ru{(*E*)-4-C=CHC$_6$H$_4$CH=CHPh}Cl(dppm)$_2$]PF_6 (**11**) (150 mg, 0.12 mmol) was stirred in dichloromethane (20 mL) with triethylamine (1.0 mL) at room temperature for 2 h. The solution was filtered through an alumina plug and the solvent reduced in volume under vacuum to afford the yellow product (109 mg, 82 %). Anal. Calcd for $C_{66.5}H_{56}Cl_2P_4Ru$: C 69.39, H 4.90 %. Found: C 69.35, H 5.35 %. IR: (CH_2Cl_2) ν(C≡C) 2073 cm^{-1}. UV-Vis: λ (thf) 397 nm, ε 23 400 M^{-1} cm^{-1}. ^1H NMR: (δ, 300 MHz, $CDCl_3$); 4.89 (m, 4H, PCH_2P), 5.27 (s, 1H, CH_2Cl_2), 6.21 (d, J_{HH} = 8 Hz, 2H, H_4), 7.10 - 7.60 (m, 49H, Ph + H_5 + H_7 + H_8). ^{31}P NMR: (δ, 121 MHz, $CDCl_3$); -6.0. SI MS; *m/z* (fragment, relative intensity): 1109 ($[M]^+$, 20), 1073 ($[M - HCl]^+$, 20), 905 ($[RuCl(dppm)_2]^+$, 90), 869 ($[Ru(dppm)_2 - H]^+$, 100).

5.7.3.8. trans-[Ru{(E)-4-C≡CC$_6$H$_4$CH=CHPh}Cl(dppe)$_2$] (13)

cis-[$RuCl_2$(dppe)$_2$] (150 mg, 0.15 mmol) and (*E*)-4-HC≡CC$_6$H$_4$CH=CHPh (**3**) (38 mg, 0.19 mmol) were stirred together in dichloromethane (25 mL) at room temperature for 20 min. NH_4PF_6 (50 mg, 0.3 mmol) was then added, and the stirring continued for another 24 h. The solvent was removed under reduced pressure and the excess acetylene removed by triturating with diethyl ether (3 x 30 mL). Dichloromethane (15 mL) and triethylamine (1 mL) were added and the solution stirred for 5 min. Petroleum spirit (40 mL) was added, and the resulting precipitate was collected to afford the yellow product (125 mg, 71 %). Anal. Calcd for $C_{68}H_{59}ClP_4Ru$:

C 71.86, H 5.23 %. Found: C 71.31, H 5.63 %. IR: (CH_2Cl_2) ν(C≡C) 2066 cm^{-1}. UV-Vis: λ (thf) 404 nm, ε 28 600 M^{-1} cm^{-1}. ^1H NMR: (δ, 300 MHz, $CDCl_3$); 2.67 (m, 8H, PCH_2CH_2P), 7.10 - 7.60 (m, 51H, Ph + H_7 + H_8). ^{31}P NMR: (δ, 121 MHz, $CDCl_3$); 50.1. SI MS; *m/z* (fragment, relative intensity): 1136 ($[M]^+$, 40), 1101 ($[M - Cl]^+$, 20), 957 ($[M - C_6H_4CH{=}CHPh]^+$, 100), 897 ($[Ru(dppe)_2 - H]^+$, 100).

*5.7.3.9. [1,3,5-(trans-[(dppm)$_2$ClRu{(E)-4-C=CHC$_6$H$_4$CH=CH}])$_3$C$_6$H$_3$](PF$_6$)$_3$ (**14**)*

cis-$[RuCl_2(dppm)_2]$ (185 mg, 0.20 mmol), 1,3,5-{(*E*)-4-$HC{\equiv}CC_6H_4CH{=}CH\}_3C_6H_3$ (**5**) (30 mg, 0.068 mmol) and NH_4PF_6 (72 mg, 0.44 mmol) were added to dichloromethane (25 mL), and stirred at room temperature for 45 h. Petroleum spirit (50 mL) was added, and the resulting precipitate was collected and washed with diethyl ether (50 mL) to afford the pale red product (223 mg, 94 %). Anal. Calcd for $C_{186}H_{156}Cl_3F_{18}P_{15}Ru_3$: C 61.93, H 4.36 %. Found: C 61.45, H 4.66 %. IR: (KBr) ν(PF) 838 cm^{-1}. UV-Vis: λ (thf) 396 nm, ε 19 700 M^{-1} cm^{-1}. ^1H NMR: (δ, 300 MHz, $CDCl_3$); 3.07 (m, 3H, =CH), 5.10 (m, 6H, PCH_2P), 5.26 (m, 6H, PCH_2P), 5.51 (d, 6H, J_{HH} = 8 Hz, H_4), 6.98 (d, 6H, J_{HH} = 8 Hz, H_5), 7.10 - 7.60 (m, 129H, Ph + H_7 + H_8). ^{31}P NMR: (δ, 121 MHz, $CDCl_3$); -15.8. SI MS; *m/z* (fragment, relative intensity): 904 ($[RuCl(dppm)_2 - 2H]^+$, 40), 868 ($[Ru(dppm)_2 - H]^+$, 100).

*5.7.3.10. 1,3,5-(trans-[(dppm)$_2$ClRu{(E)-4-C≡CC$_6$H$_4$CH=CH}])$_3$C$_6$H$_3$ (**15**)*

[1,3,5-(*trans*-[$(dppm)_2ClRu\{(E)$-4-$C{=}CHC_6H_4CH{=}CH\}$])$_3C_6H_3$](PF$_6$)$_3$ (**14**) (154 mg, 0.043 mmol) was stirred in dichloromethane (25 mL) with triethylamine (1 mL) at room temperature for 15 min. The solution was filtered through an alumina plug and the solvent reduced in volume under vacuum to afford the yellow product (110 mg, 81 %). Anal. Calcd for $C_{186}H_{153}Cl_3P_{12}Ru_3$: C 70.48, H 4.87 %. Found: C 69.46, H 5.57 %. IR: (CH_2Cl_2) ν(C≡C) 2073 cm^{-1}. UV-Vis: λ (thf) 415 nm, ε 48 500 M^{-1} cm^{-1}. ^1H NMR: (δ,

300 MHz, $CDCl_3$); 4.91 (m, 12H, PCH_2P), 6.07 (d, J_{HH} = 8 Hz, 6H, H_4), 6.90 - 7.60 (m, 135H, Ph + H_5 + H_7 + H_8). ^{31}P NMR: (δ, 121 MHz, $CDCl_3$); -5.9. SI MS; *m/z* (fragment, relative intensity): 3168 ($[M - H]^+$, 15), 2246 ($[M - RuCl(dppm)_2]^+$, 5), 904 ($[RuCl(dppm)_2 - H]^+$, 40), 869 ($[Ru(dppm)_2]^+$, 100).

5.7.3.11. 1,3,5-(trans-[(dppe)$_2$ClRu{(E)-4-C≡CC$_6$H$_4$CH=CH}])$_3$C$_6$H$_3$ (16)

cis-$[RuCl_2(dppe)_2]$ (304 mg, 0.31 mmol) and 1,3,5-{(*E*)-4-$HC{\equiv}CC_6H_4CH{=}CH\}_3C_6H_3$ (**5**) (32 mg, 0.070 mmol) were stirred together in dichloromethane (25 mL) at room temperature for 20 min. NH_4PF_6 (112 mg, 0.69 mmol) was then added, and the solution refluxed for 15 h. The solution was then cooled to room temperature and filtered through a sintered-glass funnel. Triethylamine (1.0 mL) was added to the filtrate, the resultant solution was stirred for 5 min, and then the solvent was removed under reduced pressure. The yellow residue was adsorbed onto an alumina column, with any *trans*-$[RuCl_2(dppe)_2]$ being removed by elution with diethyl ether (400 mL). Elution with dichloromethane (400 mL) gave the yellow product (173 mg, 76 %). Anal. Calcd for $C_{192}H_{165}Cl_3P_{12}Ru_3$: C 70.88, H 5.11 %. Found: C 70.60, H 5.15 %. IR: (CH_2Cl_2) ν(C≡C) 2062 cm^{-1}. UV-Vis: λ (thf) 426 nm, ε 87 400 M^{-1} cm^{-1}. ^1H NMR: (δ, 300 MHz, $CDCl_3$); 2.70 (m, 24H, PCH_2CH_2P), 6.66 (d, 6H, J_{HH} = 8 Hz, H_4), 6.90 - 7.60 (m, 135H, Ph + H_5 + H_7 + H_8). ^{31}P NMR: (δ, 121 MHz, $CDCl_3$); 50.1. SI MS; *m/z* (fragment, relative intensity): 3254 ($[M]^+$, 5), 3218 ($[M - HCl]^+$, 4), 897 ($[Ru(dppe)_2 - H]^+$, 100), 499 ($[Ru(dppe) - H]^+$, 100).

5.7.3.12. 1,3,5-(trans-[(dppe)$_2$(PhC≡C)Ru{(E)-4-C≡CC$_6$H$_4$CH=CH}])$_3$C$_6$H$_3$·CH$_2$Cl$_2$ (17)

1,3,5-(*trans*-[$(dppe)_2ClRu\{(E)$-4-$C{\equiv}CC_6H_4CH{=}CH\}])_3C_6H_3$ (**16**) (100 mg, 0.031 mmol), NH_4PF_6 (30 mg, 0.18 mmol), HC≡CPh (31 mg, 0.31 mmol) and triethylamine (1 mL) were stirred in refluxing dichloromethane (25 mL) for 5 h. After

this time the solution was cooled, the solvent removed, and the residue triturated with petroleum spirit (100 mL) to remove excess HC≡CPh. The yellow product was collected by filtration (60 mg, 57 %). Anal. Calcd for $C_{217}H_{182}Cl_2P_{12}Ru_3$: C 73.72, H 5.19 %. Found: C 73.81, H 5.83 %. IR: (CH_2Cl_2) ν(C≡C) 2057 cm^{-1}. UV-Vis: λ (thf) 421 nm, ε 129 700 M^{-1} cm^{-1}. ^1H NMR: (δ, 300 MHz, $CDCl_3$); 2.63 (m, 24H, PCH_2CH_2P), 5.27 (s, 2H, CH_2Cl_2), 6.70 - 7.60 (m, 156H, Ph + H_7 + H_8). ^{31}P NMR: (δ, 121 MHz, $CDCl_3$); 54.3. SI MS; *m/z* (fragment, relative intensity): 3451 ($[M]^+$, 3), 3351 ($[M - C{\equiv}CPh]^+$, 4), 998 ($[(dppe)_2(PhC{\equiv}C)Ru - H]^+$, 100), 897 ($[Ru(dppe)_2 - H]^+$, 100).

*5.7.3.13 1,3-{trans-[(dppe)$_2$ClRuC≡C]}$_2$-5-HC≡CC_6H_3 (**18**)*

NH_4PF_6 (65 mg, 0.40 mmol) and *cis*-$[RuCl_2(dppe)_2]$ (465 mg, 0.48 mmol) were stirred in dichloromethane (25 mL). 1,3,5-$(HC{\equiv}C)_3C_6H_3$ (30 mg, 0.20 mmol) in dichloromethane (5 mL) was added dropwise and the solution was then heated at reflux for 12 h. After this time, the solution was cooled to room temperature, and the red solution was filtered through a sintered glass funnel under nitrogen. Triethylamine (1 mL) was then added, and the solution stirred for 5 min. The solvent was removed under reduced pressure, and the yellow mixture adsorbed onto an alumina column. The by-product *trans*-$[RuCl_2(dppe)_2]$ was removed by eluting with diethyl ether (300 mL) and the product was eluted with dichloromethane (300 mL); reducing the solvent volume of the dichloromethane fraction yielded the pale yellow product (285 mg, 71 %). Anal. Calcd for $C_{116}H_{100}Cl_2P_8Ru_2$: C 69.15, H 5.00 %. Found: C 69.42, H 5.29 %. IR: (CH_2Cl_2) ν(≡CH) 3302 cm^{-1}, ν(C≡C) 2059 cm^{-1}. UV-Vis: λ (thf) 334 nm, ε 38 300 M^{-1} cm^{-1}. ^1H NMR: (δ, 300 MHz, $CDCl_3$); 2.68 (m, 16H, PCH_2CH_2P), 3.01 (s, 1H, H_{15}), 6.41 (m, 2H, H_{12}), 6.55 (m, 1H, H_{11}), 6.80 - 7.70 (m, 80H, Ph). ^{31}P NMR: (δ, 121 MHz, $CDCl_3$); 50.5. SI MS; *m/z* (fragment, relative intensity): 2016 ($[M + H]^+$, 20), 1981 ($[M - Cl]^+$, 15), 1618 ($[M - (dppe)]^+$, 15), 933 ($[RuCl(dppe)_2]^+$, 15), 897 ($[Ru(dppe)_2 - H]^+$, 100).

*5.7.3.14. 1,3-{trans-[(dppe)$_2$(PhC≡C)RuC≡C]}$_2$-5-HC≡CC$_6$H$_3$ (**19**)*

HC≡CPh (422 mg, 4.18 mmol), NH_4PF_6 (100 mg, 0.060 mmol), triethylamine (5 mL) and 1,3-{*trans*-[(dppe)$_2$ClRuC≡C]}$_2$-5-HC≡CC$_6$H$_3$ (**18**) (1.00 g, 0.50 mmol) were stirred in refluxing dichloromethane (40 mL) for 2 h. The solution was filtered through an alumina plug and the solvent was removed under reduced pressure. The residue was triturated with petroleum spirit and the resultant solid was collected, to yield the yellow product (873 mg, 82 %). Anal. Calcd for $C_{132}H_{110}P_8Ru_2$: C 73.87, H 5.17 %. Found: C 74.46, H 5.78 %. IR: (CH_2Cl_2) ν(HC≡) 3309 cm^{-1}, ν(C≡C) 2055 cm^{-1}. UV-Vis: λ (thf) 335 nm, ε 79 700 M^{-1} cm^{-1}. ^{1}H NMR: (δ, 300 MHz, $CDCl_3$); 2.64 (m, 16H, PCH_2CH_2P), 3.02 (s, 1H, H_{15}), 6.41 (m, 2H, H_{12}), 6.55 (m, 1H, H_{11}), 6.80 - 7.70 (m, 90H, Ph). ^{31}P NMR: (δ, 121 MHz, $CDCl_3$); 54.4. SI MS; *m/z* (fragment, relative intensity): 2146 ([M]$^+$, 3), 999 ([(dppe)$_2$(PhC≡C)Ru]$^+$, 98), 897 ([Ru(dppe)$_2$ - H]$^+$, 100).

*5.7.3.15. 1,3-{trans-[(dppe)$_2$(PhC≡C)RuC≡C]}$_2$-5-(Me$_3$SiC≡C-4-C$_6$H$_4$C≡C)C$_6$H$_3$·CH$_2$Cl$_2$ (**20**)*

4-Me$_3$SiC≡CC$_6$H$_4$I (372 mg, 1.24 mmol), 1,3-{*trans*-[(dppe)$_2$(PhC≡C)RuC≡C]}$_2$-5-HC≡CC$_6$H$_3$ (**19**) (275 mg, 0.13 mmol) and [Pd(PPh$_3$)$_4$] (49 mg) were stirred together in a thoroughly deoxygenated mixture of triethylamine / dichloromethane (1:1, 50 mL) for 18 h. The solution was allowed to cool to room temperature, the mixture filtered through an alumina plug and the solvent was removed under reduced pressure. The material was triturated with petroleum spirit and the yellow product was collected by filtration (226 mg, 76 %). Anal. Calcd for $C_{144}H_{124}Cl_2P_8Ru_2Si$: C 71.96, H 5.20 %. Found: C 72.07, H 5.80 %. IR: (CH_2Cl_2) ν(C≡CSiMe$_3$) 2157 cm^{-1}, ν(C≡C) 2056 cm^{-1}. UV-Vis: λ (thf) 335 nm, ε 94 900 M^{-1} cm^{-1}. ^{1}H NMR: (δ, 300 MHz, $CDCl_3$); 0.26 (s, 9H, Me), 2.67 (m, 16H, PCH_2CH_2P), 5.27 (s, 2H, CH_2Cl_2), 6.41 (m, 2H, H_{12}), 6.55 (m, 1H, H_{11}), 6.80 - 7.70 (m, 94H, Ph). ^{31}P NMR: (δ, 121 MHz, $CDCl_3$);

54.4. SI MS; *m/z* (fragment, relative intensity): 2146 ($[M]^+$, 2), 897 ($[Ru(dppe)_2 - H]^+$, 100), 499 ($[Ru(dppe) - H]^+$, 30).

5.7.3.16. 1,3-{trans-[(dppe)$_2$(PhC≡C)RuC≡C]}$_2$-5-(HC≡C-4-C$_6$H$_4$C≡C)C$_6$H$_3$ (21)

1,3-{*trans*-[(dppe)$_2$(PhC≡C)RuC≡C]}$_2$-5-(Me$_3$SiC≡C-4-C$_6$H$_4$C≡C)C$_6$H$_3$ (**20**) (185 mg, 0.080 mmol) and NBu^n_4F (2.0 mL, 1 M in thf) were stirred together in dichloromethane (25 mL) for 2 h. The solution was filtered through an alumina plug and the solvent was reduced in volume to yield the yellow product (151 mg, 84 %). Anal. Calcd for $C_{140}H_{114}P_8Ru_2$: C 74.86, H 5.12 %. Found: C 74.61, H 5.80 %. IR: (CH_2Cl_2) ν(C≡CH) 3303 cm^{-1}, ν(C≡C) 2056 cm^{-1}. UV-Vis: λ (thf) 330 nm, ε 99 400 M^{-1} cm^{-1}. ^1H NMR: (δ, 300 MHz, $CDCl_3$); 2.66 (m, 16H, PCH_2CH_2P), 3.18 (s, 1H, H_{21}), 6.70 (m, 2H, H_{11}), 6.40 (m, 1H, H_{12}), 6.80 - 7.70 (m, 94H, Ph). ^{31}P NMR: (δ, 121 MHz, $CDCl_3$); 54.4. SI MS; *m/z* (fragment, relative intensity): 2247 ($[M + H]^+$, 5), 2145 ($[M - HC≡CC_6H_4]^+$, 10), 999 $[(dppe)_2(PhC≡C)Ru]^+$, 15), 897 ($[Ru(dppe)_2 - H]^+$, 100), 499 ($[Ru(dppe) - H]^+$, 30).

5.7.3.17. (3,5-{trans-[(dppe)$_2$(PhC≡C)RuC≡C]}$_2$C$_6$H$_3$C≡C)$_2$ (22)

$Me_2NCH_2CH_2NMe_2$ (0.10 mL, 0.66 mmol) was added with stirring to a suspension of CuCl (10 mg, 0.058 mmol) in acetone. After 15 min a blue-green solution had formed, which was filtered through a glass frit. The copper catalyst thus prepared was added dropwise with stirring to a solution of 1,3-{*trans*-[(dppe)$_2$(PhC≡C)RuC≡C]}$_2$-5-HC≡CC$_6$H$_3$ (**19**) (100 mg, 0.046 mmol) in acetone (20 mL), and dioxygen was bubbled through the mixture for 2 h. The solvent was removed under reduced pressure, and the residue was dissolved in dichloromethane (50 mL) and washed with water (3 x 50 mL) using a separating funnel. The organic solvent fraction was dried with $MgSO_4$ and passed through an alumina plug. Reducing the solvent volume gave the pale-yellow product (78 mg, 78 %). Anal. Calcd for $C_{246}H_{218}P_{16}Ru_4$: C

73.91, H 5.12 %. Found: C 73.92, H 5.55 %. IR: (CH_2Cl_2) ν(C≡C) 2056 cm^{-1}. UV-Vis: λ (thf) 335 nm, ε 140 600 M^{-1} cm^{-1}. ^1H NMR: (δ, 300 MHz, $CDCl_3$); 2.63 (m, 32H, PCH_2), 6.85 - 7.60 (m, 186H, Ph). ^{31}P NMR: (δ, 121 MHz, $CDCl_3$); 54.4. SI MS; *m/z* (fragment, relative intensity): 2245 ([1,3-{*trans*-[(dppe)$_2$(PhC≡C)RuC≡C]}$_2$-5-C≡CC_6H_3]$^+$, 30), 999 ([(dppe)$_2$(PhC≡C)Ru]$^+$, 20), 897 ([Ru(dppe)$_2$ - H]$^+$, 100).

5.7.3.18. 1,3,5-(3,5-{trans-[(dppe)$_2$(PhC≡C)RuC≡C]}$_2$$C_6H_3$C≡C$C_6H_4$-4-C≡C)$_3$$C_6H_3$ (23)

1,3,5-triiodobenzene (6.8 mg, 0.015 mmol), 1,3-{*trans*-[(dppe)$_2$(PhC≡C)RuC≡C]}$_2$-5-(HC≡C-4-C_6H_4C≡C)C_6H_3 (**21**) (100 mg, 0.045 mmol) and [$Pd(PPh_3)_4$] (25 mg) were stirred together in a thoroughly deoxygenated mixture of triethylamine / dichloromethane (1:1, 50 mL) at reflux for 12 h. The solution was allowed to cool to room temperature, the mixture was filtered through an alumina plug and the solvent was removed under reduced pressure. The residue was extracted into dichloromethane and was adsorbed onto an alumina column. The column was eluted with diethyl ether (200 mL) to remove any unreacted **21**. Dichloromethane (200 mL) was then used to elute the yellow product, which was obtained as a yellow powder by reduction in solvent volume (57 mg, 56 %). Anal. Calcd for $C_{426}H_{342}P_{24}Ru_6$: C 75.12, H 5.06 %. Found: C 74.36, H 5.86 %. IR: (CH_2Cl_2) ν(C≡C) 2057 cm^{-1}. UV-Vis: λ (thf) 339 nm, ε 342 500 M^{-1} cm^{-1}. ^1H NMR: (δ, 300 MHz, $CDCl_3$); 2.65 (m, 48H, PCH_2CH_2P), 6.50 - 7.75 (m, 294H, Ph). ^{31}P NMR: (δ, 121 MHz, $CDCl_3$); 54.2. SI MS; *m/z* (fragment, relative intensity): 2247 ([1,3-{*trans*-[(dppe)$_2$(PhC≡C)RuC≡C]}$_2$-5-(C≡C-4-C_6H_4C≡C)C_6H_3 + H]$^+$, 7), 2145 (1,3-{*trans*-[(dppe)$_2$(PhC≡C)RuC≡C]}$_2$-5-(C≡C)C_6H_3]$^+$, 55), 898 ([Ru(dppe)$_2$]$^+$, 100).

5.8. References

[1] Joffre, M., Yaron, D., Silbey, R.J., Zyss, J., *J. Chem. Phys.*, **1992**, *97*, 5607.

[2] Shuai, Z., Ramasesha, S., Bredas, J.L., *Chem. Phys. Lett.*, **1996**, *250*, 14.

[3] Dehu, C., Geskin, V., Persoons, A., Bredas, J.L., *Eur. J. Org. Chem.*, **1998**, 1267.

[4] Lee, H., An, S.Y., Cho, M.H., *J. Phys. Chem. B*, **1999**, *103*, 4992.

[5] Hahn, S., Kim, D., Cho, M.H., *J. Phys. Chem. B*, **1999**, *103*, 8221.

[6] Thalladi, V.R., Brasselet, S., Weiss, H.C., Blaser, D., Katz, A.K., Carrell, H.L., Boese, R., Zyss, J., Nangia, A., Desiraju, G.R., *J. Am. Chem. Soc.*, **1998**, *120*, 2563.

[7] Brasselet, S., Cherioux, F., Audebert, P., Zyss, J., *Chem. Mater.*, **1999**, *11*, 1915.

[8] Lambert, C., Gaschler, W., Noll, G., Weber, M., Schmalzlin, E., Brauchle, C., Meerholz, K., *J. Chem. Soc., Perkin Trans. 2*, **2001**, 964.

[9] Wolff, J.J., Siegler, F., Matschiner, R., Wortmann, R., *Angew. Chem., Int. Ed. Engl.*, **2000**, *39*, 1436.

[10] Officer, D.L., Burrell, A.K., Reid, D.C.W., *J. Chem. Soc. Chem. Commun.*, **1996**, 1657.

[11] Gong, L.Z., Hu, Q.S., Pu, L., *J. Org. Chem.*, **2001**, *66*, 2358.

[12] Kleiman, V.D., Melinger, J.S., McMorrow, D., *J. Phys. Chem. B*, **2001**, *105*, 5595.

[13] Jansen, J.F.G.A., Meijer, E.W., de Brabander van den Berg, E.M.M., *J. Am. Chem. Soc.*, **1995**, *118*, 5326.

[14] van Koten, G., Jastrzebski, J.T.B.H., *J. Mol. Catal. A*, **1999**, *146*, 317.

[15] de Groot, D., de Waal, B.F.M., Reek, J.N.H., Schenning, A., Kramer, P.C.J., Meijer, E.W., van Leeuwen, P., *J. Am. Chem. Soc.,* **2001**, *123*, 8453.

[16] Osawa, M., Hoshino, M., Horiuchi, S., Wakatsuki, Y., *Organometallics,* **1999**, *18*, 112.

[17] Achar, S., Immoos, C.E., Hill, M.G., Catalano, V.J., *Inorg. Chem.,* **1997**, *36*, 2314.

[18] Nlate, S., Ruiz, J., Sartor, V., Navarro, R., Blais, J.C., Astruc, D., *Chem. Eur. J.,* **2000**, *6*, 2544.

[19] Murfee, H.J., Thoms, T.P.S., Greaves, J., Hong, B., *Inorg. Chem.,* **2000**, *39*, 5209.

[20] Turrin, C.O., Chiffre, J., Daran, J.C., de Montauzon, D., Caminade, A.M., Manoury, E., Balavoine, G., Majoral, J.P., *Tetrahedron,* **2001**, *57*, 2521.

[21] Poon, K.W., Liu, W., Chan, P.K., Yang, Q.C., Chan, T.W.D., Mak, T.C.W., Ng, D.K.P., *J. Org. Chem.,* **2001**, *66*, 1553.

[22] Ohshiro, N., Takei, F., Onitsuka, K., Takahashi, S., *Chem. Lett.,* **1996**, 872.

[23] Ohshiro, N., Takei, F., Onitsuka, K., Takahashi, S., *J. Organomet. Chem.,* **1998**, *569*, 195.

[24] Turrin, C.-O., Chiffre, J., Montauzon, D., Daran, J.-C., Caminade, M., Manoury, E., Balavoine, G., Majorla, J.-P., *Macromolecules,* **2000**, *33*, 7328.

[25] Put, E.J.H., Clays, K., Persoons, A., Biemans, H.A.M., Luijkx, C.P.M., Meijer, E.W., *Chem. Phys. Lett.,* **1996**, *260*, 136.

[26] Ma, H., Jen, A.K.Y., *Adv. Mater.,* **2001**, *13*, 1201.

[27] Varnavski, O., Leanov, A., Liu, L., Takacs, J., Goodson, T., *J. Phys. Chem. B,*, **2000**, *104*, 179.

[28] McDonagh, A.M., Humphrey, M.G., Samoc, M., Luther-Davies, B., Houbrechts, S., Wada, T., Sasabe, H., Persoons, A., *J. Am. Chem. Soc.*, **1999**, *121*, 1405.

[29] McDonagh, A.M., Humphrey, M.G., Samoc, M., Luther-Davies, B., *Organometallics,* **1999**, *18*, 5195.

[30] Derkowska, B., Mulatier, J.C., Fuks, I., Sahraoui, B., Phu, X.N., Andraud, C., *J. Opt. Soc. Am. B,* **2001**, *18*, 610.

[31] Whittall, I.R., Humphrey, M.G., Samoc, M., Luther-Davies., B., *Angew. Chem., Int. Ed. Engl.*, **1997**, *36*, 370.

[32] Cho, B.R., Lee, S.J., Lee, S.H., Son, K.H., Kim, Y.H., Doo, J.Y., Lee, G.J., Kang, T.I., Lee, Y.K., Cho, M.H., Jeon, S.J., *Chem. Mater.*, **2001**, *13*, 1438.

[33] Allred, G.D., Liebeskind, L.S., *J. Am. Chem. Soc.*, **1996**, *118*, 2748.

[34] Lee, B.Y., Bazan, G.C., *J. Am. Chem. Soc.*, **2000**, *122*, 8577.

[35] Whittall, I.R., Humphrey, M.G., Houbrechts, S., Persoons, A., Hockless, D.C.R., *Organometallics,* **1996**, *15*, 5738.

[36] Touchard, D., Haquette, P., Pirio, N., Toupet, L., Dixneuf, P.H., *Organometallics,* **1993**, *12*, 3132.

[37] Whittall, I.R., Humphrey, M.G., Houbrechts, S., Maes, J., Persoons, A., Schmid, S., Hockless, D.C.R., *J. Organomet. Chem.*, **1997**, *544*, 277.

[38] Colbert, M.C.B., Lewis, J., Long, N.J., Raithby, P.R., Younus, M., White, A.J.P., Williams, D.J., Payne, N.N., Yellowlees, L., Beljonne, D., Chawdhury, N., Friend, R.H., *Organometallics,* **1998**, *17*, 3034.

[39] Bruce, M.I., Horn, E., Matisons, J.G., Snow, M.R., *Aust. J. Chem.,* **1984**, *37*, 1163.

[40] Bruce, M.I., Duffy, D.N., *Aust. J. Chem.,* **1986**, *39*, 1697.

[41] Whittall, I.R., Humphrey, M.G., Samoc, M., Swiatkiewicz, J., Luther-Davies, B., *Organometallics,* **1995**, *14*, 5493.

[42] Hurst, S.K., Cifuentes, M.P., McDonagh, A.M., Humphrey, M.G., Samoc, M., Luther-Davies, B., Asselberghs, I., Persoons, A., *J. Organomet. Chem.,* **2001**, In press.

[43] Chaudret, B., Commenges, G., Poilblanc, R., *J. Chem. Soc., Dalton Trans.,* **1984**, 1635.

[44] Hsung, R.P., Chidsey, C.E.D., Sita, L.R., *Organometallics,* **1995**, *14*, 4808.

[45] MacBride, J.A.H., Wade, K., *Synth. Commun.,* **1996**, *26*, 2309.

[46] Lavastre, O., Cabioch, S., Dixneuf, P.H., Vohlidal, J., *Tetrahedron,* **1997**, *53*, 7595.

[47] McAuliffe, C.A., Parish, R.V., Randall, P.D., *J. Chem. Soc., Dalton Trans.,* **1979**, 1730.

[48] Diez-Barra, E., Garcia-Martinez, J.C., Rodriguez-Lopez, J., *Tetrahedron Lett.,* **1999**, *40*, 8181.